

Production of Lipid Nanoparticles for Topical Administration of Flavonoids

Raquel Pinho Costa

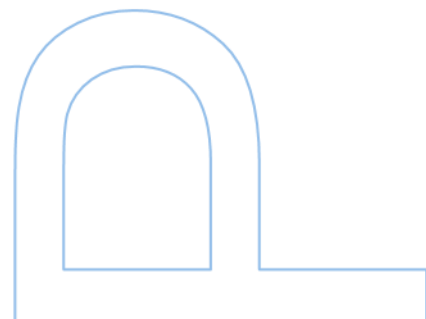
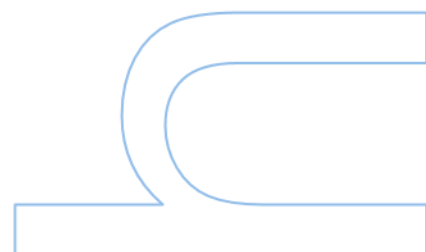
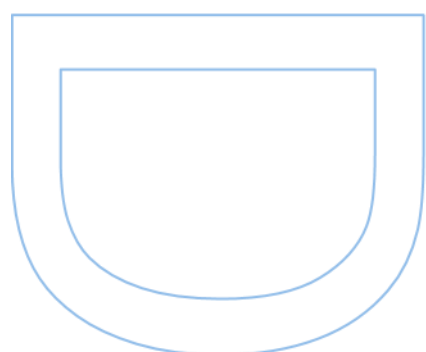
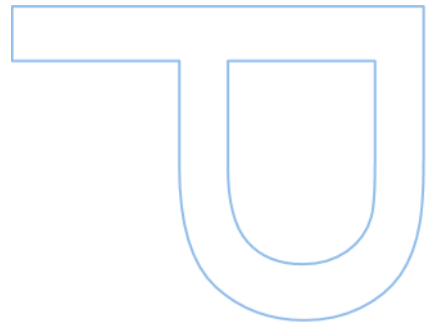
Programa Doutoral em Química Sustentável
Departamento de Química e Bioquímica
2023

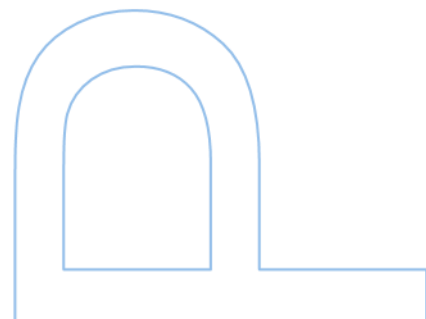
Orientador

Professora Doutora Maria de La Salette de Freitas Fernandes
Hipólito Reis Dias Rodrigues, Professor Catedrático, Faculdade de
Farmácia da Universidade do Porto

Coorientador

Professora Doutora Alberta Paula Lobo Machado Gameiro dos
Santos, Professor Auxiliar, Faculdade de Ciências da Universidade
do Porto





À minha família e amigos

Declaração de Honra

Eu, Raquel Pinho Costa, inscrita no Programa Doutoral em Química Sustentável da Faculdade de Ciências da Universidade do Porto declaro, nos termos do disposto na alínea a) do artigo 14.º do Código Ético de Conduta Académica da U.Porto, que o conteúdo da presente tese reflete as perspetivas, o trabalho de investigação e as minhas interpretações no momento da sua entrega.

Ao entregar esta tese, declaro, ainda, que a mesma é resultado do meu próprio trabalho de investigação e contém contributos que não foram utilizados previamente noutros trabalhos apresentados a esta ou outra instituição.

Mais declaro que todas as referências a outros autores respeitam escrupulosamente as regras da atribuição, encontrando-se devidamente citadas no corpo do texto e identificadas na secção de referências bibliográficas. Não são divulgados na presente tese quaisquer conteúdos cuja reprodução esteja vedada por direitos de autor.

Tenho consciência de que a prática de plágio e auto-plágio constitui um ilícito académico.

Raquel Pinho Costa

Porto, 19 de junho de 2023

Agradecimentos

O trabalho que culmina nesta dissertação não seria possível sem o contributo de um número considerável de pessoas. A todos aqueles que foram imprescindíveis durante todo este percurso expresso os meus sinceros agradecimentos.

Em primeiro lugar, agradeço à Professora Doutora Salette Reis que teve um papel central na execução desta tese. Agradeço por me ter recebido no seu laboratório e grupo e por toda a ajuda e palavras de motivação ao longo deste percurso. Agradeço conjuntamente à Professora Doutora Paula Gameiro por me ter aceite também como sua aluna e por estar sempre atenta e disponível ao longo deste percurso académico.

À Doutora Sofia Costa Lima deixo o meu agradecimento pelo apoio e pela sua disponibilidade total ao longo deste percurso. Agradeço a sua orientação durante o decorrer do trabalho que culminou nesta tese

A todos os restantes Professores do Departamento de Química Aplicada, agradeço a simpatia demonstrada.

Um enorme obrigado ao grupo MB2 por todo o apoio ao longo destes últimos anos. Em especial agradeço à Andreia Marinho, Ana Isabel Barbosa e Andreia Granja, por me terem ajudado vezes incontáveis no laboratório. Um obrigado especial também à Irina Pereira por ter sempre uma palavra de apoio quando mais precisava. Obrigada também aos restantes elementos do grupo pela boa-disposição, bom-humor e por estarem sempre disponíveis para ajudar: Tânia Moniz, Filipa Soares, Daniela Loureiro, Catarina Seabra, Zina, Thaisa.

Um obrigada especial à Renata Basto, que se tornou uma grande amiga, e que foi sem dúvida essencial ao longo destes anos. Obrigada pela tua boa-disposição, por me fazeres rir durante os momentos mais complicados e por estares sempre disponível para o que fosse preciso.

A todas as pessoas que conheci no contexto deste doutoramento e que irão certamente deixar saudades.

A todos os meus amigos e família, que fizeram e sempre irão fazer parte do meu percurso.

Por fim, o maior e mais especial agradecimento, é para a melhor e mais especial pessoa que tenho a sorte de ter na minha vida, Ricardo. É graças a ti que esta tese existe, graças ao teu apoio constante, tanto nos bons e nos maus momentos.

Funding

This work was supported from Portuguese national funds through the Foundation for Science and Technology (FCT) (project NORTE-08-5369-FSE-000050) supported by Northern Portugal Regional Operational Programme (NORTE 2020), under the Portugal 2020 Partnership Agreement, through the European Social Fund (ESF) agreement. Financial support from PT national funds (FCT/MCTES, Fundação para a Ciência e Tecnologia and Ministério da Ciência, Tecnologia e Ensino Superior), through the project UIDB/50006/2020 | UIDP/50006/2020, was also received.

The Foundation for Science and Technology (Fundação para a Ciência e Tecnologia, FCT) is a Portuguese public foundation responsible for promoting and funding scientific research and technological development in Portugal. It operates under the supervision of the Ministry of Science, Technology, and Higher Education.

The NORTE-08-5369-FSE-000050 project is supported by NORTE 2020, which is a regional development program that aims to enhance the competitiveness and sustainable development of the Northern region of Portugal. It is part of the Portugal 2020 Partnership Agreement, which is a strategic framework that promotes economic, social, and territorial cohesion in Portugal.

The European Social Fund (ESF) is one of the European Structural and Investment Funds (ESIF) that provide financial support to EU member states and regions to address social and economic disparities.

Resumo

Os flavonoides estão entre os grupos mais comuns de substâncias polifenólicas naturalmente encontradas em muitas plantas e frutas. Apesar do desenvolvimento crescente de novos medicamentos na área farmacêutica, vários compostos naturais ainda são utilizados para tratar diversas patologias humanas, tais como inflamação da pele, cancro e várias outras doenças inflamatórias.

A quercetina é um dos flavonóides mais estudados e o antioxidante mais abundante na nossa dieta. Esse composto pode ser encontrado ubiquamente distribuído em frutas, vegetais, ervas e outros produtos relacionados. Adicionalmente, as suas vastas propriedades farmacológicas, tais como atividades antioxidante, antienvhecimento e antiangiogénica, tornam a quercetina um composto altamente atrativo. No entanto, a aplicabilidade clínica da quercetina é extremamente limitada devido à sua alta hidrofobicidade, instabilidade química e tempo de meia-vida curto, aspetos que levam a uma baixa biodisponibilidade.

Para além das vias convencionais de administração, como, por exemplo, ingestão oral, métodos alternativos para a administração de quercetina, tais como administração tópica, têm sido explorados. Neste caso específico, a pele atua como uma barreira importante que dificulta a absorção e a permeabilidade de compostos, devido à organização e composição lipídica da camada mais externa da epiderme, o estrato córneo. No entanto, através da nanotecnologia, nomeadamente recorrendo à encapsulação de fármacos em sistemas de entrega, tais como nanopartículas lipídicas (transportadores lipídicos nanoestruturados, NLCs, e nanopartículas lipídicas sólidas, SLNs), lipossomas ou hidrogéis incorporando nanopartículas, torna-se possível aumentar a sua biodisponibilidade, mas também promover uma libertação controlada do fármaco.

Assim, o principal objetivo desta tese foi usar a nanotecnologia para desenvolver um sistema de administração tópica de quercetina, para a melhorar a penetração desse composto, obter uma libertação controlada e entrega direcionada da quercetina, assim como aumentar a sua solubilidade e estabilidade, proporcionando simultaneamente proteção contra condições adversas. Este sistema foi desenvolvido devido ao seu potencial para várias aplicações, tais como terapia anti-inflamatória e antioxidante, cicatrização de feridas, fotoproteção ou tratamento de doenças relacionadas com a pele.

Para esse propósito, o primeiro objetivo desta tese consistiu em produzir e otimizar NLCs para a encapsulação de quercetina. Para a fabricação dos NLCs, foi usado o óleo de romã (PO) como lípido líquido, uma vez possui várias propriedades importantes, tais como potencial anti-inflamatórios, antioxidantes e anti-apoptótico. Um desenho Box-Behnken, no qual a relação lípido líquido/lípido sólido, a quantidade de água e a quantidade de fármaco foram utilizadas como variáveis independentes, foi construído para obter a formulação otimizada das NLCs, em relação à percentagem de encapsulação e incorporação de fármaco. Para comparação da percentagem de encapsulação e incorporação de fármaco, as formulações com SLNs foram obtidas de forma semelhante. A distribuição de tamanho das NLCs otimizadas apresentou uma variação entre 200 e 300 nm, sendo adequada para administração tópica de fármacos. Adicionalmente, as NLCs otimizadas apresentaram uma eficiência de encapsulação de quercetina de aproximadamente 55%, enquanto para as SLNs essa eficiência foi de 43%. Além disso, foi observada uma estabilidade de armazenamento até 3 meses. A biocompatibilidade celular foi verificada em fibroblastos e queratinócitos após 24 horas de exposição às NLCs e SLNs com quercetina encapsulada, bem como à quercetina livre. Tanto as NLCs como as SLNs mostraram ser capazes de proteger a quercetina da fotodegradação. Particularmente, verificou-se que a quercetina mantém a sua atividade antioxidante, a qual é protegida ao ser encapsulada nas nanopartículas lipídicas, em comparação com a sua forma livre. Estudos de permeação usando um ensaio de permeação baseado em vesículas fosfolipídicas (PVPA), i.e. um modelo mimético do estrato córneo, revelaram que esta barreira retém uma maior quantidade de quercetina quando esta é encapsulada em NLCs e SLNs, em comparação com a sua forma livre.

O segundo objetivo desta tese visou incorporar as nanopartículas encapsuladas com quercetina já otimizadas em hidrogéis de alginato de sódio-álcool polivinílico (SA-PVA), de modo a obter um sistema de libertação tópica de quercetina. A biocompatibilidade do hidrogel obtido foi avaliada, juntamente com o seu potencial como agente terapêutico contra danos na pele causados pela radiação ultravioleta (UV). Hidrogéis são redes poliméricas hidrofílicas que se têm tornados altamente atrativos para fins farmacêuticos e cosméticos. Neste trabalho, hidrogéis híbridos de SA-PVA foram desenvolvidos de forma a incorporarem quercetina encapsulada em NLCs e SLNs, a fim de formular um sistema de entrega tópica combinado, com a capacidade de aumentar a retenção de quercetina na pele e melhorar a sua ação local como agente fotoprotetor. NLCs e SLNs encapsuladas com quercetina foram incorporados com sucesso na rede polimérica dos hidrogéis de SA-PVA. A análise reológica revelou que estes hidrogéis são robustos com comportamento pseudoplástico, perfil não tixotrópico e boa resistência à deformação, a

temperaturas entre 20 e 40°C. A exposição de queratinócitos aos hidrogéis incorporados com NLCs e SLNs encapsuladas com quercetina, antes da irradiação, originou um aumento da viabilidade celular, o que sugere um efeito fotoprotetor deste sistema. Adicionalmente, foi observada uma diminuição dos níveis intracelulares de espécies reativas de oxigénio (ROS) após a exposição dessas células a hidrogéis incorporados com quercetina, antes da irradiação. Por outro lado, hidrogéis com NLCs vazias também produziram uma diminuição dos níveis intracelulares de ROS, sugerindo que o PO também possui a capacidade de eliminar ROS intracelular gerados por irradiação UVB. A exposição de queratinócitos a hidrogéis com quercetina, após a irradiação, levou a um aumento significativo da viabilidade celular, demonstrando que este sistema possui um potencial efeito terapêutico contra danos na pele causados por radiação UVB.

Através deste trabalho foi possível estabelecer uma nanoplataforma promissora para a entrega tópica de quercetina. Esta nanoplataforma é baseada em nanopartículas lipídicas, nomeadamente NLCs e SLNs, as quais permitem um encapsulamento estável e eficiente da quercetina. Adicionalmente, a incorporação de nanopartículas lipídicas encapsuladas com quercetina em hidrogéis de SA-PVA deu origem a uma plataforma de entrega com a capacidade de aumentar a retenção da quercetina na pele, permitindo assim que atue como antioxidante e agente terapêutico contra danos na pele induzidos por UVB. Com vista a demonstrar o potencial desta nanoplataforma, vários aspetos foram estudados, tais como otimização da formulação, atividade antioxidante, biocompatibilidade celular e permeação através da pele.

Palavras-chave: atividade antioxidante, biocompatibilidade celular, flavonoides, transportador lipídico nanoestruturado, fotoproteção, espécies reativas de oxigénio, nanopartículas lipídicas sólidas

Abstract

Flavonoids are among the most common groups of polyphenolic substances found naturally in many plants and fruits. Despite the fast-growing development in the pharmaceutical field, natural compounds are still being used to treat various human pathologies, including conditions such as skin inflammation, cancer, and several other inflammatory diseases.

Quercetin is one of the best studied flavonoids, and the most abundant antioxidant found in the human diet. It can be found ubiquitously distributed in fruits, vegetables, herbs, and related products. Its vast pharmacological properties, that include antioxidant, anti-inflammatory, anti-aging and anti-angiogenic activities makes quercetin a highly attractive compound. However, its clinical applicability is extremely limited by its high hydrophobicity, chemical instability, and short half-life, which in turn result in low bioavailability.

Besides the conventional routes of administration, e.g. oral ingestion, alternative routes for the delivery of quercetin, such as topical delivery have been explored. However, skin acts a major barrier hindering drug absorption and permeability, given the organization and lipidic composition of the outermost epidermis layer, the stratum corneum. Thus, application of nanotechnology for drug encapsulation into delivery systems such as lipid nanoparticles (nanostructured lipid carriers, NLCs, and solid lipid nanoparticles, SLNs), liposomes, or hydrogels incorporating nanoparticles can enhance bioavailability and also promote a controlled drug release.

The main aim of this thesis was to use nanotechnology to develop a topical delivery system for quercetin, in order to improve the penetration of that compound, achieve a controlled release and targeted delivery of quercetin, as well as enhance its solubility and stability, whilst providing protection from harsh environmental conditions. As a result, this system was developed due to its potential for a variety of applications, such as anti-inflammatory and anti-oxidant therapy, wound healing, photoprotection, or for treatment of skin disorders.

For that, the first goal was to produce and optimize NLCs for the encapsulation of quercetin. For NLCs fabrication, pomegranate oil (PO) was used as the liquid lipid, since it possesses various attractive properties, e.g. anti-inflammatory, antioxidant, and anti-apoptotic effects. A three-level Box-Behnken design, in which the lipid liquid/solid lipid

ratio, amount of water, and amount of drug were used as the independent variables, was constructed in order to obtain the optimized NLCs formulation, regarding encapsulation efficiency and drug loading. The counterpart SLNs were obtained similarly for comparison of the encapsulation efficiency and drug loading. The size distribution of the optimized NLCs ranged from 200 to 300 nm, being adequate for topical drug administration. The optimized NLCs exhibited a quercetin entrapment efficiency of approximately 55%, while SLN 43%. In addition, storage stability was verified up to 3 months. Cell biocompatibility was verified in fibroblasts and keratinocytes upon 24 hours of exposure with quercetin-loaded NLCs and SLNs, as well as free-quercetin. Both NLCs and SLNs were proven to protect quercetin from photodegradation. Particularly, it was verified that quercetin's antioxidant activity is maintained but protected upon loading in the lipid nanoparticles, as compared to its free form. Permeation studies using a phospholipid vesicle-based permeation assay (PVPA), a mimetic stratum corneum model, revealed that this barrier retains a higher amount of quercetin when loaded into NLCs and SLNs in comparison to its free form.

The second goal of this thesis was to incorporate the optimized quercetin-loaded nanoparticles into sodium alginate-poly(vinyl) alcohol (SA-PVA) hydrogels with the goal of obtaining a topical delivery system for quercetin. The biocompatibility of the hydrogel system was further evaluated in addition to its potential to be used as therapeutic agent towards ultraviolet (UV)-induced skin damage. Hydrogels are hydrophilic polymeric networks that have become highly attractive candidates for pharmaceutical and cosmetic purposes. Hybrid SA-PVA hydrogels were design to incorporate quercetin encapsulated into NLCs and SLNs in order to formulate a combined topical delivery system capable of increasing quercetin's retention in the skin and improve its local action as a photoprotective agent. Quercetin-loaded NLCs and SLNs were successfully incorporated into the polymeric network of the SA-PVA hydrogels. The rheological analysis revealed robust hydrogels with pseudoplastic behavior, a non-thixotropic profile, and good resistance to deformation and temperatures from 20 to 40°C. Exposure of keratinocytes to hydrogels incorporated with quercetin-loaded NLCs and SLNs prior to irradiation resulted in an increase in cell viability, suggesting a photoprotective effect. Similarly, a decrease in the level of intracellular reactive oxygen species (ROS) was observed when cells were exposed to quercetin-loaded hydrogels prior to irradiation. Hydrogels containing empty NLCs were able to produce a decrease in the intracellular levels of ROS, which suggests that PO is also capable of scavenging the intracellular ROS generated by UVB irradiation. Exposure to quercetin-loaded hydrogels after

irradiation resulted in a significant increase in cell viability, suggesting a potential therapeutic effect against UVB-damaged skin.

Overall, this work established a nanoplatform for topical delivery of quercetin. This nanoplatform is based on lipidic nanoparticles, namely NLCs and SLNs, which provided a stable and efficient means of encapsulating quercetin. These nanoparticles were shown to protect the quercetin payload and enhance its delivery to the skin. Furthermore, the incorporation of lipidic nanoparticles encapsulating quercetin into SA-PVA hydrogels resulted in a delivery vehicle capable of increasing quercetin's absorption and retention in the skin, thus enabling its action as an antioxidant and therapeutic agent against UVB-induced skin damage. To demonstrate the potential of this nanoplatform, several aspects were studied, such as formulation optimization, antioxidant activity, cellular biocompatibility, and permeation through the skin.

Keywords: antioxidant activity, cellular biocompatibility, flavonoids, nanostructured lipid carrier, photoprotection, reactive oxygen species, solid lipid nanoparticles

Index

List of Tables	xv
List of Figures	xvi
List of Abbreviations and Symbols	xx
1. Thesis Structure.....	1
2. Introduction.....	3
2.1. Quercetin Overview	3
2.1.1. Flavonoids – an Overview.....	3
2.1.2. Quercetin.....	4
2.1.2.1. Chemical Structure	4
2.1.2.2. Absorption, Bioavailability, and Excretion.....	5
2.1.3. Mechanisms of Action.....	6
2.1.3.1. Inflammation and Immune Function	6
2.1.3.2. Antioxidant Capacity	7
2.1.3.3. Anticancer Capacity.....	8
2.1.3.4. Neuroprotective Effects.....	8
2.1.4. Nanomedicine.....	9
2.1.5. Clinical Trials Patents and Formulations in the Market.....	10
2.2. References	14
2.3. On the Development of a Cutaneous Flavonoid Delivery System: Advances and Limitations.....	26
3. Materials and Methods.....	52
3.1. Materials.....	52
3.2. Methods.....	53
3.2.1. Production of Nanostructured Lipid Carriers and Solid Lipid Nanoparticles.....	53
3.2.2. Experimental Design: Box-Behnken Design	53
3.2.3. Validation of the Optimized Quercetin-Loaded Nanostructured Lipid Carriers.....	55

3.2.4. Characterization of Quercetin-Loaded Nanoparticles.....	55
3.2.4.1. Determination of Nanoparticles' Size and Zeta Potential.....	55
3.2.4.2. Morphology Evaluation	59
3.2.4.3. Encapsulation Efficiency and Drug Loading Determination	59
3.2.4.4. Storage Stability Assessment	61
3.2.4.5. Fourier Transform Infrared Spectroscopy Analysis	61
3.2.4.6. Thermal Analysis	62
3.2.4.7. Photostability Study	63
3.2.5. Preparation of the Sodium Alginate-Poly(Vinyl Alcohol) Hydrogels.....	63
3.2.6. Rheology Studies	63
3.2.7. Morphology of SA-PVA Hydrogels Incorporating Quercetin-Loaded Nanoparticles.....	67
3.2.8. Determination of Quercetin Antioxidant Activity	70
3.2.8.1. The ABTS Assay	70
3.2.8.2. The DDPH Assay.....	71
3.2.9. Cellular Studies	72
3.2.9.1. Cell Culture Conditions	72
3.2.9.2. Biocompatibility.....	72
3.2.9.3. Ultraviolet B Irradiation Intensity Studies.....	73
3.2.9.4. Photoprotective Assay	73
3.2.9.5. Cellular Recovery Study	74
3.2.9.6. Apoptosis Analysis.....	74
3.2.9.7. Determination of Intracellular Reactive Oxygen Species	75
3.2.10. Permeation Studies Using PVPA _{sc} Model	76
3.2.10.1. Preparation of PVPA _{sc} Model	77
3.2.10.2. Permeation Assay Using PVPA _{sc} Model	77
3.2.11. Statistical Analysis.....	78
3.3. References	79
4. Results and Discussion.....	88

4.1. Design, Optimization, and Characterization of Nanostructured Lipid Carriers Containing Pomegranate Oil	88
4.1.1. Experimental Design: Optimization	88
4.1.2. Validation of the Experimental Design	91
4.1.3. Characterization of Quercetin-Loaded Lipid Nanoparticles	91
4.1.4. Morphology Assessment	92
4.1.5. Storage Stability Assessment	93
4.1.6. Fourier-Transform Infrared Spectroscopy Evaluation	94
4.1.7. Thermal Analysis	95
4.1.8. Photostability Study	97
4.1.9. Cellular Studies	98
4.1.9.1. Antioxidant Activity of Quercetin Incorporated within NLCs and SLNs	99
4.1.9.2. Assessment of Skin Permeation	100
4.1.10. Conclusion.....	101
4.2. Characterization of SA-PVA Hydrogels Incorporating Quercetin-Loaded Nanoparticles	102
4.2.1. Fourier-Transform Infrared Spectroscopy Evaluation	102
4.2.2. Rheology Analysis of SA-PVA Hydrogels	103
4.2.3. Long-Term Mechanical Stability Analysis of SA-PVA Hydrogels	107
4.2.4. Quercetin-Loaded SA-PVA Hydrogels Morphology.....	111
4.2.5. Antioxidant Activity of Quercetin-Loaded SA-PVA Hydrogels.....	112
4.2.6. Cellular Studies	113
4.2.6.1. Biocompatibility.....	113
4.2.6.2. Biocompatibility Evaluation of the Effect of Ultraviolet B Irradiation on Keranocytes Treated with the Quercetin-Based Nanoformulations – Photoprotective Assay.....	114
4.2.6.3. Effect of Quercetin-Based Nanoformulations on Intracellular ROS Levels.....	117
4.2.6.4. Evaluation of the Effect of Ultraviolet B Irradiation on Keranocytes Treated with the Quercetin-Based Nanoformulations – Cell Recovery Effect .	119

4.2.7. Conclusion.....	120
4.3. References	121
5. Conclusions and Future Perspectives.....	127
Annex 1	130

List of Tables

Table 3.1 - Composition of optimized quercetin-loaded NLCs.....	55
Table 4.1 - Formulation composition and correspondent responses of 15 different formulations obtained from BBD.	89
Table 4.2 - Physicochemical parameters of optimized quercetin-loaded lipid particles.	91
Table 4.3 - DSC parameters of optimized quercetin-loaded and unloaded formulations.	97

List of Figures

Figure 2.1 - Structure of the main flavonoid subgroups	3
Figure 2.2 - Molecular structure of quercetin.....	5
Figure 3.1 - BBD for three variables x1, x2 and x3; the circles represent experimental points and square is the central point.....	54
Figure 3.2 - Scheme of a general DLS setup	56
Figure 3.3 - Raw correlation function	57
Figure 3.4 - EDL of a negatively charged nanoparticle during electrophoresis.	58
Figure 3.5 - Schematic diagram of a HPLC system.....	60
Figure 3.6 - Flow curves of different commercial hydrogels	65
Figure 3.7 - Example of an amplitude sweep curve. (LVE – linear-viscoelastic).	66
Figure 3.8 - Schematic diagram of the main components of a SEM equipment.....	68
Figure 3.9 - Schematic diagram of the different particles emitted during electron-sample interaction at various depths	69
Figure 3.10 - Principle of the PVPA assay, mimicking the SC	76
Figure 4.1 - Response surface plots evidencing the influence of the independent variables on the selected responses particle size. (A) influence of the drug concentration and liquid lipid/solid lipid ratio on the particle size, (B) influence of the quantity of drug and water volume on the particle size, (C) influence of the water volume and liquid lipid/solid lipid ratio on the PDI, (D) influence of the quantity of drug and liquid lipid/solid lipid on PDI, (E) Influence of the water volume on the % EE, and (F) influence of drug quantity on the % EE.	90
Figure 4.2 - Quercetin-loaded and unloaded formulations morphology. Transmission electron microscopy images attained for both quercetin-loaded and non-loaded SLNs and NLCs. The red arrows in the images point to the distinct zones formed that result from a mixture of lipids in the nanoparticles. Scale bar of 100 nm.....	93
Figure 4.3 - Storage stability of quercetin-loaded NLCs (black bar), unloaded NLCs (light grey), quercetin-loaded SLNs (dark grey) and unloaded SLNs (white) at 4°C and RT.	94
Figure 4.4 - FTIR spectra of quercetin in its free form and quercetin-loaded NLCs and SLNs. Empty NLCs and SLNs are also displayed.	95
Figure 4.5 - DSC thermograms for (A) quercetin loaded and unloaded SLNs and NLCs and (B) corresponding physical mixtures.	96
Figure 4.6 - (A) Absorption spectra of quercetin in its free form and quercetin-loaded NLCs and SLNs before and after UV light exposure for 3 hours. (B) Percentage of	

quercetin photodegradation after 3 hours exposure to UV light. Values correspond to means \pm standard deviation for n = 1 replicates..... 98

Figure 4.7 - Viability of L929 fibroblasts (A) and HaCaT keratinocytes (B) upon 24 hours of exposure to unloaded and quercetin-loaded NLCs and SLNs. Tested concentrations ranged from 3.125 to 50 $\mu\text{g/mL}$. Each result represents the mean \pm standard deviation for n=4 replicates of 3 assays. Asterisks indicate statistical significance in relation to control (*P \leq 0.05; **P \leq 0.01; ***P \leq 0.001; ****P \leq 0.0001). 99

Figure 4.8 - Antioxidant activity of quercetin-loaded nanoparticles. (A) ABTS and (B) DPPH radical scavenging activity percentage of free quercetin and quercetin-loaded NLCs and SLNs. Values correspond to means \pm standard deviation for n = 3 replicates. 100

Figure 4.9 - Percentage of quercetin permeated, retained, and non-permeated through the PVPASc after 3 hours. Values correspond to means \pm standard deviation for n = 3 replicates. 101

Figure 4.10 - FTIR spectra of (A) quercetin in its free form and (B) quercetin-loaded hydrogels. Unloaded and hydrogels loaded with empty nanoparticles are also displayed. 103

Figure 4.11 - Viscosimetry analysis of control and quercetin-loaded hydrogels, as free quercetin and quercetin-loaded NLCs and SLNs, through shear stress (black line) and shear viscosity (blue line) data. Data points correspond to mean \pm standard deviation for n = 2 replicates. 104

Figure 4.12 - Thixotropy analysis of control and quercetin-loaded hydrogels, as free quercetin and quercetin-loaded NLCs and SLNs. Data points correspond to mean \pm standard deviation for n = 2 replicates. 105

Figure 4.13 - Resistance to deformation based on the determination of viscoelastic region of control and quercetin-loaded hydrogels, as free quercetin and quercetin-loaded NLCs and SLNs. Data points correspond to mean \pm standard deviation for n = 2 replicates. 106

Figure 4.14 - Resistance to temperature based on the determination of viscoelastic region of control and quercetin-loaded hydrogels, as free quercetin and quercetin-loaded NLCs and SLNs. Data points correspond to mean \pm standard deviation for n = 2 replicates. 107

Figure 15 - Viscosimetry analysis over a period of six weeks of quercetin-loaded hydrogels, as free quercetin and quercetin-loaded NLCs and SLNs, through shear stress (black line) and shear viscosity (blue line) data. Data points correspond to mean \pm standard deviation for n = 2 replicates. 108

Figure 4.16 - Thixotropy analysis over a period of six weeks of quercetin-loaded hydrogels, as free quercetin and quercetin-loaded NLCs and SLNs. Data points correspond to mean \pm standard deviation for n = 2 replicates. 109

Figure 4.17 - Resistance to deformation based on the determination of viscoelastic region over a period of six weeks of quercetin-loaded hydrogels, as free quercetin and quercetin-loaded NLCs and SLNs. Data points correspond to mean \pm standard deviation for n = 2 replicates. 110

Figure 4.18 - Resistance to temperature based on the determination of viscoelastic region over a period of 6 weeks of quercetin-loaded hydrogels, as free quercetin and quercetin-loaded NLCs and SLNs. Data points correspond to mean \pm standard deviation for n = 2 replicates. 111

Figure 19 - Analysis of the hydrogel's morphology. SEM micrographs of quercetin free and quercetin-loaded NLCs and SLNs incorporated into sodium alginate-poly(vinyl) alcohol (SA-PVA) hydrogels. Scale bar 200 μ m and 400 μ m. Red arrows indicate more compact areas presenting lower porosity. 112

Figure 4.20 - Antioxidant activity of quercetin incorporated within SA-PVA hydrogels. ABTS radical scavenging activity percentage of free quercetin and quercetin-loaded SA-PVA hydrogels, as a free quercetin or loaded into NLCs and SLNs. Data points correspond to mean \pm standard deviation for n = 3 replicates, Asterisks indicate statistical significance in relation to control (**** p < 0.0001). # Represent statistical significance in relation to quercetin in its free form (###, p \leq 0.0001). 113

Figure 4.21 - Viability HaCaT keratinocytes upon 24 hours of exposure to the developed nanoformulations, unloaded and quercetin-loaded hydrogels as free quercetin or loaded into NLCs and SLNs. Tested concentrations ranged from 1.25 to 10 μ g/mL in quercetin and equivalent polymer concentration of 20.9 to 167 mg/mL. Each result represents the mean \pm standard deviation for n=4 replicates of 3 independent assays. Asterisks indicate statistical significance in relation to non-irradiated control cells (*, p \leq 0.05). No asterisks indicate no statistical significance (p > 0.05). 114

Figure 4.22 - Effect of different UVB intensities (60, 80, 100 and 120 mJ/cm²) on the HaCaT cell's viability. 115

Figure 4.23 - Effects of free quercetin and quercetin-containing hydrogels (both quercetin free-loaded hydrogel and quercetin-loaded NLCs and SLNs incorporated into hydrogels) on cell viability in UVB (60 mJ/cm²) irradiated HaCaT keratinocytes at a concentration of quercetin of 2.5 μ g/mL. (A) Photoprotection effect on cells exposed to the hydrogels prior to irradiation and (B) Apoptosis analysis on cells exposed to the hydrogels prior to irradiation. Flow cytometry analysis was performed following staining with FITC Annexin

V and 7-AAD and the percentage of viable cells as well as early and late apoptotic cells is showed. Data are representative of tree independent experiments as mean ± SD. Asterisks indicate statistical significance in relation to irradiated control cells (*, p ≤ 0.05; **, p ≤ 0.01; *** p ≤ 0.001). No asterisks indicate no statistical significance (p > 0.05). # Represent statistical significance in relation to non-irradiated control cells (#, p ≤ 0.05; ##, p ≤ 0.01; ###, p ≤ 0.0001). 117

Figure 4.24 - Effect of quercetin-based nanoformulations on intracellular ROS levels in cultured HaCaT cells. Cells were treated with quercetin-based nanoformulations at a concentration of quercetin of 2.5 µg/mL for 24 hours, prior to UVB irradiation (60 mJ/cm²). Immediately following irradiation, the intracellular ROS levels were determined using the fluorogenic probe DCFH-DA. The intracellular ROS levels were quantitatively determined via flow cytometry. Data are representative of tree independent experiments as mean ± SD. Asterisks indicate statistical significance in relation to irradiated control cells (*, p ≤ 0.05; **** p ≤ 0.0001). No asterisks indicate no statistical significance (p > 0.05). # Represent statistical significance in relation to non-irradiated control cells (###, p ≤ 0.001). 118

Figure 4.25 - Effects of free quercetin and quercetin-loaded hydrogels (both quercetin free-loaded hydrogel and quercetin-loaded NLCs and SLNs incorporated into hydrogels) on cell viability in UVB (60 mJ/cm²) irradiated HaCaT keratinocytes at a concentration of quercetin of 2.5 µg/mL. (A) Cell recovery effect on cells exposed to the hydrogels after irradiation and (B) Apoptosis analysis on cells exposed to the hydrogels after irradiation. Flow cytometry analysis was performed following staining with FITC Annexin V and 7-AAD AAD and the percentage of viable cells as well as early and late apoptotic cells is showed. Data are representative of tree independent experiments as mean ± SD. Asterisks indicate statistical significance in relation to irradiated control cells (*, p ≤ 0.05; **, p ≤ 0.01; ***, p ≤ 0.001; **** p ≤ 0.0001). No asterisks indicate no statistical significance (p > 0.05). # Represent statistical significance in relation to non-irradiated control cells (###, p ≤ 0.001; ###, p ≤ 0.0001). 120

List of Abbreviations and Symbols

ABS	Absorbance
ABTS	2,2-azinobis (3-ethylbenzothiazoline-6-sulfonic acid)
AChE	Acetylcholinesterase
ACE2	Angiotensin converting enzyme 2
ANOVA	One-way analysis of variance
AP-1	Activator protein-1
BBD	Box-Bhenken design
BChE	Butyrylcholinesterase
CAT	Catalase
cm ⁻¹	Centimetre minus 1
CoQ10	Coenzyme q10
DCF	2',7'-dichlorofluorescein
DCFH-DA	2',7'-dichlorodihydrofluorescein diacetate
DL	Drug loading
DLS	Dynamic light scattering
DMEM	Dulbecco's Modified Eagle's Medium
DMSO	Dimethyl sulfoxide
DPPH	1,1-diphenyl-2-picrylhydrazyl
DPPH-H	2,2-diphenyl-1-hydrazine
DSC	Differential scanning calorimetry
EDL	Electric double layer
EDS	Energy dispersive x-ray spectroscopy
EDTA	Ethylenediaminetetraacetic acid
EE	Encapsulation efficiency
EPC	Egg phosphatidylcholine
ER	Estrogen receptor
ERK	Extracellular signal-related kinase
FBS	Fetal bovine serum
FITC	Fluorescein isothiocyanate
FTIR	Fourier transform infrared resonance
G'	Storage modulus
G''	Loss modulus
GSH	Glutathione

H ₂ O ₂	Hydrogen peroxide
HPLC	High performance liquid chromatography
IC ₅₀	The half maximal inhibitory concentration
IR	Infrared
J/g	Joule per gram
JNK	c-Jun NH ₂ -terminal kinase
LPS	Lipopolysaccharide
LUV	Large unilamellar liposome
MeOH	Methanol
mg	Milligram
mJ/cm ²	Millijoules per square centimeter
ml	Milliliter
MLV	Multilamellar large liposome
mM	Millimolar
MTT	3-(4,5-dimethylthiazol-2-yl)-2,5-diphenyltetrazolium bromide
mV	Millivolt
NLC	Nanostructured lipid carrier
NF-κB	Nuclear factor-kappa B
nm	Nanometer
NP	Nanoparticle
NPQ	Lecithin-chitosan nanoparticle
PBS	Phosphate Buffer Solution
PDI	Polydispersity index
PI	Propidium iodide
PLGA	Poly (lactic-co-glycolic acid)
PM	Physical mixture
PO	Pomegranate oil
PPAR γ	Peroxisome proliferator-activated receptor c
PS	Phosphatidylserine
PVA	Poly(vinyl) alcohol
PVPA	Phospholipid vesicle-based permeation
r ²	Squared correlation coefficient
ras	Rat sarcoma
ROS	Reactive oxygen species
RSC%	Radical scavenging activity

rpm	Rotation per minute
RT	Room temperature
SA	Sodium alginate
SA-PVA	Sodium alginate-poly(vinyl) alcohol
SC	Stratum corneum
SD	Standard deviation
SEM	Scanning electron microscopy
SLN	Solid lipid nanoparticle
SOD	Superoxide dismutase
TEM	Transmission electron microscopy
TNF- α	Tumor necrosis factor alpha
TPGS	d- α -Tocopheryl polyethylene glycol
TSCC	Tongue squamous cell carcinoma
UV	Ultraviolet radiation
UV-Vis	Ultraviolet- visible
UVA	Ultraviolet-A radiation
UVB	Ultraviolet-B radiation
v/v	Volume/volume
w/v	Weight/volume
w/w	Weight/weight
ZP	Zeta potential
α	Alpha
β	Beta
ζ	Zeta
%	Percentage
$^{\circ}\text{C}$	Degree Celsius
$^{\circ}\text{C}/\text{min}$	Degree Celsius per minute
ΔH	Enthalpy variation
μ_e	Electrophoretic mobility
$\mu\text{g ml}^{-1}$	Microgram per milliliter
$\mu\text{g s}^{-1}$	Microgram per second
7-AAD	7-Amino-Actinomycin

1. Thesis Structure

This thesis is organized into 5 chapters, comprising a brief description of the structure of the thesis in chapter 1, theoretical background in chapter 2, materials and methods in chapter 3, results and discussion in chapter 4 and in chapter 5 the conclusion and future perspectives.

Chapter 1. Thesis Structure

In this chapter, a summary of the thesis organization is given in addition to the description of the contents of each chapter.

Chapter 2. Theoretical Background

This chapter includes the state-of-the-art regarding flavonoids, in particular, quercetin. An overview of its structure, bioavailability and mechanisms of action is highlighted. With that purpose, two sub-chapters were included:

2.1. This sub-chapter comprises a literature review describing quercetin's structure, bioavailability, and mechanisms of action, particularly, antioxidant and anticancer capacity, as well as anti-inflammatory activity. In this sub-chapter it is also highlighted how nanotechnology has been used towards improving quercetin's bioavailability.

2.2. In this sub-chapter it is addressed the potential of nanotechnology for the development of topical delivery systems for quercetin, as well as other classes of flavonoids, by presenting a review article entitled: On the Development of a Cutaneous Flavonoid Delivery System: Advances and Limitations (Costa, R., Costa Lima, S. A., Gameiro, P., and Reis, S., On the development of a cutaneous flavonoid delivery system: Advances and limitations. *Antioxidants* **10**, 1376 (2021).

Chapter 3. Materials and Methods

In this chapter it is presented a description of the experimental methods and characterization techniques used in this thesis. It includes the production and optimization methods used to obtain nanostructured lipid carriers (NLCs) and solid lipid nanoparticles (SLNs), as well as the characterization techniques. *In vitro* studies and its procedures are also described.

Chapter 4. Results and Discussion

This chapter comprises the progress beyond the state of the art, and it is divided into two sub-chapters:

4.1. In this sub-chapter NLCs are produced and optimized using a Box-Behnken design for the encapsulation of quercetin. SLNs encapsulating quercetin are also produced. The nanoparticles are characterized in terms of morphology by transmission electron microscopy (TEM), Fourier-Transform Infrared Spectroscopy (FTIR) as well as differential scanning calorimetry (DSC). Their storage stability is assessed over a period of 12 weeks as well as their capacity to protect quercetin from UV radiation upon encapsulation. Finally, their biocompatibility, skin permeation profile, and antioxidant activity were also evaluated to validate its potential to be used as a topical delivery system for quercetin.

4.2. In this sub-chapter the previously produced NLCs and SLNs encapsulating quercetin are incorporated into hydrogels composed of sodium alginate and poly(vinyl) alcohol (SA-PVA). The SA-PVA hybrid hydrogel system is characterized in terms of structure and mechanical properties. In addition, its ability to retain quercetin's antioxidant activity is evaluated as well as the effect of UVB irradiation on keratinocytes exposed to the hybrid quercetin-loaded hydrogels. HaCaT cells were exposed to the hydrogels prior to UVB cell irradiation, in order to evaluate their potential photoprotective effect. The effect of the quercetin hydrogels on the intracellular levels of ROS is also evaluated. Finally, the cell recovery effect of these hydrogels on UVB-induced skin damage is addressed.

Chapter 5. Conclusions and Future Perspectives

In this chapter the main findings and outcomes of this thesis are discussed, and future perspectives are presented.

2. Introduction

2.1. Quercetin Overview

2.1.1. Flavonoids – an Overview

Flavonoids belong to a class of plant secondary metabolites that are found ubiquitously in fruits, vegetables and a number of beverages. Due to their well-known antioxidant, anti-inflammatory, anti-carcinogenic properties, they have been used in a variety of pharmaceutical, nutraceutical and cosmetic applications.¹ Flavonoids are low-molecular-weight polyphenolic compounds with a 15-carbon backbone structure consisting of two benzene rings connected by a 3-carbon bridge that forms a heterocycle. The presence of different substitutes creates different subclasses, including flavones, flavonols, anthocyanins, proanthocyanidins, flavanonols, isoflavones, and chalcones (Figure 2.1).²⁻⁴

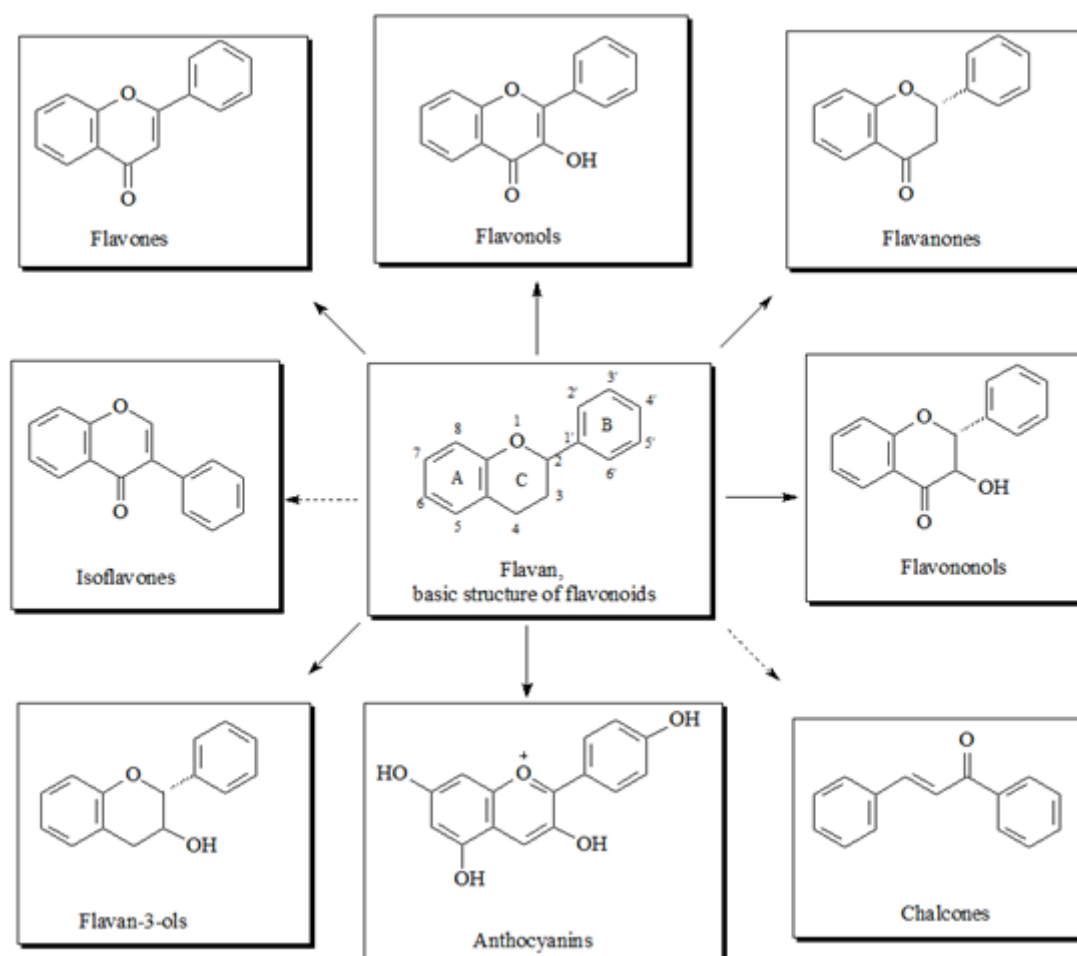


Figure 2.1 - Structure of the main flavonoid subgroups.⁵ Copyright 2020 Authors licensed under a Creative Commons Attribution (CC BY) license.

2.1.2. Quercetin

Isolated and identified in 1936 by Szent-Gyorgyi, quercetin is one of the most well-known flavonoid present in the human diet, in a variety of fruits and vegetables, such as capers, lovage, dill, cilantro, onions, apples, and berries.^{6,7} Quercetin's unique and interrelated biological properties make it an appealing pharmacological candidate for treating a variety of conditions and diseases, such as inflammatory diseases and cancer.⁸ These properties include anti-carcinogenic, anti-inflammatory, antibacterial, antiviral, and antioxidant effect, as well as the ability to stimulate mitochondrial biogenesis and inhibit lipid peroxidation, platelet aggregation and capillary permeability.⁹⁻¹⁷ Studies have shown that quercetin can inhibit the proliferation of many different types of cancer cells, namely prostate, liver, pancreatic and lung cancer cells. These anticancer properties are exerted through mechanisms that involve cellular signalling and the capacity to inhibit enzymes that are responsible for the activation of carcinogens.^{7,18} Studies have also shown that a synergistic effect is seen when quercetin is administered in combination with chemotherapeutic agents, thus improving the outcome of the traditional chemotherapeutic treatments.¹⁸ In addition, recent studies have also reported a potential role of quercetin in the prevention of cardiovascular diseases, in fact, studies showed that a regular intake of quercetin can decrease the risk of coronary artery disease.¹⁹

Other authors have verified that quercetin can assist in the protection against neurodegenerative diseases by lowering the oxidative stress, inflammation, and neuronal damage.²⁰ Furthermore, its capacity to cross the blood-brain barrier has made it an interesting compound for neurological research.²¹ Additionally, several works have revealed that quercetin can help in improving several metabolic health parameters, such as blood sugar levels or insulin sensitivity.²² Furthermore, due to its anti-inflammatory properties, some authors have investigated quercetin's potential for managing some inflammatory conditions, such as arthritis, allergies, and inflammatory bowel disease.²³

2.1.2.1. Chemical Structure

Quercetin (2-(3,4-dihydroxyphenyl)-3,5,7-trihydroxy-4H-chromen-4-one) is an aglycone, belonging to the class of flavonols, one of the subclasses of the flavonoids.¹ It contains five hydroxyl groups at 3,5,7,3' and 4' of the basic skeleton of flavonol (Figure 2.2). Quercetin exhibits a bright citron yellow colour in the form of slender needle-like crystals that are not soluble in cold water, have limited solubility in hot water (with an aqueous solubility that varies between 0.409 ppm at 25 °C and 16.139 ppm at 100 °C), but readily dissolve in alcohol and lipids.^{24,25} The glycosylation of some of the hydroxyl groups from the quercetin skeleton form various quercetin glycosides and constitute the major

quercetin derivatives.²⁶ The formation of quercetin glycoside can alter the solubility of the compound, as well as its absorption and *in vitro* properties.²⁴ Other quercetin derivatives can contain disaccharides, such as rutinose, or methyl groups, such as the case of dimethylated quercetin, named rhamnazin, that contains two methyl groups at the 3'- and 7-OH groups of quercetin.²⁶ These quercetin derivatives display various biological properties and different structures, that can present more favourable solubility and absorption profiles, thus modifications of this compound, such as glycosylation, methylation, acetylation, esterification, have also been extensively studied.²⁶

Furthermore, when exposed to light, especially in the wavelength range between 280 and 370 nm, quercetin molecules can undergo chemical reactions that result in their degradation.²⁷ However, the specific mechanisms associated with this process can depend on various factors, such as the wavelength of the irradiation light and its intensity or duration of exposure.²⁸ Therefore, the influence of structural modifications to the quercetin molecule on its stability and susceptibility to photodegradation has also been studied.²⁹ Particularly, it has been verified that some derivatives can be more stable and less prone to photodegradation when compared to quercetin, while others may present an increased sensitivity to light.³⁰

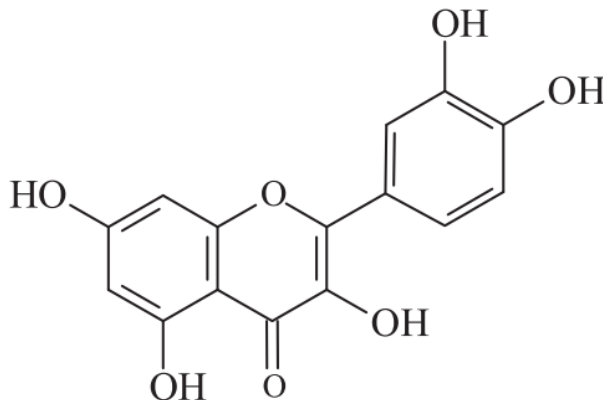


Figure 2.2 - Molecular structure of quercetin.

2.1.2.2. Absorption, Bioavailability, and Excretion

Quercetin glucoside, the naturally occurring form, has very poor oral bioavailability, which is attributed to its low absorption (as evidenced by an estimated absorption of only 3% to 17% in healthy individuals after an oral dose of 100 mg), extensive metabolism and rapid elimination.^{7,24,31} Quercetin is a hydrophobic compound that presents low water solubility (0.17–7 µg/mL), as well as low solubility in gastric fluids (5.5 µg/mL) and small intestine fluids (28.9 µg/mL) which greatly limits its bioaccessibility and bioavailability

since it has a tendency to precipitate in these fluids.^{32,33} Quercetin's absorption is affected by differences in its glycosylation, the type of food and the dietary compounds administered together, namely fibres and fat.³³ In fact, the solubility and transformation of quercetin greatly depends on the number and position of hydroxyl groups, as well as the number and type of sugar molecules attached to the quercetin molecule. Particularly, the hydroxyl groups play a pivotal role in determining its reactivity, biological activity, and solubility in different solvents, such as water and organic solvents.³⁴ Moreover, the number and type of sugar molecules attached to quercetin can affect its solubility, stability, and bioavailability. Specifically, glycosylation can improve the water solubility of that compound and modify its physicochemical properties, making it more adequate for certain applications, such as pharmaceutical formulations.³⁵

Nevertheless, if the quercetin derivate molecule presents a low water solubility, it may be too polar to cross the lipidic bilayer in the epithelium cell walls.³³

Contributing to its low bioavailability is also its rapid metabolization and elimination. In fact, quercetin and its metabolites have a propensity to be effluxed back into the intestinal lumen after enterocyte uptake.^{32,36} Quercetin glucosides interact with sodium dependent glucose transport receptors that are in the mucosal epithelium, being thus absorbed by the small intestine.²⁴ Following absorption, quercetin is metabolized in the small intestine and liver by enteric bacteria and enzymes in intestinal mucosal epithelial cells, forming metabolites such as methylated, sulfo-substituted and glucuronidated forms, that are then absorbed, transformed, or excreted later by kidney in urine.^{24,37}

2.1.3. Mechanisms of Action

Quercetin exhibits a wide range of mechanisms of action, ranging from anti-inflammatory to neuroprotective effects. In this section some of these mechanisms will be addressed.

2.1.3.1. Inflammation and Immune Function

Quercetin exhibits anti-inflammatory properties, which encompass mast cell stabilization and gastrointestinal cytoprotective activity. Moreover, this compound demonstrates a modulating, biphasic, and regulatory effect on inflammation and immunity. Additionally, it has been observed that this compound exerts an immunosuppressive effect on the function of dendritic cells, which are important antigen-presenting cells involved in immune responses.²⁴

Studies have demonstrated that quercetin inhibits lipopolysaccharide (LPS)-induced tumor necrosis factor α (TNF- α) production in macrophages.^{24,46} This prevents TNF- α

from directly activating extracellular signal-related kinase (ERK), c-Jun NH₂-terminal kinase (JNK), c-Jun, and nuclear factor- κ B (NF- κ B), that in turn are responsible for inducing inflammatory gene expression and protein secretion.^{46,47} Quercetin has been also shown to increase the activity of the peroxisome proliferator-activated receptor γ (PPAR γ) thus antagonizing NF- κ B or activator protein-1 (AP-1) transcriptional activation of inflammatory genes. All of these mechanisms can block the TNF- α -mediated induction of inflammatory cascades.⁴⁸

2.1.3.2. Antioxidant Capacity

Reactive oxygen species (ROS) generation has been reported to contribute to many diseases including diabetes, atherosclerosis, hypertension, ischemic heart disease and heart failure. Quercetin is widely known for its antioxidant capacity, that can be due to its ability to prevent oxidative stress, the major cause for generation of ROS, or by scavenging free radicals and bind transition metal ions.⁴⁹

One of the mechanisms of quercetin's antioxidant capacity, is its ability to regulate the levels of glutathione (GSH).^{50,51} When oxidative stress occurs and free oxygen radicals are produced, superoxide dismutase (SOD) captures the superoxide radical, O²⁻, and transforms it into H₂O₂.⁵¹ SOD further catalyses the decomposition of H₂O₂ to the non-toxic H₂O, but only in the presence of GSH, that acts as a proton donor. Studies have shown that quercetin has the ability to induce GSH synthesis.⁵²

Quercetin has been shown to have a stronger inhibitory effect against key enzymes acetylcholinesterase (AChE) and butyrylcholinesterase (BChE), which are correlated with oxidative properties, since the -OH groups on the side phenyl ring of quercetin are bound to important amino acid residues at the active site of these enzymes.⁵¹ Quercetin has also been shown to significantly enhance the expression levels of endogenous antioxidant enzymes such as Cu/Zn SOD, Mn SOD, catalase (CAT), and GSH peroxidase, as well as inhibit xanthine oxidase activity, which has been implicated as an important route in the oxidative injury to the tissues especially after ischemia-reperfusion.⁵⁰

Quercetin affects a number of signal transduction pathways, by activating, inhibiting, upregulating, or downregulating many molecules of the body, thus quercetin can improve the antioxidant state of the body and repair injury such as spinal cord injury, atherosclerosis, and lead or cadmium toxicity.⁵¹ For instances, quercetin's protective mechanism against acute spinal cord injury is due to its inhibitory effect on the

p38MAPK/iNOS signaling pathway, the downregulation of MDA levels, and the consequent upregulation of SOD activity.⁵³

2.1.3.3. Anticancer Capacity

Quercetin has been shown to down regulate expression of mutant p53 protein in human breast cancer cell lines, which was found to arrest the cells in the G2-M phase of the cell cycle.⁵⁴

Quercetin was found to inhibit tyrosine kinases, which are a family of proteins located in the cell membrane that are involved in the transduction of growth factor signals to the nucleus. The expression of these enzymes may be involved in oncogenesis due to its ability to override normal regulatory growth control. Studies showed that in patients with advanced cancers, intravenous administration of quercetin at dosages of 60-1700 mg/m² led to inhibition of lymphocyte tyrosine kinase at one hour in nine of eleven cases.^{50,55}

Quercetin has been shown to inhibit the production of heat shock proteins in several malignant cell lines, which are proteins known to form a complex with mutant p53, which allow tumour cells to bypass normal mechanisms of cell cycle arrest.⁵⁰ In addition it has also been found that quercetin has the capacity to inhibit the expression of rat sarcoma (*ras*) proteins. For instance, in a study quercetin inhibit the expression of the p21-*ras* oncogene in cultured colon cancer cell lines, which impair cellular GTP-ase, thus allowing the continual activation of the signal for DNA replication.⁵⁶

Quercetin has also been shown to induce ER II expression in both type I estrogen receptor positive (ER+) and type I estrogen receptor negative (ER-) human breast cancer cells, which results in a greater growth inhibition of ER- cells with quercetin treatment.⁵⁰

2.1.3.4. Neuroprotective Effects

Quercetin has also gained significant attention due to its potential neuroprotective properties. Numerous studies have demonstrated the ability of this compound to protect against neurodegenerative disorders and promote neuronal health through various mechanisms. For example, it was demonstrated that due to its potent antioxidant activity, quercetin acts as a scavenger of ROS, inhibiting lipid peroxidation and, thereby, reducing oxidative stress in the brain.^{57,58} Furthermore, quercetin has also demonstrated potential for protecting mitochondria against oxidative damage, maintain mitochondrial membrane potential, and improve energy production. Consequently, by preserving mitochondrial function, this compound helps to maintain cellular energy metabolism and, therefore, prevent neuronal dysfunction.^{59,60}

Moreover, other authors have verified that quercetin influences various neurotransmitter systems in the brain, including the dopaminergic, serotonergic, and glutamatergic systems, which are involved in mood regulation, cognition, and neuroprotection.^{61,62} Furthermore, additional studies have shown that quercetin promotes neurogenesis, i.e. the process of generating new neurons, in the hippocampus, a brain region critical for learning and memory.^{63,64} Moreover, it has also been demonstrated that this compound also enhances synaptic plasticity, facilitating the formation and strengthening of neuronal connections.⁶⁵

2.1.4. Nanomedicine

According to the European Science Foundation nanomedicine comprises nanometer size scale complex systems, consisting of at least two components, one of which being the active ingredient.⁶⁶ The loading of the active ingredient into these nanocarriers, can increase drug function, including efficacy, stability, tolerability and therapeutic index.⁶⁷ These nanocarriers can be used in combination therapy, by combining more than one therapeutic agent in the same delivery vehicle, or as theranostic agents, by combining imaging and therapeutic agents in the same delivery vehicle, thus enabling diagnosis and therapy together, with monitoring of the therapeutic response.⁶⁶

Flavonoids and other biologically active constituents of natural compounds generally display poor absorption and short half-life, as well as poor water solubility, which results in loss of bioavailability and efficacy, and can limit their clinical applicability. To overcome that, several nanomedical approaches such as liposomes, polymeric nanoparticles, lipid nanoparticles, microemulsions and hydrogels have been proposed.⁶⁸ These vehicles counteract the poor bioavailability of these compounds and allow for a controlled and site-specific drug release, thus increasing the compound's bioavailability and safety.^{69,70}

On that matter, lipid nanoparticles, which are spherical vesicles primarily composed of lipids, have proven to be an efficient drug delivery system for flavonoids and other type of drugs, with extensive clinical application, low production cost, and large-scale production capacity.⁶⁸

As a result, various researchers have explored the use of nanoparticles as delivery systems for quercetin. These nanoparticles have shown to improve the solubility, stability, and controlled release of quercetin, leading to enhanced cellular uptake and targeted delivery to specific tissues or cells.^{71,72} By encapsulating quercetin within nanoparticles, its hydrophobic nature can be overcome, resulting in improved aqueous solubility and bioavailability.⁷³ Furthermore, the nanoparticles can protect quercetin from

degradation, oxidation, and rapid elimination, thereby extending its circulation time in the body.⁷⁴

In this context, several studies have demonstrated the successful encapsulation of quercetin within different types of nanoparticles such as liposomes, polymeric nanoparticles, and lipid nanoparticles.^{75,76} Regarding liposomes, which are lipid-based vesicles, it was demonstrated that these can encapsulate such compound within their aqueous core or lipid bilayers.⁷⁷ Furthermore, these nanoparticles offer excellent biocompatibility and can be modified to enhance stability, target specific tissues, and control the release of quercetin.⁷⁸ On the other hand, polymeric nanoparticles, including polymeric micelles, nanoparticles, and nanogels, have also been employed as carriers for quercetin. As a result, it was verified that these polymeric systems could be tailored to achieve desired drug release profiles and provide protection to quercetin during circulation.^{79,80}

Furthermore, lipid nanoparticles, such as SLNs and NLCs, have also gained attention as quercetin delivery systems. These lipid-based nanoparticles demonstrated the capacity to improve the bioavailability and offer multiple advantages, such as high drug-loading capacity, sustained release, and enhanced stability of quercetin.^{81,82}

As a result, several studies have demonstrated the successful encapsulation of quercetin within nanoparticles, which have shown improved pharmacokinetic profiles and therapeutic outcomes.^{83,84} These nanoparticles could efficiently deliver quercetin to target sites, such as tumour tissues, inflamed areas, or specific cells, thereby maximizing its therapeutic effects while minimizing undesirable side effects.⁸⁵ Particularly, the use of formulations as a topical delivery system for quercetin, and other classes of flavonoids, has been addressed by various authors and will be addressed in section 2.3. Furthermore, the use of nanoparticles allows for the possibility of combination therapies, where quercetin can be co-encapsulated with other drugs or therapeutic agents so as to achieve synergistic effects.⁸⁶

2.1.5. Clinical Trials Patents and Formulations in the Market

Currently, there are various quercetin-based products available that can be used towards different purposes. For example, quercetin is available in the form of supplements, frequently combined with other bioflavonoids or antioxidants, which are commonly used for their anti-inflammatory, antihistaminic, and antioxidant effects. In this context, there are various options, such as a combination of quercetin with bromelain, which enhances the absorption of that compound in the body and is used to support for healthy immune

and inflammatory responses.⁸⁷ Examples of these supplements include Now Foods[®] Quercetin with Bromelain, Thorne[®] Quercenase, Doctor's Best[®] Quercetin Bromelain or Swanson[®] Ultra Quercetin & Bromelain. Other options, such as Life Extension[®] Optimized Quercetin, involve the combination of quercetin with vitamin C in camu camu extract, which is a natural source of vitamin C, being used for supporting the cardiovascular and immune health. Moreover, there are also supplements that are only composed of quercetin in its pure form, such as Jarrow Formulas[®] Quercetin.^{87,88}

On the other hand, there are also some quercetin-based products used for allergies, which are available in the form of capsules, tablets, nasal sprays or eye drops. Some examples, include Aller-7[®] that is a proprietary blend of natural extracts, Quercetin Plus[®], which combines quercetin with other natural ingredients, Aller-Leaf[®], i.e. a quercetin-based supplement, or Quercetin Complex-Solgar[®], which is a formulation that contains quercetin along with other bioflavonoids and nutrients.⁸⁹

Moreover, multiple quercetin-based products that can be used to improve cardiovascular health are also available in the current market. One example is Optimized Quercetin by Life Extension[®], which is composed of quercetin combined with other ingredients like resveratrol, for a comprehensive cardiovascular support.⁹⁰ Other formulations, involve coenzyme Q10 (CoQ10), which is an antioxidant that supports heart health, omega-3 fish oil, or pomegranate extract in combination with quercetin so as to support the hearth's health. Examples products that can be used for this purpose are Quercetin by Jarrow Formulas[®] or Activated Quercetin by Source Naturals[®].^{91,92}

Furthermore, there are also various quercetin-based products available for improving prostate health. These can involve, for example, saw palmetto, which is a popular herb used for prostate health, combined with quercetin, or be composed by a combination of quercetin with herbs, vitamins, minerals, and antioxidants. Examples of these products include Prostate Support by NOW Foods[®] or Prosta-Strong by Irwin Naturals[®].⁹³

Finally, there are various quercetin-based products that can be used for improving not only the performance during exercise, but also the recovery. These include pre-workout supplements, where quercetin is used as due to its antioxidant and anti-inflammatory properties, or recovery formulas, where quercetin is frequently combined with often combine quercetin with other nutrients like branched-chain amino acids, glutamine, and vitamins in order to help in muscle recovery and reduce inflammation. Examples of brands that provide these types of products include BulkSupplements[®], NOW Foods[®], and Thorne Research[®].⁹⁴

Besides these commercial products, numerous clinical trials are underway to validate the potential of quercetin to be used as a therapeutic agent. However, despite the completion of numerous studies, only a limited number have disclosed their findings, possibly owing to inconclusive outcomes.⁹⁵

These clinical trials primarily delve into the examination of quercetin's anticancer, antioxidant, anti-inflammatory, cardiovascular protective, and anti-infectious attributes, including its potential efficacy against SARS-CoV-2.⁹⁶

Due to its anticarcinogenic activity quercetin has been undergoing clinical trials to evaluate its potential as a therapeutic agent in colon, pancreas, and prostate cancer.⁹⁷ For example, Tezerji et al. performed a trial where the effect of the combination of quercetin and resveratrol in rats with stage IV colorectal cancer was evaluated. The study aimed at assessing the effects of these compounds on tumour markers, quality of life, and overall survival of the animals. As a result, it was concluded that this therapeutic approach is promising for treating such type of cancer, having led to histopathological changes, apoptosis induction and reduced cell proliferation in colon cancer.⁹⁸

In the context of cardiovascular protective potential of quercetin, Zahedi *et al.* evaluated the effects of quercetin intake on cardiovascular risk factors and inflammatory biomarkers in women possessing type 2 diabetes. By considering biomarkers such as such as blood pressure, cholesterol levels, inflammation, the authors verified that this compound considerably reduced the systolic blood pressure, whilst presenting no effects on other cardiovascular risk factors and inflammatory biomarkers.⁹⁹ Additionally, various trials on the effects of quercetin on cardiovascular health have been performed throughout the years. These have suggested that such compound has a positive effect on the cardiovascular system, namely in terms of blood pressure, protective effect against cardiovascular disease, and cardiovascular health.^{100–102}

Different clinical trials are exploring the anti-inflammatory and antioxidant properties of quercetin, for instance, in the treatment of sarcoidosis and idiopathic pulmonary fibrosis. Studies indicate a key role for oxidative stress in sarcoidosis ethology, thus an antioxidant therapy to strengthen the reduced antioxidant defence is believed to be efficacious in sarcoidosis treatment.¹⁰³ In another clinical trial, the effect of quercetin supplementation was evaluated in type 2 diabetes, namely on oxidative stress, glycemic control, lipid profile and insulin resistance. The study concluded that oral quercetin supplementation was beneficial in improving the antioxidant status of patients with type 2 diabetes despite showing no significant effect on glycemic control and lipid profile.¹⁰⁴

So far, one clinical trial is evaluating the anticancer effects of quercetin either free or encapsulated by PLGA-PEG NPs in tongue squamous cell carcinoma (TSCC) cell line.¹⁰⁵ Nevertheless, several studies have provided compelling evidence of the benefits of encapsulating quercetin in delivery vehicles, namely in terms of increased drug half-life and solubility, improved drug accumulation on the target site, and reduction of side effects.⁹⁵

In recent years, there has been a notable increase in the number of patents being filed for flavonoid-based formulations.¹⁰⁶

For example, patent IN202141046188 was filed for a novel dosage form of quercetin with the goal of enhancing tumour localization and cancer specific therapy. This formulation consists of a quercetin nanosuspension that was developed using polymers such as soya lecithin with TPGS as co-stabilizer by high pressure homogenization method. The goal of this novel formulation is to improve the dissolution and oral bioavailability of quercetin in the treatment of certain cancers and other disorders with subsequent reduction in drug dose. This quercetin nanosuspension displayed increased cytotoxicity in MCF-7 cells as compared with unformulated quercetin.¹⁰⁷

Moreover, several patents were filed for different methods of increasing quercetin bioavailability. For instance, Quercetin Phytosome[®] (patent application no. 171816341), a new delivery system based on food grade lecithin was found to increase oral absorption of quercetin. When administered orally to human volunteers, it resulted in exceptionally high plasma levels of quercetin—up to 20 times higher than the levels typically achieved with a regular quercetin dose, without causing any noticeable side effects. These findings indicate that Quercetin Phytosome[®] enables the safe and efficient oral delivery of quercetin, making it a valuable option for effectively utilizing this natural compound in the treatment of diverse human diseases.¹⁰⁸

Different compositions of quercetin were developed from the treatment of skin wounds.

In addition, taking advantage of quercetin's antiviral action patent no. WO2021259441A1 provides a composition containing quercetin and tamarixin, claiming that both have the ability to bind with ACE2, thereby impeding the binding of SARS-CoV-2 to the receptor. Additionally, they hinder the conversion of ACE1 to ACE2, leading to various advantageous effects such as vasodilatation, vascular protection, antifibrosis, antiproliferation, anti-inflammation, and increased release of nitric oxide.¹⁰⁹

In this context, patent no. WO2020153855A1 reports a composition composed of quercetin, all- trans retinoic acid, and L-ascorbic acid for the treatment of skin wounds.¹¹⁰

Overall, the clinical trials, quercetin-based products and patents demonstrate quercetin's potential to be used as a therapeutic agent in the treatment of many diseases, including cancer and anti-inflammatory conditions, as well as skin disorders.

2.2. References

1. Panche, A. N., Diwan, A. D., and Chandra, S. R., Flavonoids: an overview. *Journal of Nutritional Science* **5**, e47 (2016).
2. Leonarduzzi, G., Testa, G., Sottero, B., Gamba, P., and Poli, G., Design and Development of Nanovehicle-Based Delivery Systems for Preventive or Therapeutic Supplementation with Flavonoids. *Current Medicinal Chemistry* **17**, 74-95 (2010).
3. Verri, W. A., Vicentini, F., Baracat, M., Georgetti, S., Cardoso, R., Cunha, T., Ferreira, S., Cunha, F., Fonseca, M., and Casagrande, R., Flavonoids as anti-inflammatory and analgesic drugs: Mechanisms of action and perspectives in the development of pharmaceutical forms. In: *Studies in Natural Products Chemistry vol. 36*, 297-330 (Elsevier B.V., 2012).
4. Nagula, R. L., and Wairkar, S., Recent advances in topical delivery of flavonoids: A review. *Journal of Controlled Release* **296**, 190–201 (2019).
5. Tzanova, M., Atanasov, V., Yaneva, Z., Ivanova, D., and Dinev, T., Selectivity of Current Extraction Techniques for Flavonoids from Plant Materials. *Processes* **8**, 1222 (2020).
6. Formica, J. V., and Regelsont, W., Review of the biology of quercetin and related bioflavonoids. *Food and chemical toxicology* **33**, 1061-1080 (1995).
7. Wang, W., Sun, C., Mao, L., Ma, P., Liu, F., Yang, J., & Gao, Y., The biological activities, chemical stability, metabolism and delivery systems of quercetin: A review. *Trends in Food Science & Technology* **56**, 21–38 (2016).
8. Davis, J. M., Murphy, E. A., and Carmichael, M. D., Effects of the dietary flavonoid quercetin upon performance and health. *Current Sports Medicine Reports* **8**, 206–213 (2009).
9. Chen, S., Jiang, H., Wu, X., and Fang, J., Therapeutic Effects of Quercetin on Inflammation, Obesity, and Type 2 Diabetes. *Mediators of Inflammation* **2016**, 9340637 (2016).

10. Gaby, A. R., Quercetin derivative inhibits platelet aggregation. *Townsend Letter: The Examiner of Alternative Medicine* **285**, 64–66 (2007).
11. Prince, P. S. M., and Sathya, B., Pretreatment with quercetin ameliorates lipids, lipoproteins and marker enzymes of lipid metabolism in isoproterenol treated cardiotoxic male Wistar rats. *European Journal of Pharmacology* **635**, 142–148 (2010).
12. Schor, J., The Influence of Quercetin on Exercise Performance and Muscle Mitochondria. *Natural Medicine Journal* **2**, 3-6 (2010).
13. Batiha, G. E. S., Beshbishy, A. M., Ikram, M., Mulla, Z. S., El-Hack, M. E. A., Taha, A. E., Algammal, A. M., and Elewa, Y. H. A., The Pharmacological Activity, Biochemical Properties, and Pharmacokinetics of the Major Natural Polyphenolic Flavonoid: Quercetin. *Foods* **9**, 374 (2020).
14. Ferreira, C. G. T., Campos, M. G., Felix, D. M., Santos, M. R., de Carvalho, O. V., Diaz, M. A. N., Fietto, J. L. R., Bressan, G. C., Silva-Júnior, A., and Almeida, M. R., Evaluation of the antiviral activities of *Bacharis dracunculifolia* and quercetin on Equid herpesvirus 1 in a murine model. *Research in Veterinary Science* **120**, 70–77 (2018).
15. Catauro, M., D'Angelo, A., Fiorentino, M., Pacifico, S., Latini, A., Brutti, S., and Cipriotti, S. V., Thermal, spectroscopic characterization and evaluation of antibacterial and cytotoxicity properties of quercetin-PEG-silica hybrid materials. *Ceramics International* **49**, 14855-14863 (2022).
16. Chiang, M. C., Tsai, T. Y., and Wang, C. J., The Potential Benefits of Quercetin for Brain Health: A Review of Anti-Inflammatory and Neuroprotective Mechanisms. *International Journal of Molecular Sciences* **24**, 6328 (2023).
17. Gulay, S., Cumaoglu, A., and Yerer, M. B., Quercetin's Effects on Cell Survival of Resistant GBM Cell Line (T98G) after Repetitive Treatment Combined with Temozolomide. *Proceedings of The 3rd International conference on Natural Products for Cancer Prevention and Therapy* **40**, 28 (2019).
18. Rauf, A., Imran, M., Khan, I. A., ur-Rehman, M., Gilani, S. A., Mehmood, Z., and Mubarak, M. S., Anticancer potential of quercetin: A comprehensive review. *Phytotherapy Research* **32**, 2109–2130 (2018).
19. Hooper, L., Kroon, P. A., Rimm, E. B., Cohn, J. S., Harvey, I., Le Cornu, K. A., Ryder, J. J., Hall, W. L., and Cassidy, A., Flavonoids, flavonoid-rich foods, and cardiovascular

risk: a meta-analysis of randomized controlled trials. *The American Journal of Clinical Nutrition* **88**, 38-50 (2008).

20. Khan, H., Ullah, H., Aschner, M., Cheang, W. S., and Akkol, E. K., Neuroprotective Effects of Quercetin in Alzheimer's Disease. *Biomolecules* **10**, 59 (2019).

21. Chaturvedi, S., Malik, M. Y., Rashid, M., Singh, S., Tiwari, V., Gupta, P., Shukla, S., Singh, S., and Wahajuddin, M., Mechanistic exploration of quercetin against metronidazole induced neurotoxicity in rats: Possible role of nitric oxide isoforms and inflammatory cytokines. *Neurotoxicology* **79**, 1–10 (2020).

22. Shen, H., Wang, J., Ao, J., Hou, Y., Xi, M., Cai, Y., Li, M., and Luo, A., Structure-activity relationships and the underlying mechanism of α -amylase inhibition by hyperoside and quercetin: Multi-spectroscopy and molecular docking analyses. *Spectrochimica Acta Part A: Molecular and Biomolecular Spectroscopy* **285**, 121797 (2023).

23. El-Said, K. S., Atta, A., Mobasher, M. A., Germoush, M. O., Mohamed, T. M., and Salem, M. M., Quercetin mitigates rheumatoid arthritis by inhibiting adenosine deaminase in rats. *Molecular Medicine* **28**, 1–13 (2022).

24. Li, Y., Yao, J., Han, C., Yang, J., Chaudhry, M. T., Wang, S., Liu, H., and Yin, Y., Quercetin, inflammation and immunity. *Nutrients* **8**, 167 (2016).

25. Lončarić, A., Lamas, J. C., Guerra E., M., and Lores, M., Increasing water solubility of Quercetin by increasing the temperature. Poster in: *15th Instrumental Analysis Conference/Expoquimia* **35**, 89 (2017).

26. Magar, R. T., and Sohng, J. K., A Review on Structure, Modifications and Structure-Activity Relation of Quercetin and Its Derivatives. *Journal of Microbiology and Biotechnology* **30**, 11–20 (2020).

27. Zvezdanović, J. B., Stanojević, J. S., Marković, D. Z., and Cvetković, D. J., Irreversible UV-induced quercetin and rutin degradation in solution studied by UV spectrophotometry and HPLC chromatography. *Journal of the Serbian Chemical Society* **77**, 297–312 (2012).

28. Sadda, S. R., Schachat, A. P., Wilkinson, C. P., Hinton, D. R., Wiedemann, P., Freund, K. B., and Sarraf, D., *Ryan's Retina*. Elsevier Health Sciences (2022).

29. Wang, W., Sun, C., Mao, L., Ma, P., Liu, F., Yang, J., and Gao, Y., The biological activities, chemical stability, metabolism and delivery systems of quercetin: A review. *Trends in Food Science & Technology* **56**, 21–38 (2016).
30. Dall'Acqua, S., Miolo, G., Innocenti, G., and Caffieri, S., The Photodegradation of Quercetin: Relation to Oxidation. *Molecules* **17**, 8898 (2012).
31. Zhou, Y., Suo, W., Zhang, X., Lv, J., Liu, Z., and Liu, R., Roles and mechanisms of quercetin on cardiac arrhythmia: A review. *Biomedicine & Pharmacotherapy* **153**, 113447 (2022).
32. Kasikci, M. B., and Bagdatlioglu, N., Bioavailability of quercetin. *Current Research in Nutrition and Food Science* **4**, 146–151 (2016).
33. Kandemir, K., Tomas, M., Mcclements, D. J., and Capanoglu, E., Recent advances on the improvement of quercetin bioavailability. *Trends in Food Science & Technology* **119**, 192–200 (2022).
34. Ferenczyova, K., Kalocayova, B., and Bartekova, M., Potential Implications of Quercetin and its Derivatives in Cardioprotection. *International Journal of Molecular Sciences* **21**, 1585 (2020).
35. Liao, H., Bao, X., Zhu, J., Qu, J., Sun, Y., Ma, X., Wang, E., Guo, X., Kang, Q., and Zhen, Y., O-Alkylated derivatives of quercetin induce apoptosis of MCF-7 cells via a caspase-independent mitochondrial pathway. *Chemico-Biological Interactions* **242**, 91–98 (2015).
36. Crespy, V., Morand, C., Manach, C., Besson, C., Demigne, C., and Remesy, C., Part of quercetin absorbed in the small intestine is conjugated and further secreted in the intestinal lumen. *American Journal of Physiology-Gastrointestinal and Liver Physiology* **277**, G120-G126 (1999).
37. Day, A. J., Bao, Y., Morgan, M. R. A., and Williamson, G., Conjugation position of quercetin glucuronides and effect on biological activity. *Free Radical Biology and Medicine* **29**, 1234–1243 (2000).
38. Sindhu, R. K., Chitkara, M., and Sandhu, I. S., *Nanotechnology: principles and applications*. CRC Press (2021).
39. Das, S., and Chaudhury, A., Recent advances in lipid nanoparticle formulations with solid matrix for oral drug delivery. *AAPS PharmSciTech* **12**, 62–76 (2011).

40. Elmowafy, M., and Al-Sanea, M. M., Nanostructured lipid carriers (NLCs) as drug delivery platform: Advances in formulation and delivery strategies. *Saudi Pharmaceutical Journal* **29**, 999–1012 (2021).
41. Teixeira, M. C., Carbone, C., Sousa, M. C., Espina, M., Garcia, M. L., Sanchez-Lopez, E., and Souto, E. B., Nanomedicines for the Delivery of Antimicrobial Peptides (AMPs). *Nanomaterials* **10**, 560 (2020).
42. Giannouli, M., Karagkiozaki, V., Pappa, F., Moutsios, I., Gravalidis, C., and Logothetidis, S., Fabrication of quercetin-loaded PLGA nanoparticles via electrohydrodynamic atomization for cardiovascular disease. *Materials Today: Proceedings* **5**, 15998–16005 (2018).
43. Valencia, M. S., da Silva Júnior, M. F., Júnior, F. H. X., de Oliveira Veras, B., de Oliveira Borba, E. F., da Silva, T. G., Xavier, V. L., de Souza, M. P., and Carneiro-da-Cunha, M. G., Bioactivity and cytotoxicity of quercetin-loaded, lecithin-chitosan nanoparticles. *Biocatalysis and Agricultural Biotechnology* **31**, 101879 (2021).
44. Caló, E., and Khutoryanskiy, V. V., Biomedical applications of hydrogels: A review of patents and commercial products. *European Polymer Journal* **65**, 252–267 (2015).
45. Mirpoor, S. F., Hosseini, S. M. H., and Nekoei, A. R., Efficient delivery of quercetin after binding to beta-lactoglobulin followed by formation soft-condensed core-shell nanostructures. *Food Chemistry* **233**, 282–289 (2017).
46. K. Manjeet, R., and Ghosh, B., Quercetin inhibits LPS-induced nitric oxide and tumor necrosis factor- α production in murine macrophages. *International Journal of Immunopharmacology* **21**, 435–443 (1999).
47. Bureau, G., Longpré, F., and Martinoli, M. G., Resveratrol and quercetin, two natural polyphenols, reduce apoptotic neuronal cell death induced by neuroinflammation. *Journal of Neuroscience Research* **86**, 403–410 (2008).
48. Geraets, L., Moonen, H. J., Brauers, K., Wouters, E. F., Bast, A., and Hageman, G. J., Dietary flavones and flavonoles are inhibitors of poly(ADP-ribose)polymerase-1 in pulmonary epithelial cells. *The Journal of Nutrition* **137**, 2190–2195 (2007).
49. Kumar, R., Vijayalakshmi, S., and Nadasabapathi, S., Health benefits of quercetin. *Defence Life Science Journal* **2**, 142-151 (2017).

50. Baghel, S. S., Shrivastava, N., Baghel, R. S., Agrawal, P., and Rajput, S., A review of quercetin: antioxidant and anticancer properties. *World Journal of Pharmaceutical Sciences* **1**, 146-160 (2012).
51. Xu, D., Hu, M. J., Wang, Y. Q., and Cui, Y. L., Antioxidant Activities of Quercetin and Its Complexes for Medicinal Application. *Molecules* **24**, 1123 (2019).
52. Jia, H., Zhang, Y., Si, X., Jin, Y., Jiang, D., Dai, Z., and Wu, Z., Quercetin Alleviates Oxidative Damage by Activating Nuclear Factor Erythroid 2-Related Factor 2 Signaling in Porcine Enterocytes. *Nutrients* **13**, 1–15 (2021).
53. Song, Y., Liu, J., Zhang, F., Zhang, J., Shi, T., and Zeng, Z., Antioxidant effect of quercetin against acute spinal cord injury in rats and its correlation with the p38MAPK/iNOS signaling pathway. *Life Sciences* **92**, 1215–1221 (2013).
54. Liang, Y., Wu, J., Stancel, G. M., and Hyder, S. M., P53-dependent inhibition of progestin-induced VEGF expression in human breast cancer cells. *Journal of Steroid Biochemistry and Molecular Biology* **93**, 173–182 (2005).
55. Ferry, D. R., Smith, A., Malkhandi, J., Fyfe, D. W., deTakats, P. G., Anderson, D., Baker, J., and Kerr, D. J., Phase I clinical trial of the flavonoid quercetin: pharmacokinetics and evidence for in vivo tyrosine kinase inhibition. *Clinical Cancer Research* **2**, 659-668 (1996).
56. Ranelletti, F. O., Maggiano, N., Serra, F. G., Ricci, R., Larocca, L. M., Lanza, P., Scambia, G., Fattorossi, A., Capelli, A., and Piantelli, M., Quercetin inhibits p21-ras expression in human colon cancer cell lines and in primary colorectal tumors. *International Journal of Cancer* **85**, 438–445 (2000).
57. Costa, L. G., Garrick, J. M., Roquè, P. J., and Pellacani, C., Mechanisms of neuroprotection by quercetin: counteracting oxidative stress and more. *Oxidative Medicine and Cellular Longevity* **2016**, 2986796 (2016).
58. Le, K., Song, Z., Deng, J., Peng, X., Zhang, J., Wang, L., Zhou, L., Bi, H., Liao, Z., and Feng, Z., Quercetin alleviates neonatal hypoxic-ischemic brain injury by inhibiting microglia-derived oxidative stress and TLR4-mediated inflammation. *Inflammation Research* **69**, 1201-1213 (2020).
59. Chang, X., Li, Y., Liu, J., Wang, Y., Guan, X., Wu, Q., Zhou, Y., Zhang, X., Chen, Y., Huan, Y., and Liu, R., β -tubulin contributes to Tongyang Huoxue decoction-induced protection against hypoxia/reoxygenation-induced injury of sinoatrial node cells through

- SIRT1-mediated regulation of mitochondrial quality surveillance. *Phytomedicine* **108**, 154502 (2023).
60. de Oliveira, M. R., Nabavi, S. M., Braidy, N., Setzer, W. N., Ahmed, T., and Nabavi, S. F., Quercetin and the mitochondria: a mechanistic view. *Biotechnology Advances* **34**, 532-549 (2016).
61. Singh, S., Jamwal, S., and Kumar, P., Neuroprotective potential of Quercetin in combination with piperine against 1-methyl-4-phenyl-1,2,3,6-tetrahydropyridine-induced neurotoxicity. *Neural Regeneration Research* **12**, 1137 (2017).
62. Sharma, S., Raj, K., and Singh, S., Neuroprotective effect of quercetin in combination with piperine against rotenone-and iron supplement–induced Parkinson’s disease in experimental rats. *Neurotoxicity Research* **37**, 198-209 (2020).
63. Karimipour, M., Rahbarghazi, R., Tayefi, H., Shimia, M., Ghanadian, M., Mahmoudi, J., and Bagheri, H. S., Quercetin promotes learning and memory performance concomitantly with neural stem/progenitor cell proliferation and neurogenesis in the adult rat dentate gyrus. *International Journal of Developmental Neuroscience* **74**, 18-26 (2019).
64. Tchantchou, F., Lacor, P. N., Cao, Z., Lao, L., Hou, Y., Cui, C., Klein, W. L., and Luo, Y., Stimulation of neurogenesis and synaptogenesis by bilobalide and quercetin via common final pathway in hippocampal neurons. *Journal of Alzheimer's Disease* **18**, 787-798 (2009).
65. Hu, P., Wang, M., Chen, W. H., Liu, J., Chen, L., Yin, S. T., Yong, W., Chen, J. T., Wang, H. L., and Ruan, D. Y., Quercetin relieves chronic lead exposure-induced impairment of synaptic plasticity in rat dentate gyrus in vivo. *Naunyn-Schmiedeberg's Archives of Pharmacology* **378**, 43-51 (2008).
66. Rahman, M., Beg, S., Kumar, V., and Ahmad, F. J., *Nanomedicine for bioactives: Healthcare applications*. Springer Nature (2020).
67. Plapied, L., Duhem, N., des Rieux, A., and Pr eat, V., Fate of polymeric nanocarriers for oral drug delivery. *Current Opinion in Colloid & Interface Science* **16**, 228–237 (2011).
68. Ahmed, H. M., Nabavi, S., and Behzad, S. Herbal, Drugs and Natural Products in the light of Nanotechnology and Nanomedicine for Developing Drug Formulations. *Mini-Reviews in Medicinal Chemistry* **21**, 302–313 (2020).

69. Carullo, G., Cappello, A. R., Frattaruolo, L., Badolato, M., Armentano, B., and Aiello, F., Quercetin and derivatives: useful tools in inflammation and pain management. *Future medicinal chemistry* **9**, 79–93 (2016).
70. Menea, F., Menea, A., and Tréton, J., Polyphenols against Skin Aging. In: *Polyphenols in Human Health and Disease*, 819–830 (Academic Press, 2014).
71. Wang, G., Wang, J. J., Chen, X. L., Du, L., and Li, F., Quercetin-loaded freeze-dried nanomicelles: Improving absorption and anti-glioma efficiency in vitro and in vivo. *Journal of Controlled Release* **235**, 276-290 (2016).
72. Li, K., Zang, X., Meng, X., Li, Y., Xie, Y., and Chen, X., Targeted delivery of quercetin by biotinylated mixed micelles for non-small cell lung cancer treatment. *Drug Delivery* **29**, 970-985 (2022).
73. Pinheiro, R. G., Pinheiro, M., and Neves, A. R., Nanotechnology innovations to enhance the therapeutic efficacy of quercetin. *Nanomaterials* **11**, 2658 (2021).
74. Wang, W., Sun, C., Mao, L., Ma, P., Liu, F., Yang, J., and Gao, Y. The biological activities, chemical stability, metabolism and delivery systems of quercetin: A review. *Trends in Food Science & Technology* **56**, 21-38 (2016).
75. Souto, E. B., Severino, P., Basso, R., and Santana, M. H. A., Encapsulation of antioxidants in gastrointestinal-resistant nanoparticulate carriers. In: *Oxidative Stress and Nanotechnology: Methods and Protocols*, 37-46 (Humana Press, 2013).
76. Date, A. A., Joshi, M. D., and Patravale, V. B. Parasitic diseases: liposomes and polymeric nanoparticles versus lipid nanoparticles. *Advanced Drug Delivery Reviews* **59**, 505-521 (2007).
77. Alhodieb, F. S., Rahman, M. A., Barkat, M. A., Alanezi, A. A., Barkat, H. A., Hadi, H. A., Harwansh, R. K., and Mittal, V., Nanomedicine-driven therapeutic interventions of autophagy and stem cells in the management of Alzheimer's disease. *Nanomedicine* **18**, 145-168 (2023).
78. Wang, Y., Tao, B., Wan, Y., Sun, Y., Wang, L., Sun, J., and Li, C. Drug delivery based pharmacological enhancement and current insights of quercetin with therapeutic potential against oral diseases. *Biomedicine & Pharmacotherapy* **128**, 110372 (2020).
79. Gao, X., Wang, B., Wei, X., Men, K., Zheng, F., Zhou, Y., Zheng, Y., Gou, M., Huang, M., Guo, G., Huang, N., Qian, Z., and Wei, Y. Anticancer effect and mechanism of

polymer micelle-encapsulated quercetin on ovarian cancer. *Nanoscale* **4**, 7021-7030 (2012).

80. Nie, Z. Y., Zhang, M. Z., Zheng, D. H., Zhang, M. X., Jia, H. Q., Zhang, X. D., Yue, G. C., Xiao-Ming, L., Peng, Z., and Liang, K., Enhanced antitumoral activity of quercetin against lung cancer cells using biodegradable poly (lactic acid)-based polymeric nanoparticles. *Journal of Biomaterials and Tissue Engineering* **7**, 269-274 (2017).

81. Kumar, P., Sharma, G., Kumar, R., Singh, B., Malik, R., Katare, O. P., and Raza, K., Promises of a biocompatible nanocarrier in improved brain delivery of quercetin: Biochemical, pharmacokinetic and biodistribution evidences. *International Journal of Pharmaceutics* **515**, 307-314 (2016).

82. Huang, J., Wang, Q., Li, T., Xia, N., and Xia, Q., Nanostructured lipid carrier (NLC) as a strategy for encapsulation of quercetin and linseed oil: Preparation and *in vitro* characterization studies. *Journal of Food Engineering* **215**, 1-12 (2017).

83. Patel, G., Thakur, N. S., Kushwah, V., Patil, M. D., Nile, S. H., Jain, S., Kai, G., and Banerjee, U. C., Mycophenolate co-administration with quercetin via lipid-polymer hybrid nanoparticles for enhanced breast cancer management. *Nanomedicine: Nanotechnology, Biology and Medicine* **24**, 102147 (2020).

84. Patel, G., Thakur, N. S., Kushwah, V., Patil, M. D., Nile, S. H., Jain, S., Banerjee, U. C., and Kai, G., Liposomal delivery of mycophenolic acid with quercetin for improved breast cancer therapy in SD rats. *Frontiers in Bioengineering and Biotechnology* **8**, 631 (2020).

85. Thakur, N. S., Mandal, N., Patel, G., Kirar, S., Reddy, Y. N., Kushwah, V., Jain, S., Kalia, Y. N., Bhaumik, J., and Banerjee, U. C., Co-administration of zinc phthalocyanine and quercetin via hybrid nanoparticles for augmented photodynamic therapy. *Nanomedicine: Nanotechnology, Biology and Medicine* **33**, 102368 (2021).

86. Ganthala, P. D., Alavala, S., Chella, N., Andugulapati, S. B., Bathini, N. B., and Sistla, R., Co-encapsulated nanoparticles of Erlotinib and Quercetin for targeting lung cancer through nuclear EGFR and PI3K/AKT inhibition. *Colloids and Surfaces B: Biointerfaces* **211**, 112305 (2022).

87. Balch, P. A., and Bell, S. J., *Prescription for nutritional healing*. Penguin (2006).

88. Lyman, D., *Triple Life Threat*. Book Vine Press (2022).

89. Joe, S. A., *Rhinology and Allergy for the Facial Plastic Surgeon, An Issue of Facial Plastic Surgery Clinics*. Elsevier Health Sciences (2012).
90. Brown, G. J., *Happy and Healthy Living Towards 100 and Beyond by Gerald J. Brown, MD*. Lulu (2005).
91. Mechanick, J. I., and Brett, E. M., *Nutritional Strategies for the Diabetic/Prediabetic Patient*. CRC Press (2006).
92. Stanton, A., *The complete idiot's guide to hormone weight loss*. DK Publishing (2011).
93. Bokelmann, J. M., *Medicinal Herbs in Primary Care: An Evidence-Guided Reference for Healthcare Providers*. Elsevier (2021).
94. Contreras, B., and Cordoza, G., *Glute Lab: the Art and Science of Strength and Physique Training*. Victory Belt Publishing (2019).
95. Pinheiro, R. G. R., Pinheiro, M., and Neves, A. R., Nanotechnology innovations to enhance the therapeutic efficacy of quercetin. *Nanomaterials* **11**, 2658 (2021).
96. Saeedi-Boroujeni, A., and Mahmoudian-Sani, M. R., Anti-inflammatory potential of Quercetin in COVID-19 treatment. *Journal of Inflammation* **18**, 1–9 (2021).
97. Vafadar, A., Shabaninejad, Z., Movahedpour, A., Fallahi, F., Taghavipour, M., Ghasemi, Y., Akbari, M., Shafiee, A., Hajighadimi, S., Moradzarmehri, S., Razi, E., Savardashtaki, A., and Mirzaei, H., Quercetin and cancer: new insights into its therapeutic effects on ovarian cancer cells. *Cell & Bioscience* **10**, 1–17 (2020).
98. Tezerji, S., abdolazimi, H., Fallah, A., and Talaei, B., The effect of resveratrol and quercetin intervention on azoxymethane-induced colon cancer in Rats model. *Clinical Nutrition Open Science* **45**, 91–102 (2022).
99. Zahedi, M., Ghiasvand, R., Feizi, A., Asgari, G., and Darvish, L., Does Quercetin Improve Cardiovascular Risk factors and Inflammatory Biomarkers in Women with Type 2 Diabetes: A Double-blind Randomized Controlled Clinical Trial. *International Journal of Preventive Medicine* **4**, 777 (2013).
100. Huang, H., Liao, D., Dong, Y., and Pu, R., Effect of quercetin supplementation on plasma lipid profiles, blood pressure, and glucose levels: a systematic review and meta-analysis. *Nutrition Reviews* **78**, 615–626 (2020).

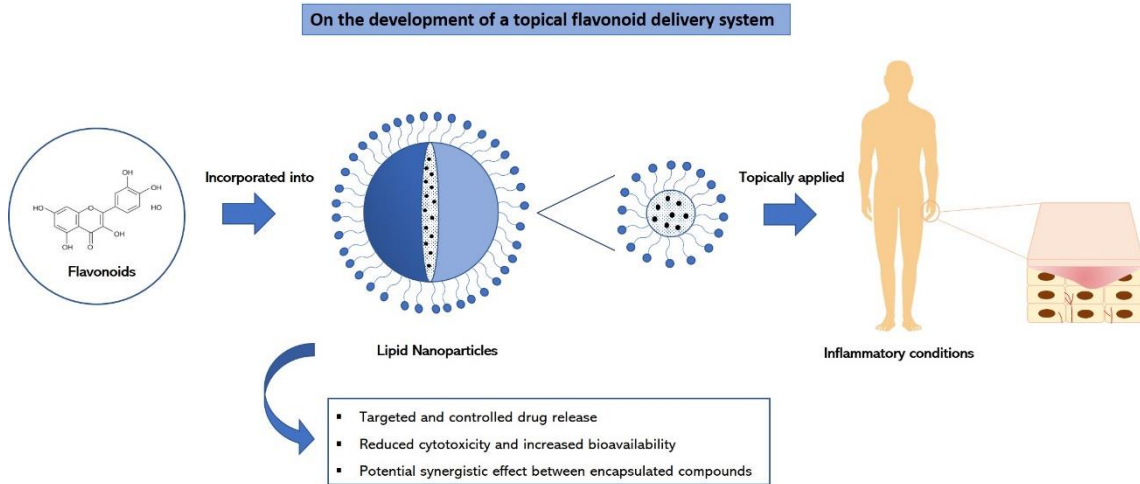
101. Serban, M. C., Sahebkar, A., Zanchetti, A., Mikhailidis, D. P., Howard, G., Antal, D., Andrica, F., Ahmed, A., Aronow, W. S., Muntner, P., Lip, G. Y. H., Graham, I., Wong, N., Rysz, J., Banach, M., and Lipid and Blood Pressure Meta-analysis Collaboration (LBPMC) Group, Effects of Quercetin on Blood Pressure: A Systematic Review and Meta-Analysis of Randomized Controlled Trials. *Journal of the American Heart Association* **5**, e002713 (2016).
102. Tabrizi, R., Tamtaji, O. R., Mirhosseini, N., Lankarani, K. B., Akbari, M., Heydari, S. T., Dadgostar, E., and Asemi, Z., The effects of quercetin supplementation on lipid profiles and inflammatory markers among patients with metabolic syndrome and related disorders: A systematic review and meta-analysis of randomized controlled trials. *Critical Reviews in Food Science and Nutrition* **60**, 1855–1868 (2020).
103. Boots, A. W., Veith, C., Albrecht, C., Bartholome, R., Drittij, M. J., Claessen, S. M., Bast, A., Rosenbruch, M., Jonkers, L., van Schooten, F.-J., and Schins, R. P., The dietary antioxidant quercetin reduces hallmarks of bleomycin-induced lung fibrogenesis in mice. *BMC Pulmonary Medicine* **20**, 1-16 (2020)
104. Mazloom, Z., Abdollahzadeh, S. M., Dabbaghmanesh, M.-H., and Rezaianzadeh, A., The Effect of Quercetin Supplementation on Oxidative Stress, Glycemic Control, Lipid Profile and Insulin Resistance in Type 2 Diabetes: A Randomized Clinical Trial. *Journal of Health Sciences and Surveillance System* **2**, 8-14 (2014).
105. Algadi, H. H. G. A., Therapeutic Efficacy of Quercetin Versus Its Encapsulated Nanoparticle on Tongue Squamous Cell Carcinoma Cell Line. ClinicalTrials.gov Identifier: NCT05456022 (2022).
106. Sharma, S., Sahni, J. K., Ali, J., and Baboota, S., Patent Perspective for Potential Antioxidant Compounds-Rutin and Quercetin. *Recent Patents on Nanomedicine* **3**, 62-68 (2013).
107. Sumathi, R., Tamizharasi, S., Punitha, S., and Sivakumar, T., Enhanced Anticancer Activity of Quercetin-Loaded TPGS Nanosuspension for Drug Impervious MCF-7 Human Breast Cancer Cells. IN202141046188 (2021).
108. Riva, A., Ronchi, M., Petrangolini, G., Bosisio, S., and Allegrini, P., Improved Oral Absorption of Quercetin from Quercetin Phytosome®, a New Delivery System Based on Food Grade Lecithin. *European Journal of Drug Metabolism and Pharmacokinetics* **44**, 169–177 (2019).

109. Khalil, I. T. T., and ABD El-Latif, S. A. E.-A. M., A new and safe pharmaceutical preparation for prophylaxis and treatment of respiratory viral infections, especially corona viruses. Patent Number WO2021259441A1 (2021).

110. Sachadyn, P., Sass, P., Kaminska, J., Sosnowski, P., Baczynski-Keller, J., and Slonimska, P., Composition for use in the treatment of skin wound. Patent Number WO2020153855A1 (2019).

2.3. On the Development of a Cutaneous Flavonoid Delivery System: Advances and Limitations

This sub-chapter comprises a literature review that describes currently available formulations that are used as a topical delivery system for different classes of flavonoids. The major advantages of the cutaneous delivery route are highlighted in addition to its limitations. The need for nanocarriers in the delivery of flavonoids to the skin is then discussed, in addition to an extensive review of the flavonoid cutaneous delivery systems that are currently under study for the treatment of skin pathologies.



Review

On the Development of a Cutaneous Flavonoid Delivery System: Advances and Limitations

Raquel Costa ^{1,2}, Sofia A. Costa Lima ¹, Paula Gameiro ² and Salette Reis ^{1,*}

- ¹ LAQV, REQUIMTE, Departamento de Ciências Químicas, Faculdade de Farmácia, Universidade do Porto, 4050-313 Porto, Portugal; up201811987@fc.up.pt (R.C.); slima@ff.up.pt (S.A.C.L.)
² LAQV, REQUIMTE, Departamento de Química e Bioquímica, Faculdade de Ciências, Universidade do Porto, 4169-007 Porto, Portugal; agsantos@fc.up.pt
 * Correspondence: shreis@ff.up.pt

Abstract: Flavonoids are one of the vital classes of natural polyphenolic compounds abundantly found in plants. Due to their wide range of therapeutic properties, which include antioxidant, anti-inflammatory, photoprotective, and depigmentation effects, flavonoids have been demonstrated to be promising agents in the treatment of several skin disorders. However, their lipophilic nature and poor water solubility invariably lead to limited oral bioavailability. In addition, they are rapidly degraded and metabolized in the human body, hindering their potential contribution to the prevention and treatment of many disorders. Thus, to overcome these challenges, several cutaneous delivery systems have been extensively studied. Topical drug delivery besides offering an alternative administration route also ensures a sustained release of the active compound at the desired site of action. Incorporation into lipid or polymer-based nanoparticles appears to be a highly effective approach for cutaneous delivery of flavonoids with good encapsulation potential and reduced toxicity. This review focuses on currently available formulations used to administer either topically or systemically different classes of flavonoids in the skin, highlighting their potential application as therapeutic and preventive agents.

Keywords: antioxidant; inflammation; skin research; topical delivery; transdermal delivery



Citation: Costa, R.; Costa Lima, S.A.; Gameiro, P.; Reis, S. On the Development of a Cutaneous Flavonoid Delivery System: Advances and Limitations. *Antioxidants* 2021, 10, 1376. <https://doi.org/10.3390/antiox10091376>

Academic Editor: Stanley Omaye

Received: 19 July 2021
 Accepted: 19 August 2021
 Published: 28 August 2021

Publisher's Note: MDPI stays neutral with regard to jurisdictional claims in published maps and institutional affiliations.



Copyright: © 2021 by the authors. Licensee MDPI, Basel, Switzerland. This article is an open access article distributed under the terms and conditions of the Creative Commons Attribution (CC BY) license (<https://creativecommons.org/licenses/by/4.0/>).

1. Introduction

For centuries, flavonoids have been used to treat various human diseases, and despite the fast-growing development of new and innovative synthetic drugs, continuous use of these natural compounds has prevailed to this day [1,2]. Flavonoids are one of the key classes of bioactive compounds abundantly found in plants and have a general structure of a 15-carbon backbone, consisting of two benzene rings connected by a 3-carbon bridge, which forms a heterocycle. They are low-molecular-weight polyphenolic compounds derived from plant metabolites, and the presence of different substitutes creates different subclasses (Figure 1) [3–5]. Due to their broad spectrum of biological activity and attractive pharmacological properties, which include antioxidant, anti-inflammatory, antiproliferative, photoprotective, and antiaging effects, flavonoids have been explored as a therapeutic option towards a great number of diseases, including several skin disorders [6,7]. However, their lipophilic nature, which results in a reduced capacity to be orally absorbed, and the fact that they undergo extensive first-pass metabolism and rapid elimination hamper their oral bioavailability [8–10]. Thus, alternative research focuses on the development of the cutaneous delivery of flavonoids, with high patient compliance and potential to surpass drawbacks associated with oral and parental routes of administration. Although skin acts as a physical barrier to drug absorption, the development of delivery systems, such as nanoparticles, hydrogels, and microneedles, allows for the delivery of both hydrophilic and lipophilic compounds as well as drugs with shorter half-time and limited therapeutic index. This results in a higher bioavailability at the target site under a

controlled release rate and avoids interactions with gastric and intestinal fluids as well as flavonoid degradation [11,12].

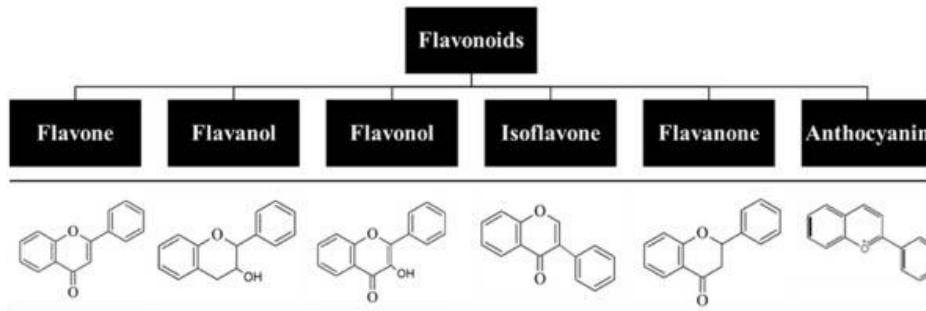


Figure 1. Classification of flavonoids based on their chemical structure.

This review focuses on the therapeutic potential of flavonoids, including their mechanisms of action and influence of several delivery systems for topical application on the improvement of their bioavailability, safety, and therapeutic capacity. In addition, current in vitro and in vivo studies of different classes of flavonoids under study for its application on the treatment of skin conditions are highlighted.

2. Human Skin: Structure and Function

The skin is the largest organ of the body and acts as a physical barrier that separates the body from the external environment. It constitutes a first line of defense in protecting the body against physical, chemical, and microbial insults and assists in a wide range of functions such as prevention of body's dehydration, thermoregulation, sensation, and synthesis of vitamin D.

The skin is divided into three major layers, namely the epidermis, dermis, and hypodermis [13–16]. The epidermis is the outermost viable layer of the skin and constitutes a barrier between the body and the external environment. As represented in Figure 2, the epidermis is composed of four layers: the *stratum basale*, *stratum spinosum*, *stratum granulosum*, and *stratum corneum* (SC). An additional layer, the *stratum lucidum*, which is often considered the lower part of the *stratum corneum* as opposed to an individual epidermal layer, can be found on the palm and sole of the foot, parts of the body with thickened skin. In addition, appendageal features such as hair follicles and sweat ducts are transversal to multiple skin layers [14].

The dermis, with a thickness of typically 1–2 mm, comprises the bulk layer of the skin and provides its elasticity, flexibility, and tensile strength. It is composed of collagenous and elastin fibers, which accommodate epidermally derived appendages such as hair follicles, nails, sebaceous glands, and sweat glands as well as sensory nerve endings, lymphatic vessels and blood capillaries, which extend to the dermal side of the dermo-epidermal junction, thus allowing for metabolic exchanges and waste removal between the epidermis and the blood system [15]. The dermis contains resident cells, primarily fibroblasts that synthesize type I collagen for the extracellular matrix, as well as cells from the immune system, including macrophages and dermal dendritic cells (DCs). Below this layer, the fibrous connective tissue starts to transition to the adipose tissue of the hypodermis, where adipocytes interconnect with the collagen fibers, forming a thermal barrier for energy storage and protection from physical shock [15,17].

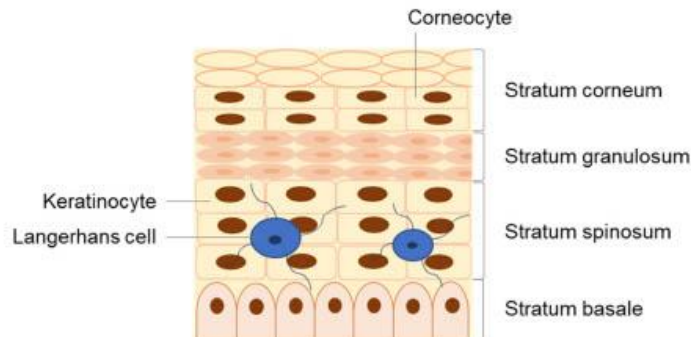


Figure 2. Detailed structure of the epidermis, composed of four distinct strata: the *stratum basale*, *stratum spinosum*, *stratum granulosum*, and *stratum corneum*.

The hypodermis is the innermost layer of the skin and may be considered part of the endocrine system. It provides the nerves, and the lymphatic and blood vessels, which permeate into the upper layers, thus playing a critical role in re-epithelization, wound healing, and angiogenesis [14,18].

3. The Skin as an Immune Organ

The skin is undoubtedly a complex organ that harbors a highly specialized immune microenvironment essential for maintaining tissue homeostasis, defense, and repair. Through a sophisticated network of resident immune and non-immune cells, biomolecules, and skin structures, the skin is able to protect the host from pathogen invasion as well as chemical and physical stress [13–15].

Resident immune cells (e.g., melanocytes and Langerhans cells) ensure tissue function in homeostasis and actively seek environmental antigens. Following an infection or tissue injury, these cells create a defense network in order to fight the insult and to restore the tissue to its original state [19,20]. Both epidermal keratinocytes and Langerhans cells (LCs) as well as dermal DCs, mast cells, and macrophages function as sentinels that not only provide a protective barrier but also trigger an early response to pathogen invasion by releasing stored antimicrobial peptides (AMPs), chemotactic proteins, and cytokines [20].

3.1. Non-Immune Cells as Key Immunological Mediators

Keratinocytes in response to multiple stimuli produce large amounts of interleukins (ILs), tumor-necrosis factor (TNF), and antimicrobial peptides, which trigger local immune responses. Moreover, they produce chemokines and immunoregulatory cytokines that act on resident immune cells such as DCs, mast cells, and macrophages, triggering the upregulation of inducible mediator expression and the recruitment of additional immune cells to the site of inflammation [21].

Similar to keratinocytes, fibroblasts also exert key immunomodulatory features. They express pattern recognition receptors (PRRs), produce AMPs, and synthesize many cytokines.

3.2. Immune Skin Cells

Langerhans cells are the only myeloid cell type in the epidermis. These cells act as key immunological mediators, with both an antigen-presenting role and a possible tolerance induction during an infection. These cells take up and process microbial fragments and lipid antigens and present them to effector T cells [19]. LCs are naturally migratory cells that continuously search the skin for signs of infection and that drain lymph nodes in order

to build tolerance in homeostasis or to initiate adaptive immune responses. In addition, they can further exert immunoregulatory and tolerogenic functions [22–24].

Mast cells are commonly found in the upper dermal layer of the skin, actively protecting it and responding to infections, venoms, and stress caused by wound healing [20]. Mast cells produce and release significant amounts of histamine, thus being naturally involved in allergic reactions, and are recognized as typical allergy cells. Recent studies show their critical role in wound healing, inflammation, angiogenesis, immune tolerance, and cancer [19].

Dermal DCs, similar to LCs, are prime antigen-presenting cells, the main role of which is to provide immunosurveillance against pathogens. These cells activate and promote the clonal expansion of skin-resident memory CD4⁺ or CD8⁺ T cells. T cell-derived pro-inflammatory cytokines and chemokines can in turn stimulate epithelial and mesenchymal cells, therefore intensifying the inflammatory response [25]. Plasmacytoid DCs are a type of DC found in the skin exclusively during an inflammatory stage. These cells produce large quantities of interferon- α (IFN- α), essential for viral defense. In addition, they have also been implicated in autoimmune disease such as psoriasis as well as fibrosis [26].

Table 1 summarizes the functions of the main cell types found in the skin and their role in the skin immunology, which leads the outcome of molecules delivered cutaneously.

Table 1. Main immunological functions of skin cells.

Cell Type	Location in the Skin	Immunological Role	Ref
Langerhans cells	Epidermis	Sentinel role Migration to lymph nodes to induce adaptive immune responses Induction of tolerance Production of pro-inflammatory cytokines and chemokines	[19,25]
Dermal DCs	Papillary dermis	Antigen presentation Cytokine and chemokine secretion	[25]
Plasmacytoid DCs	Dermis	Production of IFN- α Antimicrobial activity	[21,25]
Macrophages	Papillary and reticular dermis	Production of pro- and anti-inflammatory mediators Production of cytokines and chemokines Phagocytosis of pathogenic agents and necrotic debris	[19,25]
Mast cells	Papillary and reticular dermis	Production of inflammatory mediators involved in allergic responses and asthma Recruitment of immune cells Production of inflammatory cytokines	[19]
B lymphocytes	Reticular dermis	Production of autoantibodies specific to components of the skin Provide physical barrier and structural integrity	[27,28]
Non-immune cells (keratinocytes and fibroblasts)	Epidermis and reticular dermis	Production of inflammatory cytokines and AMPs in response to injury or pathogen invasion Phagocytosis during pathogen invasion	[20–22,25]
Neutrophils	Reticular dermis	Release of chemo-attractants to recruit other neutrophils to the site of inflammation	[29,30]
Eosinophils	Reticular dermis	Defense against parasites	[31]

4. The Skin as a Barrier in Cutaneous Delivery

Cutaneous delivery is one of the most attractive routes of administration for drugs and cosmetics, since it can overcome the many drawbacks of most common routes (e.g., parenteral and oral), including low bioavailability and cytotoxicity, while ensuring a sustained drug release at the desired site of action [32]. However, normal skin presents a serious barrier to drug absorption, mostly due to the unique lipid composition and organization of the SC, which plays a key role in skin permeability and therefore drug permeation through the skin [32–34].

Despite recent advances in the identification and elucidation of the mechanisms of drug transport through the skin and the generation of structure–activity relations that allow for an accurate prediction of the permeation profile of a drug, the development of new formulations and drug delivery systems capable of improving drug uptake via the skin barrier are still needed [5]. This is particularly relevant when it comes to routes for flavonoid administration. It is now well-established that, due to its lipophilic nature, the cutaneous route is the best delivery approach for flavonoids. In fact, an array of novel formulations for topical delivery have been developed and optimized in order to increase the solubility and permeability of flavonoids across the skin barrier [5]. Nonetheless, there are still major challenges to overcome in order to successfully deliver these compounds to the skin for therapeutic purposes, including inadequate residence time and sustained release profile as well as the scalability of formulation and manufacturing process [1,3–5].

Targeting the optimal skin penetration pathway is an essential step for effective topical drug delivery. On that matter, drugs can be administered through the skin in an invasive and noninvasive way. In the invasive route of administration, drugs can permeate through the skin via needle injections (subcutaneous, intramuscular, or intravenous routes) or via the implantation of a device [35]. In the subcutaneous route, the needle is inserted directly into the fatty tissue, thus reaching the bloodstream. For instance, insulin, similar to other proteins that are destroyed in the digestive tract, is administered through this route. For larger volumes of drugs, the intramuscular route is preferred in comparison with the subcutaneous one. On the other hand, in the intravenous route, the drug is delivered directly into the bloodstream, in a well-controlled and rapid manner. The implantation of a device inserted under the skin is another invasive drug administration method and is usually considered when a controlled release of the drug with time is needed.

Regarding noninvasive drug administration methods, there are four possible pathways of drug permeation across the skin: the intracellular, intrafollicular, transcellular, and polar pathways (Figure 3) [36]. The intrafollicular route, sometimes classified as the appendageal route, encompasses drug permeation through the skin appendages, such as lipophilic follicular ducts, sebaceous glands, or hydrophilic sweat ducts [14,37]. In the most commonly used pathway, the intercellular one, the drug travels through the lipid matrix that occupies the intercellular spaces between the corneocytes, thus making it the preferred permeation route for lipophilic molecules. On the other hand, in the transcellular way, also known as the intracellular pathway, the drug diffuses through the various skin layers and dead cells, allowing for the transport of hydrophilic or polar molecules. Finally, in the polar pathway, the drugs permeate through the skin via polar pores available at its surface. This observed flux of drugs across the various layers of the skin is called transdermal drug delivery [15,18,38,39].

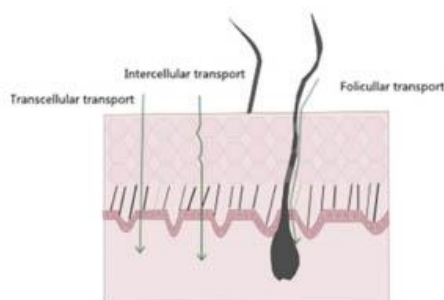


Figure 3. Schematic representation of different entry pathways for molecules into the skin.

After passing through the SC and diffusing through the viable epidermis and dermis, the drug becomes available for its uptake into the systemic circulation [5]. Systemic absorption

depends on the application site, its area, and the nature of the delivery system. Another alternative to the oral administration of drugs is topical delivery, in which the drug is intended to be absorbed at specific areas of the skin rather than being targeted for systemic delivery. Examples of drugs topically delivered to the skin include corticosteroids, antifungals, antivirals, antibiotics, antiseptics, and local anesthetics [40].

5. Flavonoids: Relevant Biochemical and Biological Properties

In addition to their well-reported strong antioxidant activity, flavonoids also exhibit the ability to modulate key cellular signaling pathways and enzymatic reactions involved in a wide range of pathophysiological events such as cell proliferation, inflammation, immune response, platelet aggregation, and cytotoxicity [41–45]. Studies indicate that the biological properties of flavonoids are beneficial in solving or controlling skin disorders. The following subsections briefly describe the antioxidant, anti-inflammatory, anticancer, and antibacterial activities of flavonoids, elucidating the molecular targets and mechanism of actions with an effect on skin disorders (Table 2).

Table 2. Synopsis of the main molecular targets and mechanisms of action of flavonoids.

Flavonoid	Molecular Targets	Biological Role	Mechanisms of Action	Ref.
Catechin, Epigallocatechin	ERK, NF- κ B, Rac1, AP-1, p38	Anticarcinogenic	Inhibition of iNOS expression Reduction of NF- κ B and AP-1 activity Inhibition of intercellular adhesion molecule-1 (ICAM-1), VCAM-1, and E-selectin expression Inhibition of prostaglandin synthesis and IL-6 production Inhibition of the upregulation of monocytes adhesion and VCAM-1 expression and NF- κ B activity	[46–49]
Apigenin	Akt, ERK, caspase-12, caspase-3, MAPK, ROS, COX-2, IL-6, TNF- α , IL-1 β , iNOS, PGE2	Anti-inflammatory, Anticarcinogenic		[9,46,47,50,51]
Luteolin	Akt, ERK, caspase-12, caspase-3, MAPK, ROS, COX-2, IL-6, TNF- α , IL-1 β , iNOS, PGE2	Anti-inflammatory, anticarcinogenic		[9,46,47,50,51]
Quercetin	PKC, AP-1, H ₂ O ₂ , iNOS, MDA, citrate synthase, MMP-9, MMP-2, COX-2, ERK	Antioxidant, anti-inflammatory	Inhibition of NO production and iNOS protein expression Inhibition of cyclooxygenase and lipoxygenase activities	[46,47,52]
Hesperetin	GSH reductase, iNOS, 3-nitropropionic acid, COX2, NF- κ B, IL-1, TNF- α	Antioxidant	Blood lipid-lowering and cholesterol-lowering agents	[46,47,52]

5.1. Antioxidant Properties

One of the best-described properties of flavonoids is their capacity to act as powerful antioxidants. In fact, flavonoids have the ability to act as free-radical scavengers and metal ion chelators as well as the capacity to affect enzymatic and non-enzymatic systems that regulate cellular redox balance [41,45,53]. Their mechanisms of antioxidant action can include (1) the suppression of reactive oxygen species formation (ROS) either through inhibition of certain enzymes or by chelating trace elements involved in the generation of free radicals, (2) scavenging ROS, and (3) the upregulation or protection of antioxidant defenses [3].

Depending on their structure, there is considerable evidence that flavonoids are effective scavengers of ROS, such as peroxy, alkyl peroxy, hydroxyl, and superoxide radicals as well as reactive nitrogen species (RNS), in particular, nitric oxide (NO) and peroxynitrite (ONOO⁻). Due to the presence of vicinal hydroxyl groups, several flavonoids

can also act as chelators of redox-active metal ions, such as copper and iron, thus preventing free radical formation and lipid peroxidation [54–57].

Free metal ions enhance the formation of ROS through the reduction of hydrogen peroxide to the highly reactive hydroxyl radical. Flavonoids, due to their lower redox potential are able to reduce highly oxidizing free radicals such as hydroxyl, superoxide, and peroxy radicals by donating a hydrogen atom. The presence of a 3',4'-catechol group in the flavonoid structure, for example, is known to enhance their capacity to inhibit lipid peroxidation. This trait makes flavonoids highly effective scavengers of peroxy, superoxide, and peroxy nitrite radicals [58–61]. Epicatechin and rutin, for instance, were shown to be strong radical scavengers and inhibitors of lipid peroxidation *in vitro* [3]. Moreover, they are known to inhibit enzymes involved in ROS formation, such as the case of xanthine oxidase, myeloperoxidase, and NADPH oxidase.

On the other hand, flavonoids have the capacity to upregulate both enzymatic and non-enzymatic systems involved in the removal and detoxification of oxidant species, particularly reduced glutathione (GSH), GSH peroxidase, GSH reductase, GSH S-transferase, superoxide dismutase, and catalase, as it has been demonstrated in animal models for rutin; quercetin; daidzein; and to a lesser extent, genistein [62,63]. Certain flavonoids, such as quercetin and the catechins, have been shown to regenerate ascorbate and α -tocopherol via electron transfer reactions, thus displaying an additional antioxidant mechanism [64–66].

It is noteworthy that, under certain conditions, flavonoids might also exert a marked pro-oxidant activity, becoming cytotoxic. In fact, they can undergo transition metal or peroxidase-catalyzed reactions, which lead to the formation of highly reactive oxygen species that can damage proteins and DNA [67].

5.2. Anti-Inflammatory Properties

Inflammation is a biological response to tissue injury, microbial infection, and chemical irritation. During an inflammatory process, the migration of immune cells from blood vessels and the release of mediators to the site of damage are followed by the recruitment of inflammatory cells and the release of ROS and pro-inflammatory cytokines that work together to eliminate pathogens and to repair injured tissues. Flavonoids are known to significantly affect the immune system [47,68]. For instance, hesperidin, apigenin, and quercetin are among a broad spectrum of flavonoids known for their anti-inflammatory and analgesic capacity. In fact, studies have shown that, both *in vitro* and *in vivo*, flavonoids have the capacity to downregulate the expression of a wide range of pro-inflammatory genes, including the inducible nitric oxide synthase (iNOS), cyclooxygenase (COX), lipoxygenase (LOX), and several key cytokines, mainly through the inhibition of the mitogen-activated protein kinase (MAPK)- and nuclear factor-kappa B (NF- κ B)-mediated signaling pathways [68–70]. This ability to inhibit the arachidonic acid pathway at the level of phospholipase A₂, COX and LOX is of particular importance since it results in a decrease in the production of prostaglandins and leukotrienes, essential mediators of the acute inflammatory response [71,72]. Flavonoids are in fact known to modulate several steps of the inflammatory cascade both in human and animal cell types. Quercetin, kaempferol, genistein, and epigallocatechin-3-gallate (EGCG) are among the flavonoids that have been extensively studied on their ability to affect iNOS activity and NO production. They have been found to inhibit iNOS expression via the downregulation of extracellular signal regulated protein kinase 1/2 (ERK 1/2) and p38 MAPK phosphorylation and by preventing the binding of NF- κ B to the iNOS gene promoter [71,73–77]. In addition, several flavonoids have been shown to interfere with the production and function of various pro-inflammatory cytokines, chemokines, and adhesion molecules, such as TNF- α ; IL-1 β , -6, and -8; monocyte chemoattractant protein-1 (MCP-1); macrophage inflammatory protein-2 (MIP-2); vascular cell adhesion molecule (VCAM); and P-selectin by inhibiting the MAPK pathways, by blocking NF- κ B nuclear translocation, and via COX-2 synthesis [78–84].

5.3. Anticancer Properties

Recent studies have demonstrated a direct link between flavonoids and their ability to prevent the development of different types of malignant tumors both in human and animal models. In fact, it is now well-established that flavonoids exert an anticarcinogenic effect by quenching oxidative stress and inflammatory response; by inducing apoptosis; by suppressing MMP secretion; and by inhibiting cell growth, tumor cell invasion, and angiogenesis [85–91].

Flavonoids might act on the initial steps of cancer development by preventing the DNA damage that can be induced by free radicals and carcinogens. In addition, flavonoids have been demonstrated to inhibit various types of cancer cell proliferation by inducing cell cycle arrest at the G1/S or G2/M phases through the downregulation of cyclins and cyclin-dependent kinases. They were also shown to stimulate apoptosis through the activation of caspases 3, 9, and 8 and proapoptotic proteins p53, p27, and Bax as well as via the inhibition of antiapoptotic proteins (Bcl-2 and Bid) and the release of cytochrome c [92–98].

Their antiproliferative and proapoptotic activity might implicate the inhibition of growth factors and its receptors such as platelet-derived growth factor (PDGF), PDGF receptor (PDGFR), and epidermal growth factor receptor (EGFR) in addition to the activation of NF- κ B and the inhibition of the Akt/PI3K, ERK and activating protein-1 (AP-1) pathways [99,100]. For instance, flavonoids such as EGCG, quercetin, genistein, luteolin, and the anthocyanins were able to reduce angiogenesis, a key event in tumor growth, invasion, and metastasis via the downregulation of VEGF, VEGFR, PDGF, PDGFR, EGFR, and MMP. Other flavonoids were also shown to affect cancer cell adhesion and movement by inducing cytoskeletal modifications, by inhibiting cell adhesion to fibronectin, by reducing integrin expression and disrupting the stress fibers, and by reducing myosin II regulatory light chain phosphorylation [86–88,101–103].

5.4. Antibacterial Properties

Flavonoids are naturally synthesized by plants in response to microbial infection. Similarly, it has been found that they exert *in vitro* antimicrobial activity against a wide range of microorganisms. In fact, flavonoids such as apigenin, galangin, flavonol glycosides, isoflavones, and flavanones have all been shown to possess strong antibacterial activity [1]. Given their antibacterial properties, flavonoids are being used as wound healing agents.

6. Bioavailability of Flavonoids

One of the major concerns regarding the use of flavonoids as therapeutic agents is their relatively low bioavailability. Even in the presence of a large daily intake of flavonoids in dietary sources, their plasma and tissue concentrations are often insufficient to exert the desired pharmacological effects [3]. Due to several factors that include chemical structure and molecular weight, relatively low water solubility, absorption and metabolism in the gastrointestinal tract, lack of site specificity in distribution, and rapid elimination, flavonoids have generally low bioavailability, which largely affects their therapeutic potential. Moreover, this class of compounds is highly susceptible to degradation upon oxygen exposure, temperature changes, ultraviolet radiation, or pH change [104–106].

After being absorbed by the intestinal epithelium, flavonoids undergo extensive biotransformation into conjugated products, namely glucuronides, sulphates, and methylated derivatives, first in the intestine and then in the liver, where they are secreted into bile [107,108]. Thus, the bioavailability and the subsequent cell and tissue accumulation of the different flavonoids essentially depend on the multidrug-resistance-associated proteins (MRP-1 and MRP-2), ubiquitously expressed as ATP-dependent efflux transporters. The actual flux of a flavonoid from the gut lumen to the blood stream and the various organs depends on the tissue distribution of MRP-1 and MRP-2 as well as on their substrate's affinity. This metabolic pathway is called phase III metabolism. However, it appears that certain phase II metabolic derivatives of flavonoids can act as competitive substrates of the MRP-mediated membrane transporters and the potential use of flavonoids as a mean to

overcome transporter-mediated chemotherapy resistance due to the frequent overexpression of MRP in several types of cancer is based on this property. The intestinal absorption of quercetin, for instance, is favored in the aglycone form, and its metabolism in the gut and liver appears to be relatively high, so that less than 2% of ingested quercetin is recovered on the plasma [3]. Additionally, after oral administration of flavonoids, a significant amount can reach the colon and can interact with microbiota. Microbiota can, for instance, metabolize some flavonoids to smaller phenolic compounds with similar biological effects and improved bioavailability; however, on the other hand, it can also extensively metabolize flavonoids via the glucuronidase and sulfatase enzymes, cleaving the heterocycle break and producing inert polar compounds that are rapidly excreted without producing any biological effect [104].

In addition, flavonoids have been reported to significantly inhibit the activity of the cytochrome P450 system, which can result in an increase of the half-life and concentration of many drugs, thus enhancing their toxicity and side effects [109]. Flavonoids such as quercetin, ECG, EGCG, and silybin have been shown to downregulate the cytochrome CYP3A4, which is the major cytochrome P450 isoenzyme in the intestine and is responsible for the metabolism of approximately 50% of all prescribed drugs, thus increasing the risk of potential toxicity, especially of drugs with a limited therapeutic window [110]. Flavonoids can also interact with ATP-binding cassette (ABC) transporters, inhibiting them, which can increase the bioavailability of poorly available drugs, on the one hand, but it can also potentiate the toxicity of other ABC transporters substrates [111]. Thus, flavonoid encapsulation in effective nano-carrier systems can not only improve their pharmacokinetics and therapeutic potential but also avoid enhancement of the toxicity and side effects of drugs that can concomitantly be administered with these compounds [104].

The rapid metabolic elimination of flavonoids, together with the evidence that they are able to interact with the metabolism of other drugs, highlights the need to develop novel ways to improve the delivery of flavonoids. Cutaneous administration emerges as an alternative option to common oral and parenteral routes [112,113]. Skin drug delivery is one of the most preferred administration routes with higher patient compliance and satisfaction. The advantages also include the avoidance of liver first pass metabolism effects, metabolic degradation associated with oral administration, and minimal systemic side effects.

7. The Need for Nanocarriers in Cutaneous Flavonoid Delivery

Despite flavonoids' pharmacological potential, dietary flavonoids present several disadvantages, mentioned in Section 6, hindering their clinical potential. In addition, the fact that flavonoids can suffer an enhanced complexation or precipitation when ingested with other food components as well as degradation by microbiota greatly reduces their bioavailability and stability. On that matter, cutaneous delivery is one of the most advantageous routes in overcoming the challenges associated with flavonoid administration [3,104].

Nonetheless, the impermeable nature of the skin presents a serious challenge to cutaneous delivery, where in most of the cases the therapeutic effect produced by the conventional drug dosage is not sufficiently effective. Thus, the development of nano-engineered delivery systems for flavonoids capable of increasing the solubility and bioavailability and of providing a site-specific delivery with improved pharmacokinetic properties is imperative. Thus far, gels are the most common form of topical drug administration, including hydrogels and oleogels. However, other delivery systems such as lipid and polymeric nanoparticles, microparticles, and transferosomes, among others, are currently being developed (Figure 4). These carriers can later be formulated into creams and gels, improving patient compliance [5].

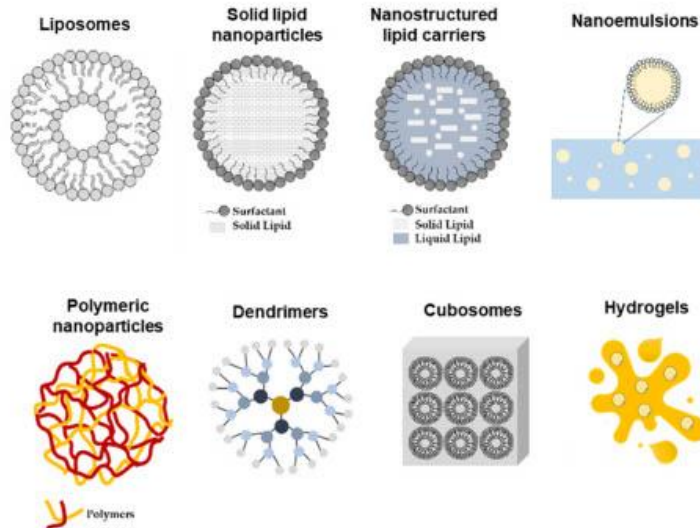


Figure 4. Schematic representation of nano-delivery systems used for topical skin delivery.

7.1. Nano-Delivery Systems: Advantages and Limitations

The development of novel drug delivery systems, which allow for the cutaneous delivery of otherwise poorly effective compounds with undesirable physicochemical and pharmacokinetics parameters, can improve their efficacy and safety. Nanotechnology tools designed for skin drug delivery include microdevices (1–1000 μm) and nanodevices (1–1000 nm) for drug delivery [112]. Micro-delivery vehicles can act as reservoirs for a drug that is released into the tissue interstitial space. Due to their size, they can cross the skin barrier and directly deliver the drug to the site of action, minimizing toxicity and prolonging release [3,51].

Despite great progress, the development of a successful drug delivery system is still a challenging task that requires meticulous selection of the vehicle according to the active agent. In fact, the safety of the chosen materials, eventual harmful degradation products, and high cost of the final product are major limitations that need to be addressed.

The use of nanocarriers allows for an improvement in crucial drug properties, including solubility, diffusivity, blood circulation half-life, and immunogenicity. However, there are some essential prerequisites for the development of a successful targeted drug delivery vehicle, including the physicochemical and biological properties of the vehicle [114]. For instance, size, charge, and surface hydrophilicity are all properties that can impact the circulating half-life of the particles as well as their biodistribution. Small molecule-, peptide-, or nucleic acids-loaded nanoparticles are not as easily recognized by the immune system; in addition, the presence of targeting ligands can increase the interaction of drug delivery systems with the cells and can enhance cellular uptake by receptor-mediated endocytosis [115]. Nevertheless, there are some limitations on the use of nanocarriers, namely storage, generation of pro-oxidant chemical species, and unexpected pro-inflammatory response, which need to be considered in their design.

In summary, the advantages of nanocarriers application for cutaneous drug delivery include (1) targeted delivery, with maximized efficacy and minimized systemic side effects; (2) controlled drug release; (3) prolonged half-life in the systemic circulation; (4) improved patient compliance; (5) improved drug solubility and permeability; (6) protection against

degradation; (7) delivery of multiple drugs with a synergistic effect; and (8) improved biocompatibility [3,115–117].

7.2. Nano-Delivery Systems Applied for Flavonoid Cutaneous Administration

Among the numerous nano-based drug delivery systems that have been developed so far, lipid-based nanoparticles, including liposomes and lipid nanoparticles as well as polymeric-based nanoparticles, are most commonly used for flavonoid delivery [3]. Liposomes are concentric vesicles consisting of an aqueous core surrounded by a membranous lipid bilayer that, thanks to their structure, can encapsulate hydrophilic, hydrophobic (in the lipid bilayers), and amphipathic molecules. To avoid the rapid elimination of liposomes from the blood by the cells of the reticuloendothelial system (RES), primarily in the liver and spleen, their structure can be modified by coating their surface with inert and biocompatible polymers such as polyethylene glycol (PEG) [118–121].

Solid lipid nanoparticles (SLN) are nanocarriers composed by a solid hydrophobic core and stabilized by a surfactant. Among the main advantages of using SLN as drug carriers, their high stability and capacity to protect the incorporated drugs from degradation, the controlled drug release, site-specific targeting, and good biocompatibility stand out. However, they often display low loading capacity as well as a short storage time with frequent drug expulsion. SLN can be administered by the parenteral, oral, transdermal, dermal, and ocular routes. In addition, they have higher stability compared with liposomes and, due to their easy biodegradability, are less toxic than polymeric nanoparticles, making them highly versatile drug delivery vehicles. Their primary applications target skin disorders; for example, curcumin loaded in SLNs featured a controlled drug release over 24 h and effective skin deposition for the reduction in pigmentation and inflammation in Balb/c mouse skin [117,122,123].

Regarding its potential application as a cutaneous drug delivery system, SLN-enhanced SC permeation is attributed to (1) prolonged contact with the skin surface; (2) their occlusive nature, since they form a film on the surface of the skin that combines with the skin lipids promoting a reduction in water loss and hydration of the skin; and (3) the interaction between the lipids in the nanoparticles and SC lipids, which facilitates permeation of lipid-soluble compounds.

The use of cationic lipids on the nanoparticle's composition allows for an interaction with the negatively charged skin surface. For instance, a highly positively charged (+51 mV) SLN using cationic phospholipids, tween 20 as a surfactant, tricaprln as a solid lipid core, and encapsulating plasma DNA was shown to have enhanced *in vitro* permeation into mouse skin and the expression of mRNA *in vivo* after topical application [124].

Liquid lipids (oils) can be added to a solid lipid, creating an irregular lipid matrix, called the nanostructured lipid carriers (NLC). The lipids' spatial structure allows for an increased drug loading capacity and better stability compared with SLN. Studies have shown that both NLC and SLN display similar mechanisms of skin permeation enhancement, through occlusion and mixing between the formulation and the SC lipids, although the presence of a liquid lipid is known to increase the solubilization and loading capacity, thus resulting in greater skin deposition [3,124].

Polymeric nanoparticles are colloidal structures composed of natural or synthetic polymers. Depending on their shape, they can be classified as nanocapsules, vesicular systems with the drug in a core surrounded by a polymeric membrane, and nanospheres, which are porous matrixes in which the drug is uniformly dispersed [125,126]. The most common synthetic polymers used in the preparation of these nanoparticles are poly(lactic acid) (PLA), poly(lactide-co-glycolide) (PLGA), poly(methyl methacrylate) (PMMA), and poly(alkylcyanoacrylate) (PACA) [127–132]. In addition, natural polymers such as alginate, gelatin, chitosan, and albumin are also frequently used since they are less toxic compared with synthetic polymers. Polymeric nanoparticles feature biocompatibility, biodegradability, stability, and surface modification potential, therefore allowing for the controlled release of both hydrophobic and hydrophilic compounds as well as proteins, peptides,

or nucleotides to the specific site of action. To avoid rapid removal from blood and to reduce its cytotoxicity, polymeric nanoparticles can be covered with a non-ionic surfactant or coated with hydrophilic substances such as PEG or carbohydrates, thus reducing opsonization [3].

8. Cutaneous Delivery Systems of Flavonoids for Treatment of Skin Pathologies

Cutaneous delivery of flavonoids is a powerful strategy to avoid systemic toxicity while restricting the therapeutic effects to the specific site of action. However, one of the major challenges that a topical delivery system faces is the ability to overcome the SC barrier against foreign substances [5]. In addition, most flavonoids are highly lipophilic compounds and their permeation across the SC into viable skin layers is hindered by their affinity for SC components and the tendency to be retained in this layer. Thus, there has been a growing interest in the use of nanotechnology as a strategy for a more efficient flavonoid delivery to the human body (Figure 5). Nano-delivery systems are in fact excellent tools to overcome the challenges associated not only with the cutaneous absorption of the drug per se but also with flavonoid pharmacology, including low solubility, short half-life, and poor bioavailability [5,124].

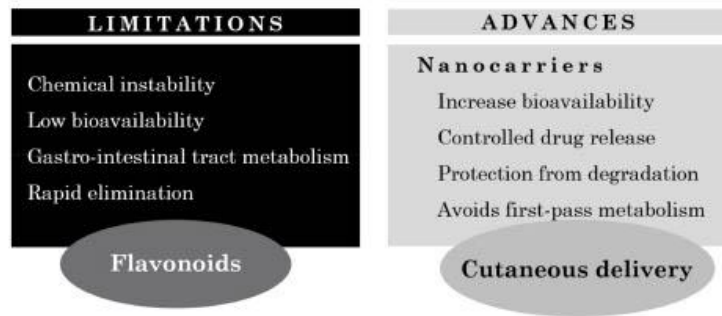


Figure 5. Limitations and advances on cutaneous flavonoid delivery.

8.1. Examples of Nanocarriers Designed for Flavonol Cutaneous Delivery

Flavonols are O-glycosidic ketonic compounds with a sugar moiety at the 3-position that act as powerful antioxidants, protecting the skin from ROS formation. Compounds belonging to this family of flavonoids are quercetin, kaempferol, and myricetin, among others [133].

Quercetin, one of the best studied and most common flavonoid found in nature, was shown to have poor permeability across excised human skin [4]. For that, this flavonoid has been incorporated into different delivery systems, including nanoemulsions, nanocapsules, lipid nanoparticles, and microemulsions, to increase its solubility and skin permeability [5]. Casagrande and colleagues incorporated quercetin into two different oil-in-water emulsions with a distinct lipid content in order to evaluate their potential application as a topical delivery system. The in vivo results demonstrated that these formulations were an effective vehicle for topical application of quercetin with the goal of controlling ultraviolet B (UVB)-induced skin damage [4,134]. Based on these results, other studies were conducted to design novel delivery systems to increase quercetin effectiveness when topically applied. For example, quercetin was incorporated into a liquid, crystalline formulation and the influence of this vehicle in the antioxidant activity of this flavonoid was evaluated in vitro. The presence of a liquid, crystalline structure allowed for an easier diffusion through the skin and a considerable solubilizing capacity for both oil- and water-soluble compounds. Scalia and colleagues also demonstrated that the incorporation of quercetin in lipid microparticles improved its photostability and chemical stability as well

as its biocompatibility [135,136]. In another study, Tan and colleagues investigated the potential of using lecithin-chitosan nanoparticles as a topical delivery system for quercetin. Compared with quercetin in its free form, the quercetin-loaded nanoparticles displayed higher permeation ability and significant accumulation of quercetin in the skin, particularly in the epidermis. In addition, microstructure observations of the skin surface following administration showed that the interaction between constituents of the nanoparticles and the skin surface markedly changed the morphology of the SC and disrupted the corneocyte layers, therefore facilitating permeation and accumulation of quercetin in the skin [137].

Nan and colleagues evaluated the efficacy of topically applying quercetin-loaded chitosan nanoparticles against UVB radiation. The authors demonstrated that quercetin, if entrapped into chitosan nanoparticles, could be efficiently up taken by HaCaT cells (keratinocytes) and could easily permeate through the epidermis layer while displaying better stability and lower cytotoxicity. Moreover, they also found that quercetin-loaded nanoparticles could enhance the effects of this flavonoid when inhibiting the NF- κ B/COX-2 signaling pathway as well as when ameliorating the skin edema caused by UVB radiation [138].

Bose and Michniak-Kohn developed a solvent-free NLC formulation of quercetin using probe ultrasonication and evaluated the feasibility for topical delivery. Formulation factors such as the nature of the lipid (solid/combination of solid and liquid) in the SLN and NLC systems and the drug loading capacity were evaluated to produce the optimal formulation with an adequate physical stability. Overall, the NLC system showed the highest improvement in the topical delivery of quercetin, manifested by the amount of quercetin retained in full-thickness human skin compared with a control formulation with a similar composition and particle size in the micrometer range, thus demonstrating the feasibility of NLC systems for improved cutaneous delivery of this compound [139].

Penetration enhancer containing vesicles (PEVs) are also known to be powerful enhancers for dermal delivery due to the presence of both phospholipids and penetration enhancers (PE), which provide a synergistic effect on skin permeation. PE increases the fluidity of the lipids of the SC, facilitating the delivery of drug-loaded vesicles and its subsequent diffusion through the skin [5]. Hence, in 2011, Chessa and colleagues developed quercetin-loaded PEVs, formulated using four different hydrophilic PE, and characterized them by size, surface charge, loading capacity, and morphological and viscoelastic features. In addition, their penetration capability and distribution through pig skin were assessed to obtain the optimal formulation for the delivery of quercetin to the skin [140]. In another study, performed by Caddeo and colleagues, quercetin-loaded phospholipid vesicles, in particular liposomes and PEVs, were developed in order to study their efficacy on 12-O-tetradecanoylphorbol-13-acetate (TPA)-induced skin inflammation. In vivo results demonstrated that the vesicles, in particular PEVs, were capable of delivering the drug to the inflammation site, that is the dermis, inhibiting oxidative stress and leukocyte accumulation as well as stimulating the repair of skin damaged induced by TPA. Through this work, the authors highlighted the use of vesicular systems, particularly PEVs, as a delivery vehicle for flavonoids, with a therapeutic potential to treat inflammatory skin disorders [141].

Kaempferol is another well-known flavonol with antioxidant, anti-inflammatory, anticancer, and antiallergic properties [142]. In fact, Wang and colleagues reported that kaempferol inhibited the iNOS mRNA expression and prostaglandin E2 production in a dose-dependent manner, by inhibiting in part the NF- κ B signaling pathway [143]. Furthermore, Park et al. reported that kaempferol was also able to inhibit the activation of inflammatory NF- κ B transcription factor via nuclear factor-inducing kinase (NIK)/I κ B kinase (IKK) and MAPKs in aged rat kidney [120]. Nonetheless, studies have shown that this flavonoid undergoes excessive first pass metabolism and, as a consequence, displays a bioavailability rate of only 2%, thus making it a good candidate for cutaneous application [142]. Keeping that in mind, Yun Chao and colleagues developed submicron emulsions to be employed as a delivery system for the topical application of kaempferol. These submicron emulsion systems are oil-in-water dispersions with small droplet sizes in

the range of 100–600 nm. In comparison with traditional drug delivery vehicles, they are easy to manufacture, are more thermodynamically stable, and exhibit enhanced drug solubilization as well as increased drug permeation rates. Additionally, submicron emulsions were demonstrated to be a potential vehicle for the transdermal and topical delivery of lipophilic and hydrophilic drugs. In this study, kaempferol-loaded submicron emulsions with different water/oil/surfactant/cosurfactant ratios were prepared, and different physicochemical properties (e.g., viscosity, droplet size, permeation rate, lag time, and deposition amount in skin) were determined in order to evaluate the effectiveness of this delivery system for the cutaneous application of kaempferol. Overall, the authors demonstrated that, based on the permeation parameters, including the increase in the cumulative amount of drug over 12 h and deposition in the skin, in addition to a shorter lag time, submicron emulsions may be a promising vehicle for cutaneous application of kaempferol [142].

8.2. Examples of Nanocarriers Designed for Other Flavonoid Classes' Topical Delivery

Isoflavones, are naturally occurring isoflavonoids mainly found in soybeans, soy foods, and legumes. They are non-steroidal compounds that act as phytoestrogens as they exert pseudohormonal activity by binding to estrogen receptors in mammals. The most common isoflavones are genistein and daidzein [5]. Huang and colleagues assessed the potential topical delivery and dermal use of soy isoflavones genistein and daidzein, using α -terpineol and oleic acid as PE, both in vitro and in vivo. As demonstrated in vivo, there was an increase in the uptake of genistein and daidzein, with no toxic effects, and a decrease in the erythema. In vitro studies showed an inhibition of UVB-induced intracellular H_2O_2 production and the consequent protection of keratinocytes against UVB radiation, suggesting that a reduction in photodamage to the skin via the topical application of antioxidants could be an efficient way to enrich the endogenous cutaneous protection system [143,144].

Apigenin is a hydrophobic, polyphenolic flavonoid known to possess antioxidant, antimicrobial, anti-inflammatory, antiviral, antidiabetic, and tumor inhibitory activities. In particular, this flavonoid was demonstrated to act as a chemo-preventive by inhibiting the enzyme CYP2C and by preventing the metabolism of many drugs and xenobiotics. Similar to the already mentioned flavonoids, the clinical potential of apigenin is suppressed by its poor aqueous solubility, low oral bioavailability, and rapid metabolism. Thus, the development of novel formulations is a necessary step to overcome these limitations and to improve apigenin delivery [5]. On that matter, several formulations have been developed so far, including liposomes, nanocrystal gel formulations, and self-micro-emulsifying drug delivery systems. Munyendo and colleagues reported that the formulation of D- α -tocopherol acid and polyethylene glycol 1000 succinate (TPGS) stabilized the mixed micelles of apigenin and phospholipids, creating an effective drug delivery vehicle capable of enhancing the bioavailability of this flavonoid [145]. Karthivashan and colleagues prepared "flavosomes", which are phytosomes loaded with multiple flavonoids, using phosphatidylcholine as a carrier and evaluated their in vitro pharmacokinetics and toxicity [146]. Shen and co-workers evaluated a novel topical delivery system for apigenin by using soy lecithin-based ethosomes, demonstrating a higher skin targeting capacity and a significant reduction in COX-2 levels in mouse skin inflammation induced by UVB light [147].

Luteolin is another promising flavonoid with potential antiarthritic activity. In addition, due to its lipophilicity, it can be used in topical formulations to treat psoriasis [148]. Niosomes are non-ionic surfactant-based colloidal systems that have the ability to encapsulate both hydrophobic and hydrophilic drugs. Abidin and co-workers prepared luteolin-loaded niosomes using different non-ionic surfactants and characterized them for their in vitro and in vivo antiarthritic activity. The optimized formulation was later converted into gel using Carbopol as a gelling agent for enhanced transdermal luteolin delivery. The in vivo bioactive studies revealed that the niotransgel formulation of luteolin was able to provide good antiarthritic activity, with the results being comparable with standard diclofenac gel formulation [149]. In another study, Shin and colleagues, established a

nanoemulsion-based follicular delivery system, in which luteolin was incorporated into oil-in-water nanoemulsions. In vivo studies proved that these luteolin-loaded nanoemulsions possessed hair-growth promotion ability. In fact, when nanoemulsions are formed by the assembly of amphiphilic polymers at the oil/water (O/W) interface, they provide an efficient system for the encapsulation of poorly water-soluble substances, resulting in better bioavailability, accurate dosing, and minimal side effects [150].

Catechins are a group of flavonoids that belong to the flavanol family and are present in high concentrations in a variety of plant-based fruits, vegetables, and beverages. Belonging to this family are catechin, epicatechin (EG), and EGCG. EGCG, in particular, has captured a lot of attention due to its broad spectrum of biological properties, including antioxidant, photoprotective, antiviral, and antibacterial as well as anticancer and neuroprotective effects. Nevertheless, its clinical use has been limited due to its poor systemic absorption and low bioavailability [5]. With the goal to overcome this problem and to increase EGCG clinical applicability, Avadhani and co-workers developed nano-transfersomal formulations of EGCG for an efficient permeation into the SC and delivery into the skin [151]. In addition, hyaluronic acid (HA) was also encapsulated in the transfersomes not only because it is widely distributed in connective tissues and is a main component of the extracellular matrix but also because it is a non-irritating biopolymer and antiaging agent with high biocompatibility, specific viscoelasticity, and hydration and lubrication properties. The optimized transfersomal formulation containing EGCG and HA displayed a high free radical scavenging effect while showing no cell toxicity. In addition, the formulation was able to suppress the MDA and ROS levels to a significant extent in human keratinocytes as well as the expression levels of MMP-2 and MMP-9. The encapsulation of EGCG in the transfersomes resulted in higher skin permeation and deposition of this flavonoid in the skin, compared with plain EGCG. Interestingly, the co-entrapment of HA in the formulation increased both the skin permeation and deposition of EGCG, thus demonstrating that this system constitutes a useful and effective EGCG cutaneous delivery vehicle, with synergistic antiaging and antioxidant benefits [151].

Fang and colleagues assessed the possibility of using multilamellar phosphatidylcholine (PC) liposomes studied for topical and intratumor delivery administration of catechin, EC, and EGCG in nude mice [152,153]. The authors showed that the inclusion of anionic species such as deoxycholic acid and dicetyl phosphate increased the encapsulation of the catechins and the permeability of the lipid bilayers. EGCG performed differently due to its higher lipophilicity. In addition, the authors reported an even higher EGCG encapsulation for deoxycholic acid-liposomes prepared in the presence of 15% ethanol as well as an increased catechin in vitro and in vivo skin permeation and deposition in basal cell carcinomas compared with both the free form and ethanol-free liposomes. This might be attributed to the fact that ethanol-enriched liposomes penetrate easily in the skin due to the increased elasticity conferred by the insertion of alcohol into the PC membranes. The results showed that optimization of the physicochemical features and composition of liposomes could control and improve the delivery of catechins. Moreover, the results suggested that the intratumor administration of liposomes might be an effective approach for the local treatment of solid tumors [152,153].

Overall, there are several strategies that can be adopted to increase the solubility and subsequent bioavailability of flavonoids with therapeutic potential. Although much progress has been recently made, novel drug delivery systems suitable for an optimized topical application should continue to be explored [112,154–157]. A summary of the therapeutic application of flavonoids and the different nanocarriers used to enhance their delivery to the skin is described in Table 3.

Table 3. In vitro and in vivo studies using different nanocarriers for enhanced topical delivery of flavonoids to the skin.

Flavonoid	Nanoformulation	Skin Model	Therapeutic Application	Ref.
Quercetin	Solid lipid nanoparticles	Human skin	Delay UVB radiation-mediated cell damage and necrosis	[139]
	Non-ionic emulsion with high lipid content	Pig ear skin	Inhibition of UVB-induced cutaneous oxidative stress and inflammation	[4]
	Anionic emulsion with low lipid content	Pig ear skin	Inhibition of UVB-induced cutaneous oxidative stress and inflammation	[4]
	Lecithin-chitosan nanoparticles	Male Kunming mice	Topical delivery system with a wide range of applications	[137]
	Lipid microparticles	n.a.	Enhance quercetin stability in topical formulations	[136]
	Colloidal silica emulsion	Human skin	Optimization of a formulation with enhance penetration into human SC	[156]
	Chitosan nanoparticles	HaCaT cells	Potential therapeutic agent for topical use against UVB radiation	[138]
	Penetration Enhancer containing Vesicles (PEVs)	New born pig skin	New formulation for dermal delivery of quercetin, with various therapeutic applications	[140]
	Poly lactide nanocapsules; Multilamellar liposomes; Niosomes	Subcutaneous injection in amistogote-infected hamsters	Antileishmanial agent	[3,157]
	Liposomes with penetration enhancing vesicles (PEV)	Female CD-1 mice	Anti-inflammatory agent	[5,157]
Lipid nanocapsules	Acute monocytic leukemia cell line (THP1-1 cell)	Antioxidant, anti-inflammatory agent	[5,158]	
Nanoparticle suspension	Mice	Antioxidant agent	[5,149]	

Table 3. Cont.

Flavonoid	Nanoformulation	Skin Model	Therapeutic Application	Ref.
Catechins	Multilamellar phosphatidylcholine liposomes	Female nude mouse (Balb/c-nu, 6–8 weeks old)	Use of liposomes for the local delivery, including skin and tumor deposition, of polyphenols	[3,151]
	Ethanol enriched liposomes	Female nude mouse (Balb/c-nu, 6–8 week)	Antioxidant and chemopreventive activity	[152]
	Cream	Iranian rabbits	Wound healing effect	[5,159]
	Tansfersomes containing EGCG and hyaluronic acid (HA)	HaCaT cells	Synergize the UV radiation-protective ability of EGCG and HA along with imparting antioxidant and antiaging effects	[5,150]
Genistein	Nanoemulsion	Pig ear skin	New formulation for dermal delivery of genistein, with various therapeutic applications	[3,160]
Kaempferol	Submicron emulsions	Sprague Dawley rat	Promising vehicle for topical kaempferol application	[142]
Resveratrol	Solid lipid Nanoparticles	Porcine skin	Protection from photodegradation	[161]
Resveratrol + curcumin	Lipid-core Nanocapsules	Human skin	Increase skin delivery of resveratrol	[162]
	Niosomes	Cell rabbit skin	Increase skin delivery of resveratrol Increased antioxidant activity	[163]
Hesperetin, hesperidin	Microemulsion	Guinea pigs	Whitening effect	[5,164]
	Topical matrix film	Albino rabbits	Release of hesperetin in posterior of eye	[5,165]
	Microemulsion based ointment	Wistar rats	Skin irritation	[5,166]
Naringenin	Gel	HRS/J mice	Antioxidant and anti-inflammatory agent	[5,162]
	Nanoparticles	Wistar rats	Photoprotective, antioxidant agent	[5,162]

Table 3. Cont.

Flavonoid	Nanoformulation	Skin Model	Therapeutic Application	Ref.
Apigenin	Phospholipid phytosomes	Albino rats	Antioxidant agent	[5,167]
	Ethosomes	Konmin mice	Anti-inflammatory agent	[5,168]
Anthocyanin	Niosome gel	Male Wistar rats	Anti-inflammatory agent	[5,169]
Luteolin	Luteolin in olive oil	ICR mice	Anti-inflammatory agent	[5,170]
	Luteolin-loaded niosomes/Niosomal transgel	Albino Wistar rats	Treatment of arthritis	[148]
	Nanoemulsion	C57BL/6 mice	Growth promoting effect	[149]

9. Concluding Remarks

In the last few years, flavonoids have been extensively studied for their remarkable antioxidant, anti-inflammatory, anticancer, and antibacterial properties. However, their lipophilic nature and poor aqueous solubility invariably lead to limited oral bioavailability. In addition, flavonoids are rapidly degraded and metabolized in the human body, which greatly hinders their clinical application. Thus, oral delivery faces many challenges, and recently, there has been a shift towards the development of new formulations and alternative delivery routes, namely cutaneous administration. Flavonoid encapsulation is also an effective way not only to improve their pharmacokinetics but also to avoid degradation and improve safety. Various novel formulations aiming at cutaneous delivery have been developed with the goal to increase the solubility and permeability of flavonoids across the skin barrier, with minimal adverse effects. However, there is still the need to overcome limitations, such as a sustained release profile and skin retention time, to achieve an effective therapeutic dosage. Within the literature, different experimental protocols have been applied, hampering comparisons and progress to clinical evaluation. There is some indication of a relation between flavonoid's chemical structure and the most suitable delivery system, but given the diversity of the skin models used, it is not possible to establish such a relation. Other technical issues can limit the translation to industrial process, as laboratorial methods are a challenge to scale up.

Currently, several cutaneous formulations for flavonoids have been described in the literature and some have been patented, which indicates the relevance of these natural compounds, and the difficulty to certify for safety and efficacy towards translation to the market. Stakeholders need to come forward and to support long clinical trials that allow for the evaluation of adverse effects and for the identification of a dosage scheme. Clinical trials must be based on solid preclinical results obtained in appropriate models. The use of animal models (e.g., mice and rabbits) in preclinical studies present limitations related to a lack of similarity to human skin. The research community's awareness to the search for alternative models finds solutions on mimetic skin models (e.g., reconstituted human epidermis and phospholipid-based permeation assays) as data show a good correlation to human skin absorption and permeability features.

Flavonoids will continue to be explored both as a therapeutic and preventive tool for several disease conditions, alone or in combination (several synergistic effects have been described). A continuous growth in the search for novel strategies to empower flavonoid use is expected given their demonstrated potential as active agent. In the future, limitations

on the cutaneous application of flavonoids will be overcome and translational advances towards commercialization will bring novel skin products to the market and to society.

Author Contributions: Writing—original draft preparation; R.C.; writing—review and editing; S.A.C.L.; funding acquisition; P.G. and S.R.; revising the manuscript; S.A.C.L., P.G., S.R. All authors have read and agreed to the published version of the manuscript.

Funding: This work received financial support from PT national funds (FCT/MCTES, Fundação para a Ciência e Tecnologia and Ministério da Ciência, Tecnologia e Ensino Superior) through the project UIDB/50006/2020 | UIDP/50006/2020.

Acknowledgments: S.C.L. acknowledges funding from FCT (CEECIND/01620/2017). R.C. acknowledges funding from project NORTE-08-5369-PSE-000050.

Conflicts of Interest: The authors declare no conflict of interest.

References

- Kumar, S.; Pandey, A.K. Chemistry and Biological Activities of Flavonoids: An Overview. *Sci. World J.* **2013**, *4*, 1–16. [[CrossRef](#)] [[PubMed](#)]
- Panche, A.N.; Diwan, A.D.; Chandra, S.R. Flavonoids: An overview. *J. Nutr. Sci.* **2016**, *5*, e47. [[CrossRef](#)] [[PubMed](#)]
- Leonarduzzi, G.; Testa, G.; Sottero, B.; Gamba, P.; Poli, G. Design and Development of Nanovehicle-Based Delivery Systems for Preventive or Therapeutic Supplementation with Flavonoids. *Curr. Med. Chem.* **2009**, *17*, 74–95. [[CrossRef](#)] [[PubMed](#)]
- Verri, W.A.; Vicentini, F.T.M.C.; Baracat, M.M.; Georgetti, S.R.; Cardoso, R.D.R.; Cunha, T.M.; Ferreira, S.H.; Cunha, F.Q.; Fonseca, M.J.V.; Casagrande, R. *Studies in Natural Products Chemistry*, 1st ed.; Elsevier: Amsterdam, The Netherlands, 2012; Volume 36.
- Nagula, R.L.; Wairkar, S.J. Recent advances in topical delivery of flavonoids: A review. *Control. Release* **2019**, *296*, 190–201. [[CrossRef](#)] [[PubMed](#)]
- Domaszewska-Szostek, A.; Puzianowska-Kuźnicka, M.; Kuryłowicz, A. Flavonoids in Skin Senescence Prevention and Treatment. *Int. J. Mol. Sci.* **2021**, *22*, 6814. [[CrossRef](#)]
- Yang, B.; Liu, H.; Yang, J.; Gupta, V.K.; Jiang, Y. New insights on bioactivities and biosynthesis of flavonoid glycosides. *Trends Food Sci. Technol.* **2018**, *79*, 116–124. [[CrossRef](#)]
- Yang Wang, T.; Li, Q.; Shun Bi, K. Bioactive flavonoids in medicinal plants: Structure, activity and biological fate. *Asian J. Pharm. Sci.* **2017**, *13*, 12–23. [[CrossRef](#)] [[PubMed](#)]
- Rengasamy, K.R.R.; Khan, H.S.; Gowrishankar, S.; Lagoa, R.J.L.; Mahomoodally, F.M.; Khan, Z.; Suroowan, S.; Tewari, D.; Zengin, G.; Hasan, S.T.S.; et al. The role of flavonoids in autoimmune diseases: Therapeutic updates. *Pharmacol. Ther.* **2018**, *194*, 107–131. [[CrossRef](#)]
- Perez-Vizcaino, E.; Fraga, C.G. Research trends in flavonoids and health. *Arch. Biochem. Biophys.* **2018**, *646*, 107–112. [[CrossRef](#)]
- Shelke, S.J.; Shinkar, D.M.; Saudagar, R.B. Topical gel: A novel approach for development of topical drug delivery system. *Int. J. Pharm. Technol.* **2013**, *5*, 2739–2763.
- Mena, F.; Mena, A.; Mena, B. Polyphenols Nano-Formulations for Topical Delivery and Skin Tissue Engineering. In *Polyphenols in Human Health and Disease*; Elsevier Inc: Amsterdam, The Netherlands, 2014; pp. 839–848.
- Lee, S.H.; Jeong, S.K.; Ahn, S.K. An Update of the Defensive Barrier Function of Skin. *Yonsei Med. J.* **2006**, *47*, 293–306. [[CrossRef](#)]
- Ng, K.W.; Lau, W.M. *Skin Deep: The Basics of Human Skin Structure and Drug Penetration*; Springer: Berlin/Heidelberg, Germany, 2015; pp. 3–11.
- Costa Lima, S.A.; Reis, S. *Nanoparticles in Life Sciences and Biomedicine*; CRC Press: Boca Raton, FL, USA, 2018.
- Prausnitz, M.R.; Elias, P.M.; Franz, T.J.; Schmuth, M.; Tsai, J.C.; Menon, G.K.; Holleran, W.M.; Feingold, K.R. Skin Barrier and Transdermal Drug Delivery. *Dermatol.* **2012**, *3*, 2065–2073.
- Forster, M.; Bolzinger, M.A.; Fessi, H.; Briançon, S. Topical delivery of cosmetics and drugs. Molecular aspects of percutaneous absorption and delivery. *Eur. J. Dermatol.* **2009**, *19*, 309–323. [[CrossRef](#)] [[PubMed](#)]
- Alkilani, A.Z.; McCrudden, M.T.; Donnelly, R.F. Transdermal Drug Delivery: Innovative Pharmaceutical Developments Based on Disruption of the Barrier Properties of the Stratum Corneum. *Pharmaceutics* **2015**, *7*, 438–470. [[CrossRef](#)] [[PubMed](#)]
- Nguyen, A.V.; Soulika, A.M. The Dynamics of the Skin's Immune System. *Int. J. Mol. Sci.* **2019**, *20*, 1811. [[CrossRef](#)] [[PubMed](#)]
- Matejuk, A. Skin Immunity. *Arch. Immunol. & Ther. Exp.* **2018**, *66*, 45–54. [[CrossRef](#)] [[PubMed](#)]
- Kupper, T.S.; Fuhlbrigge, R.C. Immune surveillance in the skin: Mechanisms and clinical consequences. *Nat. Rev. Immunol.* **2004**, *4*, 211–222. [[CrossRef](#)] [[PubMed](#)]
- Elias, P.M. The skin barrier as an innate immune element. *Semin. Immunopathol.* **2007**, *29*, 3–14. [[CrossRef](#)] [[PubMed](#)]
- Flacher, V.; Tripp, C.H.; Maithofer, D.G.; Steinman, R.M.; Stoltzner, P.; Idoyaga, J.; Romani, N. Murine Langerin+ dermal dendritic cells prime CD8+ T cells while Langerhans cells induce cross-tolerance. *EMBO Mol. Med.* **2014**, *6*, 1191–1204. [[CrossRef](#)]
- Shklovskaya, E.; O'Sullivan, B.J.; Ng, L.C.; Roediger, B.; Thomas, R.; Weninger, W.; de St Groth, B.F. Langerhans cells are precommitted to immune tolerance induction. *Proc. Natl. Acad. Sci. USA* **2011**, *108*, 18049–18054. [[CrossRef](#)] [[PubMed](#)]

25. Nestle, F.O.; Di Meglio, P.; Qin, J.Z.; Nickoloff, B.J. Skin immune sentinels in health and disease. *Nat. Rev. Immunol.* **2009**, *9*, 679–691. [CrossRef] [PubMed]
26. Kashem, S.W.; Hari, M.; Kaplan, D.H. Skin Immunity to *Candida albicans*. *Annu. Rev. Immunol.* **2017**, *35*, 469–499. [CrossRef] [PubMed]
27. Kitashima, D.Y.; Kobayashi, T.; Woodring, T.; Idouchi, K.; Dcebel, T.; Voisin, B.; Adachi, T.; Ouchi, T.; Takahashi, H.; Nishifuji, K. Langerhans Cells Prevent Autoimmunity via Expansion of Keratinocyte Antigen-Specific Regulatory T Cells. *eBioMedicine* **2018**, *27*, 293–303. [CrossRef] [PubMed]
28. King, J.K.; Phillips, R.L.; Eriksson, A.U.; Kim, P.J.; Halder, R.C.; Lee, D.J.; Singh, R.R. Langerhans cells maintain local tissue tolerance in a model of systemic autoimmune disease. *J. Immunol.* **2015**, *195*, 464–476. [CrossRef]
29. Stavrou, E.X.; Fang, C.; Bane, K.L.; Long, A.T.; Naudin, C.; Kucukal, E.; Gandhi, A.; Brett-Morris, A.; Mumaw, M.M.; Izadmehr, S.; et al. Factor XII and uPAR upregulate neutrophil functions to influence wound healing. *J. Clin. Invest.* **2018**, *128*, 944–959. [CrossRef] [PubMed]
30. Lammermann, T.; Afonso, P.V.; Angermann, B.R.; Wang, J.M.; Kastnermuller, W.; Parent, C.A.; Germain, R.N. Neutrophil swarms require LTB4 and integrins at sites of cell death *in vivo*. *Nature* **2013**, *498*, 371–375. [CrossRef]
31. Long, H.; Zhang, G.; Wang, L.; Lu, Q. Eosinophilic skin diseases: A comprehensive review. *Clin. Rev. Allergy Immunol.* **2016**, *50*, 189–213. [CrossRef]
32. Souyouf, S.A.; Saussey, K.P.; Lupo, M.P. Nutraceuticals: A review. *Dermatol. Ther.* **2018**, *8*, 5–16. [CrossRef]
33. Marks, J.G.; Miller, J.J. *Lookingbill Marks' Principles of Dermatology*; Elsevier Health Sciences: Amsterdam, The Netherlands, 2019; pp. 2–10.
34. Zaki, N.M. Progress and Problems in Nutraceuticals Delivery. *J. Bioequiv. Bioavail.* **2014**, *6*, 75–77.
35. Routes for Drug Administration through the Skin. Available online: <https://www.msdsmanuals.com/home/drugs/administration-and-kinetics-of-drugs/drug-administration> (accessed on 17 May 2019).
36. Pouillot, A.; Dayan, N.; Polla, A.S.; Polla, L.L.; Polla, B.S. The stratum corneum: A double paradox. *J. Cosmet. Dermatol.* **2008**, *7*, 143–148. [CrossRef]
37. Prausnitz, M.R.; Mitragotri, S.; Langer, R. Current status and future potential of transdermal drug delivery. *Nat. Rev. Drug Discov.* **2004**, *3*, 115–124. [CrossRef]
38. Uchechi, O.; Ogbonna, J.D.N.; Attama, A.A. *Application of Nanotechnology in Drug Delivery*; InTech: Rijeka, Croatia, 2014.
39. Van Gele, M.; Geusens, B.; Brochez, L.; Speckaert, R.; Lambert, J. Three-dimensional skin models as tools for transdermal drug delivery: Challenges and limitations. *Expert Opin Drug Deliv.* **2011**, *8*, 705–720. [CrossRef]
40. Kulkarni, V.S. *Handbook of Non-Invasive Drug Delivery Systems*; Elsevier: Amsterdam, The Netherlands, 2010; pp. 1–36.
41. Heim, K.E.; Tagliaferro, A.R.; Bobilya, D.J. Flavonoid antioxidants: Chemistry, metabolism and structure-activity relationships. *J. Nutr. Biochem.* **2002**, *13*, 572–584. [CrossRef]
42. Sang, S.; Hou, Z.; Lambert, J.D.; Yang, C.S. Redox properties of tea polyphenols and related biological activities. *Antioxid. Redox Signal.* **2005**, *7*, 1704–1714. [CrossRef]
43. Rahman, I.; Biswas, S.K.; Kirkhani, P.A. Regulation of inflammation and redox signaling by dietary polyphenols. *Biochem. Pharmacol.* **2006**, *72*, 1439–1452. [CrossRef] [PubMed]
44. Tucker, G.; Robards, K. Bioactivity and structure of biophenols as mediators of chronic diseases. *Crit. Rev. Food Sci. Nutr.* **2008**, *48*, 929–966. [CrossRef]
45. Aroni, P.M.; Kennedy, J.A. Flavan-3-ols: Nature, occurrence and biological activity. *Mod. Nutr. Food Res.* **2008**, *52*, 79–104. [CrossRef] [PubMed]
46. Rathee, P.; Chaudhary, H.; Rathee, S.; Rathee, D.; Kumar, V.; Kohli, K. Mechanism of Action of Flavonoids as Anti-inflammatory Agents: A Review. *Inflamm. Allergy Drug Targets* **2009**, *8*, 229–235. [CrossRef] [PubMed]
47. Girwala, R.; Bhavsar, R.; Chigbu, D.G.I.; Jain, P.; Khan, Z.K. Potential role of flavonoids in treating chronic inflammatory diseases with a special focus on the anti-inflammatory activity of apigenin. *Antioxidants* **2019**, *8*, 35. [CrossRef]
48. Netea, M.G.; Balkwill, F.; Chonchol, M.; Cominelli, E.; Donath, M.Y.; Giamarello-Bourboulis, E.J.; Golenbock, D.; Griesnig, M.S.; Heneka, M.T.; Hoffman, H.M. A guiding map for inflammation. *Nat. Immunol.* **2017**, *18*, 826–831. [CrossRef] [PubMed]
49. Nguyen, N.H.; Khara, R.; Ohno-Machado, L.; Sandborn, W.J.; Singh, S. Annual burden and costs of hospitalization for high-need, high-cost patients with chronic gastrointestinal and liver diseases. *Clin. Gastroenterol. Hepatol.* **2018**, *16*, 1284–1292. [CrossRef] [PubMed]
50. Li, P.; Zheng, Y.; Chen, X. Drugs for autoimmune inflammatory diseases: From small molecule compounds to anti-TNF biologics. *Front. Pharmacol.* **2017**, *8*, 460. [CrossRef]
51. Baker, D.; Marta, M.; Pryce, G.; Giovannoni, G.; Schmierer, K. Memory B cells are major targets for effective immunotherapy in relapsing multiple sclerosis. *eBioMedicine* **2017**, *16*, 41–50. [CrossRef]
52. Mak, P.; Leung, Y.K.; Tang, W.Y.; Harwood, C.; Ho, S.M. Apigenin Suppresses Cancer Cell Growth through ERβ1. *Neoplasia* **2006**, *8*, 896–904.
53. Laguerre, M.; Lecomte, J.; Villeneuve, P. Evaluation of the ability of antioxidants to counteract lipid oxidation: Existing methods, new trends and challenges. *Prog. Lipid Res.* **2007**, *46*, 244–282. [CrossRef]
54. Yen, G.C.; Lai, H.H. Inhibition of reactive nitrogen species effects *in vitro* and *in vivo* by isoflavones and soy-based food extracts. *J. Agric. Food Chem.* **2003**, *51*, 7892–7900. [CrossRef]

55. DiSchia, M.; Parzella, L.; Manini, P.; Napoletano, A. The chemical basis of the antinitrosating action of polyphenolic cancer chemopreventive agents. *Curr. Med. Chem.* **2006**, *13*, 3133–3144. [[CrossRef](#)] [[PubMed](#)]
56. Kraemer, T.; Prakosay, I.; Date, R.A.; Sies, H.; Schewe, T. Oxidative modification of low-density lipoprotein: Lipid peroxidation by myeloperoxidase in the presence of nitrite. *Biol. Chem.* **2004**, *385*, 809–818. [[CrossRef](#)] [[PubMed](#)]
57. Van Acker, S.A.; Tromp, M.N.; Haenen, G.R.; van der Vijgh, W.J.; Bast, A.A. Flavonoids as scavengers of nitric oxide radical. *Biophys. Res. Commun.* **1995**, *214*, 755–759. [[CrossRef](#)]
58. Trujillo, M.; Ferre-Sueta, G.; Radi, R. Peroxynitrite detoxification and its biologic implications. *Antioxid. Redox Signal.* **2008**, *10*, 1607–1619. [[CrossRef](#)]
59. Sugihara, N.; Arakawa, T.; Ohnishi, M.; Furuno, K. Anti- and pro-oxidative effects of flavonoids on metal-induced lipid hydroperoxide-dependent lipid peroxidation in cultured hepatocytes loaded with alpha-linolenic acid. *Free Radic. Biol. Med.* **1999**, *27*, 1313–1323. [[CrossRef](#)]
60. Arora, A.; Nair, M.G.; Strasburg, G.M. Structure–Activity Relationships for Antioxidant Activities of a Series of Flavonoids in a Liposomal System. *Free Radic. Biol. Med.* **1998**, *24*, 1355–1363. [[CrossRef](#)]
61. Steffen, Y.; Gruber, C.; Schewe, T.; Sies, H. How do dietary flavanols improve vascular function? A position paper. *Arch. Biochem. Biophys.* **2008**, *469*, 209–219. [[CrossRef](#)] [[PubMed](#)]
62. Hsu, C.L.; Wu, C.H.; Huang, S.L.; Yen, G.C. Phenolic Compounds Rutin and o-Coumaric Acid Ameliorate Obesity Induced by High-Fat Diet in Rats. *J. Agric. Food Chem.* **2009**, *57*, 425–431. [[CrossRef](#)]
63. Amália, P.M.; Pessa, M.N.; Augusto, M.C.; Francisca, L.S. Quercetin prevents oxidative stress in cirrhotic rats. *Dig. Dis. Sci.* **2007**, *52*, 2616–2621. [[CrossRef](#)] [[PubMed](#)]
64. Zhou, B.; Wu, L.M.; Yang, L.; Liu, Z.L. Evidence for α -tocopherol regeneration reaction of green tea polyphenols in SDS micelles. *Free Radic. Biol. Med.* **2005**, *38*, 78–84. [[CrossRef](#)]
65. Frank, J.; Budek, A.; Lundh, T.; Parker, R.S.; Swanson, J.E.; Lourenço, C.F.; Gago, B.; Laranjinha, J.; Vessby, B.; Kamal-Eldin, A. Dietary flavonoids with a catechol structure increase α -tocopherol in rats and protect the vitamin from oxidation in vitro. *J. Lipid Res.* **2006**, *47*, 2718–2725. [[CrossRef](#)] [[PubMed](#)]
66. Fujisawa, S.; Ishihara, M.; Atsumi, T.; Kadoma, Y. A quantitative approach to the free radical interaction between alpha-tocopherol or ascorbate and flavonoids. *In Vivo* **2006**, *20*, 445–452. [[PubMed](#)]
67. Galati, G.; O'Brien, P.J. Potential toxicity of flavonoids and other dietary phenolics: Significance for their chemopreventive and anticancer properties. *Free Radic. Biol. Med.* **2004**, *37*, 287–303. [[CrossRef](#)]
68. García-Lafuente, A.; Guillamón, E.; Villares, A.; Ristagno, M.A.; Martínez, J.A. Flavonoids as anti-inflammatory agents: Implications in cancer and cardiovascular disease. *Inflamm. Res.* **2009**, *58*, 537–552. [[CrossRef](#)]
69. Santangelo, C.; Vari, R.; Scazzocchio, B.; Di Benedetto, R.; Filasi, C.; Masella, R. Polyphenols, intracellular signalling and inflammation. *Ann. Ist. Super. Sanità.* **2007**, *43*, 394–405.
70. Biesalski, H.K. Polyphenols and inflammation: Basic interactions. *Curr. Opin. Clin. Nutr. Metab. Care.* **2007**, *10*, 724–728. [[CrossRef](#)]
71. Kim, H.P.; Son, K.H.; Chang, H.W.; Kang, S.S. Anti-inflammatory plant flavonoids and cellular action mechanisms. *J. Pharmacol. Sci.* **2004**, *96*, 229–245. [[CrossRef](#)]
72. Yoon, J.H.; Baek, S.J. Molecular targets of dietary polyphenols with anti-inflammatory properties. *Med. J.* **2005**, *46*, 585–596. [[CrossRef](#)] [[PubMed](#)]
73. Paquay, J.B.; Haenen, G.R.; Stender, G.; Wiseman, S.A.; Tijburg, L.B.; Bast, A.J. Protection against nitric oxide toxicity by tea. *Agric. Food Chem.* **2000**, *48*, 5768–5772. [[CrossRef](#)]
74. Sutherland, B.A.; Rahman, R.M.; Appleton, I.J. Mechanisms of action of green tea catechins, with a focus on ischemia-induced neurodegeneration. *Nutr. Biochem.* **2006**, *17*, 291–306. [[CrossRef](#)]
75. Ciz, M.; Pavelková, M.; Gallová, L.; Králová, J.; Kubala, L.; Lojek, A. The influence of wine polyphenols on reactive oxygen and nitrogen species production by murine macrophages RAW 264.7. *Physiol. Res.* **2008**, *57*, 393–402. [[CrossRef](#)] [[PubMed](#)]
76. Lee, J.S.; Oh, T.Y.; Kim, Y.K.; Baik, J.H.; So, S.; Hahn, K.B.; Surh, Y.J. Protective effects of green tea polyphenol extracts against ethanol-induced gastric mucosal damages in rats: Stress-responsive transcription factors and MAP kinases as potential targets. *Mutat. Res.* **2005**, *579*, 214–224. [[CrossRef](#)]
77. Lin, Y.L.; Lin, J.K. (–)-Epigallocatechin-3-gallate Blocks the Induction of Nitric Oxide Synthase by Down-Regulating Lipopolysaccharide-Induced Activity of Transcription Factor Nuclear Factor- κ B. *Mol. Pharmacol.* **1997**, *52*, 465–472. [[CrossRef](#)] [[PubMed](#)]
78. Min, Y.D.; Choi, C.H.; Bark, H.; Son, H.Y.; Park, H.H.; Lee, S.; Park, J.W.; Park, E.K.; Shin, H.I.; Kim, S.H. Quercetin inhibits expression of inflammatory cytokines through attenuation of NF- κ B and p38 MAPK in HMC-1 human mast cell line. *Inflamm. Res.* **2007**, *56*, 210–215. [[CrossRef](#)] [[PubMed](#)]
79. Calixto, J.B.; Campos, M.M.; Otuki, M.F.; Santos, A.R. Anti-inflammatory compounds of plant origin. Part II. Modulation of pro-inflammatory cytokines, chemokines and adhesion molecules. *Planta Med.* **2004**, *70*, 93–103.
80. Comalada, M.; Ballester, I.; Bailón, E.; Sierra, S.; Xaus, J.; Gálvez, J.; de Medina, F.S.; Zarzuelo, A. Inhibition of pro-inflammatory markers in primary bone marrow-derived mouse macrophages by naturally occurring flavonoids: Analysis of the structure–activity relationship. *Biochem. Pharmacol.* **2006**, *72*, 1010–1021. [[CrossRef](#)]

81. Huang, S.M.; Wu, C.H.; Yen, G.C. Effects of flavonoids on the expression of the pro-inflammatory response in human monocytes induced by ligation of the receptor for AGEs. *Mol. Nutr. Food Res.* **2006**, *50*, 1129–1139. [[CrossRef](#)]
82. Sharma, V.; Mishra, M.; Ghosh, S.; Tewari, R.; Basu, A.; Seth, P.; Sen, E. Modulation of interleukin-1 β mediated inflammatory response in human astrocytes by flavonoids: Implications in neuroprotection. *Brain Res. Bull.* **2007**, *73*, 55–63. [[CrossRef](#)] [[PubMed](#)]
83. Kim, S.J.; Jeong, H.J.; Lee, K.M.; Myung, N.Y.; An, N.H.; Yang, W.M.; Park, S.K.; Lee, H.J.; Hong, S.H.; Kim, H.M.; et al. Epigallocatechin-3-gallate suppresses NF- κ B activation and phosphorylation of p38 MAPK and JNK in human astrocytoma U373MG cells. *J. Nutr. Biochem.* **2007**, *18*, 587–596. [[CrossRef](#)] [[PubMed](#)]
84. Kundu, J.K.; Suh, Y.J. Epigallocatechin Gallate Inhibits Phorbol Ester-Induced Activation of NF- κ B and CREB in Mouse Skin: Role of p38 MAPK. *Ann. N. Y. Acad. Sci.* **2007**, *1095*, 504–512. [[CrossRef](#)] [[PubMed](#)]
85. Ramos, S. Cancer chemoprevention and chemotherapy: Dietary polyphenols and signalling pathways. *Md. Nutr. Food Res.* **2008**, *52*, 507–526. [[CrossRef](#)] [[PubMed](#)]
86. Filip, A.; Clichici, S.; Daicoviciu, D.; Adriana, M.; Postescu, I.D. Photochemoprevention of cutaneous neoplasia through natural products. *Exp. Oncol.* **2009**, *31*, 9–15. [[PubMed](#)]
87. Ren, W.; Qiao, Z.; Wang, H.; Zhu, L.; Zhang, L. Flavonoids: Promising anticancer agents. *Med. Res. Rev.* **2003**, *23*, 519–534. [[CrossRef](#)]
88. Kandaswami, C.; Lee, L.T.; Lee, P.P.; Hwang, J.J.; Ke, F.C.; Huang, Y.T.; Lee, M.T. The antitumor activities of flavonoids. *In Vitro* **2005**, *19*, 895–909. [[PubMed](#)]
89. Soobrattee, M.A.; Bahorun, T.; Aruoma, O.I. Chemopreventive actions of polyphenolic compounds in cancer. *Biofactors* **2006**, *27*, 19–35. [[CrossRef](#)]
90. Lee, K.W.; Lee, H.J. The roles of polyphenols in cancer chemoprevention. *Biofactors* **2006**, *26*, 105–121. [[CrossRef](#)]
91. Chen, D.; Milacic, V.; Chen, M.S.; Wan, S.B.; Lam, W.H.; Huo, C.; Landis-Piwowar, K.R.; Cui, Q.C.; Wali, A.; Chan, T.H.; et al. Tea polyphenols, their biological effects and potential molecular targets. *Histol. Histopathol.* **2008**, *23*, 487–496.
92. Thangapazham, R.L.; Singh, A.K.; Sharma, A.; Warren, J.; Gaddipati, J.P.; Maheshwari, R.K. Green tea polyphenols and its constituent epigallocatechin gallate inhibits proliferation of human breast cancer cells in vitro and in vivo. *Cancer Lett.* **2007**, *245*, 232–241. [[CrossRef](#)]
93. Choi, E.J.; Kim, G.H. Daidzein causes cell cycle arrest at the G1 and G2/M phases in human breast cancer MCF-7 and MDA-MB-453 cells. *Phytomedicine* **2008**, *15*, 683–690. [[CrossRef](#)] [[PubMed](#)]
94. Jeong, J.H.; An, J.Y.; Kwon, Y.T.; Rhee, J.G.; Lee, Y.J. Effects of low dose quercetin: Cancer cell-specific inhibition of cell cycle progression. *J. Cell. Biochem.* **2009**, *106*, 73–82. [[CrossRef](#)] [[PubMed](#)]
95. Nakazato, T.; Ito, K.; Ikeda, Y.; Kizaki, M. Green Tea Component, Catechin, Induces Apoptosis of Human Malignant B Cells via Production of Reactive Oxygen Species. *Clin. Cancer Res.* **2005**, *11*, 6040–6049. [[CrossRef](#)] [[PubMed](#)]
96. Granado-Serrano, A.B.; Martín, M.A.; Bravo, L.; Goya, L.; Ramos, S.J. Quercetin induces apoptosis via caspase activation, regulation of Bcl-2, and inhibition of PI-3-kinase/Akt and ERK pathways in a human hepatoma cell line (HepG2). *Nutrients* **2006**, *136*, 2715–2721. [[CrossRef](#)] [[PubMed](#)]
97. Manna, S.; Banerjee, S.; Mukherjee, S.; Das, S.; Panda, C.K. Epigallocatechin gallate induced apoptosis in Sarcoma180 cells in vivo: Mediated by p53 pathway and inhibition in U1B, U4-U6 UsnRNAs expression. *Apoptosis* **2006**, *11*, 2267–2276. [[CrossRef](#)] [[PubMed](#)]
98. Nishikawa, T.; Nakajima, T.; Moriguchi, M.; Jo, M.; Sekoguchi, S.; Ishii, M.; Takashima, H.; Katagishi, T.; Kimura, H.; Minami, M.; et al. A green tea polyphenol, epigallocatechin-3-gallate, induces apoptosis of human hepatocellular carcinoma, possibly through inhibition of Bcl-2 family proteins. *Hepatology* **2006**, *44*, 1074–1082. [[CrossRef](#)]
99. Sah, J.F.; Balasubramanian, S.; Eckert, R.L.; Rorke, E.A. Epigallocatechin-3-gallate inhibits epidermal growth factor receptor signaling pathway: Evidence for direct inhibition of ERK1/2 and AKT kinases. *J. Biol. Chem.* **2004**, *279*, 12755–12762. [[CrossRef](#)] [[PubMed](#)]
100. Siddiqui, I.A.; Adhami, V.M.; Afaq, E.; Ahmad, N.; Mukhtar, H.J. Modulation of phosphatidylinositol-3-kinase/protein kinase B-and mitogen-activated protein kinase-pathways by tea polyphenols in human prostate cancer cells. *Cell. Biochem.* **2004**, *91*, 232–242. [[CrossRef](#)] [[PubMed](#)]
101. Vijayababu, M.R.; Arunkumar, A.; Kanagara, P.; Venkataraman, P.; Krishnamoorthy, G.; Arunakaran, J. Quercetin downregulates matrix metalloproteinases 2 and 9 proteins expression in prostate cancer cells (PC-3). *Mol. Cell. Biochem.* **2006**, *287*, 109–116. [[CrossRef](#)]
102. Zhen, M.C.; Huang, X.H.; Wang, Q.; Sun, K.; Liu, Y.J.; Li, W.; Zhang, L.J.; Cao, L.Q.; Chen, X.L. Green tea polyphenol epigallocatechin-3-gallate suppresses rat hepatic stellate cell invasion by inhibition of MMP-2 expression and its activation. *Acta Pharmacol. Sin.* **2006**, *27*, 1600–1607. [[CrossRef](#)]
103. Mojzis, J.; Varinska, L.; Mojzisova, G.; Kostova, I.; Mirossay, L. Antiangiogenic effects of flavonoids and chalcones. *Pharmacol. Res.* **2008**, *57*, 259–265. [[CrossRef](#)]
104. Khan, H.; Ullah, H.; Martorell, M.; Valdes, S.E.; Belwal, T.; Tejada, S.; Sureda, A.; Kamal, M.A. Flavonoids nanoparticles in cancer: Treatment, prevention and clinical prospects. *Semin. Cancer Biol.* **2021**, *69*, 200–211. [[CrossRef](#)]

105. Ruenroengklin, N.; Zhong, J.; Duan, X.; Yang, B.; Li, J.; Jiang, Y. Effects of Various Temperatures and pH Values on the Extraction Yield of Phenolics from Litchi Fruit Pericarp Tissue and the Antioxidant Activity of the Extracted Anthocyanins. *Int. J. Mol.* **2008**, *9*, 1333–1341. [[CrossRef](#)]
106. Palafox-Carlos, H.; Ayala-Zavala, J.F.; González-Aguilar, G.A. The role of dietary fiber in the bioaccessibility and bioavailability of fruit and vegetable antioxidants. *J. Food Sci.* **2011**, *76*, R6–R15. [[CrossRef](#)]
107. Li, C.; Lee, M.J.; Sheng, S.; Meng, X.; Prabhu, S.; Winnik, B.; Huang, B.; Chung, J.Y.; Yan, S.; Ho, C.T.; et al. Structural identification of two metabolites of catechins and their kinetics in human urine and blood after tea ingestion. *Chem. Res. Toxicol.* **2000**, *13*, 177–184. [[CrossRef](#)]
108. Lambert, J.D.; Sang, S.; Yang, C.S. Biotransformation of green tea polyphenols and the biological activities of those metabolites. *Mol. Pharm.* **2007**, *4*, 819–825. [[CrossRef](#)] [[PubMed](#)]
109. Schubert, W.; Eriksson, U.; Edgar, B.; Cullberg, G.; Hedner, T. Flavonoids in grapefruit juice inhibit the in vitro hepatic metabolism of 17 β -estradiol. *Eur. J. Drug Metab. Pharmacol.* **1995**, *20*, 219–224. [[CrossRef](#)]
110. Ramadan, D.; McCrudden, M.T.C.; Courtenay, A.J.; Donnelly, R.F. Enhancement strategies for transdermal drug delivery systems: Current trends and applications. *Drug Deliv. Transl. Res.* **2021**, *11*, 1–34.
111. Cermak, R.; Wolfram, S. Effect of dietary flavonoids on pathways involved in drug metabolism. *Expert Opin. Drug Metab. Toxicol.* **2008**, *4*, 17–35. [[CrossRef](#)]
112. Rahman, H.S.; Othman, H.H.; Hammadi, N.I.; Yeap, S.K.; Amin, K.M.; Samad, N.A.; Alitheen, N.B. Novel drug delivery systems for loading of natural plant extracts and their biomedical applications. *Int. J. Nanomed.* **2020**, *15*, 2439. [[CrossRef](#)]
113. Jain, K.K. Nanomedicine: Application of nanobiotechnology in medical practice. *Med. Princ. Pract.* **2008**, *17*, 89–101. [[CrossRef](#)] [[PubMed](#)]
114. Farokhzad, O.C.; Langer, R. Impact of nanotechnology on drug delivery. *ACS Nano.* **2009**, *3*, 16–20. [[CrossRef](#)] [[PubMed](#)]
115. Zhang, L.; Gu, F.X.; Chan, J.M.; Wang, A.Z.; Langer, R.S.; Farokhzad, O.C. Nanoparticles in medicine: Therapeutic applications and developments. *Clin. Pharmacol. Ther.* **2008**, *83*, 761–769. [[CrossRef](#)] [[PubMed](#)]
116. Emerich, D.F.; Thanos, C.G. The pinpoint promise of nanoparticle-based drug delivery and molecular diagnosis. *Biomol. Eng.* **2006**, *23*, 171–184. [[CrossRef](#)]
117. Emerich, D.F.; Thanos, C.G. Targeted nanoparticle-based drug delivery and diagnosis. *J. Drug Target.* **2007**, *15*, 163–183. [[CrossRef](#)]
118. Torchilin, V.P. Recent advances with liposomes as pharmaceutical carriers. *Nat. Rev. Drug Discov.* **2005**, *4*, 145–160. [[CrossRef](#)]
119. Klibanov, A.L.; Maruyama, K.; Torchilin, V.P.; Huang, L. Amphipathic polyethylene glycols effectively prolong the circulation time of liposomes. *FEBS Lett.* **1990**, *268*, 235–238. [[CrossRef](#)]
120. Simões, S.; Moreira, J.N.; Fonseca, C.; Düzgüneş, N.; de Lima, M.C. On the formulation of pH-sensitive liposomes with long circulation times. *Adv. Drug Deliv. Rev.* **2004**, *56*, 947–965. [[CrossRef](#)]
121. Gasco, M.R. Lipid nanoparticles: Perspectives and challenges. *Adv. Drug Deliv. Rev.* **2007**, *59*, 377–378. [[CrossRef](#)]
122. Faraji, A.H.; Wipf, P. Nanoparticles in cellular drug delivery. *Med. Chem.* **2009**, *17*, 2950–2962. [[CrossRef](#)]
123. Benson, H.A.E.; Grice, J.E.; Mohammed, Y.; Namjoshi, S.; Roberts, M.S. Topical and transdermal drug delivery: From simple poisons to smart technologies. *Curr. Drug Deliv.* **2019**, *16*, 444–460. [[CrossRef](#)] [[PubMed](#)]
124. Kreuter, J. Nanoparticles. In *Encyclopaedia of Pharmaceutical Technology*; Marcel Dekker Inc: New York, NY, USA, 1994.
125. Singh, R.; Lillard, J.W., Jr. Nanoparticle-based targeted drug delivery. *Exp. Mol. Pathol.* **2009**, *86*, 215–223. [[CrossRef](#)] [[PubMed](#)]
126. Soppimath, K.S.; Aminabhavi, T.M.; Kulkarni, A.R.; Rudzinski, W.E. Biodegradable polymeric nanoparticles as drug delivery devices. *J. Control. Release* **2001**, *70*, 1–20. [[CrossRef](#)]
127. Panyam, J.; Sahoo, S.K.; Prabha, S.; Bargar, T.; Labhasetwar, V. Fluorescence and electron microscopy probes for cellular and tissue uptake of poly (D, L-lactide-co-glycolide) nanoparticles. *Int. J. Pharm.* **2003**, *262*, 1–11. [[CrossRef](#)]
128. Bala, I.; Hariharan, S.; Kumar, M.N. Critical Reviews™ in Therapeutic Drug Carrier Systems. *Crit. Rev. Ther. Drug Carrier Syst.* **2004**, *21*, 387–422. [[CrossRef](#)] [[PubMed](#)]
129. Zhang, K.; Serizawa, T.J. Preparation and Characterization of Surfactant-Free Nanoparticles Composed of Stereoregular Poly(methyl methacrylate)s. *Nanosci. Nanotechnol.* **2009**, *9*, 591–597. [[CrossRef](#)]
130. Chana, J.; Forbes, B.; Jones, S.A. The synthesis of high molecular weight partially hydrolysed poly (vinyl alcohol) grades suitable for nanoparticle fabrication. *J. Nanosci. Nanotechnol.* **2008**, *8*, 5739–5747. [[CrossRef](#)]
131. Vauthier, C.; Dubernet, C.; Fattal, E.; Pinto-Alphandary, H.; Couvreur, P. Poly (alkylcyanoacrylates) as biodegradable materials for biomedical applications. *Adv. Drug Deliv. Rev.* **2003**, *55*, 519–548. [[CrossRef](#)]
132. Wang, H.; Helliwell, K. Determination of flavonols in green and black tea leaves and green tea infusions by high-performance liquid chromatography. *Food Res. Int.* **2001**, *34*, 223–227. [[CrossRef](#)]
133. Casagrande, R.; Georgetti, S.R.; Verri, W.A., Jr.; Borin, M.F.; Lopez, R.F.; Fonseca, M.J. In vitro evaluation of quercetin cutaneous absorption from topical formulations and its functional stability by antioxidant activity. *Int. J. Pharm.* **2007**, *328*, 183–190. [[CrossRef](#)] [[PubMed](#)]
134. Casagrande, R.; Georgetti, S.R.; Verri, W.A., Jr.; Dorta, D.J.; dos Santos, A.C.; Fonseca, M.J. Protective effect of topical formulations containing quercetin against UVB-induced oxidative stress in hairless mice. *J. Photochem. Photobiol.* **2006**, *84*, 21–27. [[CrossRef](#)] [[PubMed](#)]
135. Vicentini, F.T.; Casagrande, R.; Verri, W.A., Jr.; Georgetti, S.R.; Bentley, M.V.; Fonseca, M.J. Quercetin in lyotropic liquid crystalline formulations: Physical, chemical and functional stability. *AAPS Pharm. Sci. Technol.* **2008**, *9*, 591–596. [[CrossRef](#)]

136. Scalia, S.; Mezzena, M.J. Incorporation of quercetin in lipid microparticles: Effect on photo-and chemical-stability. *Pharm. Biomed. Anal.* **2009**, *49*, 90–94. [[CrossRef](#)] [[PubMed](#)]
137. Tan, Q.; Liu, W.; Guo, C.; Zhai, G. Design of self-assembling peptides and their biomedical applications. *Int. J. Nanomed.* **2011**, *6*, 1621.
138. Nan, W.; Ding, L.; Chen, H.; Khan, F.U.; Yu, L.; Sui, X.; Shi, X. Discovery of the consistently well-performed analysis chain for SWATH-MS based pharmacoproteomic quantification. *Front. Pharmacol.* **2018**, *9*, 1–11.
139. Bose, S.; Michniak-Kohn, B. Preparation and characterization of lipid based nanosystems for topical delivery of quercetin. *Eur. J. Pharm. Sci.* **2013**, *48*, 442–452. [[CrossRef](#)]
140. Chessa, M.; Caddeo, C.; Valenti, D.; Manconi, M.; Sinico, C.; Fadda, A.M. Effect of penetration enhancer containing vesicles on the percutaneous delivery of quercetin through new born pig skin. *Pharmaceutics* **2011**, *3*, 497–509. [[CrossRef](#)]
141. Caddeo, C.; Diez-Sales, O.; Pons, R.; Fernández-Busquets, X.; Fadda, A.M.; Manconi, M. Topical Anti-Inflammatory Potential of Quercetin in Lipid-Based Nanosystems: In Vivo and In Vitro Evaluation. *Pharmaceut. Res.* **2014**, *31*, 959–968. [[CrossRef](#)]
142. Chao, Y.; Huang, C.-T.; Fu, L.-T.; Huang, Y.-B.; Tsai, Y.-H.; Wu, P.-C. The Effect of Submicron Emulsion Systems on Transdermal Delivery of Kaempferol. *Chem. Pharmaceut. Bull.* **2012**, *60*, 1171–1175. [[CrossRef](#)]
143. Wang, L.; Tu, Y.C.; Lian, T.W.; Hung, J.T.; Yen, J.H.; Wu, M.J. Distinctive Antioxidant and Antiinflammatory Effects of Flavonols. *J. Agric. Food Chem.* **2006**, *54*, 9798–9804. [[CrossRef](#)] [[PubMed](#)]
144. Huang, Z.-R.; Hung, C.-F.; Lin, Y.-K.; Fang, J.-Y. In vitro and in vivo evaluation of topical delivery and potential dermal use of soy isoflavones genistein and daidzein. *Int. J. Pharm.* **2008**, *364*, 36–44. [[CrossRef](#)] [[PubMed](#)]
145. Munyendo, W.L.L.; Zhang, Z.; Abbad, S.; Waddad, A.Y.; Lv, H.; Baraza, L.D.; Zhou, J. Micelles of TPGS modified apigenin phospholipid complex for oral administration: Preparation, in vitro and in vivo evaluation. *J. Biomed. Nanotechnol.* **2013**, *9*, 2034–2047. [[CrossRef](#)] [[PubMed](#)]
146. Shen, L.N.; Zhang, Y.T.; Wang, Q.; Xu, L.; Feng, N.P. Enhanced in vitro and in vivo skin deposition of apigenin delivered using ethosomes. *Int. J. Pharm.* **2014**, *460*, 280–288. [[CrossRef](#)] [[PubMed](#)]
147. Karthivashan, G.; Masarudin, M.J.; Umar Kura, A.; Abas, F.; Fakurazi, S. Optimization, formulation, and characterization of multiflavonoids-loaded flavanosome by bulk or sequential technique. *Int. J. Nanomed.* **2016**, *11*, 3417–3434. [[CrossRef](#)] [[PubMed](#)]
148. Abidin, L.; Mujeeb, M.; Imam, S.S.; Aqil, M.; Khurana, D. Enhanced transdermal delivery of luteolin via non-ionic surfactant-based vesicle: Quality evaluation and anti-arthritis assessment. *Drug Deliv.* **2016**, *23*, 1069–1074. [[CrossRef](#)]
149. Shin, K.; Choi, H.; Song, S.K.; Yu, J.W.; Lee, J.Y.; Choi, E.J.; Lee, D.H.; Do, S.H.; Kim, J.W. Nanoemulsion Vehicles as Carriers for Follicular Delivery of Luteolin. *ACS Biomater. Sci. Eng.* **2018**, *4*, 1723–1729. [[CrossRef](#)]
150. Avadhani, K.S.; Manikkath, J.; Tiwari, M.; Chandrasekhar, M.; Godavarthi, A.; Vidya, S.M.; Hariharapura, R.C.; Kalthur, G.; Udupa, N.; Mutalik, S. Skin delivery of epigallocatechin-3-gallate (EGCG) and hyaluronic acid loaded nano-transfersomes for antioxidant and anti-aging effects in UV radiation induced skin damage. *Drug Deliv.* **2017**, *4*, 61–74. [[CrossRef](#)] [[PubMed](#)]
151. Fang, J.Y.; Hung, C.F.; Hwang, T.L.; Huang, Y.L. Physicochemical characteristics and in vivo deposition of liposome-encapsulated tea catechins by topical and intratumor administrations. *J. Drug Target* **2005**, *13*, 19–27. [[CrossRef](#)] [[PubMed](#)]
152. Fang, J.Y.; Hwang, T.L.; Huang, Y.L.; Fang, C.L. Enhancement of the transdermal delivery of catechins by liposomes incorporating anionic surfactants and ethanol. *Int. J. Pharm.* **2006**, *310*, 131–138. [[CrossRef](#)] [[PubMed](#)]
153. Bhia, M.; Motallebi, M.; Abadi, B.; Zarepour, A.; Pereira-Silva, M.; Saemnejad, F.; Santos, A.C.; Zarrabi, A.; Melero, A.; Jafari, S.M.; et al. Naringenin Nano-Delivery Systems and Their Therapeutic Applications. *Pharmaceutics* **2021**, *13*, 291. [[CrossRef](#)] [[PubMed](#)]
154. Nasr, M.; Al-Karak, R. Nanotechnological Innovations Enhancing the Topical Therapeutic Efficacy of Quercetin: A Succinct Review. *Curr. Drug Deliv.* **2020**, *17*, 270–278. [[CrossRef](#)]
155. Guan, F.; Wang, Q.; Bao, Y.; Chao, Y. Anti-rheumatic effect of quercetin and recent developments in nano formulation. *RSC Adv.* **2021**, *11*, 7280–7293. [[CrossRef](#)]
156. Scalia, S.; Franceschini, E.; Bertelli, D.; Iannuccelli, V. Comparative Evaluation of the Effect of Permeation Enhancers, Lipid Nanoparticles and Colloidal Silica on in vivo Human Skin Penetration of Quercetin. *Skin Pharmacol. Physiol.* **2013**, *25*, 57–67. [[CrossRef](#)] [[PubMed](#)]
157. Sarkar, S.; Mandal, S.; Sinha, J.; Mukhopadhyay, S.; Das, N.; Basu, M.K. Quercetin: Critical evaluation as an antileishmanial agent in vivo in hamsters using different vesicular delivery modes. *J. Drug Target* **2002**, *10*, 573–578. [[CrossRef](#)] [[PubMed](#)]
158. Hatahet, T.; Morille, M.; Shamseddin, A.; Aubert-Pouëssel, A.; Devoisselle, J.M.; Begu, S. Dermal quercetin lipid nanocapsules: Influence of the formulation on antioxidant activity and cellular protection against hydrogen peroxide. *Int. J. Pharm.* **2017**, *518*, 167–176. [[CrossRef](#)]
159. Tan, Q.; Liu, W.; Zhai, G. Preparation and evaluation of quercetin-loaded lecithin-chitosan nanoparticles for topical delivery. *Int. J. Nanomed.* **2011**, *6*, 1621–1630.
160. Silva, A.P.; Nunes, B.R.; De Oliveira, M.C.; Koester, L.S.; Mayorga, P.; Bassani, V.L.; Teixeira, H.F. Development of topical nanoemulsions containing the isoflavone genistein. *Pharmazie* **2009**, *64*, 32–35. [[PubMed](#)]
161. Carlotti, M.; Sapino, S.; Ugazio, E.; Gallarate, M.; Moiel, S.J. Resveratrol in Solid Lipid Nanoparticles. *Dispers. Sci. Technol.* **2012**, *33*, 465–471. [[CrossRef](#)]
162. Friedrich, R.B.; Kann, B.; Coradini, K.; Offerhaus, H.L.; Beck, R.C.; Windbergs, M. Skin penetration behavior of lipid-core nanocapsules for simultaneous delivery of resveratrol and curcumin. *Eur. J. Pharm. Sci.* **2015**, *78*, 204–213. [[CrossRef](#)]

163. Tavano, L.; Muzzalupo, R.; Picci, N.; de Cindio, B. Co-encapsulation of lipophilic antioxidants into niosomal carriers: Percutaneous permeation studies for cosmetic applications. *Colloids Surf. B* **2014**, *114*, 144–149. [[CrossRef](#)]
164. Tsai, Y.; Lee, K.; Huang, Y.; Huang, C. In vitro permeation and in vivo whitening effect of topical hesperetin microemulsion delivery system. *Int. J. Pharm.* **2010**, *388*, 257–262. [[CrossRef](#)] [[PubMed](#)]
165. Adelli, G.R.; Hingorani, T.; Punyamurthula, N.; Pracheta, S.; Majumdar, S. Evaluation of topical hesperetin matrix film for back-of-the-eye delivery. *Eur. J. Pharm. Biopharm.* **2015**, *92*, 74–82. [[CrossRef](#)]
166. Kilot, V.; Sapkal, N.; Vaidya, G. Design and development of novel microemulsion based topical formulation of Hesperidin. *Int. J. Pharm. Pharm. Sci.* **2015**, *7*, 142–148.
167. Haritima, J. Paper reduction using scs-slm technique in stfbc mimo-ofdm. *ARPN J. Eng. Appl. Sci.* **2017**, *12*, 3218–3221.
168. Telange, D.R.; Patil, A.T. Formulation and characterization of an apigenin-phospholipid phytosome (APLC) for improved solubility, in vivo bioavailability, and antioxidant potential. *Eur. J. Pharm. Sci.* **2016**, *108*, 36–49. [[CrossRef](#)]
169. Pripem, A.; Limsitthichaikoon, S.; Thappasaraong, S.; Complex, A.A. Preparation, Anti-inflammatory Activity of Topical Anthocyanins by Complexation and Niosomal Encapsulation. *Int. J. Chem. Mol. Eng.* **2015**, *9*, 133–137.
170. Baolin, L.; Weiwei, W.; Ning, T. Topical Application of Luteolin Inhibits Scratching Behavior Associated with Allergic Cutaneous Reaction in Mice. *Planta Med.* **2005**, *71*, 424–428. [[CrossRef](#)] [[PubMed](#)]

This article is an open access article distributed under the terms and conditions of the Creative Commons Attribution (CC BY) license (<https://creativecommons.org/licenses/by/4.0/>).

3. Materials and Methods

3.1. Materials

For lipid nanoparticles preparation, cetyl palmitate was kindly supplied by Gatefossé (Nanterre, France), Tween[®] 80, quercetin (2-(3,4-dihydroxyphenyl)-3,5,7-trihydroxy-4Hchromen-4-one), 2,2-azinobis (3-ethylbenzothiazoline-6-sulfonic acid) (ABTS), and 1,1-diphenyl-2-picrylhydrazyl (DPPH) were obtained from Sigma-Aldrich[®] (St Louis, MO, USA), and pomegranate oil was purchased at a local herb shop (Porto, Portugal). Ethanol absolute ($\geq 99,8\%$) was obtained from Fisher Chemical (Thermo Fisher Scientific, Loughborough, UK).

Hydrogels were prepared with sodium alginate (SA) purchased from ACROS Organics[™] (Thermo Fisher Scientific, Waltham, MA, USA), and poly(vinyl alcohol) (PVA) from Sigma-Aldrich[®] (St Louis, MO, USA).

The preparation of PVPA_{SC} membranes, i.e. lipid-based membranes designed to mimic the *stratum corneum*, involved the use of egg phosphatidylcholine (EPC), cholesterol, free fatty acids, ceramides and cholesteryl sulphate obtained from Sigma-Aldrich[®] (St Louis, MO, USA).

For high performance liquid chromatography (HPLC) analysis of quercetin, methanol ($\geq 99,8\%$ HPLC grade) and acetonitrile ($\geq 99,8\%$ HPLC grade) were obtained from Fisher Chemical (Thermo Fisher Scientific, Loughborough, UK), and dimethyl sulphoxide (DMSO, $\geq 99,9\%$) was obtained from Sigma-Aldrich[®] (St Louis, MO, USA).

Cellular assays were performed using two cell lines: L929 fibroblast cell line and HaCaT human keratinocyte purchased from Cell Lines Service (CLS, Eppelheim, Germany). Cell culture was conducted using culture medium Dulbecco's Modified Eagle's Medium (DMEM), supplemented with fetal bovine serum (FBS) and penicillin-streptomycin (10000 U/mL) acquired from Gibco[®] (Invitrogen Corporation, United Kingdom). Trypsin-EDTA 0.25% (v/v) was purchased from Gibco[®] (Invitrogen Corporation, UK), and isopropanol and 3-[4,5-dimethylthiazol-2-yl]-2,5-diphenyltetrazolium bromide (MTT) from Sigma-Aldrich Co. (Merck KGaA, Germany). FITC Annexin V Apoptosis Detection Kit with 7-AAD was obtained from Biolegend (United Kingdom). 2',7'-dichlorodihydrofluorescein diacetate (DCFH-DA) and hydrogen peroxide were acquired from Sigma-Aldrich[®] (St Louis, MO, USA).

All experiments were performed with double-deionized water (resistivity = 18.2 MΩ·cm) supplied through an ultra-pure water system (Arium Pro, Sartorius AG, Göttingen, Germany). Additionally, the pH measurements were executed in a Crison pH meter GLP 22, which was equipped with a Crison 52-02 tip (Crison; Barcelona, Spain).

3.2. Methods

3.2.1. Production of Nanostructured Lipid Carriers and Solid Lipid Nanoparticles

Quercetin was incorporated into NLCs and SLNs by hot emulsification followed by sonication.¹ In this process, drugs, or bioactives, are premixed with lipids and, subsequently, the temperature is raised to 5-10 °C above the temperature associated with the lipid that has the highest melting point.^{1,2} Then, the resulting mixture is mixed with a surfactant solution at an identical temperature. As a result, the surfactant adsorption at the oil and water interface is going to lower the energy barrier required to form new surfaces, as well as a stabilized nanoemulsion.^{1,3} Afterwards, a nanoemulsion is synthesized by applying external energy, which, in this case, was provided in the form of sound waves by sonication.² Following, the nanoemulsion is cooled down and the melted lipids return to the solid state. The resulting particle size depends directly on the energy dissipation, as well as on the surfactant nature.³

The amount of cetyl palmitate (150 mg), selected amount of quercetin (Table 3.1), and the defined ratio liquid lipid/solid lipid (Table 3.1) were heated separately from the Tween 80 solution in a water bath at 60°C to solubilize the lipids and the drug. The volume of aqueous phase containing Tween 80 (Table 3.1) was added into the lipid phase and homogenized using a probe sonicator (VCX130; Sonics & Materials, Inc., Newtown, CT, USA), at 70% of amplitude for 5 minutes. Similarly, SLNs were prepared using cetyl palmitate as the solid lipid, in the same amount as the lipidic content of optimized NLCs (section 3.2.3), quercetin and Tween 80. In addition, drug-free NLCs and SLNs were prepared using the previously described method.

3.2.2. Experimental Design: Box-Behnken Design

The NLCs prepared using pomegranate oil (PO) as the liquid lipid were optimized using a three factor-three level Box–Behnken design (BBD) with 15 runs. This is a commonly applied type of response surface design used for optimizing the response of a system, or process, that is controlled by various factors.⁴ Particularly, BBD is composed by a

central point together with the middle points of the edges of a cube circumscribed on a sphere of radius $\sqrt{2}$ (Figure 3.1).^{5,6}

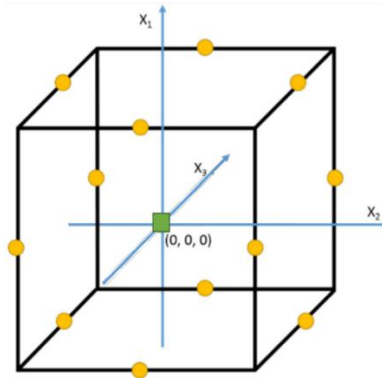


Figure 3.1 - BBD for three variables x_1 , x_2 and x_3 ; the circles represent experimental points and square is the central point.⁷ Copyright 2022 Authors licensed under a Creative Commons Attribution (CC BY) license.

BBD approach is efficient, since it requires a reduced number of experiments when compared to a full factorial design.⁷ Furthermore, as the BBD does not involve any experimental points at the vertices of the cube, it can be advantageous when the experiments at these points are costly or unfeasible due to practical reasons.⁸ The number of experimental runs is determined by the following expression:⁷

$$2k(k - 1) + c_p \tag{1}$$

Where k is the number of factors and c_p represents the number of replicates located at the central point.

The chosen independent variables were (X_1) the liquid lipid/solid lipid ratio, (X_2) the quantity of water and, (X_3) the quantity of drug. All the other parameters were maintained constant, namely the type and amount of solid lipid (cetyl palmitate, 150 mg), type and amount of surfactant (Tween 80, 47 mg), and the method of nanoparticle production (hot emulsification followed by ultrasonication). The correspondent responses were analyzed in terms of Y_1 = mean particle diameter, Y_2 = polydispersity index (PDI), Y_3 = % of loaded drug and Y_4 = drug loading (DL), and the data calculated through the regression coefficient associated with each response, following the equation:

$$Y = b_0 + b_1X_1 + b_2X_2 + b_3X_3 + b_{12}X_1X_2 + b_{13}X_1X_3 + b_{23}X_2X_3 + b_{11}X_1^2 + b_{22}X_2^2 + b_{33}X_3^2$$

In which the Y refers to the response, b_0 , represents the results average and b_1 to b_{33} are the associated coefficient. X_1 , X_2 and X_3 represent the lipid liquid/solid lipid ratio (X_1); water volume (X_2); and quantity of drug (X_3) correspondently. X_iX_j and X_i^2 express the

combination of factors and quadratic terms, correspondently. The optimal formulation resulted of the analyzes of the variables using STATISTICA 10 software and considering the optimal conditions including maximal drug encapsulation and drug loading.

3.2.3. Validation of the Optimized Quercetin-Loaded Nanostructured Lipid Carriers

The optimal formulation indicated by STATISTICA 10 software, that resulted of the analyses of the variables studied in the Box-Behnken experimental design, was prepared in triplicate, in order to validate the theoretical data predicted by the software, namely, size, PDI, entrapment efficiency (EE) and DL. For optimized NLCs preparation, the lipids were melted with 1.32% (2.49 mg) of a previously prepared solution of quercetin dissolved in ethanol 70% (v/v) and homogenized in 4 mL of double-deionized water (Table 3.1) Unloaded NLCs and quercetin-loaded and unloaded SLNs were also prepared for comparison.

Table 3.1 - Composition of optimized quercetin-loaded NLCs.

Compound	Quantity (mg)
Cetyl Palmitate	150
Pomegranate oil	39
Tween 80	47
Quercetin	2.5

3.2.4. Characterization of Quercetin-Loaded Nanoparticles

3.2.4.1. Determination of Nanoparticles' Size and Zeta Potential

The average size, polydispersity index (PDI), and surface potential of all the optimized formulations under study were measured in a ZetaPALS zeta potential analyzer (Brookhaven Instruments Corporation, Holtsville, NY, USA). Before the analysis, the samples were diluted by a factor of 200 in double-deionized water.

The average size and PDI were determined through dynamic light scattering (DLS), a technique also known as photon correlation spectroscopy or quasi-elastic light scattering. This method measures the Brownian motion of particles in suspension, which results from the bombardment of solvent molecules that surround a particle, relating such

motion to the particle size.^{9,10} This measure is dependent on temperature as well as on the solvent viscosity.⁹ A scheme of a general DLS setup is represented in Figure 3.2.

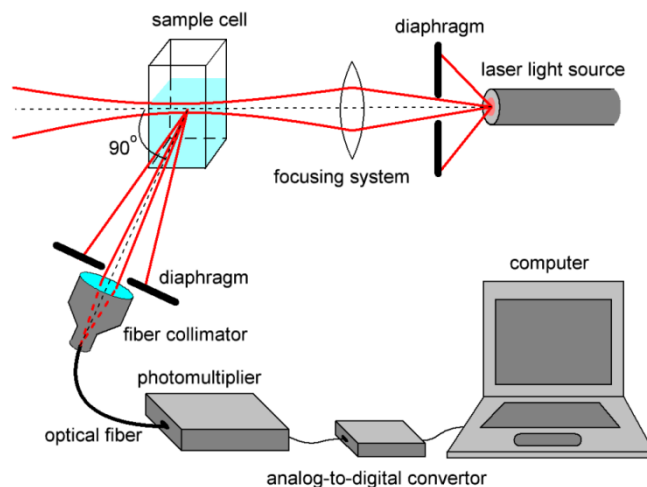


Figure 3.2 - Scheme of a general DLS setup.¹¹ Copyright 2020 Authors licensed under a Creative Commons Attribution (CC BY) license.

When particles are illuminated by a laser over time, the scattered light intensity fluctuates at a rate which is dependent on the particle size. Particularly, smaller particles are projected a larger distance by the solvent molecules and they also move quicker, leading to fast fluctuations. On the other hand, bigger particles will diffuse slower, originating slower fluctuations.¹² In a DLS instrument, the intensity of the light that reaches the detector, at any instant, is dependent on the interference pattern resulting from the light scattered by all the particles in the scattering volume. The scattered light will either result in mutually destructive phases, which will cancel each other out, or in mutually constructive phases, originating a detectable signal.¹²

Then, a correlogram, where the raw correlation function is plotted (Figure 3.3), is produced.¹³

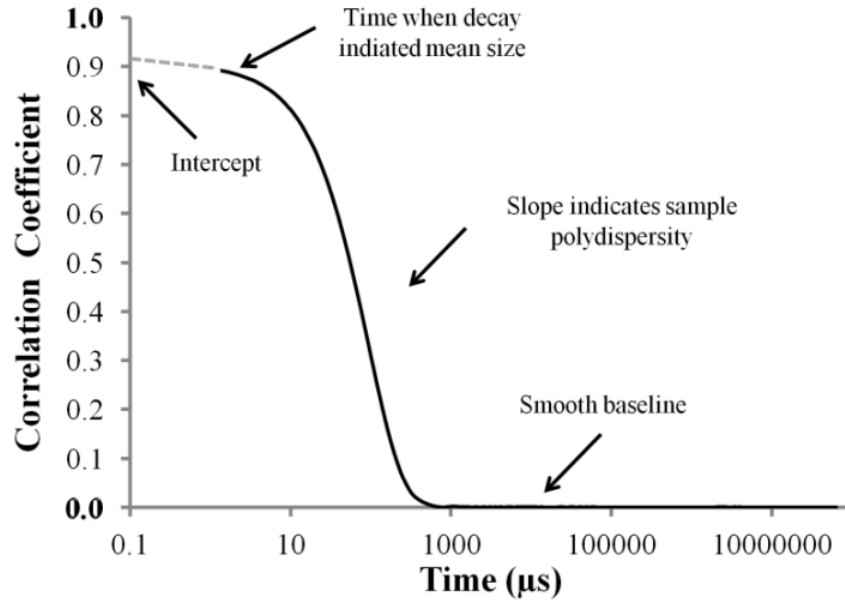


Figure 3.3 - Raw correlation function.¹³ Copyright 2015 Authors licensed under a Creative Commons Attribution (CC BY) license.

As a result, if the particles have a spherical shape and do not interact, their hydrodynamic diameter, d_h , can be determined from the diffusion coefficient by considering the Stokes-Einstein equation:¹⁴

$$d_h = \frac{K_b T}{3\pi\eta D} \quad (3)$$

Where K_b is the Boltzmann constant ($1.38064852 \times 10^{-23}$ J/K), T is the temperature, η represents the absolute viscosity of the medium, and D is the diffusion coefficient.

DLS also provides information about the size distribution of the nanoparticles in the form of a polydispersity index, which is given by the slope of the correlation function (Figure 3.3). Particularly, steeper lines indicate more monodispersed the systems.¹⁵ In our experiments, 6 runs of 2 minutes were completed to determine particle size and the polydispersity index of the produced samples.

The surface potential of the fabricated samples was determined through the zeta potential. This parameter assesses the potential difference among the electric double layer (EDL) associated with electrophoretically mobile particles and the dispersant medium around them in the sliding plane (Figure 3.4).¹⁶

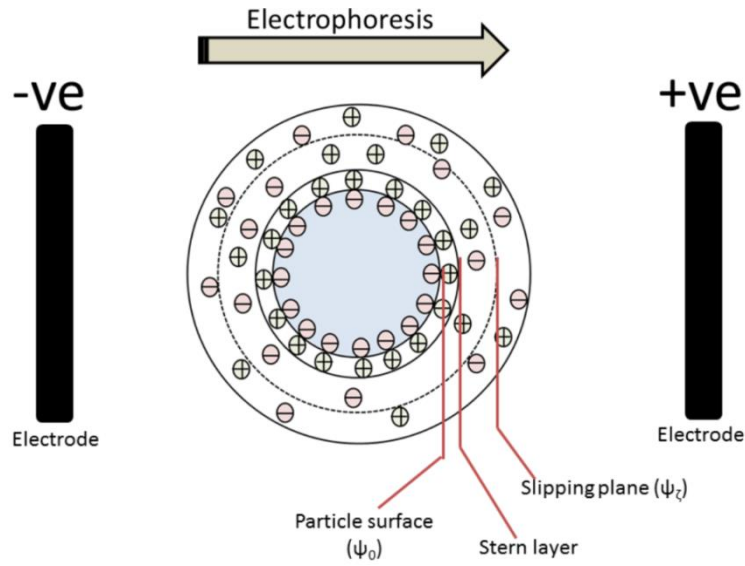


Figure 3.4 - EDL of a negatively charged nanoparticle during electrophoresis.¹⁷ Reprinted from Journal of Controlled Release 10, Bhattacharjee, S., DLS and zeta potential – What they are and what they are not?, 337-351, Copyright (2016), with permission from Elsevier.

As can be observed in the above figure, at the particle surface there is a strongly adhered layer, known as stern layer, composed by ions of opposite charge. Additionally, there is the development of a diffuse layer that is constituted by positive and negative charges.^{17,18} This double layer adsorbed on the particle surface is known as EDL and its composition depends on multiple factors, such as pH, ionic strength, or concentration.¹⁹

As a result, during electrophoresis, the particle with the adsorbed EDL will move in the direction of the electrode with the opposite charge and the slipping plane becomes the interface between the mobile particles and dispersant. The zeta potential is the electrokinetic potential at this slipping plane.¹⁷

Since the zeta potential cannot be directly measured, it is determined by the electrophoretic mobility (μ_e) of charged particles under the application of an external electric field. Firstly, μ_e is calculated by the following equation:^{17,20}

$$\mu_e = \frac{V}{E} \tag{4}$$

Where V is particle velocity ($\mu\text{m/s}$) and E the applied electric field strength (V/cm). Then, the zeta potential is calculated using the Henry's equation:^{17,20}

$$\mu_e = \frac{2\varepsilon_r\varepsilon_0\xi f(Ka)}{3\eta} \tag{5}$$

Where ε_r is the relative permittivity/dielectric constant, ε_0 represents the vacuum permittivity, ξ is the zeta potential, $f(Ka)$ is the Henry's function, and η represents viscosity at the experimental temperature.

In the produced samples, the zeta potential was measured with an electrode working at a scattering angle of 90° at 20°C . 6 runs of 10 cycles were carried out for each assay and the Smoluchowski mathematical model was employed to acquire the respective measurements. Three independent batches of each formulation were examined, in terms of size and zeta potential, as described.

3.2.4.2. Morphology Evaluation

The nanoparticles' morphology was evaluated through transmission electron microscopy (TEM). In this imaging technique, a highly focused beam of electrons passes through a thin sample. As a result, those particles pass through the sample, they are either transmitted or scattered by the atoms in the analyzed material, which are detected.²¹ Those electrons provide detailed information about the interior of the sample, its crystalline structure, morphology, and stress state information, allowing the formation of an image.²²

For the TEM analysis of the samples considered in this work, $20\ \mu\text{L}$ of each optimized type of lipid nanoparticle was set in a copper grid for 1 minute, using 0.75% (w/v) uranyl acetate as a contrast agent. The grid was submitted to an accelerating voltage equal to 60 kV, and images were acquired using a JEM-1400 transmission electron microscope (Jeol JEM-1400, JEOL, Ltd., Tokyo, Japan).

3.2.4.3. Encapsulation Efficiency and Drug Loading Determination

The encapsulation efficiency (EE) of the previously prepared nanoparticles was determined by analyzing the amount of quercetin loaded in each formulation. The EE% and DL% were determined using direct quantification method. Briefly, NLCs and SLNs were diluted 1:200 in water, placed into centrifugal filter units (Amicon® Ultra Centrifugal Filters Ultracell-50 kDa, MERCK Millipore, Ltd.; Cork, Ireland) and centrifuged at $2500\ \text{xg}$ (Allegra®X-15R centrifuge, Beckman Coulter, Pasadena, CA, USA) until the complete separation of the lipid and the aqueous phase. The lipid samples were diluted 1:10 in methanol, vortexed for 1 minute and centrifuged at $10,000\ \text{xg}$ for 10 minutes using an Allegra®X-15R centrifuge (Beckman Coulter, Pasadena, CA, USA). The supernatant was then recovered and further diluted 1:10 in mobile phase (solution prepared with methanol 60% (v/v), acetonitrile 20% (v/v) and water 20% (v/v)).²³ The quantity of

quercetin was then determined through High Performance Liquid Chromatography (HPLC).

HPLC is an analytical technique that allows the separation of compounds soluble in a particular solvent. This technique involves the migration of a lipid mixture through a column containing a stationary phase (liquid).²⁴ Particularly, the liquid phase is pumped at a constant rate to a column packed with the stationary phase. On the other hand, before entering the column, the sample is injected into the carrier stream and, when it reaches the column, its components are selectively retained depending on the physico-chemical interactions between the analyte molecules and the stationary phase.²⁵ The detection and quantification of the eluted molecules is typically performed using an ultraviolet (UV) or UV-visible detector (Figure 3.5).²⁶

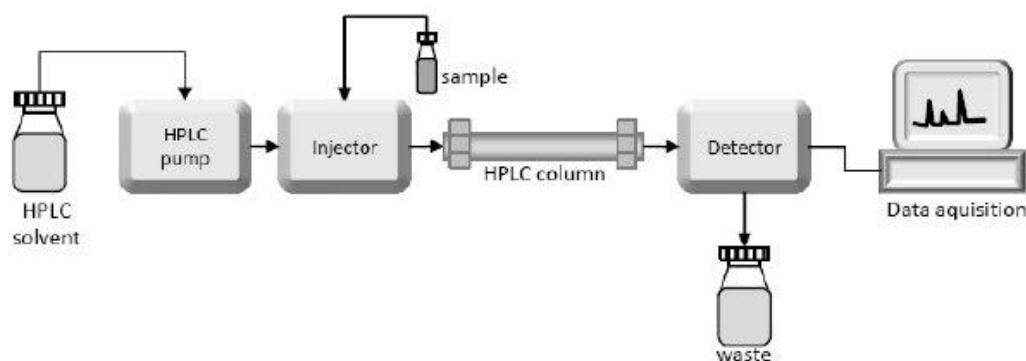


Figure 3.5 - Schematic diagram of a HPLC system.²⁴ Copyright 2013 Authors licensed under a Creative Commons Attribution (CC BY) license.

Then, the EE, i.e., the percentage quercetin successfully entrapped into the nanoparticles, was calculated using the following formula²⁷:

$$EE (\%) = \frac{\text{Amount of encapsulated compound}}{\text{Total amount of compound initially added}} \times 100 \quad (6)$$

where the "Amount of encapsulated compound" refers to the quantity of the compound measured by HPLC after being extracted from the formulation, while the "Total amount of compound initially added" is associated with the initial amount of the compound that was added during the formulation fabrication process.

Additionally, the drug loading, i.e. the quantity of drug loaded *per* unit weight of the nanoparticle, was also determined through this technique using the following equation²⁸:

$$DL(\%) = \frac{\text{Amount of total entrapped drug}}{\text{Total nanoparticle weight}} \times 100 \quad (7)$$

In this work, a HPLC equipped with a reversed-phase monolithic column (Chromolith® RP-18e, 100 mm x 4.6 mm i.d., Merck) connected to a Jasco (Easton, PA, USA) HPLC system (pump PU-4180, autosampler AS-4050, and LC-Net II/ADC controller) coupled to a PDA detector (Jasco MD-4010, start wavelength = 200 nm, end wavelength = 400 nm) was used. The data processing was performed by ChromNAV 2.0 HPLC software (Easton, PA, USA). The chromatographic separation was performed using an injection volume equal to 10 µL, flow rate of 1.0 mL/min, column temperature of 30°C and a detection wavelength of 374 nm.

3.2.4.4. Storage Stability Assessment

The nanoparticles storage stability was assessed over a period of 12 weeks. For that two different batches of nanoparticles were kept at 4°C and at room temperature (RT), and characterized every two weeks by measuring size, PDI, zeta potential as well as drug content as described in 2.2.4.3.

3.2.4.5. Fourier Transform Infrared Spectroscopy Analysis

In order to assess whether quercetin was successfully incorporated in the nanoparticles and evaluate the existence of possible chemical interactions between quercetin and the lipid matrix, Fourier Transform Infrared Spectroscopy (FTIR) spectroscopy was conducted. This analysis was also conducted to identify the functional groups in the developed hydrogels based on SA and PVA (section 2.2.5) as well as to evaluate whether quercetin was successfully incorporated in the hydrogels and the existence of possible chemical interactions between quercetin and the polymeric matrix.

FTIR is a method that allows the acquisition of the infrared (IR) spectrum of absorption, emission, photoconductivity, or Raman scattering associated with a solid, liquid, or gas. In this technique, IR radiation is used to determine the structures, chemical bonding, as well as functional groups present in molecules.²⁹ Particularly, when exposed to IR radiation, the molecules in a given sample selectively absorb at specific wavelengths, transitioning to a higher vibrational state. In this process, the wavelength associated with the radiation absorbed by a particular molecule is a function of the energy difference among its ground and excited, i.e. higher energy, vibrational state.³⁰ Consequently, the intensity of the transmitted, or reflected, IR radiation is then measured as a function of its wavelength, being plotted in a single-beam IR spectrum.³¹

FTIR (Frontier™, Perkin Elmer, Santa Clara, CA, USA) coupled to an attenuated total reflectance (ATR) sampling device possessing a diamond/ZnSe crystal was employed to obtain the spectra of quercetin-loaded and unloaded lipid nanoparticles. The

formulations were previously frozen at -80°C (Deep freezer, GFL®, Burgwedel, Germany), and freeze-dried in a LyoQuest 85 plus v.407 Telstar freeze dryer (Telstar® Life Science Solutions, Terrassa, Spain) during 72 hours at -80°C , under pressure of 0.40 mbar. Then, samples were placed in a temperature and humidity-controlled environment. Spectra were then acquired by merging 16 scans and recorded between 4000 and 600 cm^{-1} with a resolution of 4 cm^{-1} . Three analyses were performed for each sample.

3.2.4.6. Thermal Analysis

Differential scanning calorimetry (DSC) analysis was used to assess the physical state of the optimized nanoparticles core, and to investigate the existence of possible drug and lipid interactions within the nanoparticles. DSC is a technique that allows the measurement of the quantity of heat flow required to increase the temperature of a substance, under controlled conditions.³² In this method, the heat flow rate difference into the sample material and the reference material is continuously measured as a function of temperature, whilst both materials are subjected to a controlled temperature program.³³ In an adequate environment, the measured temperature difference is proportional to the sample's heat capacity, as well as to the heat flowing into and out of it. The resulting record is known as DSC curve.³⁴

In this work DSC measurements of cetyl palmitate, quercetin-loaded, and non-loaded NLCs and SLNs were achieved utilizing a Perkin Elmer Pyris 1 differential scanning calorimeter (PerkinElmer, Waltham, MA, USA). Samples were measured (0.5 – 2 mg) directly in aluminum pans and scanned between 25°C and 75°C , considering a heating rate of $10^{\circ}\text{C}/\text{min}$ and a cooling rate equal to $40^{\circ}\text{C}/\text{min}$, under nitrogen gas ($20\text{ mL}/\text{min}$). A vacant aluminum pan was considered as the reference. Origin software (Northampton, MA, USA) was used to analyze the data. Raw data was baseline-corrected and then normalized with regard to the scan rate and the gram mass of the sample in the pan, yielding the excess heat capacity (C_p , $\text{J}\cdot\text{g}^{-1}\cdot\text{C}^{-1}$). The melting point was taken as the temperature at which the heat capacity was maximum and calorimetric enthalpy changes (ΔH) were determined by integrating the area below the endothermic peak, expressed in J/g . The same software was also employed to calculate the width of peak in its half height ($\Delta T_{1/2}$) and, when peaks overlapped, it was used to estimate thermodynamic parameters of each single component peak. DSC studies were performed in collaboration with Dra. Catarina Morais, Professor Dra. Amália Jurado and Professor Dra. Maria Pedroso de Lima, from Center for Neuroscience and Molecular Biology, from University of Coimbra.

3.2.4.7. Photostability Study

In order to evaluate the protection effect of the lipid nanoparticles against UV-induced quercetin's photodegradation a photostability study was performed. In this assay, solutions of 10 µg/mL of quercetin in its free form and quercetin-loaded NLCs and SLNs were exposed for 3 hours to radiation with a wavelength of 254 nm. At 0, 1, 2 and 3 hours of irradiation, aliquots were withdrawn from each sample, diluted with ethanol 70% (v/v) by a factor of 1:3, vortexed for 1 minute and centrifuged at 10,000 xg for 10 minutes using an Allegra®X-15R centrifuge (Beckman Coulter, Pasadena, CA, USA). Ethanol was used to promote the disruption of the lipidic composition of the nanoparticles, allowing the quantification of quercetin in solution. The quantification of quercetin was performed by spectrophotometric detection in a wavelength range of 250-500 nm in a V-660 spectrophotometer (Jasco, Easton, MD, USA).

3.2.5. Preparation of the Sodium Alginate-Poly(Vinyl Alcohol) Hydrogels

The hydrogels were prepared as described elsewhere.³⁵ Shortly, SA was dissolved in sterile double-deionized water (7.5% w/v) with the help of a glass rod. Simultaneously, a PVA solution (8% w/v) was also dissolved in sterile double-deionized water. In order to facilitate the dissolution process the PVA solution was heated until 70°C, and then added to the SA in a SA-PVA ratio of 2:1. Both SA and PVA solutions were then mixed using a glass rod.³⁵ In the hydrogels loaded with quercetin in its free form, a concentration of 0.1 mg/mL of quercetin was added to the hydrogel in the SA dissolution step. Likewise, in the hydrogels prepared with quercetin loaded into both NLCs and SLNs, the nanoparticles were added to the hydrogel in the SA dissolution step to achieve 0.1 mg/mL concentration of quercetin. Quercetin-loaded NLCs and SLNs were prepared by hot emulsification/ sonication technique and made of cetyl palmitate as the solid lipid and pomegranate oil (PO) as the liquid lipid for NLCs, in the presence of tween 80, as described in section 3.2.1. In order to remove the air bubbles, all hydrogels were left degassing in an incubator shaker (ES-60E Incubator Shaker, Miulab, Hangzhou, Zhejiang, China) at room temperature and 125 rpm for 48 hours. The hydrogels were prepared under sterile conditions in a flow chamber.

3.2.6. Rheology Studies

In order to better understand the mechanical properties of the hydrogels under study control and quercetin-containing (as free or loaded in nanoparticles) hydrogels were submitted to rheology studies, in particular viscosimetry, thixotropy, and resistance to

deformation and temperature. From a cutaneous application point of view, gathering information regarding the rigidity and elasticity of the polymeric network is essential.

The determination of the response of a given material to an externally applied mechanical stress is crucial for its successful application in the industry, since it allows not only a fine tuning of its response to external conditions so as to achieve the desired final result, but also to acquire insight on its structure, properties, and microscale structural organization.³⁶ In this context, rheometers appear as important equipments, since they allow assessing how a liquid, suspension, or slurry flows in response to applied forces, measuring its rheology, being employed for fluids whose viscosity cannot be defined by a single value.³⁷

Depending on the measuring principle, two types of rheometers can be distinguished, namely rotational, or shear, rheometers, which control the applied shear stress and measure the shear strain (or vice-versa), and extensional rheometers, which control the applied extensional stress and measure the extensional strain (or vice-versa).³⁸ The experiments carried out in this work were performed using a rotational rheometer. In this type of equipment the sample is set among two plates: the lower plate is fixed and the upper plate rotates, imposing a controlled torque (stress-controlled rheometer) or a controlled strain (strain-controlled rheometer). Our measurements were performed with the first type of device, where the strain is measured as a function of the applied stress. On the other hand, a strain-controlled instrument measures the torque as a function of the imposed strain.³⁹

Furthermore, the upper plate can possess distinct shapes in order to address different measurement requisites. In our case, a geometry composed of two parallel plates, which allows tuning the thickness among both of them and, therefore, investigating different deformation regimes depending on the gap height between the two plates, was used. Nevertheless, this configuration has the disadvantage that the strain/strain rate is not uniform. This problem can be overcome through a cone-plate geometry, which is composed by a fixed plate together with a rotating cone, however these two elements have to be placed at a fixed distance.⁴⁰

Through the use of rheometers it is possible to study various physical properties associated with the considered material. For example, in this work, we studied the viscosity of the fabricated samples by acquiring their flow curve. This curve is obtained either by increasing the shear rate applied to the material as a function of time and measuring the shear stress that is necessary to obtain such shear rate, or by increasing the applied shear stress and measuring the resulting shear rate.⁴¹ Then, the curve is

presented as the viscosity, or shear stress, as a function of the shear rate (Figure 3.6). This curve presents the flow behaviour for reduced shear rates (slow motions) and large shear rates (fast motion), allowing the determination of the viscosity for the desired shear rates.⁴²

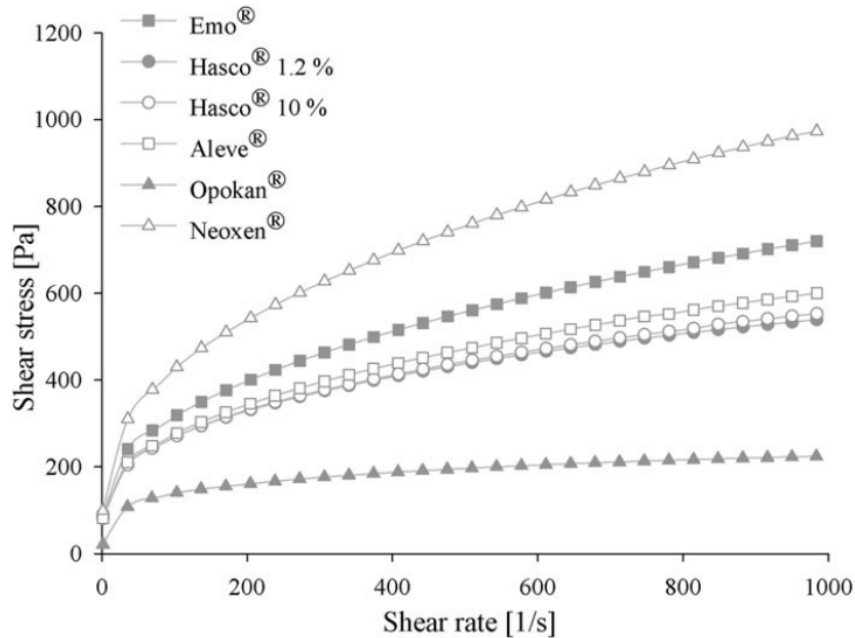


Figure 3.6 - Flow curves of different commercial hydrogels.⁴³ Reprinted from Pharmaceutical Development and Technology 22, Osmatek, T., Milanowski, B., Froelich, A., Górska, S., Białas, W., Szybowicz, M., and Kapela, M Novel organogels for topical delivery of naproxen: Design, physicochemical characteristics and in vitro drug permeation, 521-536, Copyright (2016), with permission from Taylor & Francis.

Thixotropy of the synthesized hydrogels was also studied using the rheometer. This property represents the tendency of a material's viscosity to decrease over time, when under shear, and to recover during rest periods.⁴⁴ In this work, thixotropy was determined using three-step shear rate method where the measurement is divided in three distinct segments, so as to assess the structure breakdown and recovery as a function of time.⁴⁵ In the first part, a low shear rate is applied in order to simulate the quiescent state of the material, with the goal of obtaining a constant viscosity at a constant low shear rate, providing the reference viscosity of the considered sample at rest. The following section simulates structural breakdown of the sample, therefore a large shear rate is applied. Finally, in the last section, the sample structural regeneration at rest after the second step is simulated, using the same shear rate considered in the first part. Typically, the obtained result is represented as a time-dependent viscosity function.^{46,47}

Additionally, the linear viscoelastic region of the hydrogels was determined through an amplitude sweep method, using the same equipment. In this technique, the deformation amplitude (or, alternatively, shear stress amplitude) is varied, while the frequency is

fixed.⁴⁸ Then, the analysis is performed by plotting the storage modulus, G' , and the loss modulus, G'' , as a function of the deformation (strain sweep curve), see Figure 3.7.⁴⁹

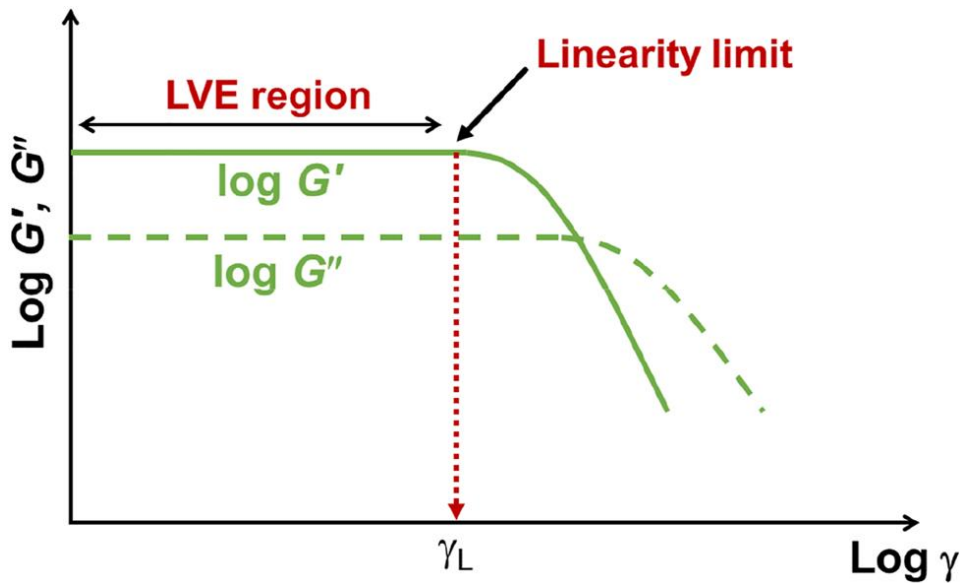


Figure 3.7 - Example of an amplitude sweep curve. (LVE – linear-viscoelastic).⁵⁰ Copyright 2022 Authors licensed under a Creative Commons Attribution (CC BY) license.

As can be observed in figure 3.7, when the deformation is low the two moduli are constant, meaning that the sample structure is not affected. This region is known as linear-viscoelastic. When those moduli start to decrease, the material structure is disturbed, indicating the end of the linear-viscoelastic region.⁵¹ In that region, the plateau value exhibited by G' indicates the rigidity of the sample at rest, while the plateau value associated with G'' represents a measure of the unsheared sample viscosity.^{52,53} Furthermore, the ratio between the two moduli, in the linear viscoelastic region, provides information on the sample characteristic, namely if $G' > G''$, the material behaviour is similar to that of a viscoelastic solid, while if the opposite is true it possesses properties of a viscoelastic fluid.⁵⁴ With this technique, two additional points can be determined, namely the yield point, given by the shear stress value at the limit of the linear-viscoelastic region; and the flow point, given by the shear stress value at the crossover point, i.e. when $G' = G''$.^{55,56}

The effect of temperature on the hydrogels was also evaluated with the rheometer. This evaluation was performed using a single frequency temperature ramp where the temperature was varied continuously at a constant frequency, under constant shear conditions, i.e. the shear-strain/shear stress was kept at a fixed value, and the material response was monitored. This examination provides information on the softening or melting behaviour of the considered material when temperature is increased; or on

solidification, crystallization, or cold gelation when its temperature is reduced.⁵⁷ In the particular case of polymers, this characterizes their architecture as well as describe the internal superstructure and configuration associated with the macromolecules. The acquired data is typically presented as G' and G'' as a function of temperature. From these curves, it is possible to determine the melting temperature, i.e. the temperature at which a material changes from a solid to a liquid state, corresponding to the temperature where $G' = G''$.^{58,59} Moreover, it is also possible to obtain the glass-transition temperature, which, usually, is considered as the temperature corresponding to the G'' maximum and represents the temperature at which an amorphous material changes from a hard/glassy state to a soft/leathery state, or vice versa.^{60,61}

The developed hydrogels were analysed in terms of their rheological properties using a rheometer (Malvern Kinexus Lab+; Malvern Instruments; Worcestershire, UK), in which four different methods were deployed. Rheological properties were also performed following a storage period of six weeks at room temperature in order to assess the hydrogel's stability over time. Viscosimetry analysis was performed, using a shear rate table method (0.1 to 100.0 s^{-1} , 10 samples per decade, 25 °C). For the thixotropy test a three-step shear rate method (1st phase: 0.1 s^{-1} , 2 min; 2nd phase: 100.0 s^{-1} , 30 s; 3rd phase: 0.1 s^{-1} , 15 min, 25 °C) was applied. In addition, to determine the linear viscoelastic region of the hydrogels, an amplitude sweep method (0.1 to 100%, 10 samples per decade, 1.0 Hz, 25 °C), and, finally, the temperature effect on the hydrogels was evaluated, using a single frequency temperature ramp with an initial temperature of 20 °C, final temperature of 40 °C, a 1 °C/min ramp, and a frequency of 1 Hz. All analysis were conducted with a plate-plate configuration (geometry PU20 SR4367) with a 1 mm gap (Peltier Plate Cartridge). The data were collected using the rSpace software® (Kinexus 1.75: PSS0211-17).

3.2.7. Morphology of SA-PVA Hydrogels Incorporating Quercetin-Loaded Nanoparticles

In order to obtain information about the morphology associated with the produced hydrogels, scanning electron microscopy (SEM) was used. This technique allows a direct observation of the fabricated samples with a resolution ranging from a few millimeters until 5 nm, and a magnification of up to 500.000 times. Additionally, the chemical composition of the analysed materials can also be determined through this technique, since SEM is typically coupled with an energy dispersive X-ray spectroscopy (EDS) detector.^{62,63}

Electronic microscopy is based on the irradiation of a sample by an electron beam, which possesses a controlled kinetic energy and is under high vacuum. This beam hits a small spot of the sample, causing the emission of electrons or photons. Through the use of a set of electrostatic and magnetic lenses, which allow the control of the focused electron beam, the sample is scanned. Subsequently, the intensity of the emitted particles is used to form the SEM image through convolution of the sample spots that were hit by the focused electron beam.^{64,65}

A schematic diagram of the main components of a SEM equipment is presented in Figure 3.8. These involve an electron column, condenser lenses, and a detector.

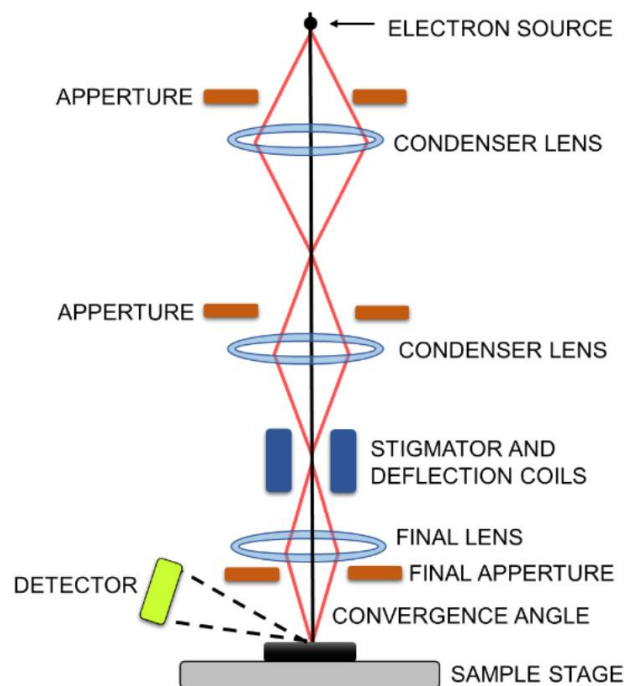


Figure 3.8 - Schematic diagram of the main components of a SEM equipment.⁶⁶ Reprinted from Encyclopedia of Materials Characterization Surfaces, Interfaces, Thin Films, 1st edition, Bindell, J. B., 2.2 - SEM: Scanning Electron Microscopy, 70-84, Copyright (1992), with permission from Elsevier.

Particularly, the electron column is composed by an electron source, such as a tungsten filament cathode, which is responsible for emitting an accelerated electron beam that can have energies between 0.1 and 40 KeV, under pressures of $\sim 10^{-4}$ Pa.⁶⁷ The diameter of this beam is reduced, i.e. the beam is focused, using a series of magnetic focusing lenses that have defines apertures, so as to converge the electron beam towards the sample. In the sample chamber, two types of detectors exist, namely secondary and backscattered detectors. In order to obtain an image, the focused electron beam is scanned, in a raster scan pattern, over the sample surface and the electrons emitted at each spot hit are gathered by the detectors and subsequently processed. Then, the SEM

image is constructed by mapping (point-to-point) the intensity of the detected signals to the position of the scanning beam.⁶⁷

When the focused electron beams hits the sample and interacts with its atoms, different types of particles are emitted at different depths within the sample (Figure 3.9). The most commonly used ones for image formation are secondary electrons and backscattered electrons.⁶⁶⁻⁶⁹

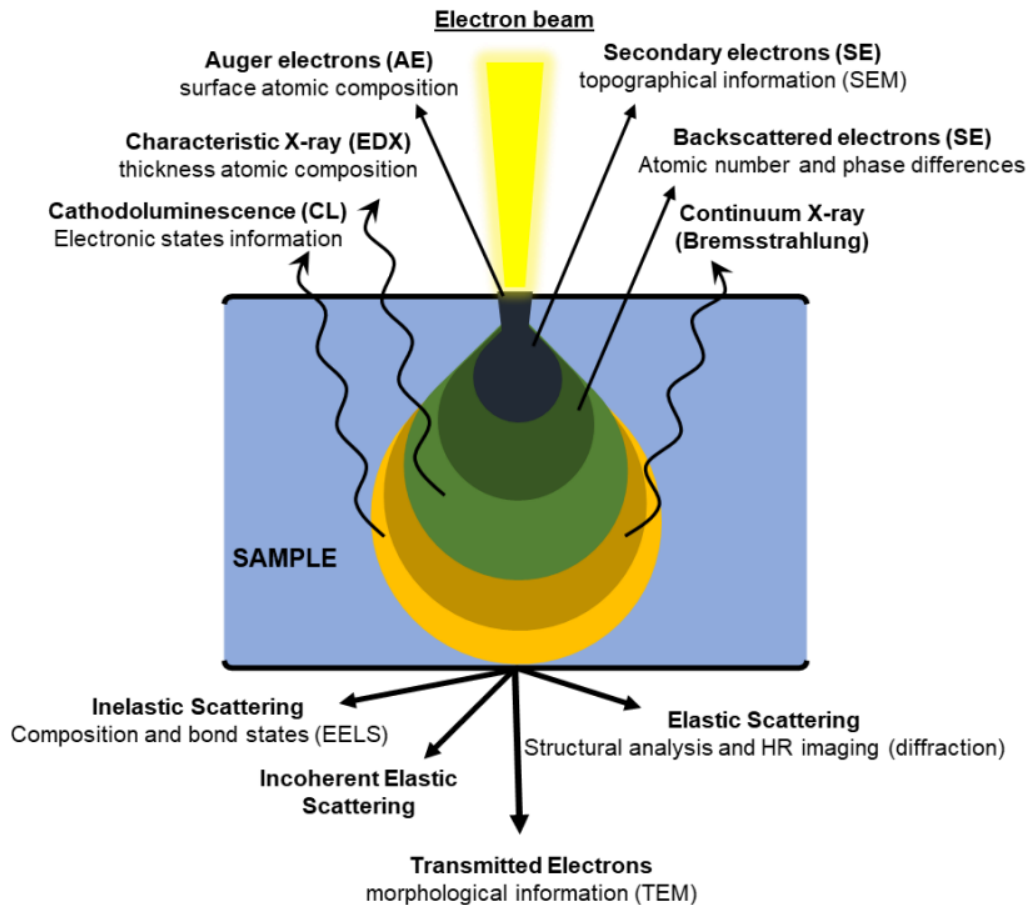


Figure 3.9 - Schematic diagram of the different particles emitted during electron-sample interaction at various depths.⁷⁰ Copyright 2013 Author licensed under a Creative Commons Attribution (CC BY) license.

The secondary electrons have a low energy, i.e. <50 eV, and they originate due to inelastic collisions of the primary electrons beam with superficial atoms, which are located a few nanometers from the sample surface and are weakly bound. The SEM images obtained using these particles give information of the sample topography.⁶⁶

On the other hand, backscattered electrons possess a high energy, i.e. >50 eV, and they originate from the elastic collision between the primary electron beam and atoms of the sample that are in a deeper location. These particles can be used to obtain a composition contrast image, since the intensity of the backscattered electrons emission is associated

with the atomic number of the material, namely chemical elements that have a greater atomic number emit more backscattered electrons than those with a lower atomic number, appearing brighter in the resulting image.^{62,71}

The developed hydrogels were analysed by SEM using a FEI Quanta 400 FEG ESEM/EDAX Pegasus X4M with an accelerating voltage of 10 kV. Briefly, all hydrogels were kept overnight in a -80 °C freezer (Deep Freezer, GFL®, Burgwedel, Germany), to be further lyophilized in a freeze drier (LyoQuest –85 plus v.407, Telstar® Life Science Solutions, Terrassa, Spain) for 72 hours, continuously kept at -80 °C and 0.40 mbar of pressure. Hydrogels were then fixed onto carbon-taped metal pins and coated with Au/Pd by sputtering for 45 seconds.

3.2.8. Determination of Quercetin Antioxidant Activity

3.2.8.1. The ABTS Assay

In order to understand how quercetin's encapsulation in the drug delivery systems (optimized nanoparticles and SA-PVA hydrogels, either in its free form or within lipid nanoparticles), affects its antioxidant capacity the 2,2-azinobis (3-ethylbenzothiazoline-6-sulfonic acid) (ABTS) assay was performed.

The ABTS assay is considered one of the most sensitive techniques to identify antioxidant activity, since it has faster reaction kinetics and a heightened response to antioxidants.⁷² This assay is based on measurement of the ability of the studied compounds to reduce the radical cation ABTS⁺, which possesses a characteristic long wavelength absorption spectrum with a maximum at a wavelength of 734 nm. This radical cation, which has a dark green color, is generated by reaction of the ABTS salt with a strong oxidizing agent (eg, potassium permanganate or potassium persulfate).⁷³ Then, when an antioxidant transfers electrons, or donates hydrogen atoms, to this ABTS radical cation, its color fades leading to a decrease in absorbance.⁷⁴

In this work, the ABTS radical cation decolorization test was employed to determine the antioxidant activity associated with the formulations under study⁷⁵. Free quercetin and quercetin-loaded nanoparticles ranging from 1.25 until 25 µg mL⁻¹ were prepared and the test was carried out following previously described methods.^{76–78} Briefly, 7 mM ABTS in water and 2.45 mM potassium persulfate aqueous stock solution were mixed in equal volumes and left in the dark overnight at ambient temperature, previous to the utilization. Then, the ABTS solution was mixed with the sample buffer till an absorbance equal 0.90 ± 0.02 at 734 nm was achieved. In a 96-well plate, 100 µL of the previously diluted ABTS solution were added to 100 µL of each sample. After 15 minutes the absorbance (A_{sample})

was read using a microplate reader (BioTek Instruments Inc., Winooski, VT, USA). All determinations were performed in triplicate and results are presented as mean \pm standard deviation. The radical scavenging activity percentage (% RSC) was determined through following equation:

$$RCS (\%) = \frac{A(\text{Control}) - A(\text{Sample})}{A(\text{Control})} \times 100 \quad (8)$$

3.2.8.2. The DPPH Assay

To complement the results of the ABTS assay, the 1,1-diphenyl-2-picrylhydrazyl (DPPH) assay was employed to assess the free radical scavenging activity associated with free quercetin and the nanoparticles under study. This is fast, simple, cheap, and commonly used technique to assess the capacity of compounds to act as free radical scavengers or hydrogen donors,⁷⁹ based on the scavenging ability of antioxidants towards DPPH.⁸⁰ This molecule is known as stable free radical, due to the delocalization of a spare electron over the whole molecule, which prevents dimer formation and leads to a deep violet color.⁸¹ This molecule has an absorption maximum at 515 nm, when dissolved in methanol.⁸² Antioxidants, or other radical species, can react with DPPH by providing an electron, or hydrogen atom, which reduces it to 2,2-diphenyl-1-hydrazine (DPPH-H) or a substituted analogous hydrazine (DPPH-R), characterized by a colorless or pale-yellow color. This decolorization can be monitored using a spectrophotometer.⁸³

In our work, a range of 0.10 until 1.56 $\mu\text{g mL}^{-1}$ was tested following a previously described method.⁷⁸ Briefly, a DPPH solution at 0.2 mM in methanol was prepared by dissolving 3.94 mg of DPPH reagent in 50 mL of MeOH.

In a 96-well plate 100 μL of the previously prepared DPPH solution were added to 100 μL of each sample. The 96-well plate was subsequently protected with aluminum foil to avoid radical degradation by light and incubated during 30 minutes at room temperature. The reaction solution absorbance (A_{sample}) was measured at 515 nm using a microplate reader (BioTek Instruments Inc., Winooski, VT, USA). All determinations were carried out in triplicate and results are exhibited as mean \pm standard deviation. The percentage of free radicals scavenging by the sample was determined using the following equation:

$$\text{Scavenging capacity } (\%) = \frac{1 - A(\text{Sample})}{A(\text{Control})} \times 100 \quad (9)$$

3.2.9. Cellular Studies

3.2.9.1. Cell Culture Conditions

Murine fibroblasts L929 and Human HaCaT cells were grown in DMEM supplemented with 10% (v/v) of FBS and 1% (v/v) Penicillin- Streptomycin and maintained at 37°C in a 5% CO₂ atmosphere (Unitherm CO₂ Incubator 3503 Uniequip; Planegg, Germany). After achieving approximately 90% confluence, L929 fibroblasts were removed from the cell culture flask utilizing a scrapper (Nunc™ Cell Scrapers, Thermofisher Scientific; Waltham, MA USA), and HaCaT keratinocytes were recovered by incubating the cells at 37°C in a 5% CO₂ atmosphere for approximately 5 minutes with a solution of 0.25% (w/v) trypsin-EDTA. Cells were counted and then plated in fresh supplemented DMEM in order to maintain the cell culture or plated in 24- or 96-wells to proceed with the studies.

3.2.9.2. Biocompatibility

Cell viability was evaluated through the 3-[4,5-dimethylthiazol-2-yl]-2,5-diphenyltetrazolium bromide (MTT) assay, with the goal of evaluating the quercetin-loaded lipid nanoparticles' biocompatibility.

In this colorimetric assay, cell viability is examined through cellular metabolic activity. Particularly, viable cells contain NAD(P)H-dependent oxidoreductase enzymes, which are capable of reducing the yellow MTT to purple formazan crystals.⁸⁴ Subsequently, these crystals, which have an absorbance maximum at 570 nm, are dissolved using a solubilization solution (dimethyl sulfoxide, DMSO, in this case), originating a colored solution that can be quantified by measuring their absorbance in the 500-600 nm range. The amount of formazan produced is proportional to the number of viable cells.⁸⁵

In this work, L929 and HaCaT cells reaching confluence were collected and seeded in 96-well plates, considering a density of 4×10^4 cells per well in 100 μ L of supplemented DMEM, and incubated for 24 hours at 37°C in a 5% CO₂ atmosphere. Following this step, the cell medium was removed and various concentrations of free quercetin as well as loaded and unloaded SLNs and NLCs were diluted in supplemented DMEM and added to the cells.

To determine the effect of the hydrogels on human keratinocytes (HaCaT cells), the cell viability was evaluated through the MTT assay. After reaching confluence, the cells were collected and seeded in 96-well plates, with a density of 4×10^4 cells per well in 100 μ L of supplemented DMEM and incubated for 24 hours at 37°C in a 5% CO₂ atmosphere. After cell adhesion, the culture medium was removed and replaced by serial dilutions (1.25 to

10 µg/mL in quercetin) of empty hydrogel, free quercetin-containing hydrogels, as well as unloaded and quercetin-loaded nanoparticles incorporated into hydrogels. In these assays, Triton X-100 (1% (v/v)) was considered the positive control for cytotoxicity, and untreated cells were used as the negative control. Then, cells were then incubated for another 24 hours at 37°C in a 5% CO₂ atmosphere.

For viability assessment, the culture medium was removed and 100 µL of an MTT solution prepared at a concentration of 0.5 mg/mL in supplemented DMEM was added. Cells were then incubated 4 hours at 37°C in 5% CO₂, following which the MTT solution was removed and 100 µL of DMSO were added to solubilize the formazan crystals. A microplate reader (BioTek Instruments Inc., Winooski, VT, USA) was used to determine the absorbance at 570 nm and 630 nm for background subtraction. The percentage of viable cells was compared to that of control cells through the corrected absorbance ratio (570–630 nm) measured for the analyzed conditions and the untreated cells.

3.2.9.3. Ultraviolet B Irradiation Intensity Studies

In order to infer the UVB radiation intensity necessary to reduce cell viability by about 50%, a preliminary evaluation was performed using four UVB pulses of 60, 80, 100, and 120 mJ/cm². Briefly, HaCaT cells were plated in a 96-well plate, at a density of 4x10⁴ cells *per* well, and left in an incubator for 24 hours at 37°C in a 5% CO₂ atmosphere, for cell adhesion. Following 24 hours of incubation, cells were irradiated using an illuminator system with UVB lamp (TRIWOOD 31/36, Helios Italquartz, Milan, Italy) at 60, 80, 100 and 120 mJ/cm². The cells were then incubated in fresh culture media for another 24 hours prior to cell viability assessment using the MTT assay, as previously described. An intensity of 60 mJ/cm², corresponding to a decrease in cell viability of approximately 50%, was selected to proceed for the photoprotective studies.

3.2.9.4. Photoprotective Assay

To assess the photoprotective effect of the SA-PVA hydrogels under study against UV-induced damage, HaCaT cells were plated in 96-well plates, at a density of 4x10⁴ cells *per* well, and left in an incubator for 24 hours at 37°C in a 5% CO₂ atmosphere, for cell adhesion. Then, cells were incubated for 24 hours with serial dilutions (2.5 to 10 µg/mL) of free quercetin-containing hydrogels, as well as unloaded and quercetin-loaded nanoparticles incorporated into hydrogels. Empty hydrogels as well as non-irradiated cells were used as a control. On the following day, cells were irradiated using an illuminator system with UVB lamp (TRIWOOD 31/36, Helios Italquartz, Milan, Italy) for 60 seconds (60 mJ/cm²). The cells were then incubated in fresh culture media for another

24 hours prior to cell viability assessment using the MTT assay, as previously described above. A similar assay was performed in order to evaluate cell apoptosis.

3.2.9.5. Cellular Recovery Study

The potential cell recovery effect of quercetin-loaded hydrogels on UVB-induced skin damage was also evaluated. As previously described HaCaT cells were plated in 96-well plates, at a density of 4×10^4 cells *per* well and left in an incubator for 24 hours at 37°C in a 5% CO₂ atmosphere. Cells were then irradiated using an illuminator system with UVB lamp (TRIWOOD 31/36, Helios Italquartz, Milan, Italy) for 60 seconds (60 mJ/cm²). Following irradiation, cells were incubated with serial dilutions (2.5 to 10 µg/mL) of free quercetin-containing hydrogels, as well as unloaded and quercetin-loaded nanoparticles incorporated into hydrogels. Empty hydrogels as well as non-irradiated cells were used as a control. After 24 hours of incubation, cell viability was assessed using the MTT assay, as described previously. A similar assay was performed in order to evaluate cell apoptosis.

3.2.9.6. Apoptosis Analysis

When cells undergo apoptosis, they can be identified by certain morphologic features, such as loss of plasma membrane asymmetry and attachment, condensation of the cytoplasm and nucleus, as well as internucleosomal cleavage of DNA.⁸⁶ One of the earliest structural changes in those cells is the modification in the plasma membrane involving the redistribution of phospholipids.⁸⁷ Namely, in healthy cells, the phospholipids are asymmetrically distributed at the plasma membrane. Particularly, phosphatidylcholine and sphingomyelin are mainly present in the external leaflet, while the majority of the phosphatidylethanolamine and all the phosphatidylserine (PS) are confined to the inner leaflet of the plasma membrane. However, in early apoptosis, the lipid asymmetry is lost, and PS is translocated from the inner to the external leaflet of the plasma membrane, which leads to its appearance on the cell surface, exposing it to the extracellular environment. Consequently, the monitoring of the appearance of PS on the cell surface provides an indication of apoptosis.^{86,88}

One compound typically used for this purpose is Annexin V, which is a 35-36 kDa Ca²⁺ dependent phospholipid-binding protein with a high affinity for PS, binding to cells with exposed PS.⁸⁹ Additionally, it can be conjugated to a fluorochrome, such as fluorescein isothiocyanate (FITC), so as to obtain a sensitive probe for flow cytometry examination of cells undergoing apoptosis.⁹⁰ Since FITC Annexin V staining precedes the loss of the plasma membrane's capacity to exclude vital dyes, such as propidium

iodide (PI) or 7-Amino-Actinomycin (7-AAD), it is commonly used together with those substances in order to distinguish between viable, early apoptotic, and necrotic or late apoptotic cells.⁸⁹ Particularly, such dyes are excluded by cells with intact membranes, while those that are dead or have damaged membranes are permeable to them⁹¹. Therefore, cells that are considered viable are FITC Annexin V and 7-AAD negative; cells in early apoptosis are FITC Annexin V positive and 7-AAD negative; and cells in late apoptosis, or dead, are FITC Annexin V and 7-AAD positive.⁸⁹

The apoptosis analysis was performed for both the photoprotective assay and the cellular recovery assay. Following both assays, cells were washed with phosphate buffer and detached using 0.25% trypsin. Then cells were centrifuged at 300 xg for 5 minutes and resuspended in 100 μ L of binding buffer, following the addition of 10 μ L of FITC Annexin V, and 10 μ L of 7-AAD, and incubation for 15 minutes at room temperature protected from light. After the incubation period, cells were analysed using a BD Accuri C6 flow cytometer with a minimum of 10,000 events. The assays were performed in triplicate and the results were analysed by Accuri C6 analysis software.

3.2.9.7. Determination of Intracellular Reactive Oxygen Species

To assess whether quercetin-loaded hydrogels have the ability to reduce UVB-induced ROS generation, the intracellular level of ROS was measured using the 2',7'-dichlorodihydrofluorescein diacetate (DCFH-DA) assay. The DCFH-DA is a nonpolar, non-fluorescent, and non-ionic molecule that can easily cross the cell membrane through passive diffusion.⁹² After diffusing into the cells, the DCFH-DA is deacetylated by intracellular esterases, originating non-fluorescent 2',7'-dichlorodihydrofluorescein (DCFH). Then, in the presence of ROS, such as hydrogen peroxide (H_2O_2), lipid hydroperoxides, and peroxyxynitrite, DCFH is quickly oxidized to 2',7'-dichlorofluorescein (DCF), which is highly fluorescent, possessing excitation and emission wavelengths of 498 and 522 nm, correspondingly.⁹³⁻⁹⁵

In the performed experiments, HaCaT cells were plated in 24-well plates, at a density of 2×10^5 cells *per* well and left in an incubator for 4 hours at 37°C in a 5% CO_2 atmosphere, for cell adhesion. Following cell plating, cells were incubated for 24 hours with 2.5 μ g/mL of free quercetin-loaded hydrogels, as well as unloaded and quercetin-loaded nanoparticles incorporated into hydrogels. Empty hydrogels as well as non-irradiated cells were used as a control. On the following day, cells were irradiated using an illuminator system with UVB lamp (TRIWOOD 31/36, Helios Italquartz, Milan, Italy) for 60 seconds (60 mJ/cm^2). Cells were then washed twice with PBS and incubated for 30 minutes with 5 μ g/mL of DCFH-DA. Following incubation, cells were washed twice with

PBS, digested with trypsin, and finally collected. Then cells were centrifuged at 300 xg for 5 minutes and resuspended in 150 µL of PBS, following the addition of 1.5 µL of Trypan Blue, and 1.5 µL of PI. Cells were then analysed using a BD Accuri C6 flow cytometer with a minimum of 10,000 events. The assays were performed in triplicate and the results were analysed by Accuri C6 analysis software. The relative fluorescent intensity was calculated compared to the control, corresponding to non-irradiated cells, using the following equation:

$$\text{Relative Fluorescent Intensity} = \frac{\text{Fluorescence of Experimental Group}}{\text{Fluorescence of Control Group}} \quad (10)$$

3.2.10. Permeation Studies Using PVPA_{SC} Model

To evaluate the potential of the quercetin-loaded NLCs and SLNs to permeate through the skin, the *ex vivo stratum corneum* mimetic model PVPA_{SC} was used.⁹⁶

Since the diffusion through the skin is controlled by its outermost layer, i.e. *stratum corneum* (SC), can be thought as diffusion through a passive membrane, the skin permeability of the produced formulations was evaluated by a phospholipid vesicle-based permeation (PVPA) assay with a lipid composition close to that of a human SC layer.^{96,97} This assay consists of a tightly packed layer of liposomes, formed by centrifugation, on a filter support, allowing the screening of passive permeability through biological membranes Figure 3.10.⁹⁸

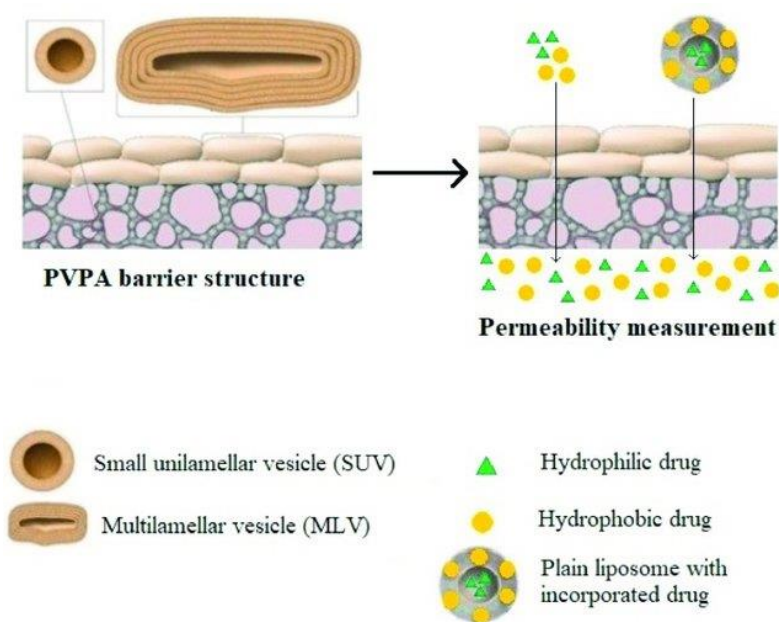


Figure 3.10 - Principle of the PVPA assay, mimicking the SC.⁹⁹ Copyright 2013 Authors licensed under a Creative Commons Attribution (CC BY) license.

3.2.10.1. Preparation of PVPA_{SC} Model

The PVPA_{SC} model systems were prepared as previously described.⁹⁶ The PVPA_{SC} model is made of liposomes composed of ceramide (50% w/w), egg phosphatidylcholine (EPC) (25% w/w), cholesterol (12.5% w/w), free fatty acids (10% w/w) and cholesteryl sulphate (2.5% w/w). The lipid mixtures were prepared as a close approximation to the composition of human SC, excluding the small proportions of cholesteryl esters and other minor constituents.^{96,100} Briefly, the lipid mixtures composed by ceramides, EPC, cholesterol, stearic acid and cholesteryl sulfate were dissolved in a mixture of chloroform and methanol (3:2 v/v), and then transferred into a 100-mL glass round-bottom flask. Using a rotary evaporator under nitrogen stream (P=1.0 Bar) and a heating bath at a temperature of 40 °C, the solvents were evaporated until complete dryness. 5 mL of phosphate buffered saline were added to the dry lipid film and vortexed 10 minutes at room temperature, with repeated cycles of 5 minutes heating and vortex until the lipid film was totally detached, allowing the formation of multilamellar large liposomes (MLVs). To assure an efficient hydration of the lipid materials, the lipid MLVs were left overnight at 4 °C. On the following day, two cycles of heating/vortex were performed again. The suspension of MLVs was divided into two portions and one was sonicated (Ultrasonic Processor for Small Volume Applications, Sonic Vibra-Cell) with amplitude 70% to obtain large unilamellar liposomes (LUVs).

In order to obtain the PVPA_{SC} barrier for the permeability studies, the liposomes were inserted into a filter support, as previously described.¹⁰¹ Briefly, the freshly prepared LUVs were incorporated into sterile culture inserts (Millicell membrane with 0.4 µm pore size) by two cycles of centrifugation (Allegra X-15R, Beckman Coulter) at 950 ×g for 15 minutes at 20 °C and one step at 45 °C for 60 minutes, in order to enhance the viscosity of the suspension and to promote filling the insert. Following that, MLVs were added to the insert and centrifuged at 1030 ×g for 60 minutes at 20 °C, followed by a 200×g centrifugation for 5 minutes at 20 °C in an inverted position to remove excess of liposomes. Then, inserts were transferred to 15 mL falcon tubes and frozen at -80 °C. Prior to use inserts were thawed at 30 °C for 90 min.

3.2.10.2. Permeation Assay Using PVPA_{SC} Model

Quercetin permeation studies were carried out at 32°C, with agitation and protection from light. Briefly, falcons containing the inserts comprising the PVPA_{SC} membranes were collected and inverted quickly, to avoid defrost of residual liquid in the tubes and incubated in a water bath during 90 minutes at 30°C.

The inserts were then positioned in a 24-well plate containing 2 mL of PBS (pH 7.4) with 10% (v/v) ethanol as the acceptor chamber. The use of ethanol was known in permeation studies to improve drugs' solubility in an aqueous medium.¹⁰² 500 μ L of each quercetin-loaded nanoparticle formulation containing approximately 150 μ g of drug was added to the donor chamber. The free drug permeation was performed similarly, 500 μ L of the same amount of quercetin dissolved in Mygliol, were added to the donor chamber. Mygliol was used to dissolve quercetin since ethanol can enhance skin permeation of drugs when simultaneously applied with drugs.¹⁰³ 200 μ L aliquots were then collected at 1-, 3- and 6-hours' time points, while the receptor chamber medium was replaced by an identical quantity of fresh buffer. 800 μ L of mobile phase were added to the collected samples and the amount of quercetin was then assessed through HPLC, as described in section 2.2.4.3.

A calibration curve (absorbance = 18163 [quercetin] – 3533.9) was acquired in mobile phase for concentrations ranging from 0.313 until 20 μ g/mL of quercetin, with a r^2 equal to 0.9998.

After 6 hours, the donor chamber samples were recovered and diluted by a factor of 1:10 in DMSO. Subsequently, a 2 minutes vortex and an ultrasonic bath of 45 minutes were performed in order to destroy the lipid nanoparticles and free the entrapped drug. Followingly, the samples were centrifuged during 15 minutes at 10000 xg in an Allegra X-15R centrifuge (Beckman Coulter, Pasadena, CA, USA). The concentration of quercetin in the supernatant was quantified through HPLC, as described above. A calibration curve (absorbance = 33037 [quercetin] – 23076) was acquired in DMSO for concentrations ranging from 0.625 until 20 μ g/mL of quercetin, with a r^2 equal to 0.9931.

3.2.11. Statistical Analysis

All the statistical analysis were performed using the GraphPad Prism Software (Version 7.03 for Windows; GraphPad Software Inc, San Diego, CA, USA). Considering the obtained data consists of at least three independent experiments, the results are expressed as mean \pm standard deviation (SD), and Ordinary one-way Anova or two-way Anova with multiple comparisons were performed to assess the differences between control and treatment groups. A p-value < 0.05 considered statistically significant.

3.3. References

1. Martins, S. A. M., *Drug delivery across blood-brain barrier by means of intravenous administration of lipid nanoparticles*. PhD thesis, Faculty of Pharmacy of the University of Porto (2012).
2. Nandvikar, N. Y., Lala, R. R., and Shinde, A. S., Nanostructured Lipid Carrier: the Advanced Lipid Carriers. *International Journal of Pharmaceutical Sciences and Research* **10**, 5252–5265 (2019).
3. Du, Y. *Fabrication and Characterization of Low Crystalline Curcumin Loaded Lipid Nanoparticles*. MSc thesis, Graduate School-New Brunswick Rutgers, The State University of New Jersey (2011).
4. Fu, S., Dou, B., Zhang, X., and Li, K., An Interactive Analysis of Influencing Factors on the Separation Performance of the Screw Press. *Separations* **10**, 245 (2023).
5. Manohar, M., Joseph, J., Selvaraj, T., and Sivakumar, D., Application of Box Behnken design to optimize the parameters for turning Inconel 718 using coated carbide tools. *International Journal of Scientific Engineering and Research* **4**, 620-642 (2013).
6. Chaichi, M. J., Azizi, S. N., Alijanpour, O., Heidarpour, M., and Qandalee, M. Application of Box-Behnken design in the optimization of new peroxyoxalate-H₂O₂ chemiluminescence system using furan derivatives as blue activators. *Journal of Luminescence* **138**, 65–71 (2013).
7. Leyva-Jiménez, F. J., Fernández-Ochoa, Á., Cádiz-Gurrea, M. D. L. L., Lozano-Sánchez, J., Oliver-Simancas, R., Alañón, M. E., Castangia, I., Segura-Carretero, A., and Arráez-Román, D., Application of Response Surface Methodologies to Optimize High-Added Value Products Developments: Cosmetic Formulations as an Example. *Antioxidants* **11**, 1552 (2022).
8. Jankovic, A., Chaudhary, G., and Goia, F., Designing the design of experiments (DOE) – An investigation on the influence of different factorial designs on the characterization of complex systems. *Energy and Buildings* **250**, 111298 (2021).
9. Housmans, J. A. J., Wu, G., Schymkowitz, J., and Rousseau, F., A guide to studying protein aggregation. *The FEBS Journal* **290**, 554–583 (2023).
10. Joshi, M., Bhattacharyya, A., and Ali, S. W., Characterization techniques for nanotechnology applications in textiles. *Indian Journal of Fibre and Textile Research* **33**, 304-317 (2008).

11. Velichko, E., Makarov, S., Nepomnyashchaya, E., and Dong, G., Molecular Aggregation in Immune System Activation Studied by Dynamic Light Scattering. *Biology* **9**, 123 (2020).
12. Stetefeld, J., McKenna, S. A., and Patel, T. R., Dynamic light scattering: a practical guide and applications in biomedical sciences. *Biophysical Reviews* **8**, 409–427 (2016).
13. Varenne, F., Botton, J., Merlet, C., Beck-Broichsitter, M., Legrand, F. X., and Vauthier, C., Toward a standardization of physico-chemical protocols for nanomedicine characterization: I. Size measurements. In: *17th International Congress of Metrology*, 14002 (EDP Sciences, 2015).
14. Misono, T., Dynamic Light Scattering (DLS). In: *Measurement Techniques and Practices of Colloid and Interface Phenomena*, 65–69 (Springer, 2019).
15. Varenne, F., Botton, J., Merlet, C., Hillaireau, H., Legrand, F. X., Barratt, G., and Vauthier, C., Size of monodispersed nanomaterials evaluated by dynamic light scattering: Protocol validated for measurements of 60 and 203 nm diameter nanomaterials is now extended to 100 and 400 nm. *International Journal of Pharmaceutics* **515**, 245–253 (2016).
16. Ploetz, E., Engelke, H., Lächelt, U., and Wuttke, S., The Chemistry of Reticular Framework Nanoparticles: MOF, ZIF, and COF Materials. *Advanced Functional Materials* **30**, 1909062 (2020).
17. Bhattacharjee, S., DLS and zeta potential – What they are and what they are not? *Journal of Controlled Release* **235**, 337–351 (2016).
18. Amran Tengku Mohd, T., Zaidi Jaafar, M., Anugerah Ali Rasol, A., and Fauzi Hamid, M., Measurement of Streaming Potential in Downhole Application: An Insight for Enhanced Oil Recovery Monitoring. In: *MATEC Web of Conferences* **87**, p. 03002 (EDP Sciences, 2017)
19. Sharma, S., Shukla, P., Misra, A., and Mishra, P. R., Interfacial and colloidal properties of emulsified systems: Pharmaceutical and biological perspective. In: *Colloid and Interface Science in Pharmaceutical Research and Development*, 149–172 (Elsevier, 2014).
20. Lowry, G. V., Hill, R. J., Harper, S., Rawle, A. F., Hendren, C. O., Klaessig, F., Nobbmann, U., Sayre, P., and Rumble, J., Guidance to improve the scientific value of zeta-potential measurements in nanoEHS. *Environmental Science: Nano* **3**, 953–965 (2016).

21. Inkson, B. J., Scanning electron microscopy (SEM) and transmission electron microscopy (TEM) for materials characterization. In: *Materials Characterization Using Nondestructive Evaluation (NDE) Methods*, 17–43 (Woodhead publishing, 2016).
22. Malatesta, M., Transmission Electron Microscopy as a Powerful Tool to Investigate the Interaction of Nanoparticles with Subcellular Structures. *International Journal of Molecular Sciences* **22**, 12789 (2021).
23. Bose, S., and Michniak-Kohn, B., Preparation and characterization of lipid based nanosystems for topical delivery of quercetin. *European Journal of Pharmaceutical Sciences* **48**, 442–452 (2013).
24. Czaplicki, S., Chromatography in Bioactivity Analysis of Compounds. In: *Column Chromatography*, 99-122 (IntechOpen, 2013).
25. Paul, S., Saikia, A., Majhi, V., and Pandey, V. K., Analytical instruments. In: *Introduction to Biomedical Instrumentation and Its Applications*, 213–250 (Springer, 2021).
26. Katz, V. L., Lentz, G., Lobo, R. A., Gershenson, D., and Willard, M., *Small Animal Clinical Diagnosis by Laboratory Methods*. Elsevier Health Sciences (2012).
27. Ali, H., Kalashnikova, I., White, M. A., Sherman, M., and Rytting, E., Preparation, characterization, and transport of dexamethasone-loaded polymeric nanoparticles across a human placental in vitro model. *International Journal of Pharmaceutics* **454**, 149–157 (2013).
28. Xu, J., Zhang, S., Machado, A., Lecommandoux, S., Sandre, O., Gu, F., and Colin, A., Controllable Microfluidic Production of Drug-Loaded PLGA Nanoparticles Using Partially Water-Miscible Mixed Solvent Microdroplets as a Precursor. *Scientific Reports* **7**, 1-12 (2017).
29. Nagy, E., *Basic Equations of Mass Transport through a Membrane Layer*. Elsevier Science (2018).
30. Saleh, T. Abdo., and Gupta, V. Kumar., *Surface Science of Adsorbents and Nanoadsorbents: Properties and Applications in Environmental Remediation*. Academic Press (2022).
31. Iqbal, H. M. N., Bilal, Muhammad., and Nguyen, T. Anh., *Nano-Bioremediation: Fundamentals and Applications*. Elsevier Science (2021).

32. Ong, K. L. L., Lovald, S., and Black, J., *Orthopaedic Biomaterials in Research and Practice*. CRC Press (2017).
33. Menczel, J. D., and Grebowicz, J., *Handbook of Differential Scanning Calorimetry: Techniques, Instrumentation, Inorganic, Organic and Pharmaceutical Substances*. Elsevier (2023).
34. Maehly, A., and Williams, R. L., *Forensic Science Progress*. Springer (1988).
35. Esposito, L., Barbosa, A. I., Moniz, T., Costa Lima, S., Costa, P., Celia, C., and Reis, S., Design and characterization of sodium alginate and poly(Vinyl) alcohol hydrogels for enhanced skin delivery of quercetin. *Pharmaceutics* **12**, 1–15 (2020).
36. Vitali, V., Nava, G., Zanchetta, G., Bragheri, F., Crespi, A., Osellame, R., Bellini, T., Cristiani, I., and Minzioni, P., Integrated Optofluidic Chip for Oscillatory Microrheology. *Scientific Reports* **10**, 5831 (2020).
37. Narayan, D. A., & Salunke, P. J., Workability & Rheological Parameter of Concrete. *GRD Journal for Engineering* **1**, (2016).
38. Ali, M. F., *Development of mucoadhesive biopolymers for food formulation*. PhD Thesis, University of Birmingham (2015).
39. Higham, R. G., *A biophysical analysis of the Ocr protein gel*. PhD Thesis, University of Edinburgh (2007).
40. Tanner, R. I., and Keentok, M., Shear Fracture in Cone-Plate Rheometry. *Journal of Rheology* **27**, 47–57 (1983).
41. Jaganath, N., *The Application of Rheological Techniques in the Characterization of Semisolids in the Pharmaceutical Industry*. PhD Thesis, Nelson Mandela Metropolitan University (2004).
42. Bair, S., and Qureshi, F. The high pressure rheology of polymer-oil solutions. *Tribology international* **36**, 637–645 (2003).
43. Osmatek, T., Milanowski, B., Froelich, A., Górska, S., Białas, W., Szybowicz, M., and Kapela, M., Novel organogels for topical delivery of naproxen: Design, physicochemical characteristics and *in vitro* drug permeation. *Pharmaceutical Development and Technology* **22**, 521-536 (2017).
44. Mazzoni, G., Stimilli, A., and Canestrari, F., Self-healing capability and thixotropy of bituminous mastics. *International Journal of Fatigue* **92**, 8–17 (2016).

45. Rial, R., Liu, Z., and Ruso, J. M., Soft Actuated Hybrid Hydrogel with Bioinspired Complexity to Control Mechanical Flexure Behavior for Tissue Engineering. *Nanomaterials* **10**, 1–20 (2020).
46. Mezger, T., *The Rheology Handbook: For users of rotational and oscillatory rheometers*. Vincentz Network (2020).
47. Galindo-Rosales, F. J., Campo-Deaño, L., Afonso, A. M., Alves, M. A., and Pinho, F. T., *Proceedings of the Iberian Meeting on Rheology (IBEREO 2019)*. Springer Nature (2019).
48. Nelson, C., Tuladhar, S., and Habib, A. Physical Modification of Hybrid Hydrogels to Fabricate Full-Scale Construct Using Three-Dimensional Bio-Printing Process. *Journal of Micro and Nano-Manufacturing* **10**, 011005 (2022).
49. Tian, T. F., Li, W. H., Ding, J., Alici, G., and Du, H., Study of shear-stiffened elastomers. *Smart materials and structures* **21**, 125009 (2012).
50. Ramli, H., Zainal, N. F. A., Hess, M., and Chan, C. H., Basic principle and good practices of rheology for polymers for teachers and beginners. *Chemistry Teacher International* **4**, 307–326 (2022).
51. Kim, J. K., Thomas, S., and Saha, P., *Multicomponent polymeric materials*. Springer (2016).
52. Zhang, L., Yue, L. N., Qian, J. Y., and Ding, X. L., Effect of Curdlan on the Rheological Properties of Hydroxypropyl Methylcellulose. *Foods* **10**, 34 (2020).
53. Yadav, R., and Purwar, R., Influence of metal oxide nanoparticles on morphological, structural, rheological and conductive properties of mulberry silk fibroin nanocomposite solutions. *Polymer Testing* **93**, 106916 (2021).
54. Zhang, X., Ding, Y., Zhang, G., Li, L., and Yan, Y., Preparation and rheological studies on the solvent based acrylic pressure sensitive adhesives with different crosslinking density. *International journal of adhesion and adhesives* **31**, 760–766 (2011).
55. Horvat, M., Pannuri, A., Romeo, T., Dogsa, I. & Stopar, D. Viscoelastic response of Escherichia coli biofilms to genetically altered expression of extracellular matrix components. *Soft Matter* **15**, 5042–5051 (2019).
56. Bilek, V., Iliushchenko, V., Hruby, P., and Kalina, L., Effectiveness of common water-reducing admixtures in alkali-activated slag pastes with different types of activator. In:

IOP Conference Series: Materials Science and Engineering **1205**, 012001 (IOP Publishing, 2021).

57. Mattice, K. D., and Marangoni, A. G., Evaluating the use of zein in structuring plant-based products. *Current Research in Food Science* **3**, 59–66 (2020).

58. Osorio, F. A., Bilbao, E., Bustos, R., and Alvarez, F. Effects of Concentration, Bloom Degree, and pH on Gelatin Melting and Gelling Temperatures Using Small Amplitude Oscillatory Rheology. *International Journal of Food Properties* **10**, 841–851 (2007).

59. Mawardi, I., Jannifar, A., and Lubis, H., Effect Of Injection Temperature On Defect Plastic Products. In: *In IOP Conference Series: Materials Science and Engineering* **536**, 012102 (IOP Publishing, 2019).

60. Polacco, G., Biondi, D., Stastna, J., Vlachovicova, Z., and Zanzotto, L., Effect of SBS on rheological properties of different base asphalts. In: *Macromolecular Symposia* **218**, 333–342 (Weinheim: Wiley-VCH Verlag, 2004).

61. Kim, T. H., and Chang Song, K., Effect of types of hydrophilic acrylic monomers in reducing glistenings of hydrophobic acrylic intraocular lenses. *Optical Materials* **119**, 111401 (2021).

62. Goldstein, J. I., Newbury, D. E., Michael, J. R., Ritchie, N. W. M., Scott, J. H. J., and Joy, D. C., *Scanning Electron Microscopy and X-Ray Microanalysis*. Springer (2018).

63. Huang, J., Wu, P., Dong, S., and Gao, B., Occurrences and impacts of microplastics in soils and groundwater. In: *Emerging Contaminants in Soil and Groundwater Systems: Occurrence, Impact, Fate and Transport* 253–299 (Elsevier, 2022).

64. Zhu, Y., and Dürr, H., The future of electron microscopy. *Physics Today* **68**, 32–38 (2015).

65. Mafu, L. D., Msagati, T. A. M., and Mamba, B. B., Ion-imprinted polymers for environmental monitoring of inorganic pollutants: Synthesis, characterization, and applications. *Environmental Science and Pollution Research* **20**, 790–802 (2013).

66. Brundle, C. R., Evans, C. A., and Wilson, S., *Encyclopedia of Materials Characterization: Surfaces, Interfaces, Thin Films*. Gulf Professional Publishing (1992).

67. Echlin, P., Fiori, C. E., Goldstein, J., Joy, D. C., and Newbury, D. E., *Advanced scanning electron microscopy and X-ray microanalysis*. Springer Science & Business Media (2013).

68. Li, L., *Versatile Applications of Nanostructured Metal Oxides*. PhD Thesis, University of Cambridge (2014).
69. Zhou, W., Apkarian, R. P., Lin Wang, Z., and Joy, D. *Fundamentals of Scanning Electron Microscopy*. Springer (2006).
70. Claudionico, *Available Source*:
https://upload.wikimedia.org/wikipedia/commons/4/49/Electron_Interaction_with_Matter.svg (2019; Accessed May 21, 2013).
71. Grote, K. H., and Hefazi, H., *Springer handbook of mechanical engineering*. Springer Nature (2020).
72. Hernández-Rodríguez, P., Baquero, L. P., and Larrota, H. R., Flavonoids: Potential Therapeutic Agents by Their Antioxidant Capacity. In: *Bioactive Compounds: Health Benefits and Potential Applications*, 265–288 (Woodhead Publishing, 2019).
73. Ratnavathi, C. V., and Komala, V. V., Sorghum Grain Quality. In: *Sorghum Biochemistry: An Industrial Perspective* (Academic Press, 2016).
74. Zhang, X. L., Zhang, Y. D., Wang, T., Guo, H. Y., Liu, Q. M., and Su, H. X., Evaluation on Antioxidant Effect of Xanthohumol by Different Antioxidant Capacity Analytical Methods. *Journal of Chemistry* **2014**, 249485 (2014).
75. Barbosa, A. I., Costa Lima, S. A., and Reis, S., Development of methotrexate loaded fucoidan/chitosan nanoparticles with anti-inflammatory potential and enhanced skin permeation. *International Journal of Biological Macromolecules* **124**, 1115–1122 (2019).
76. Magalhães, L. M., Barreiros, L., Reis, S., and Segundo, M. A., Kinetic matching approach applied to ABTS assay for high-throughput determination of total antioxidant capacity of food products. *Journal of Food Composition and Analysis* **33**, 187–194 (2014).
77. Re, R., Pellegrini, N., Proteggente, A., Pannala, A., Yang, M., & Rice-Evans, C., Antioxidant activity applying an improved ABTS radical cation decolorization assay. *Free Radical Biology and Medicine* **26**, 1231–1237 (1999).
78. Fang, R., Jing, H., Chai, Z., Zhao, G., Stoll, S., Ren, F., Liu, F., and Leng, X., Design and characterization of protein-quercetin bioactive nanoparticles. *Journal of Nanobiotechnology* **9**, 19 (2011).
79. Kedare, S. B., and Singh, R. P., Genesis and development of DPPH method of antioxidant assay. *Journal of Food Science and Technology* **48**, 412–422 (2011).

80. Zhang, M., Cao, J., Dai, X., Chen, X., and Wang, Q., Flavonoid Contents and Free Radical Scavenging Activity of Extracts from Leaves, Stems, Rachis and Roots of *Dryopteris erythrosora*. *Iranian Journal of Pharmaceutical Research: IJPR* **11**, 991 (2012).
81. Gangwar, M., Gautam, M. K., Sharma, A. K., Tripathi, Y. B., Goel, R. K., and Nath, G., Antioxidant capacity and radical scavenging effect of polyphenol rich *Mallotus philippinensis* fruit extract on human erythrocytes: an in vitro study. *The Scientific World Journal* **2014**, 27945 (2014)
82. Njoya, E. M., Medicinal plants, antioxidant potential, and cancer. In: *Cancer: Oxidative Stress and Dietary Antioxidants*, 349–357 (Elsevier, 2021).
83. Patel, V. B., and Preedy, V. R., *Toxicology: oxidative stress and dietary antioxidants*. Academic Press (2020).
84. Milojević, M., Harih, G., Vihar, B., Vajda, J., Gradišnik, L., Zidarič, T., Kleinschek, K. S., Maver, U., and Maver, T., Hybrid 3D Printing of Advanced Hydrogel-Based Wound Dressings with Tailorable Properties. *Pharmaceutics* **13**, 564 (2021).
85. Malfa, G. A., Tomasello, B., Acquaviva, R., Genovese, C., La Mantia, A., Cammarata, F. P., Ragusa, M., Renis, M., and Di Giacomo, C., *Betula etnensis* raf. (betulaceae) extract induced HO-1 expression and ferroptosis cell death in human colon cancer cells. *International Journal of Molecular Sciences* **20**, (2019).
86. Yin, X. M., and Dong, Z., *Essentials of Apoptosis*. Totowa: Humana Press (2003).
87. Diaz, C., Lee, A. T., McConkey, D. J., and Schroit, A. J., Phosphatidylserine externalization during differentiation-triggered apoptosis of erythroleukemic cells. *Cell Death & Differentiation* **6**, 218–226 (1999).
88. Barbucci, R., *Integrated Biomaterials Science*. Springer Science & Business Media (2002).
89. Leporatti, S., *Nanocolloids for Nanomedicine and Drug Delivery*. MDPI (2019).
90. Gillan, L., Evans, G., and Maxwell, W. M. C. Flow cytometric evaluation of sperm parameters in relation to fertility potential. *Theriogenology* **63**, 445–457 (2005).
91. Rowland-Jones, S. L., and McMichael, A. J., *Lymphocytes: a practical approach*. Oxford University Press (2000).

92. Srivastava, A. K., *Advances in citrus nutrition*. Springer Science & Business Media (2012).
93. Galluzzi, L., and Kroemer, G., *Conceptual background and bioenergetic/mitochondrial aspects of oncometabolism*. Elsevier (2014).
94. Kowluru, R. A., and Chan, P. S., Oxidative stress and diabetic retinopathy. *Experimental diabetes research* **2007**, 43603 (2007).
95. Clift, M. J., Fytianos, K., Vanhecke, D., Hočevár, S., Petri-Fink, A., and Rothen-Rutishauser, B., A novel technique to determine the cell type specific response within an in vitro co-culture model via multi-colour flow cytometry. *Scientific Reports* **7**, 434 (2017).
96. Shakel, Z., Nunes, C., Costa Lima, S. A., and Reis, S., Development of a novel human stratum corneum model, as a tool in the optimization of drug formulations. *International Journal of Pharmaceutics* **569**, 118571 (2019).
97. Zidarič, T., Kleinschek, K. S., Maver, U., and Maver, T., *Function-oriented bioengineered skin equivalents: continuous development towards complete skin replication*. Springer (2023).
98. Fischer, S. M., Buckley, S. T., Kirchmeyer, W., Fricker, G., and Brandl, M., Application of simulated intestinal fluid on the phospholipid vesicle-based drug permeation assay. *International Journal of Pharmaceutics* **422**, 52–58 (2012).
99. Varga-Medveczky, Z., Kocsis, D., Naszlady, M. B., Fónagy, K., and Erdő, F., Skin-on-a-Chip Technology for Testing Transdermal Drug Delivery—Starting Points and Recent Developments. *Pharmaceutics* **13**, 1852 (2021).
100. Abd, E., Yousef, S. A., Pastore, M. N., Telaprolu, K., Mohammed, Y. H., Namjoshi, S., Grice, J. E., and Roberts, M. S., Skin models for the testing of transdermal drugs. *Clinical Pharmacology: Advances and Applications* **8**, 163 (2016).
101. Flaten, G. E., Dhanikula, A. B., Luthman, K., and Brandl, M., Drug permeability across a phospholipid vesicle based barrier: A novel approach for studying passive diffusion. *European Journal of Pharmaceutical Sciences* **27**, 80–90 (2006).
102. Moniz, T., Costa Lima, S. A., and Reis, S., Application of the human stratum corneum lipid-based mimetic model in assessment of drug-loaded nanoparticles for skin administration. *International Journal of Pharmaceutics* **591**, 119960 (2020).
103. Horita, D., Todo, H., and Sugibayashi, K., Effect of Ethanol Pretreatment on Skin Permeation of Drugs. *Biological and Pharmaceutical Bulletin* **35**, 1343-1348 (2012).

4. Results and Discussion

4.1. Design, Optimization, and Characterization of Nanostructured Lipid Carriers Containing Pomegranate Oil

4.1.1. Experimental Design: Optimization

In this study, NLCs were optimized for skin delivery of the antioxidant molecule, quercetin. Pomegranate oil was selected for the nanoparticle's composition as the incorporation of a liquid lipid obtained from a natural product could bring additional beneficial features, namely, anti-inflammatory, antioxidant, and anti-apoptotic effects.¹⁻³ On that matter, SLNs with no pomegranate oil were produced as control. To optimize the production conditions of the quercetin-loaded NLCs toward achieving maximal drug encapsulation efficiency and DL capacity, a three-level BBD was made. The liquid lipid/solid lipid ratio (X_1), amount of water (X_2) and quantity of drug (X_3) were varied to explore individual and synergic effects on particle size, PDI, EE and DL. All the other variables were maintained constant. Thus, 15 formulations were prepared and analyzed regarding the adopted responses (Table 4.1). Three-dimensional response surface analyses were plotted as a graphical representation of the behavior of each response with the simultaneous changing of two factors at a time, maintaining non-used variables fixed at their middle level (Figure 4.1).

Table 4.1 - Formulation composition and correspondent responses of 15 different formulations obtained from BBD.

Formulation	Independent Variables			Dependent Variables			
	Liquid lipid/ Solid Lipid ratio	Water Volume (mL)	Quercetin (%)	Size (nm)	PDI	EE (%)	DL (%)
1	0.200	4.0	2.5	280.10	0.106	42.40	0.95
2	0.467	4.0	2.5	155.80	0.126	31.80	0.87
3	0.200	10.0	2.5	250.50	0.116	21.48	0.48
4	0.467	10.0	2.5	218.30	0.120	17.19	0.47
5	0.200	7.0	1.0	246.80	0.140	31.24	0.28
6	0.467	7.0	1.0	264.00	0.138	33.56	0.37
7	0.200	7.0	4.0	234.80	0.134	23.89	0.86
8	0.467	7.0	4.0	201.70	0.260	24.88	1.10
9	0.333	4.0	1.0	270.60	0.138	60.98	0.61
10	0.333	10.0	1.0	198.50	0.150	26.90	0.27
11	0.333	4.0	4.0	2675.00	0.345	31.05	1.24
12	0.333	10.0	4.0	237.90	0.097	20.95	0.84
13	0.333	7.0	2.5	256.10	0.183	31.37	0.78
14	0.333	7.0	2.5	250.70	0.137	29.97	0.75
15	0.333	7.0	2.5	257.30	0.172	34.55	0.86

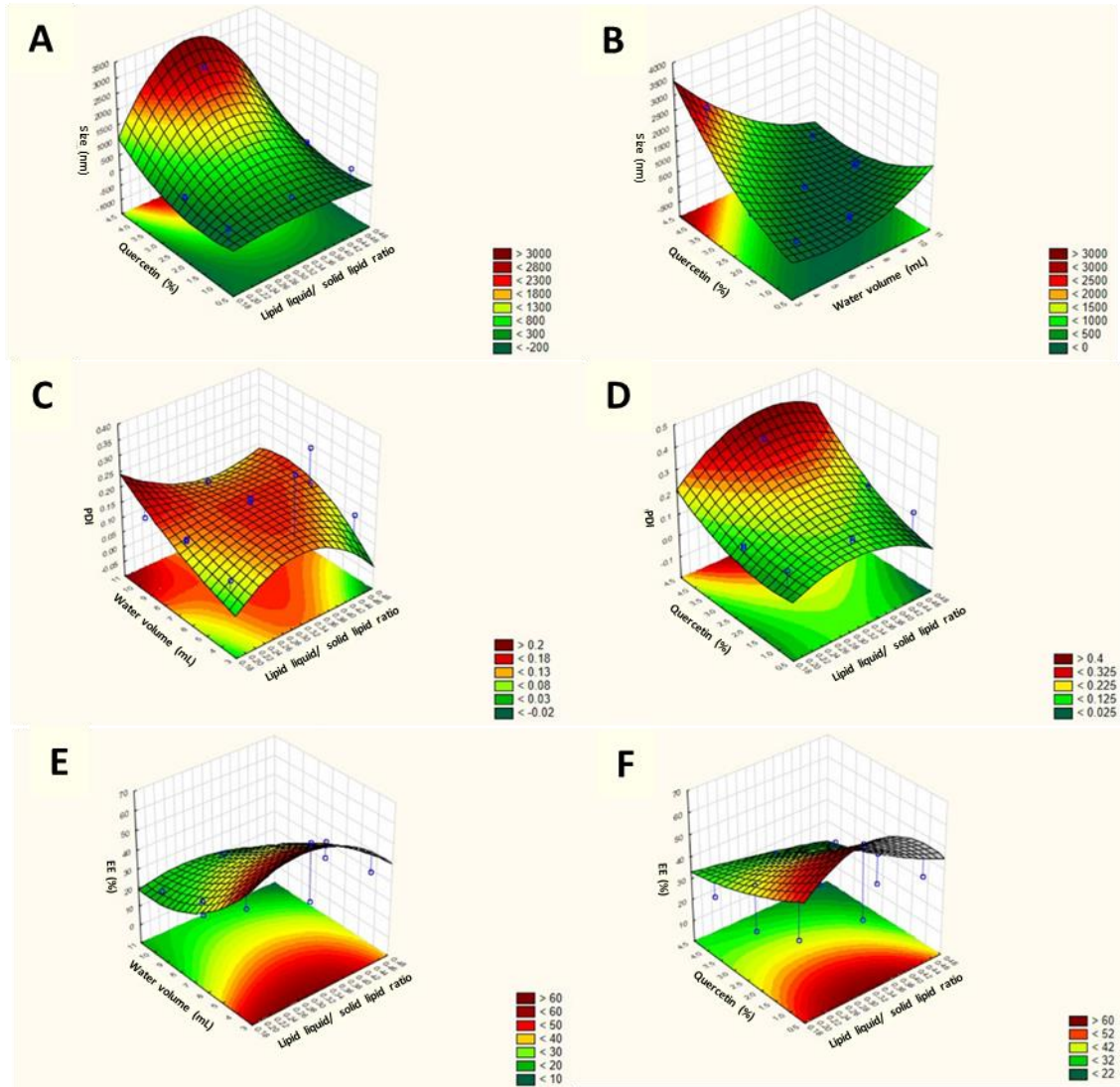


Figure 4.1 - Response surface plots evidencing the influence of the independent variables on the selected responses particle size. (A) influence of the drug concentration and liquid lipid/solid lipid ratio on the particle size, (B) influence of the quantity of drug and water volume on the particle size, (C) influence of the water volume and liquid lipid/solid lipid ratio on the PDI, (D) influence of the quantity of drug and liquid lipid/solid lipid on PDI, (E) Influence of the water volume on the % EE, and (F) influence of drug quantity on the % EE.

The obtained values of particle size from the formulations ranged from 155 nm to 300 nm. As observed in Figure 4.1A and 4.1B, the particle size increases with the simultaneous increase of the liquid lipid/solid lipid ratio and quantity of drug in the nanoparticle. Moreover, the solvent volume significantly influenced the particle size, i.e., the higher the volume the larger the nanoparticle.

Apart from formulations 8 and 11, all the others exhibited PDI values lower than 0.2, indicating a narrow distribution. As observed in Figure 4.1C and 4.1D, the simultaneous increase in water value and liquid lipid/solid lipid ratio influenced PDI of the formulations, resulting in an increase in the values. In addition, the simultaneous increase in the

quantity of drug and liquid lipid/solid lipid ratio also resulted in an increase in polydispersity.

The EE obtained varied from 17.2% to 60.9%, with the majority of the formulations presenting an EE between 20 to 40%. As observed in Figure 4.1E and 4.1F, the amount of solvent as well as the quantity of drug on the formulations affected the encapsulation efficiency. The lower the solvent volume and the quantity of quercetin, the higher the encapsulation efficiency.

4.1.2. Validation of the Experimental Design

The validation of the experimental design model was performed by formulating the optimized formulation, indicated by STATISTICA 10 software, with (X_1) 0.259 of liquid lipid/solid lipid ratio, (X_2) 4 mL of amount of water and (X_3) 2.49 of quantity of drug (Table 4.1) and comparing the experimental data (Table 4.2) with the theoretical data predicted by the software (size of 271 ± 21 nm, PDI 0.137 ± 0.1 , EE $60 \pm 14\%$ and DL 0.61 ± 0.3). The obtained data for all the responses displayed good correlation with the model, thus being an indicator of the robustness and high extrapolative ability of prediction of the experimental design. Table 4.2 displays the obtained results for optimized quercetin-loaded NLCs, as well as control quercetin-loaded SLNs and drug-free lipid nanoparticles.

Table 4.2 - Physicochemical parameters of optimized quercetin-loaded lipid particles.

	Size (nm)	PDI	EE (%)	DL (%)
NLCs	234 ± 14	0.124 ± 0.007		
Quercetin-loaded NLCs	$306 \pm 13^{**}$	0.134 ± 0.02	$55 \pm 2^*$	0.52 ± 0.05
SLNs	194 ± 13	0.115 ± 0.01		
Quercetin-loaded SLNs	$262 \pm 11^{**}$	0.150 ± 0.007	43 ± 4	0.41 ± 0.03

Data are represented as mean \pm SD (n = 3). Statistical differences are in relation to unloaded nanoparticles; **p < 0.01 in relation to blank nanoparticles, *p < 0.05 in relation to SLN

4.1.3. Characterization of Quercetin-Loaded Lipid Nanoparticles

The obtained nanoparticles, including both quercetin-loaded and unloaded counterparts, are approximately 200 and 300 nm in size, thus being within the recommended size of 500 nm for topical delivery.⁴ Quercetin incorporation had an impact on the nanoparticle' size, resulting in a significant statistical increase for both SLNs and NLCs. A possible

reason for this was that the loaded drug disturbed the lattice structure of the nanoparticles resulting in a higher size.⁴ In a previous study, the average size of quercetin-loaded silica nanoparticles increased with an increasing concentration of quercetin of 0.02%, 0.04%, 0.06%, 0.08% and 0.1%.⁵ The average size of the quercetin-loaded silica nanoparticles ranged from 90 ± 0.5 to 306 ± 11.3 nm.⁵ All PDI values are under 0.2 and thus illustrative of monodisperse populations with a narrow size distribution.⁶

As expected, optimized NLCs exhibited an entrapment efficiency of 55%, with a loading capacity of 0.5%, while their counterpart SLNs had significantly lower encapsulation efficiency (ca. 43%) with a loading capability of 0.4%. The presence of a liquid lipid within the NLCs might lead to less ordered matrix with more space to load molecules of interest as compared to the SLNs.^{7,8}

4.1.4. Morphology Assessment

Transmission electron microscopy (TEM) was employed to evaluate the formulations morphology. TEM images in Figure 4.2 revealed that both NLCs and SLNs had similar size, with particle diameters ranging from 200 to 300 nm. NLCs display a rough surface, non-spherical shape, and irregular morphology, as previously reported.^{9,10} In addition, these images show a clear presence of a mixture of lipids forming distinct zones (red arrow). The incorporation of quercetin in the nanoparticles did not affect their morphology.¹¹ Both loaded and unloaded SLNs displayed a spherical appearance, smooth surface, uniform morphology, and a solid character, that were not affected with the presence of quercetin. This agrees with data published by Lee *et al.* (2016) and Morales *et al.* (2015), in which SLNs appear to have a spherical profile with a narrow diameter distribution and lack of aggregation⁵⁻⁷. The images also revealed, for both NLCs and SLNs, no visible aggregation of the particles, which is a good indicator of the stability of the formulations, and in line with observations already reported.⁸

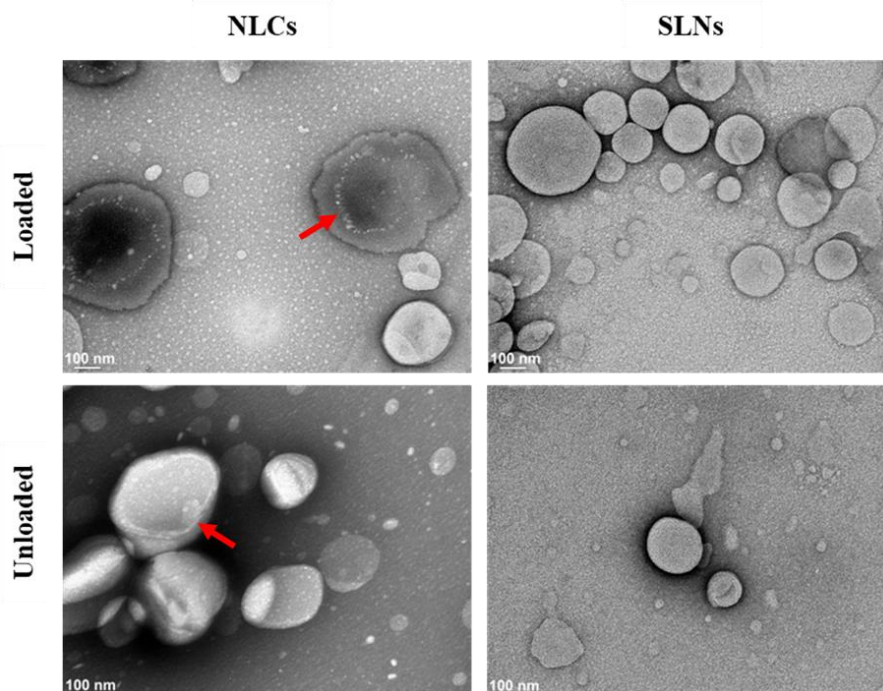


Figure 4.2 - Quercetin-loaded and unloaded formulations morphology. Transmission electron microscopy images attained for both quercetin-loaded and non-loaded SLNs and NLCs. The red arrows in the images point to the distinct zones formed that result from a mixture of lipids in the nanoparticles. Scale bar of 100 nm.

4.1.5. Storage Stability Assessment

A storage stability study of both NLCs and SLNs was performed over 12 weeks by analyzing every two weeks particle size, PDI, zeta potential, and drug content (Figure 4.3). The obtained results show that both types of lipid nanoparticles are stable for at least 12 weeks, with no considerable differences being observed between freshly produced and stored formulations. In addition, quercetin loading had no significant influence on the nanoparticle's storage stability. During the studied period of time quercetin remained inside NLCs and SLNs when stored at RT and at -4°C (data not shown). Visual observations of the developed nanoparticles did not show any significant alterations. Nonetheless, it is possible to observe that the measured parameters, in particular size, PDI and zeta potential, presented a higher variability for all the formulations stored at RT, as compared to the ones stored at -4°C . Since only minimal differences ($p > 0.05$) occur in the physicochemical data gathered to assess the storage stability of the nanoparticles under study, it may be inferred that they remain stable for at least 12 weeks at both studied conditions. Surface potential remains its negativity ranging from -20 to -35 mV, assuring colloidal stability of the nanoparticles.³ These results correlate with data previously published by Ni *et al.* (2015), which showed quercetin-loaded NLCs stable for at least 8 weeks when stored at RT.¹²

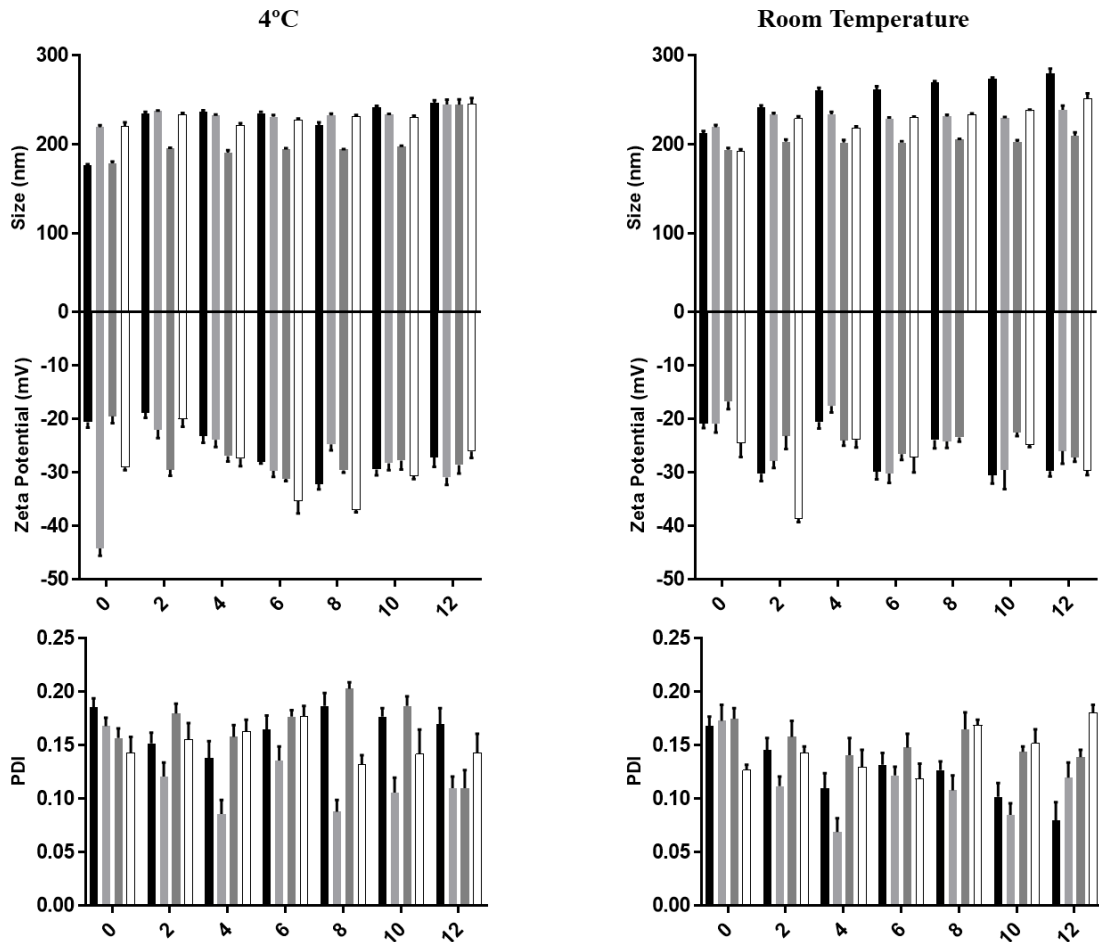


Figure 4.3 - Storage stability of quercetin-loaded NLCs (black bar), unloaded NLCs (light grey), quercetin-loaded SLNs (dark grey) and unloaded SLNs (white) at 4°C and RT.

4.1.6. Fourier-Transform Infrared Spectroscopy Evaluation

To evaluate whether quercetin was successfully incorporated in the nanoparticles and assess possible chemical interactions between quercetin and the lipid matrix, FTIR spectroscopy was conducted. The FTIR spectra for both loaded and unloaded particles are displayed in Figure 4.4. Quercetin spectrum includes a number of characteristic bands representing O-H stretching (3700 to 3100 cm^{-1}), C=O stretching (1730 cm^{-1}), C-C stretching (1649 cm^{-1}), C-H bending (1461 , 1369 , and 838 cm^{-1}), C-O stretching in the ring structure (1272 cm^{-1}), and C-O stretching (1070 to 1089 cm^{-1}).¹³ The FTIR spectra of SLNs were analogous to the NLCs spectra. Regarding the spectra of both quercetin-loaded SLNs and NLCs, it appears that the major characteristic bands of quercetin disappeared in the peaks of loaded nanoparticles, which may be due to the relation between the amount of flavonoid versus amount of lipid in the nanoparticles, or even an indirect confirmation of its encapsulation within the nanoparticles. Similar results

reporting the major characteristic bands corresponding to quercetin disappearing or being buried in NLCs peaks were also observed.¹⁴

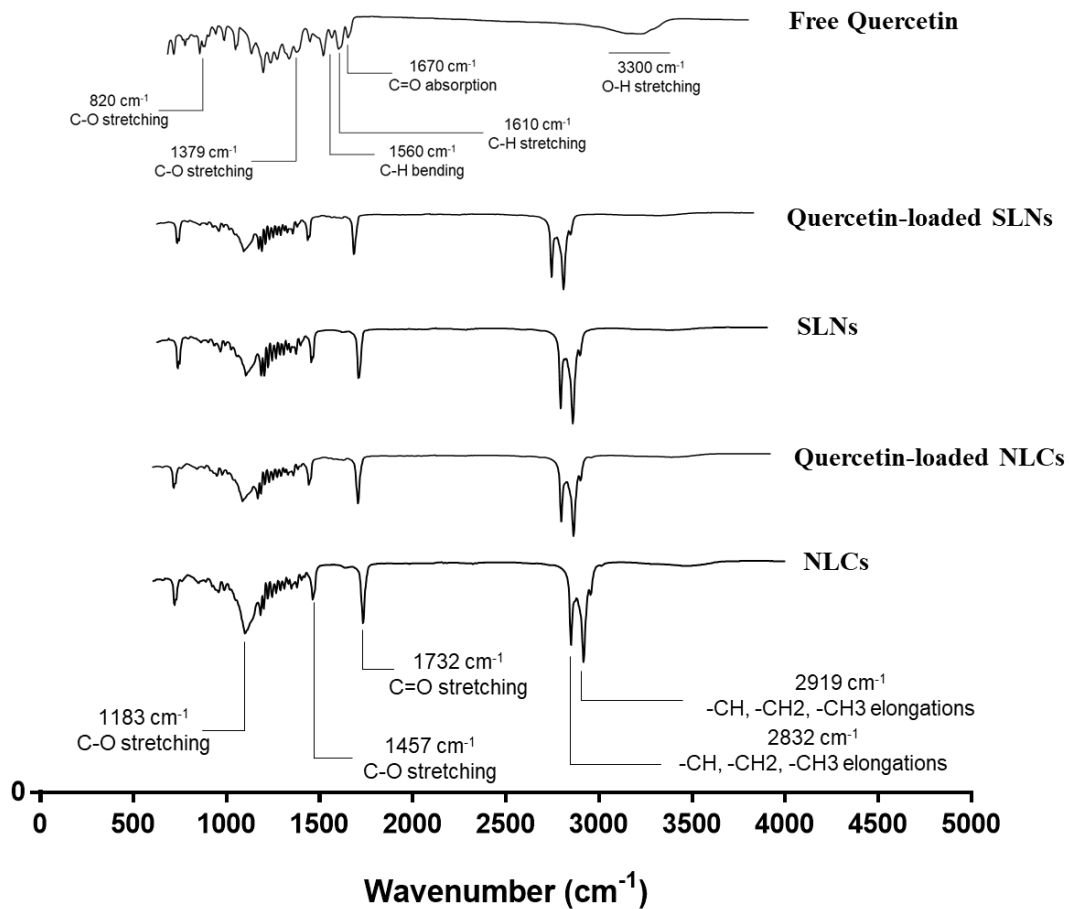


Figure 4.4 - FTIR spectra of quercetin in its free form and quercetin-loaded NLCs and SLNs. Empty NLCs and SLNs are also displayed.

4.1.7. Thermal Analysis

DSC analysis was used to assess the physical state of the optimized nanoparticles core, and to investigate the existence of possible drug and lipid interactions within the nanoparticles. The thermograms of unloaded and quercetin loaded SLNs and NLCs, as well as the corresponding physical mixtures are shown in Figure 4.5. On the heating curve of the pure solid lipid, cetyl palmitate, it is possible to observe two distinct melting peaks corresponding to two different phase transitions. The first one presented a smaller melting point (43.1°C) which corresponds to the α -polymorphic form, while the second peak (53.4°C) corresponds to the β -polymorphic form.¹⁵ The curves for the physical mixtures of both loaded and unloaded NLCs and SLNs are displayed in Figure 4.5B. As observed, the thermograms corresponding to both physical mixtures of the lipid

nanoparticles uncovered a maximum peak at 53°C, which correlates with the β -form of the cetyl palmitate (53.4°C).

The DSC thermogram obtained for the optimized NLCs displayed a single melting transition peak 2°C lower than that of the physical mixture. This is described as the Gibbs–Thompson effect and is due to the larger surface area to volume ratio of the nanoparticles, as described in the literature by Kovacevic *et al.* (2011).¹⁶ On the other hand, the thermogram obtained for the SLNs formulation displayed melting transition peak correspondent to that of the physical mixture counterpart.

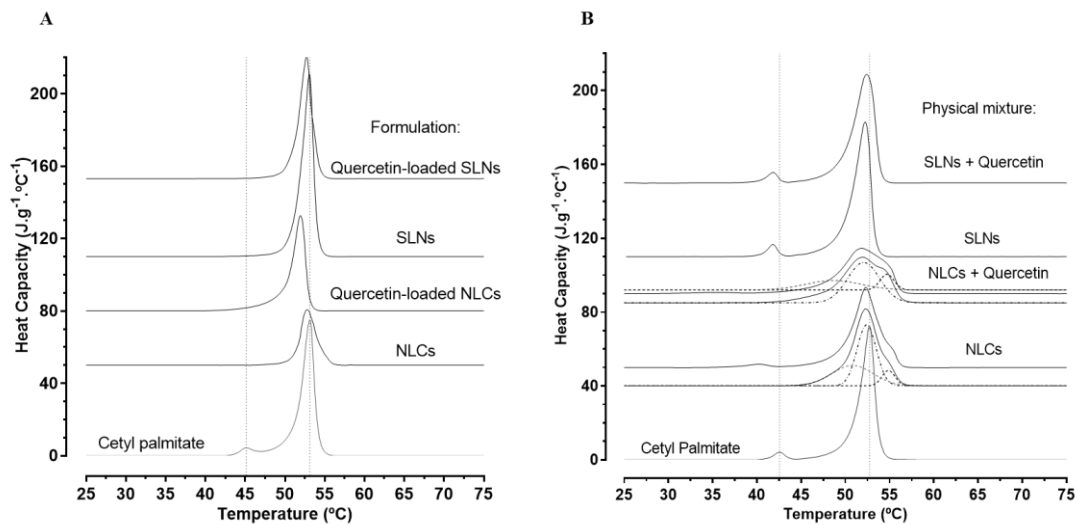


Figure 4.5 - DSC thermograms for (A) quercetin loaded and unloaded SLNs and NLCs and (B) corresponding physical mixtures.

DSC results also reveal that no significant changes in the melting point of the formulations were seen, after quercetin encapsulation (Table 4.3). Yet, the melting enthalpy increased after drug incorporation, in NLCs from 95.7 J/g to 135.7 J/g, that indicates a lipid matrix stabilization with the addition of the drug into the lipid phase.⁴ Whereas for the SLN formulation, quercetin incorporation resulted in a decrease the melting enthalpy, from 182.35 J/g to 146.2 J/g, thus suggesting less crystal lattice organization. Lipid nanoparticles loaded with cyclosporine A were reported to exhibit higher transition enthalpies, suggesting that the incorporation of the drug into the lipid phases provide a stabilizing effect due to its inclusion within the lipid matrix.^{4,17} Here, the decreased in the melting enthalpy observed in the SLNs, following quercetin loading, might be attributed to the smaller size of the bioactive molecule as compared to cyclosporine A.

Table 4.3 - DSC parameters of optimized quercetin-loaded and unloaded formulations.

Samples	Melting Point (T1) °C	ΔH (j/g)	Melting Point (T2) °C	ΔH (j/g)
NLCs	52.7	96.51	52.2	95.73
Quercetin-loaded NLCs	51.9	137.25	51.7	135.77
SLNs	52.8	186.52	52.5	182.35
Quercetin-loaded SLNs	52.8	150.51	52.5	146.16

4.1.8. Photostability Study

In order to assess whether both lipid nanoparticles, NLCs and SLNs, have the ability to protect quercetin against photodegradation, a photostability study was performed. Figure 4.6A displays the absorption spectra of quercetin in its free form and quercetin encapsulated into both NLCs and SLNs before and after UV light exposure for 3 hours. The results show a decrease of approximately 30% in free quercetin's absorption intensity at 373 nm after 3 hours of UV light exposure, as compared to the compound's absorption intensity protected from UV light (Figure 4.6B). The spectra of quercetin encapsulated into SLNs and NLCs suggests that these nanoparticles are able to protect the compound from photodegradation, as only a small decrease in quercetin's absorption intensity was displayed. In fact, the results demonstrate that quercetin encapsulated into SLNs showed only around 7% of degradation and approximately 17% of degradation when encapsulated into NLCs (Figure 4.6B). Similar results have been previously shown by Pinheiro *et al.* (2020). In this study, the authors assessed the protection effect of lipid nanoparticles against photodegradation of quercetin, by exposing both ethanol formulations of quercetin in its free form (0.7 mg/mL) and quercetin encapsulated into NLCs and SLNs, to UVA light for 6 hours. The authors concluded that around 55% of free quercetin in solution was photodegraded after UV exposure, while the encapsulated compound inside lipid nanoparticles showed only around 10% of degradation, thus confirming that nanoparticles have the ability to protect quercetin from photodegradation.

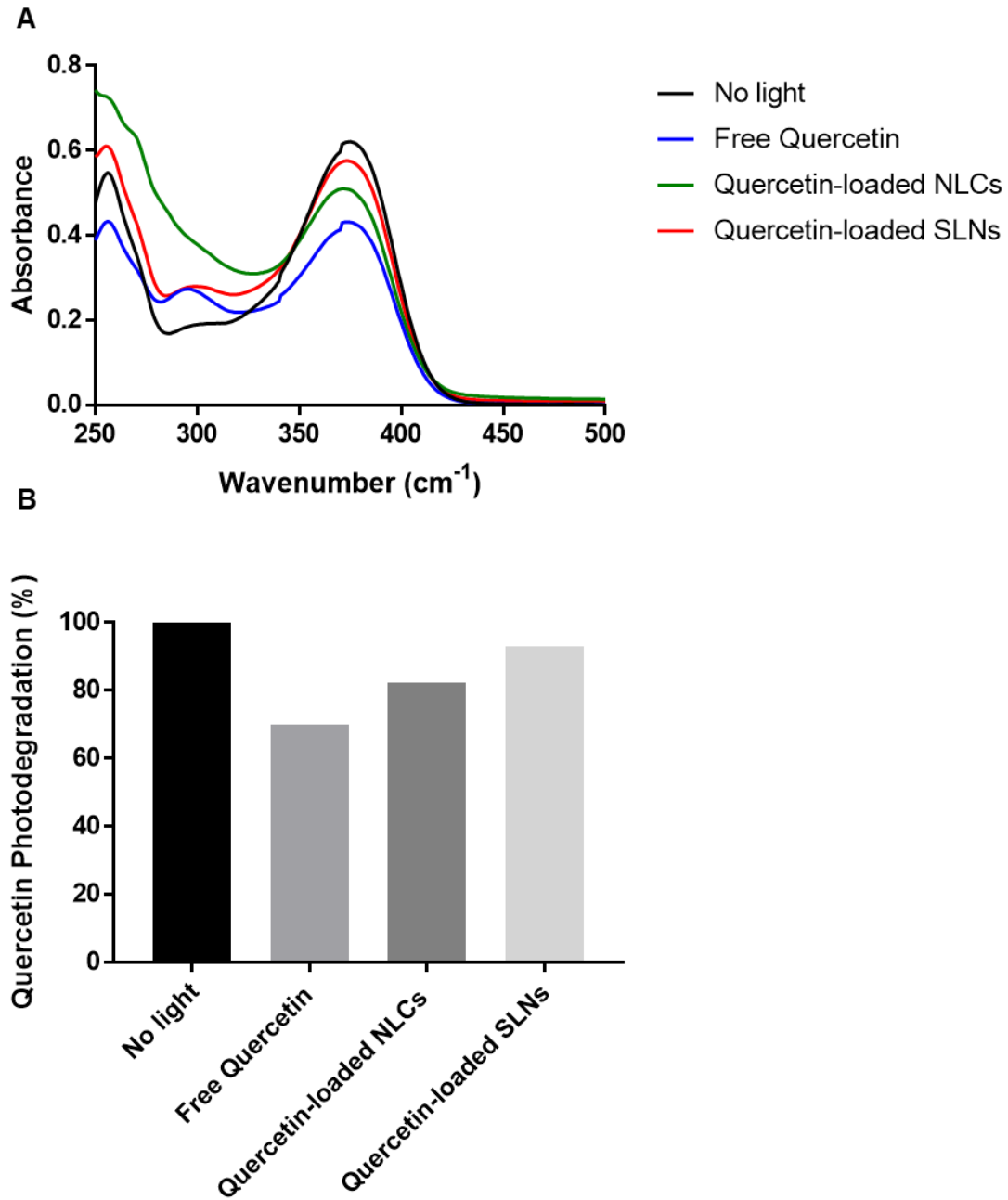


Figure 4.6 - (A) Absorption spectra of quercetin in its free form and quercetin-loaded NLCs and SLNs before and after UV light exposure for 3 hours. (B) Percentage of quercetin photodegradation after 3 hours exposure to UV light. Values correspond to means \pm standard deviation for n = 1 replicates.

4.1.9. Cellular Studies

The biocompatibility of both quercetin-loaded and unloaded NLCs and SLNs was assessed in L929 fibroblasts, following ISO 10993-1:2009.¹⁹ The effect of these nanoparticles on Human HaCaT keratinocytes' viability was also assessed, as a skin cell model. Figure 4.7 shows the *in vitro* cell viability after exposure to free quercetin and

quercetin-loaded in both NLCs and SLNs at equivalent concentrations of 3, 6.25, 12.5, 25, 50 µg/mL.

According to the obtained results, exposure of both L929 cells and keratinocytes with the different concentrations of quercetin-loaded NLCs and SLNs resulted in a concentration-dependent cell cytotoxicity. In addition, keratinocytes were also more sensitive to all evaluated nanoparticles in comparison to the L929 fibroblasts. In fact, significant loss of HaCaT cell viability was found for concentrations of quercetin loaded in the lipid nanoparticles above 12.5 µg/mL ($P \leq 0.05-0.0001$), whereas no relevant loss of cell viability was found in L929 cells for quercetin concentrations under study ($P \leq 0.001$).

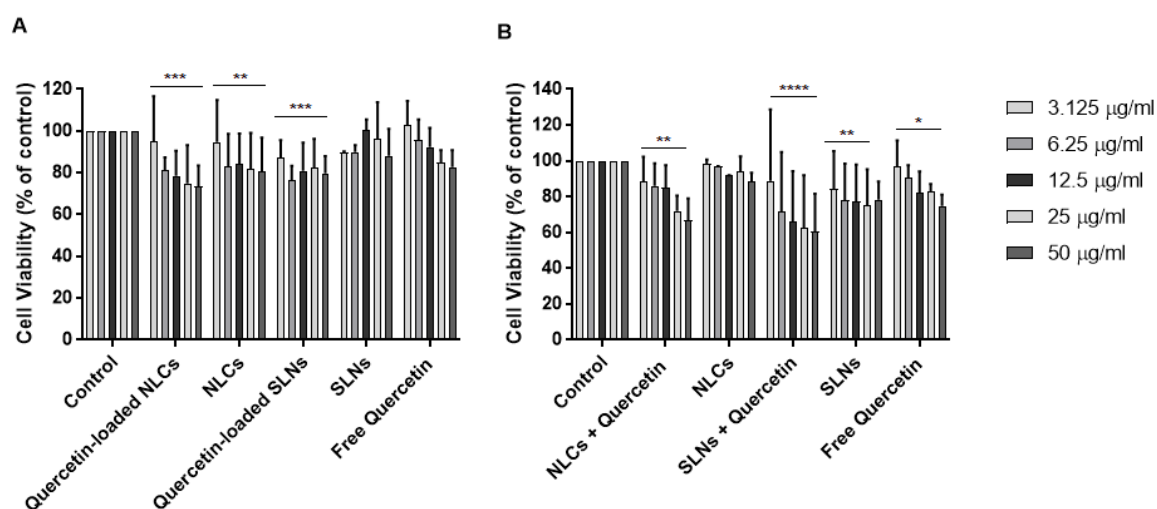


Figure 4.7 - Viability of L929 fibroblasts (A) and HaCaT keratinocytes (B) upon 24 hours of exposure to unloaded and quercetin-loaded NLCs and SLNs. Tested concentrations ranged from 3.125 to 50 µg/mL. Each result represents the mean ± standard deviation for n=4 replicates of 3 assays. Asterisks indicate statistical significance in relation to control (* $P \leq 0.05$; ** $P \leq 0.01$; *** $P \leq 0.001$; **** $P \leq 0.0001$).

4.1.9.1. Antioxidant Activity of Quercetin Incorporated within NLCs and SLNs

Quercetin has been extensively studied for its attractive pharmacological properties, in particular its antioxidant effect. Hence, in order to understand how its encapsulation in the optimized nanoparticles affects quercetin's antioxidant capacity, two scavenging assays, ABTS and DDPH, were performed (Figure 4.8A and 4.8B, respectively). According to the obtained results, the scavenging activity of quercetin-loaded nanoparticles as well as its free form increases with the concentration. Furthermore, upon incorporation into both, NLCs and SLNs, the antioxidant activity of quercetin decreased as compared to its free form for the ABTS scavenging assay. Similar results have been reported upon quercetin incorporation in hydrogels, where drug loading resulted in a decrease of quercetin's antioxidant activity in relation to its free form in approximately 20%.⁹ A similar decrease in the antioxidant activity of quercetin upon its

incorporation into both NLCs and SLNs, as compared to its free form, was not observed for the DPPH assay. This may be attributed to the fact that compared to DPPH assay the ABTS assay better estimates the antioxidant capacity of hydrophilic, lipophilic, and high-pigmented antioxidant compounds.²⁰

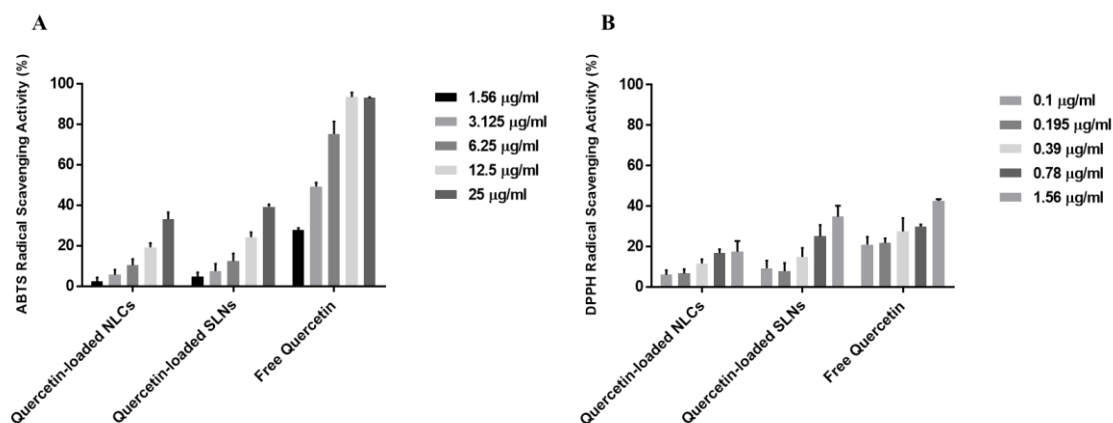


Figure 4.8 - Antioxidant activity of quercetin-loaded nanoparticles. (A) ABTS and (B) DPPH radical scavenging activity percentage of free quercetin and quercetin-loaded NLCs and SLNs. Values correspond to means \pm standard deviation for n = 3 replicates.

4.1.9.2. Assessment of Skin Permeation

To evaluate the potential of the quercetin-loaded NLCs and SLNs to permeate through the skin, the *ex vivo stratum corneum* mimetic model PVPA_{sc} was used.²¹ Data on Figure 4.9 shows that quercetin loaded in the lipid nanoparticles was more retained within the PVPA_{sc} barrier than in its free form. In fact, after 3 hours assay, about 90% of quercetin *per se* was in the apical compartment, evidencing its low absorption and permeation profile. Quercetin loading in NLCs and SLNs lead to a statistically significant increase in the absorption with low permeation, which highlights the local application of lipid nanoparticles in the skin for this flavonoid delivery. In fact, about 30% of quercetin-loaded NLCs, corresponding to approximately 60 µg of quercetin, was retained within the PVPA_{sc} barrier, whereas only 28 µg of quercetin remained in the PVPA_{sc} barrier, when applied in its free form. Similarly, Pivetta and co-workers described that using NLCs produced from Illipe butter and Calendula oil, quercetin did not permeate the skin, but was retained in the dermis and epidermis.²² Bose and collaborators addressed the permeation quercetin-loaded NLCs, produced with glyceryl dibehenate and oleic acid, as well as SLNs produced glyceryl dibehenate using human skin. Here, the authors also verified that there was no transdermal delivery for quercetin from both nanosystems.²³

Overall, the results demonstrate that encapsulation of quercetin in lipid nanoparticles, as opposed to its administration as a free drug dissolved in agents such as Mygliol, results

in a decreased permeation rate and increased retention and interaction of the drug with the skin. In turn, this advantage can result in a localized effect, with minimized release into the systemic circulation and non-specific antioxidant and anti-inflammatory effects.

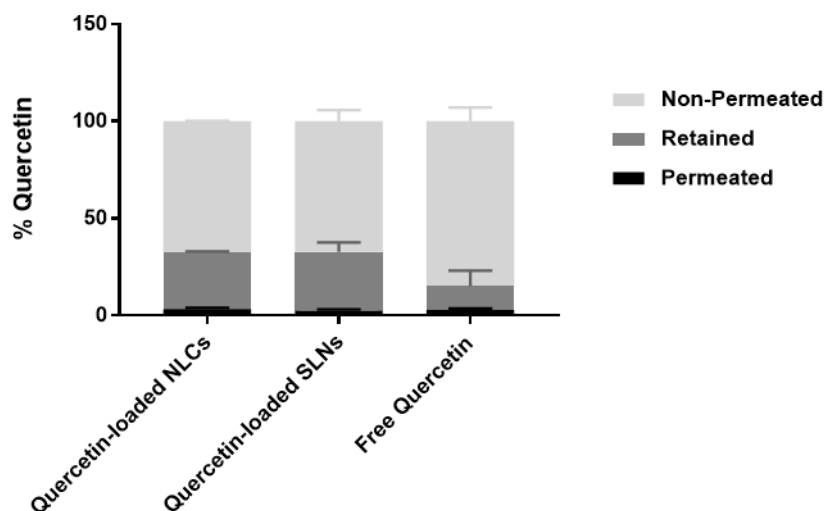


Figure 4.9 - Percentage of quercetin permeated, retained, and non-permeated through the PVPA_{SC} after 3 hours. Values correspond to means \pm standard deviation for $n = 3$ replicates.

4.1.10. Conclusion

In this chapter, NLCs were optimized for loading quercetin. The optimized NLCs displayed a high encapsulation efficiency, storage stability at 20°C and 4°C up to 12 weeks, and biocompatibility with fibroblasts and keratinocytes. The counterpart SLNs were obtained similarly for comparison and exhibited lower encapsulation efficiency and similar storage stability and biocompatibility. Thus, the presence of a natural lipid from pomegranate improved quercetin loading in the lipid nanoparticle without causing significant cytotoxicity. Additionally, skin permeation studies in a mimetic SC model revealed that encapsulation of quercetin results in an increase of quercetin in the skin, whilst allowing the retention of its antioxidant activity. These results demonstrate that the optimized NLCs may represent an advantageous topical delivery system for flavonoids contributing to the application of this natural product as preventive and therapeutic skin agent.

4.2. Characterization of SA-PVA Hydrogels Incorporating Quercetin-Loaded Nanoparticles

4.2.1. Fourier-Transform Infrared Spectroscopy Evaluation

FTIR spectroscopy was conducted to identify the functional groups in the developed hydrogels based on SA and PVA molecules as well as to evaluate whether quercetin was successfully incorporated in the hydrogels and the existence of possible chemical interactions between quercetin and the polymeric matrix. The FTIR spectra for unloaded and quercetin-loaded hydrogels as free quercetin or loaded into NLCs and SLNs are displayed in Figure 4.10. The FTIR spectrum of PVA exhibits absorption of C–OH at 1050–1150 cm^{-1} , O–H stretching at 3200–3600 cm^{-1} , CH_2 twisting vibration around 1023 cm^{-1} and C–H stretching of CH_2 group at 2850–3000 cm^{-1} .²⁴ The characteristic IR spectrum of pure SA exhibits absorption bands at 1574 cm^{-1} and 1416 cm^{-1} that are related to the asymmetric and symmetric stretching modes of the carboxylate anion, as well as an absorption band at 1032 cm^{-1} related to the stretching vibrations of CO-C group.^{21,24,25} The IR spectra of SA/PVA hydrogels show the characteristic peaks described for both pure SA and PVA, which indicates the formation of an effective blend of polymers. Similar results were obtained by Esposito *et al.* (2020), using different ratios of SA and PVA.²¹ Quercetin spectrum shows a number of characteristic bands representing O-H stretching (3700 to 3100 cm^{-1}), C=O stretching (1730 cm^{-1}), C–C stretching (1649 cm^{-1}), C–H bending (1461, 1369, and 838 cm^{-1}), C–O stretching in the ring structure (1272 cm^{-1}), and C–O stretching (1070 to 1089 cm^{-1}).²⁶ However, the major characteristic bands of quercetin are not observed in the peaks of quercetin-loaded hydrogels, which may be attributed to the higher ratio of polymer versus quercetin in the hydrogels. In addition, the disappearance of quercetin characteristic peaks may present itself as an indirect confirmation of its incorporation within the polymeric matrix of the hydrogels. Different authors report the disappearance of quercetin characteristic peaks upon incorporation of quercetin into different vehicles.^{27–29} The disappearance of characteristic peaks of quercetin after encapsulation into NLCs was also observed by Ni *et al.* (2015).¹²

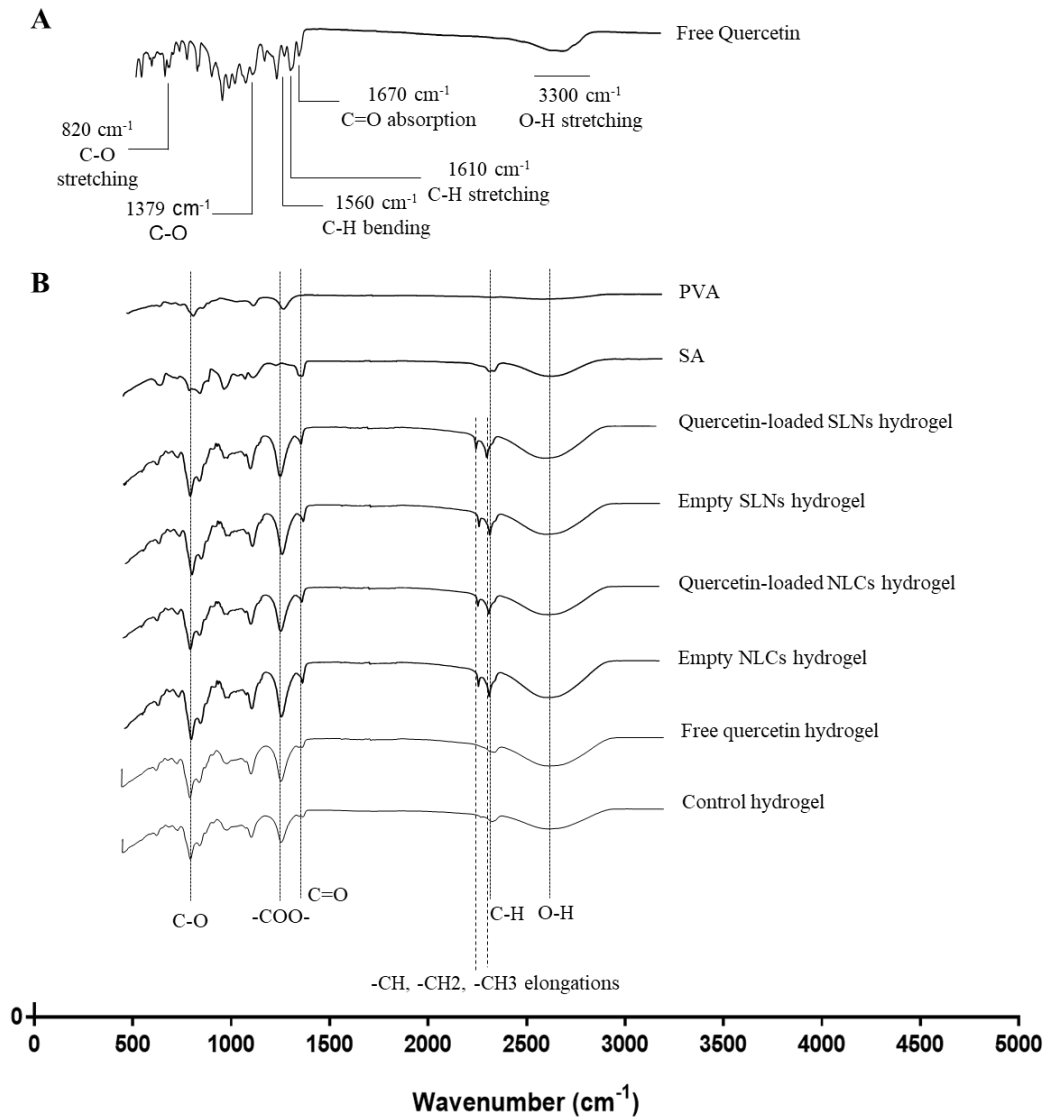


Figure 4.10 - FTIR spectra of (A) quercetin in its free form and (B) quercetin-loaded hydrogels. Unloaded and hydrogels loaded with empty nanoparticles are also displayed.

4.2.2. Rheology Analysis of SA-PVA Hydrogels

Rheological characterization of hydrogel systems design to be used in cutaneous applications is of extreme importance since it provides information regarding the rigidity and elasticity of the polymeric network.³⁰ Cutaneous application implies that hydrogels are subjected to oscillatory stress, temperature, and moisture, thus its import to assess their effects on the rheological properties of the hydrogels in order to ensure their clinical applicability.^{30,31} In order to better understand their mechanical properties, control and

quercetin-loaded hydrogels were submitted to rheology studies, in particular viscosimetry, thixotropy, and resistance to deformation and temperature.

Figure 4.11 represents the viscosimetry analysis of the control hydrogel as well quercetin-loaded hydrogels as free quercetin and quercetin loaded into NLCs and SLNs. According to the obtained results incorporation of quercetin in the hydrogel matrix did not affect its structure or mechanical properties. In addition, in all unloaded and quercetin-loaded hydrogels it is possible to observe that with an increase in shear rate, the shear stress increases as the shear viscosity decreases, being that consistent with a pseudoplastic behaviour. Pseudoplastic formulations are viscous under static conditions and become thinner or less viscous following the application of shear-stress, thus resulting in easier spreadability, which is an important characteristic of systems design for a topical application, since it facilitates its application and improved drug permeation through the skin.^{21,31–33} Souto *et al.* (2006) demonstrated that formulations based on NLCs and SLNs prepared using Carbopol 934 as carriers for imidazole antifungal agents, demonstrated pseudoplastic behaviour with thixotropic properties, proving its usefulness to be used as topical delivery systems.³⁴

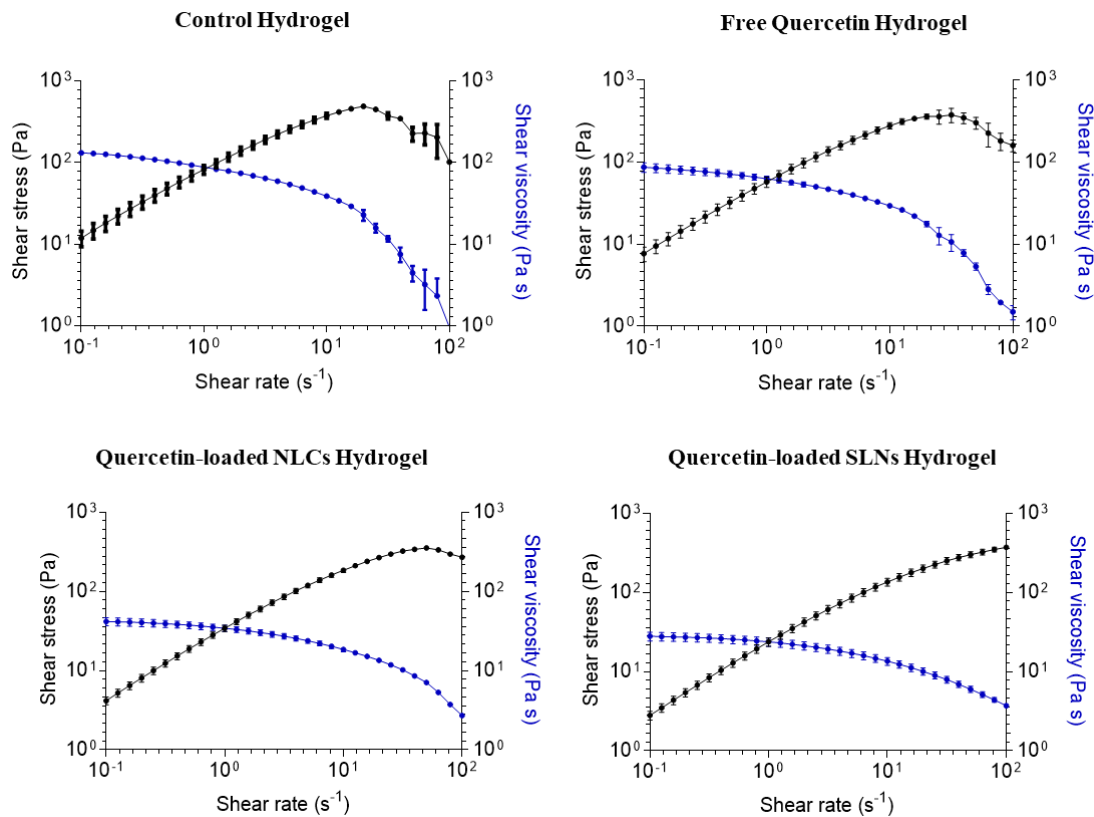


Figure 4.11 - Viscosimetry analysis of control and quercetin-loaded hydrogels, as free quercetin and quercetin-loaded NLCs and SLNs, through shear stress (black line) and shear viscosity (blue line) data. Data points correspond to mean \pm standard deviation for $n = 2$ replicates.

Thixotropy is when the rheological manifestation of viscosity-induced structural changes is reversible and time-dependent.³³ According to Figure 4.12, all hydrogels are non-thixotropic since the initial viscosity was almost completely regained after a high shear was applied during thirty seconds to replicate extreme stress conditions. Similar results were observed by Esposito *et al.* (2020) and Wu *et al.* (2020). The authors reported that similar SA-PVA hydrogels displayed self-healing capacity to regain their initial state after stress being induced.^{21,35}

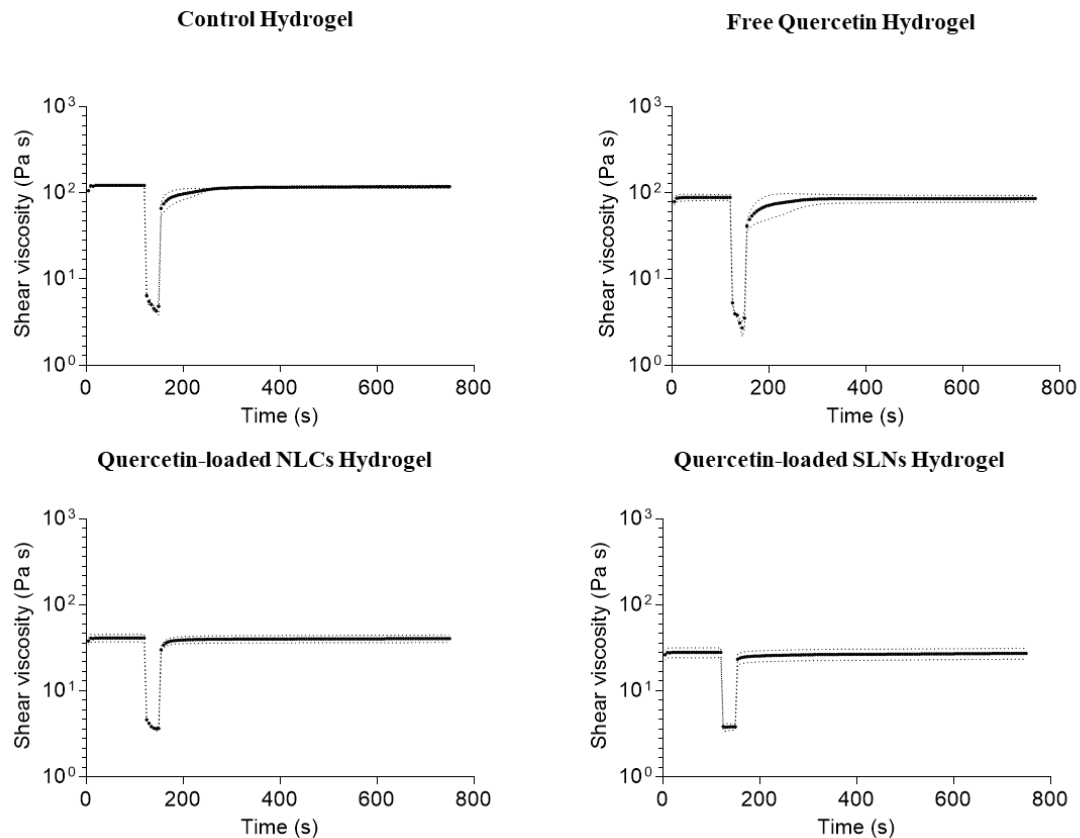


Figure 4.12 - Thixotropy analysis of control and quercetin-loaded hydrogels, as free quercetin and quercetin-loaded NLCs and SLNs. Data points correspond to mean \pm standard deviation for n = 2 replicates.

Stress application can result in polymeric matrix rearrangement, thus in order to assess whether all hydrogels are stable and resistant to deformation, an amplitude sweep test was performed.³⁴ The hydrogels were submitted to a range of amplitudes in order to determine the linear viscoelastic region. According to Figure 4.13, both elastic and viscous modulus exhibit a constant profile, which indicates a high resistance to deformation. Similarly, all hydrogels display good resistance to a temperature increase from 20 to 40° C, which is shown by the constant maintenance of the elastic and viscous modulus through the increase in temperature (Figure 4.14). Considering a potential topical application, resistance to temperatures between 32 and 37° C is of extreme

importance. These results agree with data published by Esposito *et al.* (2020), in which similar SA-PVA hydrogels incorporating free quercetin were highly resistance to both deformation and a temperature increase from 20 to 40 °C.²¹

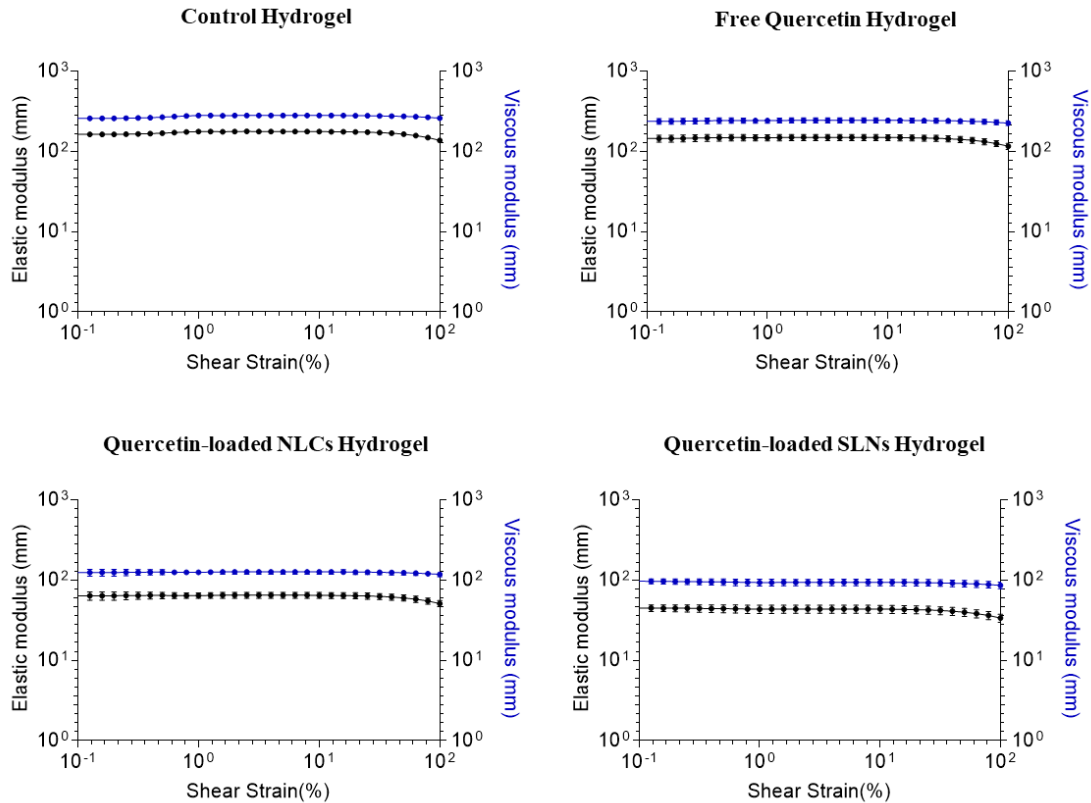


Figure 4.13 - Resistance to deformation based on the determination of viscoelastic region of control and quercetin-loaded hydrogels, as free quercetin and quercetin-loaded NLCs and SLNs. Data points correspond to mean ± standard deviation for n = 2 replicates.

Overall, the rheological analysis revealed that all tested hydrogels displayed pseudoplastic behavior, a non-thixotropic profile, and good resistance to deformation and temperatures ranging from 20 to 40°C. In addition, incorporation of quercetin either in its free form, or encapsulated into both NLCs and SLNs, did not significantly affect their mechanical properties, thus making them highly attractive topical delivery systems.

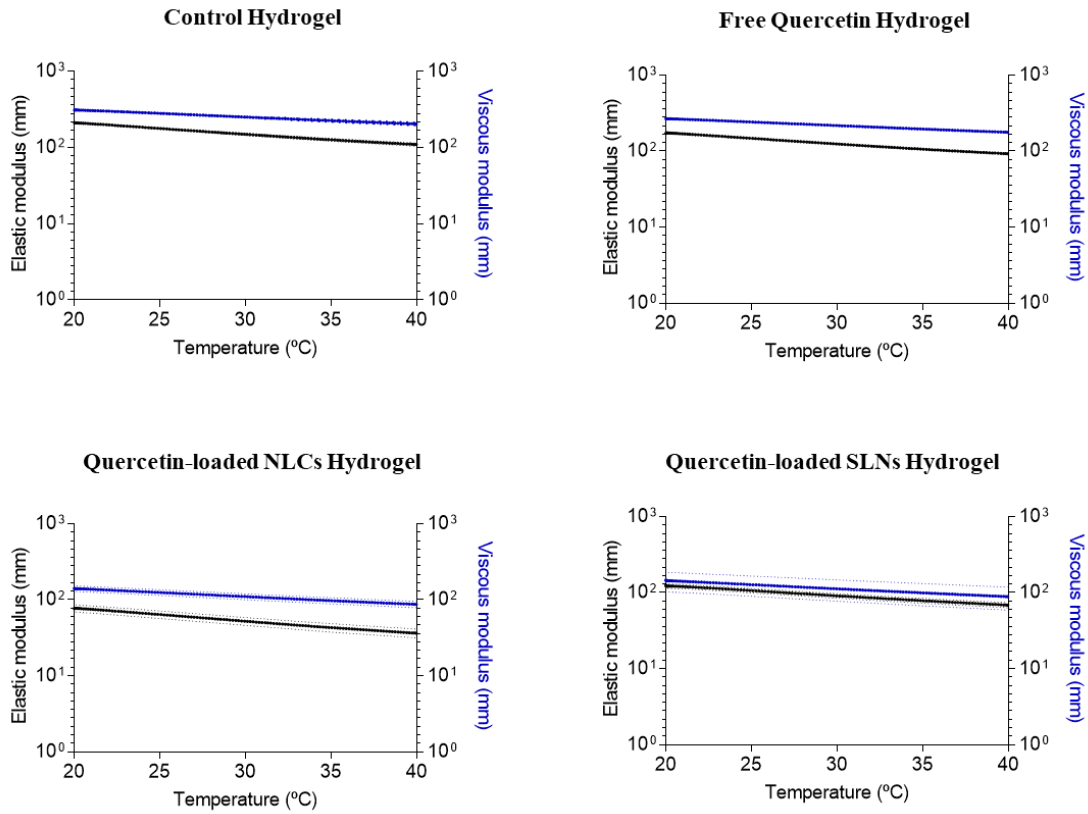


Figure 4.14 - Resistance to temperature based on the determination of viscoelastic region of control and quercetin-loaded hydrogels, as free quercetin and quercetin-loaded NLCs and SLNs. Data points correspond to mean \pm standard deviation for n = 2 replicates.

4.2.3. Long-Term Mechanical Stability Analysis of SA-PVA Hydrogels

In order to evaluate the storage stability of the hydrogels over a period of six weeks, quercetin-loaded hydrogels as free quercetin and quercetin loaded into NLCs and SLNs were submitted to previous rheology studies, in particular viscosimetry, thixotropy, and resistance to deformation and temperature. Figure 4.15 represents the viscosimetry analysis of all hydrogels after a period of six weeks. According to the obtained results all hydrogels retained their shear thinning behaviour, as shear stress increases, and shear viscosity decreases with increasing shear rate. It is possible to conclude that all hydrogels continued to display a pseudoplastic behaviour, however, the overall viscosity of hydrogels incorporated with quercetin loaded NLCs and SLNs decreased in 50%. The initial viscosity of the hydrogels loaded with quercetin in its free form maintain their viscosity profile, thus being stable over a period of six weeks.

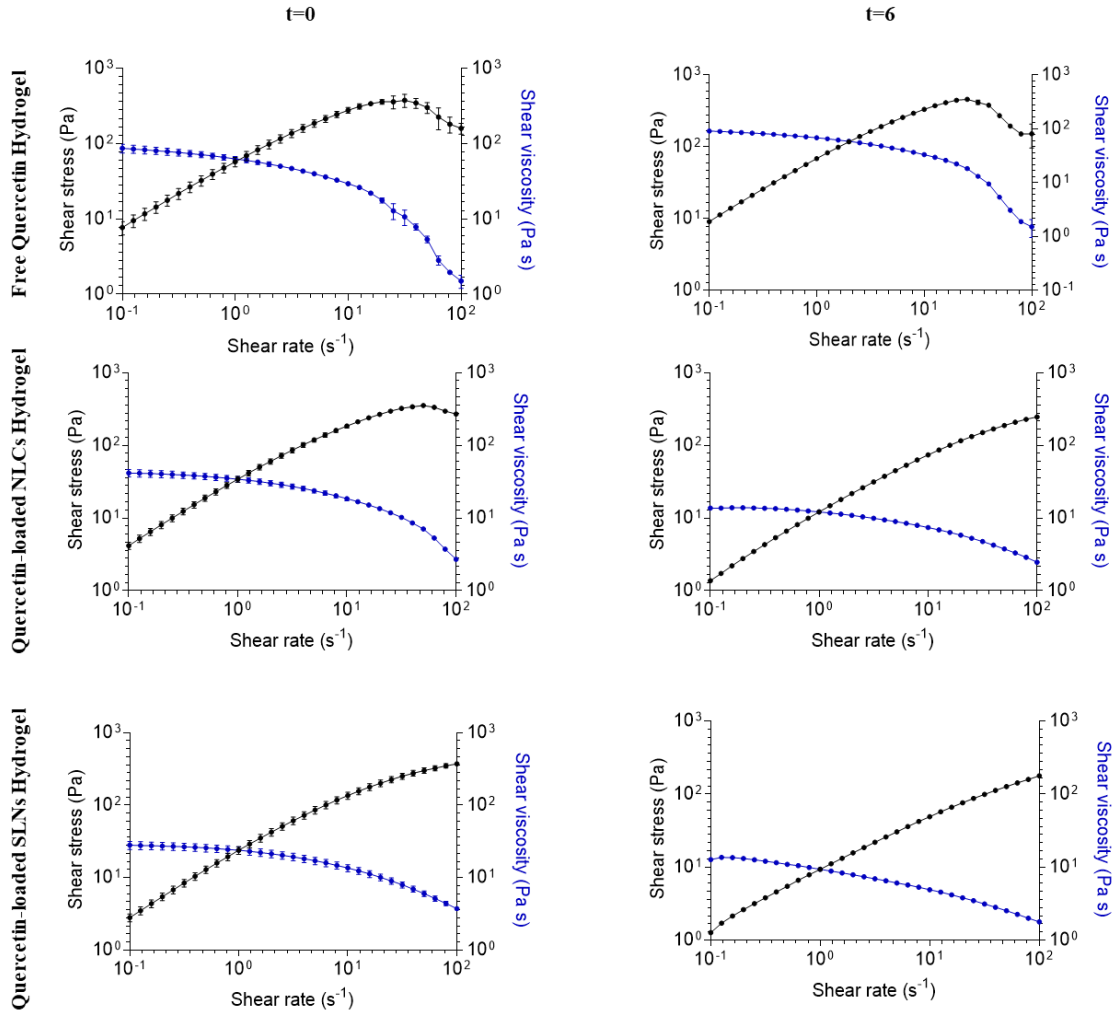


Figure 15 - Viscosimetry analysis over a period of six weeks of quercetin-loaded hydrogels, as free quercetin and quercetin-loaded NLCs and SLNs, through shear stress (black line) and shear viscosity (blue line) data. Data points correspond to mean \pm standard deviation for $n = 2$ replicates.

These results are consistent with the thixotropy analysis. All hydrogels are non-thixotropic, maintaining their self-healing capacity to regain their initial viscosity after shear stress is applied, although the amount of time necessary to regain their initial viscosity is higher as compared to fresh hydrogels (Figure 4.16). Again, a decrease in the viscosity of the hydrogels incorporated with quercetin-loaded nanoparticles is observed.

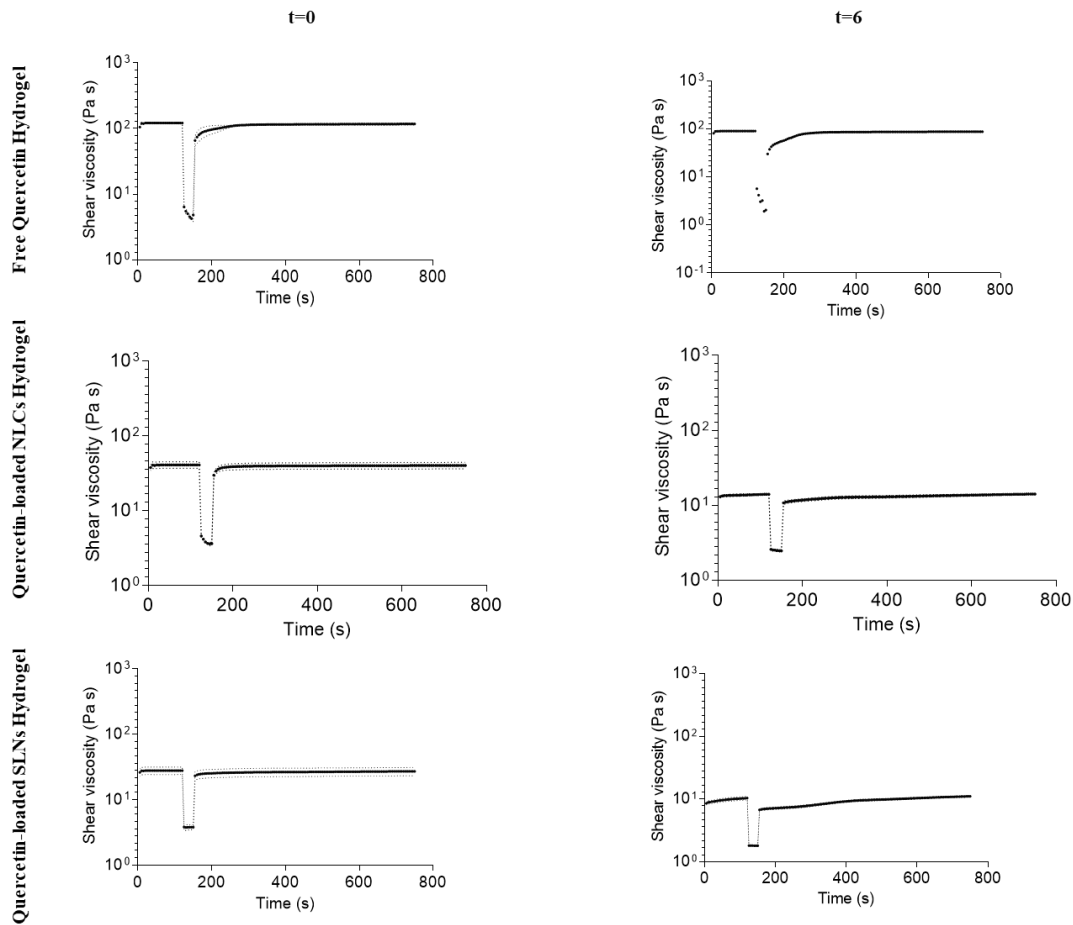


Figure 4.16 - Thixotropy analysis over a period of six weeks of quercetin-loaded hydrogels, as free quercetin and quercetin-loaded NLCs and SLNs. Data points correspond to mean \pm standard deviation for $n = 2$ replicates.

As observed in Figure 4.17, after six weeks of storage all hydrogels appear to continue to be resistant to deformation, demonstrated by the overall constant profile of both elastic and viscous modulus. Deformation only occurred for higher values of shear strain. A decrease in resistance to temperate (Figure 4.18) after a six-week storage period appear to be higher for hydrogels incorporated with quercetin-loaded SLNs, whereas only small changes in viscosity are observed for free quercetin and quercetin-loaded NLCs incorporated into the hydrogels. Overall, the results demonstrate that the incorporation of nanoparticles into hydrogels affect their stability over a period of six weeks, resulting in a decrease of the hydrogel's viscoelastic properties.

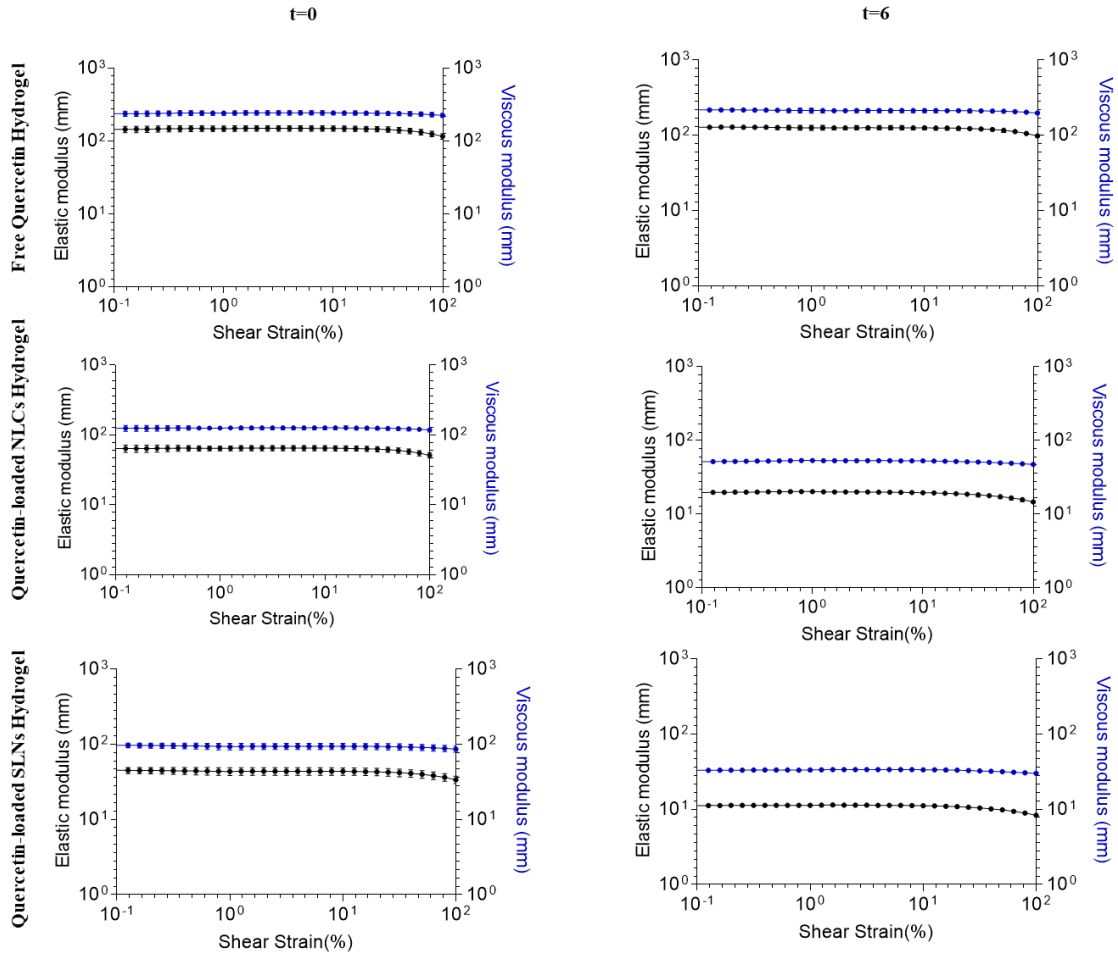


Figure 4.17 - Resistance to deformation based on the determination of viscoelastic region over a period of six weeks of quercetin-loaded hydrogels, as free quercetin and quercetin-loaded NLCs and SLNs. Data points correspond to mean \pm standard deviation for $n = 2$ replicates.

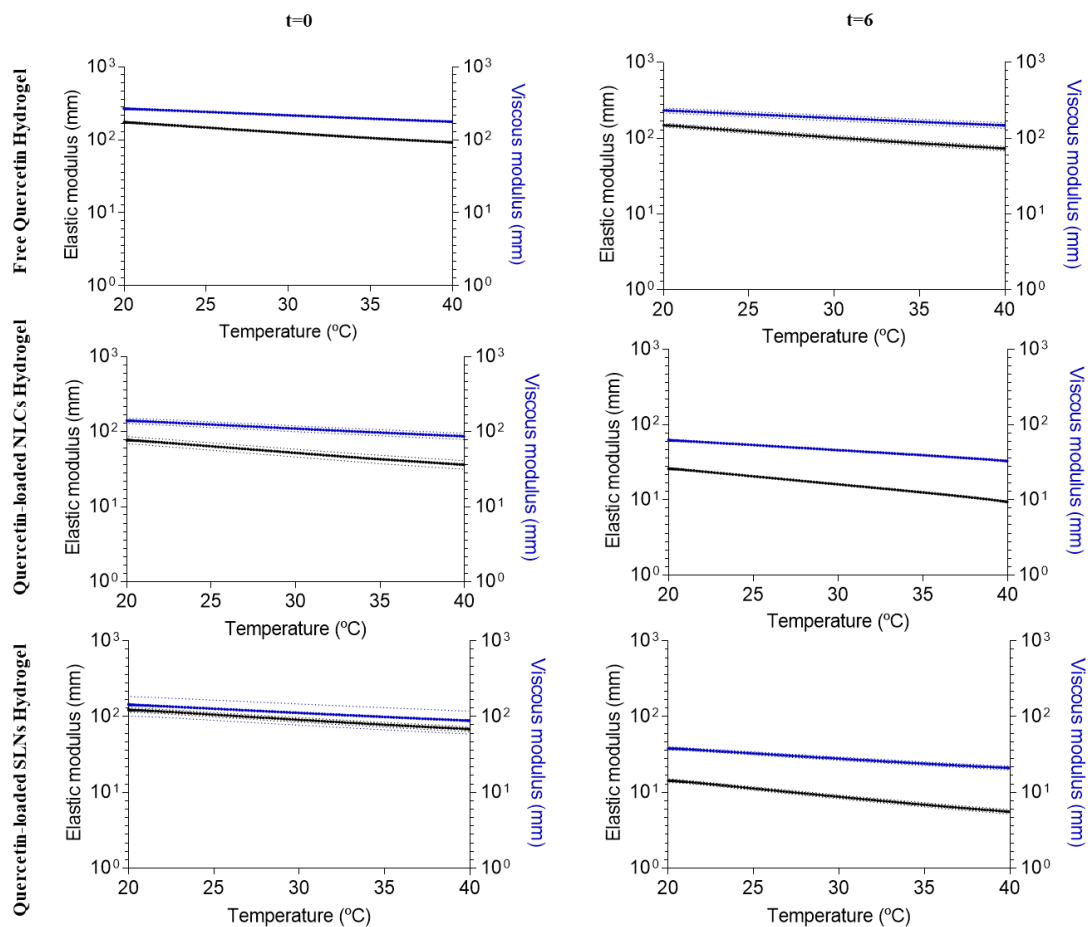


Figure 4.18 - Resistance to temperature based on the determination of viscoelastic region over a period of 6 weeks of quercetin-loaded hydrogels, as free quercetin and quercetin-loaded NLCs and SLNs. Data points correspond to mean \pm standard deviation for $n = 2$ replicates.

4.2.4. Quercetin-Loaded SA-PVA Hydrogels Morphology

The morphology of free quercetin and quercetin-loaded SA-PVA hydrogels was observed at different magnitudes on SEM (Figure 4.19). The SA-PVA hydrogel matrix displayed an interconnected branch structure. Similar results have previously been shown with SA-PVA hydrogels containing quercetin.²¹ The authors observed that incorporation of quercetin resulted in an increase in branching and formation of micropores.²¹ Here, the incorporation of quercetin-loaded and empty nanoparticles significantly affected the hydrogel matrix. The network structured of these hydrogels became more compact and the porosity significantly decreased. These results suggest that quercetin nanoparticles were successfully incorporated into the hydrogel matrix.

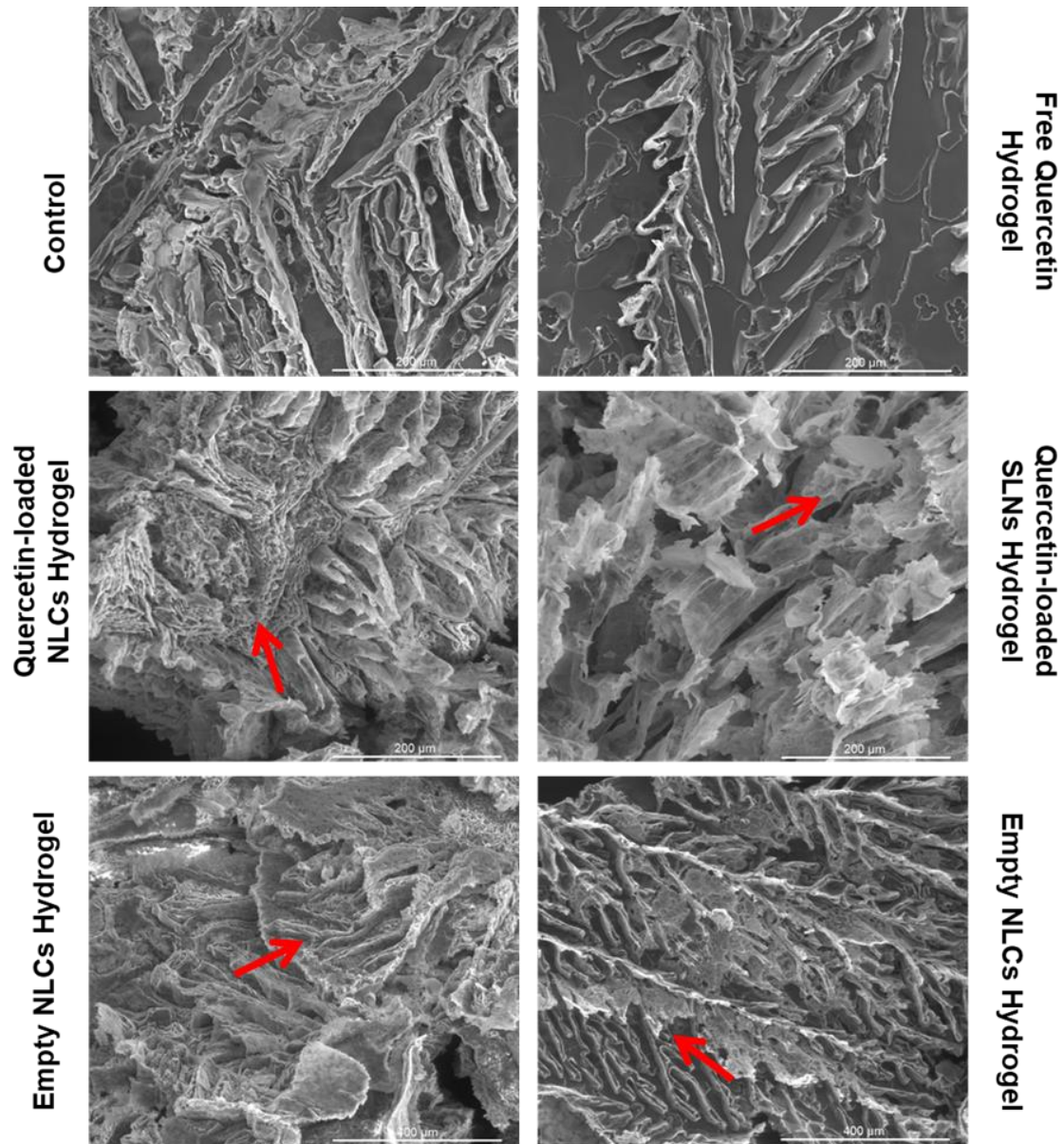


Figure 19 - Analysis of the hydrogel's morphology. SEM micrographs of quercetin free and quercetin-loaded NLCs and SLNs incorporated into sodium alginate-poly(vinyl) alcohol (SA-PVA) hydrogels. Scale bar 200 μm and 400 μm . Red arrows indicate more compact areas presenting lower porosity.

4.2.5. Antioxidant Activity of Quercetin-Loaded SA-PVA Hydrogels

One of the most attractive pharmacological properties of quercetin is its antioxidant capacity. Thus, in order to assess whether its incorporation into SA-PVA hydrogels, either in its free form or encapsulated into NLCs and SLNs, affects quercetin's antioxidant activity, the ABTS scavenging assay was performed (Figure 4.20). According to the obtained results, the scavenging activity of quercetin, either free or incorporated within the SA-PVA hydrogels, is concentration-dependent. In addition, incorporation of quercetin in its free form into the hydrogel matrix did not significantly affect its antioxidant

capacity ($P < 0.05$). However, when quercetin is encapsulated into either NLCs and SLNs prior to its incorporation within the SA-PVA hydrogels, its antioxidant capacity significantly decreases as compared to its free form ($p < 0.0001$) in approximately 20%. This decrease in quercetin's antioxidant activity is consistent with the higher protection provided by the nanoparticles' lipidic matrix. A similar result was obtained upon incorporation of quercetin into SA-PVA hydrogels.²¹

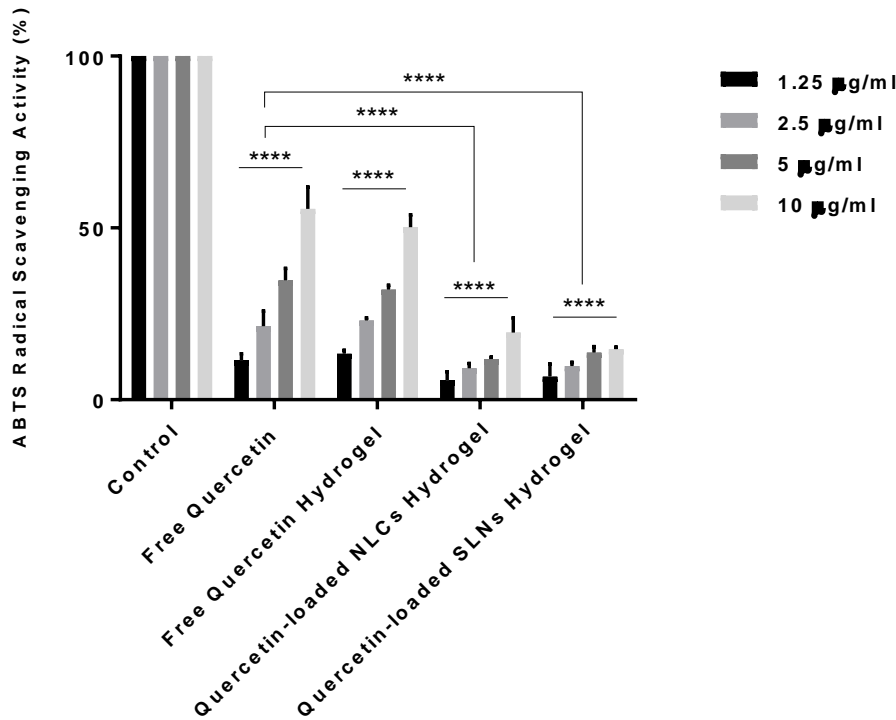


Figure 4.20 - Antioxidant activity of quercetin incorporated within SA-PVA hydrogels. ABTS radical scavenging activity percentage of free quercetin and quercetin-loaded SA-PVA hydrogels, as a free quercetin or loaded into NLCs and SLNs. Data points correspond to mean \pm standard deviation for $n = 3$ replicates, Asterisks indicate statistical significance in relation to control (**** $p < 0.0001$). # Represent statistical significance in relation to quercetin in its free form (###, $p \leq 0.0001$).

4.2.6. Cellular Studies

4.2.6.1. Biocompatibility

To investigate the biocompatibility of the SA-PVA hydrogels, HaCaT cells were treated with quercetin-loaded hydrogels (both free quercetin and quercetin loaded into NLCs and SLNs) and the cell viability was determined. Unloaded hydrogels and unloaded nanoparticles incorporated into the hydrogels were used as controls. According to Figure 4.21, exposure of keratinocytes to different concentrations of quercetin-loaded hydrogels resulted in a concentration-dependent cell cytotoxicity. In addition, no significant loss of cell viability was observed for concentrations of quercetin loaded in the hydrogels under

5 µg/mL ($P \leq 0.001$), which is demonstrated by the acceptable cell viability ($>70\%$) based on the ISO 10993-5:2009 cutoff of 70% cell viability.³⁶ However an increase in cytotoxicity was observed for quercetin concentrations of 10 µg/mL. In addition, keratinocytes were more sensitive to exposure to hydrogels loaded with empty NLCs ($P \leq 0.05$), whereas exposure to hydrogels loaded with empty SLNs had no significant effect on cell viability. In a similar way, keratinocytes were more sensitive to quercetin loaded in its free form in the hydrogels, as compared to quercetin encapsulated into NLCs and SLNs. Overall, these results demonstrate that concentrations of quercetin equal or under 5 µg/mL are safe to be used, since no significant loss of cell viability was observed for all the hydrogels under study.

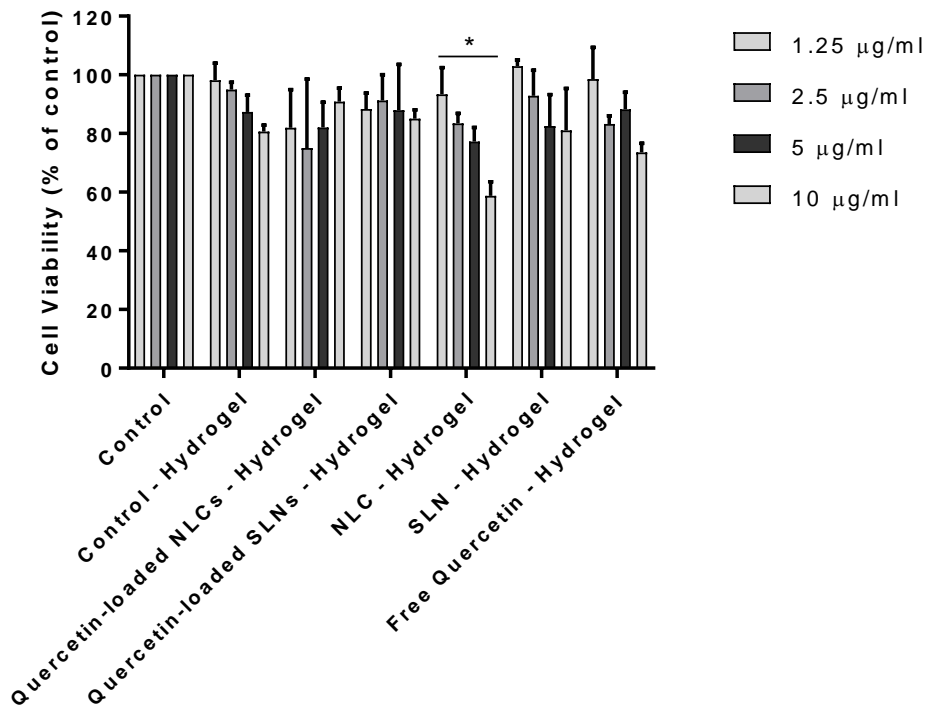


Figure 4.21 - Viability HaCaT keratinocytes upon 24 hours of exposure to the developed nanoformulations, unloaded and quercetin-loaded hydrogels as free quercetin or loaded into NLCs and SLNs. Tested concentrations ranged from 1.25 to 10 µg/mL in quercetin and equivalent polymer concentration of 20.9 to 167 mg/mL. Each result represents the mean \pm standard deviation for $n=4$ replicates of 3 independent assays. Asterisks indicate statistical significance in relation to non-irradiated control cells (*, $p \leq 0.05$). No asterisks indicate no statistical significance ($p > 0.05$).

4.2.6.2. Biocompatibility Evaluation of the Effect of Ultraviolet B Irradiation on Keranocytes Treated with the Quercetin-Based Nanoformulations – Photoprotective Assay

A preliminary study evaluated the effect of different UVB intensities (60, 80, 100 and 120 mJ/cm²) on the HaCaT cell's viability. An intensity of 60 mJ/cm² resulted in a decrease

of HaCaT viability of approximately 50% (Figure 4.22). Based on these results the intensity of 60 mJ/cm² was chosen for further studies.

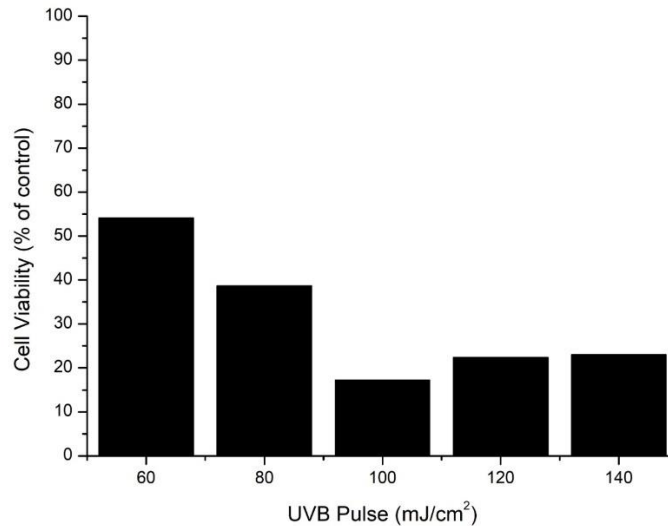


Figure 4.22 - Effect of different UVB intensities (60, 80, 100 and 120 mJ/cm²) on the HaCaT cell's viability.

To assess the photoprotective effect of the SA-PVA hydrogels under study, HaCaT cells were exposed for 24 hours with an equivalent concentration of quercetin-containing hydrogels (free quercetin-loaded hydrogels and quercetin-loaded NLCs and SLNs incorporated into the hydrogels) of 2.5 µg/mL. Following exposure, cells were irradiated at an intensity of 60 mJ/cm², and then incubated for 24 hours, prior to cell viability measurement. According to the obtained results (Figure 4.23A), HaCaT exposure to quercetin-free hydrogels showed no protective effect on UVB radiation, with a loss of approximately 30% in cell viability compared to the irradiated control group. However, a significant increase of approximately 40% and 30% in cell viability was observed when cells were exposed respectively to hydrogels containing quercetin encapsulated into NLCs and SLNs ($p \leq 0.001$). In addition, a significant increase of approximately 20% in cell viability was observed when cell were exposed to containing quercetin in its free form ($p \leq 0.05$), thus suggesting that these delivery systems may have a photoprotective effect against UVB irradiation. Control hydrogels show no statistically significant protective effect on UVB radiation. The photoprotective effect appears to be more significant when quercetin is encapsulated into nanoparticles rather than incorporated in its free form on the hydrogels. Previously treatment of keratinocytes with quercetin-loaded chitosan nanoparticles resulted in an increase in cell viability following exposure to irradiation.

This effect was attributed to the successful internalization and sustained retention of quercetin by skin cells.³⁷

Here, the lipid nanoparticles used to encapsulate quercetin were previously shown to increase its permeation and retention in the SC barrier, as compared to its free form (Figure 4.8). Hence, the combination of quercetin-loaded nanoparticles with a hybrid hydrogel was used as a tool to enhance quercetin's skin bioavailability and simultaneously reinforce its photoprotective effect against skin UVB-induced disorders.³⁸

It is well described that UVB radiation leads to cell death mediated by apoptosis.³⁸ Figure 4.8 points out the apoptotic profile of HaCaT cells upon the photoprotective assay. Cells were incubated with quercetin-containing SA-PVA hydrogels prior to irradiation on UVB-induced apoptosis. The percentage of apoptotic cells was calculated by flow cytometric analysis of the cells that were coincidentally stained with FITC Annexin V and 7-AAD-Annexin V is a member of the annexin family of intracellular proteins that binds to phosphatidylserine (PS) in a calcium-dependent manner. In healthy cells, PS is found on the intracellular leaflet of the plasma membrane, but during early apoptosis, PS translocates to the external leaflet due to membrane asymmetry loss. Fluorochrome-labelled Annexin V can then be used to specifically target and identify apoptotic cells. However, Annexin V binding alone cannot differentiate between apoptotic and necrotic cells, requiring the use of 7-AAD, a DNA intercalator. Late apoptotic cells and necrotic cells lose their cell membrane integrity thus being permeable to 7-AAD, while early apoptotic cells will exclude 7-AAD.^{39,40}

According to the obtained results (Figure 4.23B), the percentage of cells in early apoptosis is significantly increased in UVB-irradiated control cells (ca. 44 %), whereas the percentage of viable cells is significantly decreased in ca. 54%. No considerable cells in late apoptosis are observed in UVB-irradiated control cells (less than 0.5%). However, following treatment with quercetin-containing hydrogels a significant decreased (ca. 25%) of cells in early apoptosis was observed as compared to the irradiated control group. This is accompanied by a significant increase in the percentage of viable cells (ca. 26%) as compared to the irradiated control group. These results correlate with the increase in cell viability observed, thus suggesting a photoprotective effect.

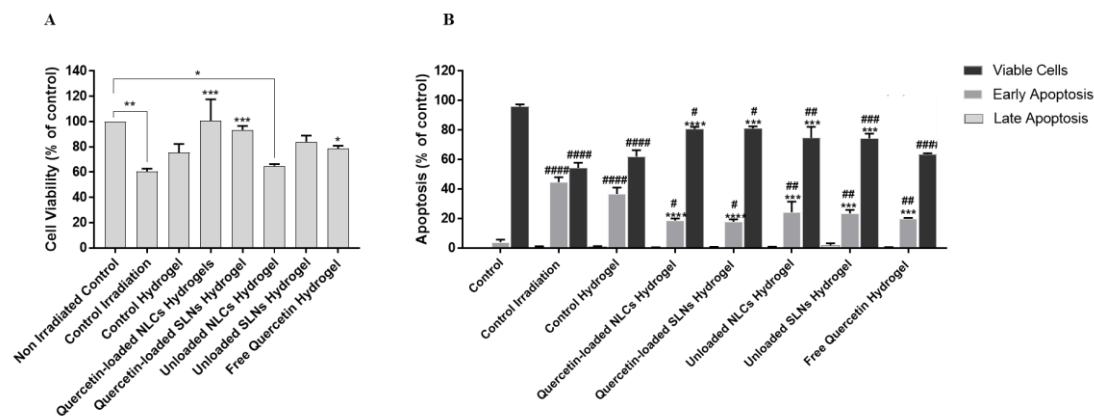


Figure 4.23 - Effects of free quercetin and quercetin-containing hydrogels (both quercetin free-loaded hydrogel and quercetin-loaded NLCs and SLNs incorporated into hydrogels) on cell viability in UVB (60 mJ/cm²) irradiated HaCaT keratinocytes at a concentration of quercetin of 2.5 µg/mL. (A) Photoprotection effect on cells exposed to the hydrogels prior to irradiation and (B) Apoptosis analysis on cells exposed to the hydrogels prior to irradiation. Flow cytometry analysis was performed following staining with FITC Annexin V and 7-AAD and the percentage of viable cells as well as early and late apoptotic cells is showed. Data are representative of three independent experiments as mean ± SD. Asterisks indicate statistical significance in relation to irradiated control cells (*, p ≤ 0.05; **, p ≤ 0.01; ***, p ≤ 0.001). No asterisks indicate no statistical significance (p > 0.05). # Represent statistical significance in relation to non-irradiated control cells (#, p ≤ 0.05; ##, p ≤ 0.01; ###, p ≤ 0.0001).

4.2.6.3. Effect of Quercetin-Based Nanoformulations on Intracellular ROS Levels

UV radiation is known to induce DNA damage, either directly or via ROS generation.⁴¹ Thus, in order to assess whether quercetin-loaded hydrogels have the ability to reduce UVB-induced ROS generation, a fluorescence assay using DCFH-DA was performed. DCFH-DA is a non-fluorescent lipophilic molecule that penetrates the plasma membrane into the cytosol, where it's activated by esterase-mediated cleavage of acetate forming DCFH. In the presence of ROS, DCFH is oxidized resulting in the formation of DCF, a green fluoresce probe. The fluorescence intensity is proportional to the level of intracellular ROS.⁴¹ The results obtained are shown in Figure 4.24. Compared to the non-irradiated control cells, UVB irradiation significantly increased the DCF fluorescence intensity, thus indicating that UVB irradiation causes the production of intracellular ROS in HaCaT cells that were not treated in quercetin-based nanoformulations. When HaCaT cells were treated with quercetin hydrogels (either quercetin in its free form or quercetin encapsulated NLCs and SLNs incorporated in the hydrogel matrix) a significant decrease of approximately 70% in the DCF fluorescence intensity was observed, thus suggesting a decrease in the level of intracellular ROS due to quercetin's scavenging ability. In addition, a decrease in the intracellular levels of ROS was also observed when cells were treated with hydrogels incorporated with empty NLCs, which suggests that the pomegranate oil is also capable of scavenging the intracellular ROS generated by UVB irradiation. The results also show that no cumulative effect between quercetin and

pomegranate oil was observed. Previously, different authors have reported a protective effect of pomegranate oil against both H₂O₂ and UVB-induced oxidative stress.⁴²⁻⁴⁴ On the other hand, a similar decrease in the intracellular ROS levels was not observed when cells were treated with hydrogels containing empty SLNs, thus confirming the potential beneficial role of the lipid liquid PO. These results demonstrate that the ability of antioxidants such as quercetin to scavenge or suppress the generation of intracellular ROS may be an effective strategy to prevent UVB-induced cell death. Similar results were obtained using quercetin in its free form and encapsulated into liposomes.^{41,45} In fact, Zhu and co-workers reported that quercetin's (20 μM) ability to inhibit HaCaT UVB-induced cell damage is attributed to its ROS clearance ability. This prevented cell membrane and mitochondria from ROS attack and inhibited cell membrane fluidity decrease and mitochondrial membrane depolarization. The author reported that the outflow of cytochrome c and apoptosis were markedly inhibited, concluding that the photoprotective effect was mediated by quercetin's ROS scavenging ability.⁴⁵

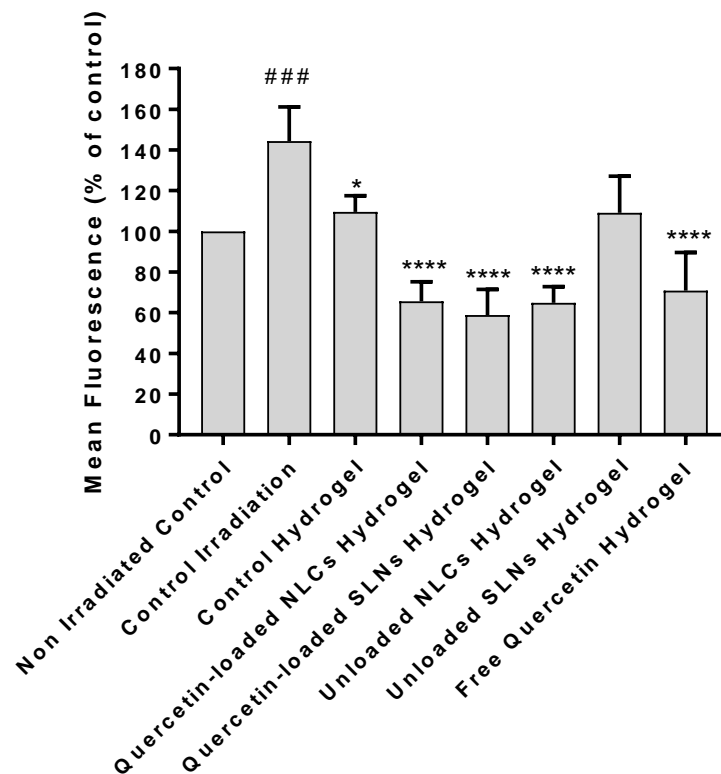


Figure 4.24 - Effect of quercetin-based nanoformulations on intracellular ROS levels in cultured HaCaT cells. Cells were treated with quercetin-based nanoformulations at a concentration of quercetin of 2.5 μg/mL for 24 hours, prior to UVB irradiation (60 mJ/cm²). Immediately following irradiation, the intracellular ROS levels were determined using the fluorogenic probe DCFH-DA. The intracellular ROS levels were quantitatively determined via flow cytometry. Data are representative of three independent experiments as mean ± SD. Asterisks indicate statistical significance in relation to irradiated control cells (*, p ≤ 0.05; **** p ≤ 0.0001). No asterisks indicate no statistical significance (p > 0.05). # Represent statistical significance in relation to non-irradiated control cells (###, p ≤ 0.001).

4.2.6.4. Evaluation of the Effect of Ultraviolet B Irradiation on Keranocytes Treated with the Quercetin-Based Nanoformulations – Cell Recovery Effect

To evaluate whether quercetin-loaded hydrogels had a cell recovery effect on UVB-induced skin damage, HaCaT cells were irradiated at an intensity of 60 mJ/cm² and incubated for 24 h prior to exposure to with a concentration of quercetin-loaded hydrogels (free quercetin-loaded hydrogels and quercetin-loaded NLCs and SLNs incorporated into the hydrogels) of 2.5 µg/mL. According to the obtained results (Figure 4.25A) exposure of cells to control hydrogel and unloaded nanoparticles incorporated at the hydrogels had no effect on cell viability as compared to the irradiated control group, with no visible recovery being observed. On the other hand, a significant increase in cell viability up to 90% was observed for cells exposed to quercetin-loaded NLCs incorporated into SA-PVA hydrogels. A similar increase in cell viability was observed in cells exposed to quercetin-loaded SLNs hydrogels, although not as significant as quercetin loaded NLCs counterparts (ca. 65%). These results suggest that quercetin-loaded hydrogels have a potential therapeutic effect against UVB-damaged skin. These results are in correlation with a previous study by Casagrande *et al.* (2006), who reported the effectiveness of topical formulations containing quercetin against damage induced by UVB radiation exposure.⁴⁶

Quercetin is a well-known dietary flavonoid with antioxidant, anti-inflammatory and anti-carcinogenic capacity.⁴⁷ In addition, quercetin has been shown to reduced UVB radiation-mediated oxidative damage to the skin. However, its action requires an effective percutaneous absorption.⁴⁸ Thus, prior encapsulation of this compound into lipid nanoparticles, such as NLCs and SLNs, may prove to be an effective strategy to increase quercetin's percutaneous absorption profile and get the most out of its therapeutic potential.

Figure 4.25B displays the effect of exposure to quercetin-loaded SA-PVA hydrogels after irradiation on UVB-induced apoptosis. HaCaT cells were irradiated at an intensity of 60 mJ/cm² and incubated for 24 h prior to exposure to with a concentration of quercetin-loaded hydrogels (free quercetin-loaded hydrogels and quercetin-loaded NLCs and SLNs incorporated into the hydrogels) of 2.5 µg/mL. The percentage of cells in early and late apoptosis as well as viable cells is shown. No visible cells in late apoptosis are observed for either the control irradiated cells or the cells incubated with all tested hydrogels. In addition, according to the obtained results, the percentage of cells in early apoptosis is significantly increased in UVB-irradiated control cells (ca. 45%) as compared to non-irradiated control cells, whereas a significant decrease in the number of viable

cells is observed (ca. 53%). An increase in the percentage of cells in early apoptosis is also observed in cells exposed to quercetin free control hydrogels (ca. 32 %) and quercetin loaded hydrogel as free quercetin (ca. 33 %), suggesting that these hydrogels had no effect on preventing early cell apoptosis. However, following the incubation with hydrogels incorporating quercetin encapsulated NLCs, the number of cells in early apoptosis was 38% lower, when compared to the irradiated control group. In addition, an increase to approximately 85% of viable cells as compared to irradiated control group was observed.

A decrease in 29 % of cells in early apoptosis was also displayed following exposure to quercetin loaded SLNs hydrogels. These results correlate with the increase in cell viability, thus being an indicative of the ability of these hydrogels to increase cell recovery capacity after UVB-induced apoptosis. Several studies have reported the protective effect of formulations containing quercetin against irradiation-induced cell damage.^{46,49,50}

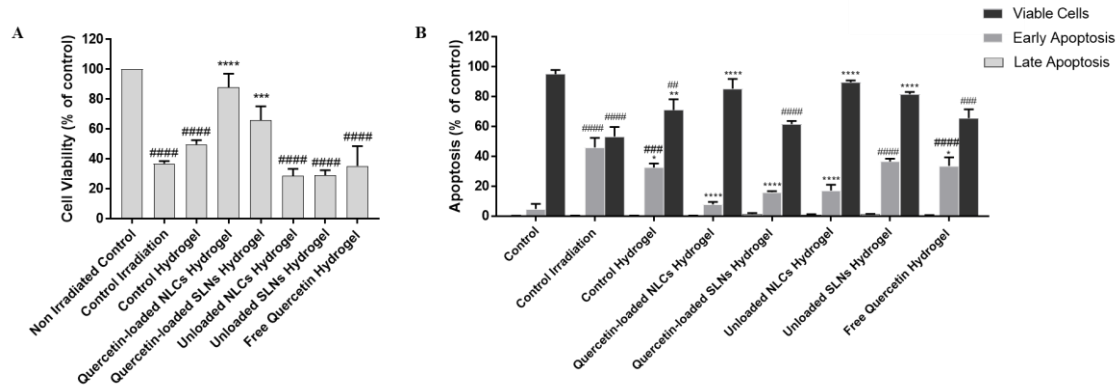


Figure 4.25 - Effects of free quercetin and quercetin-loaded hydrogels (both quercetin free-loaded hydrogel and quercetin-loaded NLCs and SLNs incorporated into hydrogels) on cell viability in UVB (60 mJ/cm²) irradiated HaCaT keratinocytes at a concentration of quercetin of 2.5 µg/mL. (A) Cell recovery effect on cells exposed to the hydrogels after irradiation and (B) Apoptosis analysis on cells exposed to the hydrogels after irradiation. Flow cytometry analysis was performed following staining with FITC Annexin V and 7-AAD AAD and the percentage of viable cells as well as early and late apoptotic cells is showed. Data are representative of three independent experiments as mean ± SD. Asterisks indicate statistical significance in relation to irradiated control cells (*, p ≤ 0.05; **, p ≤ 0.01; ***, p ≤ 0.001; **** p ≤ 0.0001). No asterisks indicate no statistical significance (p > 0.05). # Represent statistical significance in relation to non-irradiated control cells (###, p ≤ 0.001; ####, p ≤ 0.0001).

4.2.7. Conclusion

In this chapter, SA-PVA hybrid hydrogels were design as a cutaneous delivery system for quercetin. The quercetin-loaded NLCs and SLNs were successfully incorporated into SA-PVA hydrogels, with the goal of obtaining a topical delivery system for quercetin. Rheological analysis showed that the hydrogels displayed pseudoplastic behavior, a

non-thixotropic profile, and good resistance to deformation and temperatures from 20 to 40°C, making them promising candidates for cutaneous applications. Exposure of keratinocytes to hydrogels incorporated with quercetin-loaded NLCs and SLNs significantly increased cell viability after UVB-induced cell damage. Similarly, exposure of keratinocytes to hydrogels incorporated with quercetin loaded NLCs and SLNs prior to irradiation resulted in an increased cell viability, suggesting a photoprotective effect. In addition, it also resulted in a decrease in the level of intracellular ROS due to quercetin's scavenging ability, thus suggesting it may be an effective strategy to prevent UVB-induced cell death. Overall, the hybrid hydrogels may represent a promising platform for the delivery of flavonoids for skin therapeutic and cosmetic applications, including as an antiaging and solar filter.

4.3. References

1. Cevc, G., Lipid vesicles and other colloids as drug carriers on the skin. *Advanced Drug Delivery Reviews* **56**, 675–711 (2004).
2. Gupta, M., Agrawal, U., and Vyas, S. P., Nanocarrier-based topical drug delivery for the treatment of skin diseases. *Expert Opinion on Drug Delivery* **9**, 783–804 (2012).
3. Pardeike, J., Hommoss, A., and Müller, R. H., Lipid nanoparticles (SLN, NLC) in cosmetic and pharmaceutical dermal products. *International Journal of Pharmaceutics* **366**, 170–184 (2009).
4. Tan, Q., Liu, W., Guo, C., and Zhai, G., Preparation and evaluation of quercetin-loaded lecithin-chitosan nanoparticles for topical delivery. *International Journal of Nanomedicine* **6**, 1621-1630 (2011).
5. Lee, G. H., Lee, S. J., Jeong, S. W., Kim, H. C., Park, G. Y., Lee, S. G., and Choi, J. H., Antioxidative and antiinflammatory activities of quercetin-loaded silica nanoparticles. *Colloids and Surfaces B: Biointerfaces* **143**, 511–517 (2016).
6. Morales, J. O., Valdés, K., Morales, J., and Oyarzun-Ampuero, F., Lipid nanoparticles for the topical delivery of retinoids and derivatives. *Nanomedicine* **10**, 253–269 (2015).
7. Yoon, G., Park, J. W., and Yoon, I. S., Solid lipid nanoparticles (SLNs) and nanostructured lipid carriers (NLCs): Recent advances in drug delivery. *Journal of Pharmaceutical Investigation* vol. **43**, 353–362 (2013).
8. Das, S., Ng, W. K., and Tan, R. B. H., Are nanostructured lipid carriers (NLCs) better than solid lipid nanoparticles (SLNs): Development, characterizations and comparative

evaluations of clotrimazole-loaded SLNs and NLCs? *European Journal of Pharmaceutical Sciences* **47**, 139–151 (2012).

9. Dora, C. L., Putaux, J. L., Pignot-Paintrand, I., Dubreuil, F., Soldi, V., Borsali, R., and Lemos-Senna, E., Physicochemical and Morphological Characterizations of Glyceryl Tristearate/Castor Oil Nanocarriers Prepared by the Solvent Diffusion Method. *Journal of the Brazilian Chemical Society* **23**, 1972-1981 (2012).

10. Khalil, R. M., Abd-Elbary, A., Kassem, M. A., Ghorab, M. M., and Basha, M., Nanostructured lipid carriers (NLCs) versus solid lipid nanoparticles (SLNs) for topical delivery of meloxicam. *Pharmaceutical Development and Technology* **19**, 304–314 (2014).

11. Pinheiro, R. G. R., Granja, A., Loureiro, J. A., Pereira, M. C., Pinheiro, M., Neves, A. R., and Reis, S., RVG29-Functionalized Lipid Nanoparticles for Quercetin Brain Delivery and Alzheimer's Disease. *Pharmaceutical Research* **37**, 1-12 (2020).

12. Ni, S., Sun, R., Zhao, G., and Xia, Q., Quercetin Loaded Nanostructured Lipid Carrier for Food Fortification: Preparation, Characterization and *in vitro* Study. *Journal of Food Process Engineering* **38**, 93–106 (2015).

13. Dinesh Kumar, V., Verma, P. R. P., and Singh, S. K., Development and evaluation of biodegradable polymeric nanoparticles for the effective delivery of quercetin using a quality by design approach. *LWT - Food Science and Technology* **61**, 330–338 (2015).

14. Gokhale, J. P., and Surana, S. S., Quercetin Loaded Nanostructured Lipid Carriers-based Gel for Rheumatoid Arthritis: Formulation, Characterization and *in vivo* Evaluation. *International Journal of Pharmaceutical Sciences and Nanotechnology* **11**, 3967-3977 (2018)

15. Teeranachaidekul, V., Souto, E. B., Junyaprasert, V. B., and Müller, R. H., Cetyl palmitate-based NLC for topical delivery of Coenzyme Q10 - Development, physicochemical characterization and *in vitro* release studies. *European Journal of Pharmaceutics and Biopharmaceutics* **67**, 141–148 (2007).

16. Kovacevic, A., Savic, S., Vuleta, G., Müller, R. H., and Keck, C. M., Polyhydroxy surfactants for the formulation of lipid nanoparticles (SLN and NLC): Effects on size, physical stability and particle matrix structure. *International Journal of Pharmaceutics* **406**, 163–172 (2011).

17. Essaghraoui, A., Belfkira, A., Hamdaoui, B., Nunes, C., Lima, S. A. C., and Reis, S., Improved dermal delivery of cyclosporine a loaded in solid lipid nanoparticles. *Nanomaterials* **9**, 1204 (2019).
18. Pinheiro, R. G. R., Granja, A., Loureiro, J. A., Pereira, M. C., Pinheiro, M., Neves, A. R., and Reis, S., Quercetin lipid nanoparticles functionalized with transferrin for Alzheimer's disease. *European Journal of Pharmaceutical Sciences* **148**, 105314 (2020).
19. Mardashev, S. R., Nikolaev Ya., A., and Sokolov, N. N., Isolation and properties of a homogenous L asparaginase preparation from *Pseudomonas fluorescens* AG. *Biokhimiya* **40**, 984–989 (1975).
20. Floegel, A., Kim, D. O., Chung, S. J., Koo, S. I., and Chun, O. K., Comparison of ABTS/DPPH assays to measure antioxidant capacity in popular antioxidant-rich US foods. *Journal of Food Composition and Analysis* **24**, 1043–1048 (2011).
21. Esposito, L., Barbosa, A. I., Moniz, T., Costa Lima, S., Costa, P., Celia, C., and Reis, S., Design and characterization of sodium alginate and poly(Vinyl) alcohol hydrogels for enhanced skin delivery of quercetin. *Pharmaceutics* **12**, 1–15 (2020).
22. Pivetta, T. P., Silva, L. B., Kawakami, C. M., Araujo, M. M., Del Lama, M. P. F., Naal, R. M. Z., Maria-Engler, S. S., Gaspar, L. R., and Marcato, P. D., Topical formulation of quercetin encapsulated in natural lipid nanocarriers: Evaluation of biological properties and phototoxic effect. *Journal of Drug Delivery Science and Technology* **53**, 101148 (2019).
23. Bose, S., and Michniak-Kohn, B., Preparation and characterization of lipid based nanosystems for topical delivery of quercetin. *European Journal of Pharmaceutical Sciences* **48**, 442–452 (2013).
24. Wang, T., Zhang, F., Zhao, R., Wang, C., Hu, K., Sun, Y., Politis, C., Shavandi, A., and Nie, L., Polyvinyl Alcohol/Sodium Alginate Hydrogels Incorporated with Silver Nanoclusters via Green Tea Extract for Antibacterial Applications. *Designed Monomers and Polymers* **23**, (2020) 118-133.
25. Anarkoli, A. O., Khorasani, S. N., Modares, M. P., and Anvari-Yazdi, A. F., Effects of pH on Polyvinyl alcohol/Sodium Alginate Electrospun nanofibers morphology for Biomedical applications. In: *The second international and the 7th joint conference of Iranian metallurgical engineering society and Iranian foundrymen scientific society* (2013).

26. Catauro, M., Papale, F., Bollino, F., Piccolella, S., Marciano, S., Nocera, P., and Pacifico, S., Silica/quercetin sol-gel hybrids as antioxidant dental implant materials. *Science and Technology of Advanced Materials* **16**, 035001 (2015).
27. Moon, H., Lertpatipanpong, P., Hong, Y., Kim, C. T., and Baek, S. J., Nano-encapsulated quercetin by soluble soybean polysaccharide/chitosan enhances anti-cancer, anti-inflammation, and anti-oxidant activities. *Journal of Functional Foods* **87**, 104756 (2021).
28. Souza, M. P., Vaz, A. F., Correia, M. T., Cerqueira, M. A., Vicente, A. A., and Carneiro-da-Cunha, M. G., Quercetin-Loaded Lecithin/Chitosan Nanoparticles for Functional Food Applications. *Food and Bioprocess Technology* **7**, 1149–1159 (2014).
29. Zhang, Y., Yang, Y., Tang, K., Hu, X., and Zou, G., Physicochemical characterization and antioxidant activity of quercetin-loaded chitosan nanoparticles. *Journal of Applied Polymer Science* **107**, 891–897 (2008).
30. Carvalho, F. C., Calixto, G., Hatakeyama, I. N., Luz, G. M., Gremião, M. P. D., and Chorilli, M., Rheological, mechanical, and bioadhesive behavior of hydrogels to optimize skin delivery systems. *Drug Development and Industrial Pharmacy* **39**, 1750–1757 (2013).
31. Jones, D. S., Woolfson, A. D., and Brown, A. F., Viscoelastic properties of bioadhesive, chlorhexidine-containing semi-solids for topical application to the oropharynx. *Pharmaceutical Research* **15**, 1131–1136 (1998).
32. Md, S., Alhakamy, N. A., Aldawsari, H. M., Kotta, S., Ahmad, J., Akhter, S., Alam, M. S., Khan, M. A., Awan, Z., and Sivakumar, P. M., Improved analgesic and anti-inflammatory effect of diclofenac sodium by topical nanoemulgel: Formulation development—in vitro and in vivo studies. *Journal of Chemistry* **2020**, 4071818 (2020).
33. Lee, C. H., Moturi, V., and Lee, Y., Thixotropic property in pharmaceutical formulations. *Journal of Controlled Release* **136**, 88–98 (2009).
34. Souto, E. B., and Müller, R. H., The use of SLN® and NLC® as topical particulate carriers for imidazole antifungal agents. *Die Pharmazie* **61**, 431-437 (2006).
35. Wu, G., Jin, K., Liu, L., and Zhang, H., A rapid self-healing hydrogel based on PVA and sodium alginate with conductive and cold-resistant properties. *Soft Matter* **16**, 3319–3324 (2020).

36. ISO/TC 194, Biological evaluation of medical devices — Part 5: Tests for in vitro cytotoxicity. *ISO 10993-5:2009* (2009).
37. Nan, W., Ding, L., Chen, H., Khan, F. U., Yu, L., Sui, X., and Shi, X., Topical Use of Quercetin-Loaded Chitosan Nanoparticles Against Ultraviolet B Radiation. *Frontiers in Pharmacology* **9**, 826 (2018).
38. Zhu, X., Li, N., Wang, Y., Ding, L., Chen, H., Yu, Y., and Shi, X., Protective effects of quercetin on UVB irradiation-induced cytotoxicity through ROS clearance in keratinocyte cells. *Oncology Reports* **37**, 209–218 (2017).
39. Maciel, E., Neves, B. M., Santinha, D., Reis, A., Domingues, P., Cruz, M. T., Pitt, A. R., Spickett, C. M., and Domingues, M. R. M., Detection of phosphatidylserine with a modified polar head group in human keratinocytes exposed to the radical generator AAPH. *Archives of Biochemistry and Biophysics* **548**, 38–45 (2014).
40. Zimmermann, M., and Meyer, N., Annexin V/7-AAD staining in keratinocytes. In: *Mammalian Cell Viability: Methods and Protocols*, 57–63 (Humana Press, 2011).
41. Liu, D., Hu, H., Lin, Z., Chen, D., Zhu, Y., Hou, S., and Shi, X., Quercetin deformable liposome: Preparation and efficacy against ultraviolet B induced skin damages in vitro and in vivo. *Journal of Photochemistry and Photobiology B: Biology* **127**, 8–17 (2013).
42. Afaq, F., Zaid, M. A., Khan, N., Dreher, M., and Mukhtar, H., Protective effect of pomegranate-derived products on UVB-mediated damage in human reconstituted skin. *Experimental Dermatology* **18**, 553–561 (2009).
43. Bihamta, M., Hosseini, A., Ghorbani, A., and Boroushaki, M. T., Protective effect of pomegranate seed oil against H₂O₂-induced oxidative stress in cardiomyocytes. *Avicenna Journal of Phytomedicine* **7**, 46 (2017).
44. Al-Sabahi, B. N., Fatope, M. O., Essa, M. M., Subash, S., Al-Busafi, S. N., Al-Kusaibi, F. S., and Manivasagam, T., Pomegranate seed oil: Effect on 3-nitropropionic acid-induced neurotoxicity in PC12 cells and elucidation of unsaturated fatty acids composition. *Nutritional Neuroscience* **20**, 40–48 (2017).
45. Zhu, X., Li, N., Wang, Y., Ding, L., Chen, H., Yu, Y., and Shi, X., Protective effects of quercetin on UVB irradiation-induced cytotoxicity through ROS clearance in keratinocyte cells. *Oncology Reports* **37**, 209–218 (2017).
46. Casagrande, R., Georgetti, S. R., Verri Jr, W. A., Dorta, D. J., dos Santos, A. C., and Fonseca, M. J., Protective effect of topical formulations containing quercetin against

UVB-induced oxidative stress in hairless mice. *Journal of Photochemistry and Photobiology B: Biology* **84**, 21–27 (2006).

47. Nisar, M. F., Yousaf, M., Saleem, M., Khalid, H., Niaz, K., Yaqub, M., Waqas, M. Y., Ahmed, A., Abaid-Ullah, M., and Wan, C. C., Development of Iron Sequester Antioxidant Quercetin@ZnO Nanoparticles with Photoprotective Effects on UVA-Irradiated HaCaT Cells. *Oxidative Medicine and Cellular Longevity* **2021**, 6072631 (2021).

48. Vicentini, F. T., Simi, T. R., Del Ciampo, J. O., Wolga, N. O., Pitol, D. L., Iyomasa, M. M., Bentley, M. V. L. B., and Fonseca, M. J., Quercetin in w/o microemulsion: *In vitro* and *in vivo* skin penetration and efficacy against UVB-induced skin damages evaluated *in vivo*. *European Journal of Pharmaceutics and Biopharmaceutics* **69**, 948-957 (2008).

49. Liu, D., Hu, H., Lin, Z., Chen, D., Zhu, Y., Hou, S., & Shi, X., Quercetin deformable liposome: Preparation and efficacy against ultraviolet B induced skin damages *in vitro* and *in vivo*. *Journal of Photochemistry and Photobiology B: Biology* **127**, 8–17 (2013).

50. Rajnochová Svobodová, A., Ryšavá, A., Čížková, K., Roubalová, L., Ulrichová, J., Vrba, J., Zálešák, B., and Vostálová, J., Effect of the flavonoids quercetin and taxifolin on UVA-induced damage to human primary skin keratinocytes and fibroblasts. *Photochemical & Photobiological Sciences* **21**, 59–75 (2022).

5. Conclusions and Future Perspectives

This thesis is based in a multidisciplinary work involving two main research lines: (i) optimization, production and characterization of nanostructured lipid carriers with encapsulated quercetin, and (ii) incorporation of the optimized quercetin-loaded nanoparticles into hydrogels with the goal of obtaining a cutaneous delivery system for the flavonoid as therapeutic tool towards UV-induced skin damage.

Quercetin-loaded NLCs were optimized to enhance quercetin's skin absorption capacity and improve its bioavailability. Due to its numerous appealing properties such as anti-inflammatory, antioxidant, and anti-apoptotic effects, pomegranate oil was employed as a liquid lipid in the fabrication of NLCs.¹⁻³ A three-level BBD was constructed to achieve the optimal formulation of NLCs. The resulting nanoparticles, which included both quercetin-loaded and unloaded counterparts, exhibited sizes ranging from 200 to 300 nm, which falls within the recommended limit of 500 nm for topical delivery.⁴ The inclusion of quercetin had a noticeable effect on the size of the nanoparticles, leading to a statistically significant increase in both SLNs and NLCs. PDI values indicate populations with a narrow size distribution.⁵ The optimized NLCs displayed an entrapment efficiency of 55%, with a drug loading of 0.5% (12.5 µg), while their counterpart SLNs had significantly lower encapsulation efficiency (ca. 43%) with a drug loading of 0.4% (10 µg). The inclusion of quercetin did not impact the morphology of NLCs, in contrast to SLNs. Both lipid nanoparticles are stable for at least 12 weeks. DSC demonstrated that no significant changes in the melting point of the formulations were seen, after quercetin encapsulation. Yet, the melting enthalpy increased after drug incorporation in NLCs, suggesting a lipid matrix stabilization with the addition of the drug into the lipid phase. Whereas for the SLN formulation, quercetin incorporation resulted in a decrease the melting enthalpy, thus indicating less crystal lattice organization. The optimized nanoparticles are able to protect quercetin from photodegradation, as only a small decrease in quercetin's absorption intensity was displayed. Keratinocytes were more sensitive to all evaluated nanoparticles in comparison to the L929 fibroblasts. Upon incorporation into both NLCs and SLNs, the antioxidant activity of quercetin decreased as compared to its free form for the ABTS scavenging assay. A similar decrease in the antioxidant activity of quercetin upon its incorporation into both NLCs and SLNS, as compared to its free form, was not observed for the DPPH assay. Quercetin loaded in the lipid nanoparticles was more retained within the PVPA_{sc} barrier than in its free form, thus highlighting the local application of lipid nanoparticles in the skin for this flavonoid delivery.

Quercetin-loaded NLCs and SLNs were successfully incorporated into SA-PVA hydrogels, with the goal of obtaining a topical delivery system for quercetin. All developed hydrogels were non-thixotropic, highly resistant to deformation and to temperatures between 32 and 37° C. In addition, incorporation of quercetin either in its free form, or encapsulated into both NLCs and SLNs, did not significantly affect their mechanical properties, thus making them highly attractive topical delivery systems. After a period of six weeks, quercetin-loaded hydrogels as free quercetin and quercetin-loaded into NLCs and SLNs continued to display a pseudoplastic behaviour, however, the overall viscosity of hydrogels incorporated with quercetin loaded NLCs and SLNs decreased in 50%. The hydrogels remained non-thixotropic, and resistant to deformation and temperature. The morphology of the hydrogels was significantly affected upon incorporation of quercetin-loaded and empty nanoparticles. The hydrogel's network structure became more compact, and the porosity significantly decreased, suggesting that quercetin nanoparticles were successfully incorporated into the hydrogel matrix. The ABTS assay revealed that quercetin incorporated in its free form in the hydrogels retained its antioxidant capacity. However, when quercetin is encapsulated into either NLCs or SLNs prior to its incorporation within the SA-PVA hydrogels, its antioxidant capacity significantly decreases as compared to its free form in approximately 20%. This may be attributed to a protection effect provided by the nanoparticles' lipidic matrix. In terms of biocompatibility, exposure of keratinocytes to different concentrations of quercetin-loaded hydrogels resulted in a concentration-dependent cell cytotoxicity. Exposure of keratinocytes to hydrogels containing quercetin encapsulated into NLCs and SLNs lead to increase in cell viability, while in the presence of quercetin-free hydrogels showed no protective effect on UVB radiation. Moreover, following treatment with quercetin-containing hydrogels a significant decreased of cells in early apoptosis was observed as compared to the irradiated control group, which correlate with the increase in cell viability, suggesting a photoprotective effect. Cell treatment with quercetin hydrogels (either quercetin in its free form or quercetin encapsulated NLCs and SLNs incorporated in the hydrogel matrix) resulted in a decrease in the level of intracellular ROS due to quercetin's scavenging ability. Similarly, hydrogels containing empty NLCs were able to produce a decrease in the intracellular levels of ROS, which suggests that the PO is also capable of scavenging the intracellular ROS generated by UVB irradiation. Overall, these results demonstrate that the ability of antioxidants such as quercetin to scavenge or suppress the generation of intracellular ROS may be an effective strategy to prevent UVB-induced cell death.

A significant increase in cell viability was observed for keratinocytes exposed to quercetin-loaded NLCs or SLNs incorporated into SA-PVA hydrogels. These results suggest that quercetin-loaded hydrogels have a potential therapeutic effect against UVB-damaged skin. The apoptosis profile revealed a decrease in the percentage of apoptotic cells for these nanoplateforms whereas an increase in early apoptosis is observed in cells exposed to quercetin free control hydrogels and quercetin loaded hydrogel as free quercetin. These results are an indicative of the ability of these hydrogels to increase cell recovery capacity after UVB-induced apoptosis.

To conclude, flavonoids such as quercetin will continue to be explored as therapeutic and/or preventive agents for many diseases, either alone or in combination with other drugs. NLCs offer many advantages over conventional drug delivery systems, including low production costs and the fact that their manufacturing is easily scaled up. In addition, because of their tuneable properties and their biocompatibility, hydrogels are promising topical drug delivery platforms. Hydrogels are capable of increasing drug's retention in the skin, potentiating their therapeutic action, which makes them very attractive delivery platforms towards not only therapeutic but also cosmetic applications.

In this thesis a nanoplateform for the delivery of flavonoids to the skin was established, constituting the basis for the start of new scientific works such as optimization of the hydrogel-lipid nanoparticles system, incorporation of different flavonoids and combination of flavonoids with potential synergistic effects.

Annex 1

Copyright licenses:

- Figure 2.10

27/06/23, 14:34

Creative Commons — Attribution 4.0 International — CC BY 4.0

This page is available in the following languages:



**Creative Commons License
Deed**

Attribution 4.0 International (CC BY 4.0)



This is a human-readable summary of (and not a substitute for) the [license](#).

You are free to:

Share — copy and redistribute the material in any medium or format

Adapt — remix, transform, and build upon the material

for any purpose, even commercially.

The licensor cannot revoke these freedoms as long as you follow the license terms.

Under the following terms:

Attribution — You must give appropriate credit, provide a link to the license, and indicate if changes were made. You may do so in any reasonable manner, but not in any way that suggests the licensor endorses you or your use.

No additional restrictions — You may not apply legal terms or technological measures that legally restrict others from doing anything the license permits.

Notices:

You do not have to comply with the license for elements of the material in the public domain or where your use is permitted by an applicable exception or limitation.

No warranties are given. The license may not give you all of the permissions necessary for your intended use. For example, other rights such as publicity, privacy, or moral rights may limit how you use the material.

- Costa, R., Costa Lima, S. A., Gameiro, P., and Reis, S., On the development of a cutaneous flavonoid delivery system: Advances and limitations. *Antioxidants* 10, 1376 (2021)

26/06/23, 22:39

Creative Commons — Attribution 4.0 International — CC BY 4.0

This page is available in the following languages:



**Creative Commons License
Deed**

Attribution 4.0 International (CC BY 4.0)



This is a human-readable summary of (and not a substitute for) the [license](#).

You are free to:

Share — copy and redistribute the material in any medium or format

Adapt — remix, transform, and build upon the material

for any purpose, even commercially.

The licensor cannot revoke these freedoms as long as you follow the license terms.

Under the following terms:

Attribution — You must give appropriate credit, provide a link to the license, and indicate if changes were made. You may do so in any reasonable manner, but not in any way that suggests the licensor endorses you or your use.

No additional restrictions — You may not apply legal terms or technological measures that legally restrict others from doing anything the license permits.

Notices:

You do not have to comply with the license for elements of the material in the public domain or where your use is permitted by an applicable exception or limitation.

No warranties are given. The license may not give you all of the permissions necessary for your intended use. For example, other rights such as publicity, privacy, or moral rights may limit how you use the material.

- Figure 3.1

27/06/23, 14:36

Creative Commons — Attribution 4.0 International — CC BY 4.0

This page is available in the following languages:



**Creative Commons License
Deed**

Attribution 4.0 International (CC BY 4.0)



This is a human-readable summary of (and not a substitute for) the [license](#).

You are free to:

Share — copy and redistribute the material in any medium or format

Adapt — remix, transform, and build upon the material

for any purpose, even commercially.

The licensor cannot revoke these freedoms as long as you follow the license terms.

Under the following terms:

Attribution — You must give appropriate credit, provide a link to the license, and indicate if changes were made. You may do so in any reasonable manner, but not in any way that suggests the licensor endorses you or your use.

No additional restrictions — You may not apply legal terms or technological measures that legally restrict others from doing anything the license permits.

Notices:

You do not have to comply with the license for elements of the material in the public domain or where your use is permitted by an applicable exception or limitation.

No warranties are given. The license may not give you all of the permissions necessary for your intended use. For example, other rights such as publicity, privacy, or moral rights may limit how you use the material.

- Figure 3.2

27/06/23, 14:39

Creative Commons — Attribution 4.0 International — CC BY 4.0

This page is available in the following languages:



**Creative Commons License
Deed**



Attribution 4.0 International (CC BY 4.0)

This is a human-readable summary of (and not a substitute for) the [license](#).

You are free to:

Share — copy and redistribute the material in any medium or format

Adapt — remix, transform, and build upon the material

for any purpose, even commercially.

The licensor cannot revoke these freedoms as long as you follow the license terms.

Under the following terms:

Attribution — You must give appropriate credit, provide a link to the license, and indicate if changes were made. You may do so in any reasonable manner, but not in any way that suggests the licensor endorses you or your use.

No additional restrictions — You may not apply legal terms or technological measures that legally restrict others from doing anything the license permits.

Notices:

You do not have to comply with the license for elements of the material in the public domain or where your use is permitted by an applicable exception or limitation.

No warranties are given. The license may not give you all of the permissions necessary for your intended use. For example, other rights such as publicity, privacy, or moral rights may limit how you use the material.

- Figure 3.3

27/06/23, 14:39

Creative Commons — Attribution 4.0 International — CC BY 4.0

This page is available in the following languages:



**Creative Commons License
Deed**

Attribution 4.0 International (CC BY 4.0)



This is a human-readable summary of (and not a substitute for) the [license](#).

You are free to:

Share — copy and redistribute the material in any medium or format

Adapt — remix, transform, and build upon the material

for any purpose, even commercially.

The licensor cannot revoke these freedoms as long as you follow the license terms.

Under the following terms:

Attribution — You must give appropriate credit, provide a link to the license, and indicate if changes were made. You may do so in any reasonable manner, but not in any way that suggests the licensor endorses you or your use.

No additional restrictions — You may not apply legal terms or technological measures that legally restrict others from doing anything the license permits.

Notices:

You do not have to comply with the license for elements of the material in the public domain or where your use is permitted by an applicable exception or limitation.

No warranties are given. The license may not give you all of the permissions necessary for your intended use. For example, other rights such as publicity, privacy, or moral rights may limit how you use the material.

- Figure 3.4

27/06/23, 12:38

RightsLink Printable License

ELSEVIER LICENSE
TERMS AND CONDITIONS

Jun 27, 2023

This Agreement between Faculdade de Farmácia da Universidade do Porto -- Raquel Costa ("You") and Elsevier ("Elsevier") consists of your license details and the terms and conditions provided by Elsevier and Copyright Clearance Center.

License Number	5577031304013
License date	Jun 27, 2023
Licensed Content Publisher	Elsevier
Licensed Content Publication	Journal of Controlled Release
Licensed Content Title	DLS and zeta potential – What they are and what they are not?
Licensed Content Author	Sourav Bhattacharjee
Licensed Content Date	Aug 10, 2016
Licensed Content Volume	235
Licensed Content Issue	n/a
Licensed Content Pages	15
Start Page	337
End Page	351
Type of Use	reuse in a thesis/dissertation
Portion	figures/tables/illustrations

27/06/23, 12:38

RightsLink Printable License

Number of figures/tables/illustrations	1
Format	both print and electronic
Are you the author of this Elsevier article?	No
Will you be translating?	No
Title	Production of Lipid Nanoparticles for Topical Administration of Flavonoids
Institution name	Faculdade de Ciências da Universidade do Porto
Expected presentation date	Oct 2023
Portions	Figure 6
Requestor Location	Faculdade de Farmácia da Universidade do Porto Rua Conselheiro Boaventura de Sousa, nº2
	Oliveira de Azeméis, Aveiro 3720-210 Portugal Attn: Faculdade de Farmácia da Universidade do Porto
Publisher Tax ID	GB 494 6272 12
Total	0.00 EUR
Terms and Conditions	

INTRODUCTION

1. The publisher for this copyrighted material is Elsevier. By clicking "accept" in connection with completing this licensing transaction, you agree that the following terms and conditions apply to this transaction (along with the Billing and Payment terms and conditions established by Copyright Clearance Center, Inc. ("CCC"), at the time that you opened your RightsLink account and that are available at any time at <https://myaccount.copyright.com>).

GENERAL TERMS

2. Elsevier hereby grants you permission to reproduce the aforementioned material subject to the terms and conditions indicated.

27/06/23, 12:38

RightsLink Printable License

3. Acknowledgement: If any part of the material to be used (for example, figures) has appeared in our publication with credit or acknowledgement to another source, permission must also be sought from that source. If such permission is not obtained then that material may not be included in your publication/copies. Suitable acknowledgement to the source must be made, either as a footnote or in a reference list at the end of your publication, as follows:

"Reprinted from Publication title, Vol /edition number, Author(s), Title of article / title of chapter, Pages No., Copyright (Year), with permission from Elsevier [OR APPLICABLE SOCIETY COPYRIGHT OWNER]." Also Lancet special credit - "Reprinted from The Lancet, Vol. number, Author(s), Title of article, Pages No., Copyright (Year), with permission from Elsevier."

4. Reproduction of this material is confined to the purpose and/or media for which permission is hereby given. The material may not be reproduced or used in any other way, including use in combination with an artificial intelligence tool (including to train an algorithm, test, process, analyse, generate output and/or develop any form of artificial intelligence tool), or to create any derivative work and/or service (including resulting from the use of artificial intelligence tools).

5. Altering/Modifying Material: Not Permitted. However figures and illustrations may be altered/adapted minimally to serve your work. Any other abbreviations, additions, deletions and/or any other alterations shall be made only with prior written authorization of Elsevier Ltd. (Please contact Elsevier's permissions helpdesk [here](#)). No modifications can be made to any Lancet figures/tables and they must be reproduced in full.

6. If the permission fee for the requested use of our material is waived in this instance, please be advised that your future requests for Elsevier materials may attract a fee.

7. Reservation of Rights: Publisher reserves all rights not specifically granted in the combination of (i) the license details provided by you and accepted in the course of this licensing transaction, (ii) these terms and conditions and (iii) CCC's Billing and Payment terms and conditions.

8. License Contingent Upon Payment: While you may exercise the rights licensed immediately upon issuance of the license at the end of the licensing process for the transaction, provided that you have disclosed complete and accurate details of your proposed use, no license is finally effective unless and until full payment is received from you (either by publisher or by CCC) as provided in CCC's Billing and Payment terms and conditions. If full payment is not received on a timely basis, then any license preliminarily granted shall be deemed automatically revoked and shall be void as if never granted. Further, in the event that you breach any of these terms and conditions or any of CCC's Billing and Payment terms and conditions, the license is automatically revoked and shall be void as if never granted. Use of materials as described in a revoked license, as well as any use of the materials beyond the scope of an unrevoked license, may constitute copyright infringement and publisher reserves the right to take any and all action to protect its copyright in the materials.

9. Warranties: Publisher makes no representations or warranties with respect to the licensed material.

10. Indemnity: You hereby indemnify and agree to hold harmless publisher and CCC, and their respective officers, directors, employees and agents, from and against any and all claims arising out of your use of the licensed material other than as specifically authorized pursuant to this license.

11. No Transfer of License: This license is personal to you and may not be sublicensed, assigned, or transferred by you to any other person without publisher's written permission.

27/06/23, 12:38

RightsLink Printable License

12. **No Amendment Except in Writing:** This license may not be amended except in a writing signed by both parties (or, in the case of publisher, by CCC on publisher's behalf).

13. **Objection to Contrary Terms:** Publisher hereby objects to any terms contained in any purchase order, acknowledgment, check endorsement or other writing prepared by you, which terms are inconsistent with these terms and conditions or CCC's Billing and Payment terms and conditions. These terms and conditions, together with CCC's Billing and Payment terms and conditions (which are incorporated herein), comprise the entire agreement between you and publisher (and CCC) concerning this licensing transaction. In the event of any conflict between your obligations established by these terms and conditions and those established by CCC's Billing and Payment terms and conditions, these terms and conditions shall control.

14. **Revocation:** Elsevier or Copyright Clearance Center may deny the permissions described in this License at their sole discretion, for any reason or no reason, with a full refund payable to you. Notice of such denial will be made using the contact information provided by you. Failure to receive such notice will not alter or invalidate the denial. In no event will Elsevier or Copyright Clearance Center be responsible or liable for any costs, expenses or damage incurred by you as a result of a denial of your permission request, other than a refund of the amount(s) paid by you to Elsevier and/or Copyright Clearance Center for denied permissions.

LIMITED LICENSE

The following terms and conditions apply only to specific license types:

15. **Translation:** This permission is granted for non-exclusive world **English** rights only unless your license was granted for translation rights. If you licensed translation rights you may only translate this content into the languages you requested. A professional translator must perform all translations and reproduce the content word for word preserving the integrity of the article.

16. **Posting licensed content on any Website:** The following terms and conditions apply as follows: Licensing material from an Elsevier journal: All content posted to the web site must maintain the copyright information line on the bottom of each image; A hyper-text must be included to the Homepage of the journal from which you are licensing at <http://www.sciencedirect.com/science/journal/xxxx> or the Elsevier homepage for books at <http://www.elsevier.com>; Central Storage: This license does not include permission for a scanned version of the material to be stored in a central repository such as that provided by Heron/XanEdu.

Licensing material from an Elsevier book: A hyper-text link must be included to the Elsevier homepage at <http://www.elsevier.com>. All content posted to the web site must maintain the copyright information line on the bottom of each image.

Posting licensed content on Electronic reserve: In addition to the above the following clauses are applicable: The web site must be password-protected and made available only to bona fide students registered on a relevant course. This permission is granted for 1 year only. You may obtain a new license for future website posting.

17. **For journal authors:** the following clauses are applicable in addition to the above:

Preprints:

A preprint is an author's own write-up of research results and analysis, it has not been peer-reviewed, nor has it had any other value added to it by a publisher (such as formatting, copyright, technical enhancement etc.).

27/06/23, 12:38

RightsLink Printable License

Authors can share their preprints anywhere at any time. Preprints should not be added to or enhanced in any way in order to appear more like, or to substitute for, the final versions of articles however authors can update their preprints on arXiv or RePEc with their Accepted Author Manuscript (see below).

If accepted for publication, we encourage authors to link from the preprint to their formal publication via its DOI. Millions of researchers have access to the formal publications on ScienceDirect, and so links will help users to find, access, cite and use the best available version. Please note that Cell Press, The Lancet and some society-owned have different preprint policies. Information on these policies is available on the journal homepage.

Accepted Author Manuscripts: An accepted author manuscript is the manuscript of an article that has been accepted for publication and which typically includes author-incorporated changes suggested during submission, peer review and editor-author communications.

Authors can share their accepted author manuscript:

- immediately
 - via their non-commercial person homepage or blog
 - by updating a preprint in arXiv or RePEc with the accepted manuscript
 - via their research institute or institutional repository for internal institutional uses or as part of an invitation-only research collaboration work-group
 - directly by providing copies to their students or to research collaborators for their personal use
 - for private scholarly sharing as part of an invitation-only work group on commercial sites with which Elsevier has an agreement
- After the embargo period
 - via non-commercial hosting platforms such as their institutional repository
 - via commercial sites with which Elsevier has an agreement

In all cases accepted manuscripts should:

- link to the formal publication via its DOI
- bear a CC-BY-NC-ND license - this is easy to do
- if aggregated with other manuscripts, for example in a repository or other site, be shared in alignment with our hosting policy not be added to or enhanced in any way to appear more like, or to substitute for, the published journal article.

Published journal article (JPA): A published journal article (PJA) is the definitive final record of published research that appears or will appear in the journal and embodies all value-adding publishing activities including peer review co-ordination, copy-editing, formatting, (if relevant) pagination and online enrichment.

Policies for sharing publishing journal articles differ for subscription and gold open access articles:

Subscription Articles: If you are an author, please share a link to your article rather than the full-text. Millions of researchers have access to the formal publications on ScienceDirect, and so links will help your users to find, access, cite, and use the best available version.

Theses and dissertations which contain embedded PJAs as part of the formal submission can be posted publicly by the awarding institution with DOI links back to the formal publications on ScienceDirect.

If you are affiliated with a library that subscribes to ScienceDirect you have additional private sharing rights for others' research accessed under that agreement. This includes use for classroom teaching and internal training at the institution (including use in course packs and courseware programs), and inclusion of the article for grant funding purposes.

27/06/23, 12:38

RightsLink Printable License

Gold Open Access Articles: May be shared according to the author-selected end-user license and should contain a [CrossMark logo](#), the end user license, and a DOI link to the formal publication on ScienceDirect.

Please refer to Elsevier's [posting policy](#) for further information.

18. For book authors the following clauses are applicable in addition to the above: Authors are permitted to place a brief summary of their work online only. You are not allowed to download and post the published electronic version of your chapter, nor may you scan the printed edition to create an electronic version. **Posting to a repository:** Authors are permitted to post a summary of their chapter only in their institution's repository.

19. Thesis/Dissertation: If your license is for use in a thesis/dissertation your thesis may be submitted to your institution in either print or electronic form. Should your thesis be published commercially, please reapply for permission. These requirements include permission for the Library and Archives of Canada to supply single copies, on demand, of the complete thesis and include permission for Proquest/UMI to supply single copies, on demand, of the complete thesis. Should your thesis be published commercially, please reapply for permission. Theses and dissertations which contain embedded PJAs as part of the formal submission can be posted publicly by the awarding institution with DOI links back to the formal publications on ScienceDirect.

Elsevier Open Access Terms and Conditions

You can publish open access with Elsevier in hundreds of open access journals or in nearly 2000 established subscription journals that support open access publishing. Permitted third party re-use of these open access articles is defined by the author's choice of Creative Commons user license. See our [open access license policy](#) for more information.

Terms & Conditions applicable to all Open Access articles published with Elsevier:

Any reuse of the article must not represent the author as endorsing the adaptation of the article nor should the article be modified in such a way as to damage the author's honour or reputation. If any changes have been made, such changes must be clearly indicated.

The author(s) must be appropriately credited and we ask that you include the end user license and a DOI link to the formal publication on ScienceDirect.

If any part of the material to be used (for example, figures) has appeared in our publication with credit or acknowledgement to another source it is the responsibility of the user to ensure their reuse complies with the terms and conditions determined by the rights holder.

Additional Terms & Conditions applicable to each Creative Commons user license:

CC BY: The CC-BY license allows users to copy, to create extracts, abstracts and new works from the Article, to alter and revise the Article and to make commercial use of the Article (including reuse and/or resale of the Article by commercial entities), provided the user gives appropriate credit (with a link to the formal publication through the relevant DOI), provides a link to the license, indicates if changes were made and the licensor is not represented as endorsing the use made of the work. The full details of the license are available at <http://creativecommons.org/licenses/by/4.0>.

CC BY NC SA: The CC BY-NC-SA license allows users to copy, to create extracts, abstracts and new works from the Article, to alter and revise the Article, provided this is not done for commercial purposes, and that the user gives appropriate credit (with a link to the formal publication through the relevant DOI), provides a link to the license, indicates if changes were made and the licensor is not represented as endorsing the use made of the

27/06/23, 12:38

RightsLink Printable License

work. Further, any new works must be made available on the same conditions. The full details of the license are available at <http://creativecommons.org/licenses/by-nc-sa/4.0>.

CC BY NC ND: The CC BY-NC-ND license allows users to copy and distribute the Article, provided this is not done for commercial purposes and further does not permit distribution of the Article if it is changed or edited in any way, and provided the user gives appropriate credit (with a link to the formal publication through the relevant DOI), provides a link to the license, and that the licensor is not represented as endorsing the use made of the work. The full details of the license are available at <http://creativecommons.org/licenses/by-nc-nd/4.0>. Any commercial reuse of Open Access articles published with a CC BY NC SA or CC BY NC ND license requires permission from Elsevier and will be subject to a fee.

Commercial reuse includes:

- Associating advertising with the full text of the Article
- Charging fees for document delivery or access
- Article aggregation
- Systematic distribution via e-mail lists or share buttons

Posting or linking by commercial companies for use by customers of those companies.

20. Other Conditions:

v1.10

Questions? customercare@copyright.com.



- Figure 3.5

27/06/23, 14:40

Creative Commons — Attribution 3.0 Unported — CC BY 3.0

This page is available in the following languages:



**Creative Commons License
Deed**

Attribution 3.0 Unported (CC BY 3.0)



This is a human-readable summary of (and not a substitute for) the [license](#).

You are free to:

Share — copy and redistribute the material in any medium or format

Adapt — remix, transform, and build upon the material

for any purpose, even commercially.

The licensor cannot revoke these freedoms as long as you follow the license terms.

Under the following terms:

Attribution — You must give appropriate credit, provide a link to the license, and indicate if changes were made. You may do so in any reasonable manner, but not in any way that suggests the licensor endorses you or your use.

No additional restrictions — You may not apply legal terms or technological measures that legally restrict others from doing anything the license permits.

Notices:



You do not have to comply with the license for elements of the material in the public domain or where your use is permitted by an applicable exception or limitation.


No warranties are given. The license may not give you all of the permissions necessary for your intended use. For example, other rights such as publicity, privacy, or moral rights may limit how you use the material.

- Figure 3.6

27/06/23, 14:56

Rightslink® by Copyright Clearance Center





Novel organogels for topical delivery of naproxen: design, physicochemical characteristics and in vitro drug permeation
Author: Tomasz Osmalek, , Bartłomiej Milanowski, et al
Publication: Pharmaceutical Development and Technology
Publisher: Taylor & Francis
Date: May 19, 2017
Rights managed by Taylor & Francis

Thesis/Dissertation Reuse Request

Taylor & Francis is pleased to offer reuses of its content for a thesis or dissertation free of charge contingent on resubmission of permission request if work is published.

BACK CLOSE

© 2023 Copyright - All Rights Reserved | Copyright Clearance Center, Inc. | [Privacy statement](#) | [Data Security and Privacy](#)
| [For California Residents](#) | [Terms and Conditions](#)Comments? We would like to hear from you. E-mail us at customer-care@copyright.com

- Figure 3.7

27/06/23, 14:59

Creative Commons — Attribution-NonCommercial-NoDerivatives 4.0 International — CC BY-NC-ND 4.0

This page is available in the following languages:



Creative Commons License Deed

Attribution-NonCommercial-NoDerivatives 4.0 International (CC BY-NC-ND 4.0)

This is a human-readable summary of (and not a substitute for) the [license](#).

You are free to:

Share — copy and redistribute the material in any medium or format

The licensor cannot revoke these freedoms as long as you follow the license terms.

Under the following terms:

Attribution — You must give appropriate credit, provide a link to the license, and indicate if changes were made. You may do so in any reasonable manner, but not in any way that suggests the licensor endorses you or your use.

NonCommercial — You may not use the material for commercial purposes.

NoDerivatives — If you remix, transform, or build upon the material, you may not distribute the modified material.

No additional restrictions — You may not apply legal terms or technological measures that legally restrict others from doing anything the license permits.

Notices:

You do not have to comply with the license for elements of the material in the public domain or where your use is permitted by an applicable exception or limitation.

No warranties are given. The license may not give you all of the permissions necessary for your intended use. For example, other rights such as publicity, privacy, or moral rights may limit how you use the material.

- Figure 3.8

27/06/23, 13:12

RightsLink Printable License

ELSEVIER LICENSE
TERMS AND CONDITIONS

Jun 27, 2023

This Agreement between Faculdade de Farmácia da Universidade do Porto -- Raquel Costa ("You") and Elsevier ("Elsevier") consists of your license details and the terms and conditions provided by Elsevier and Copyright Clearance Center.

License Number	5577050365920
License date	Jun 27, 2023
Licensed Content Publisher	Elsevier
Licensed Content Publication	Elsevier Books
Licensed Content Title	Encyclopedia of Materials Characterization
Licensed Content Author	JEFFREY B. BINDELL
Licensed Content Date	Jan 1, 1992
Licensed Content Pages	15
Start Page	70
End Page	84
Type of Use	reuse in a thesis/dissertation
Portion	figures/tables/illustrations
Number of figures/tables/illustrations	1
Format	both print and electronic

27/06/23, 13:12

RightsLink Printable License

Are you the author of this Elsevier chapter?	No
Will you be translating?	No
Title	Production of Lipid Nanoparticles for Topical Administration of Flavonoids
Institution name	Faculdade de Ciências da Universidade do Porto
Expected presentation date	Oct 2023
Portions	Figure 4
Requestor Location	Faculade de Farmácia da Universidade do Porto Rua Conselheiro Boaventura de Sousa, nº2
	Oliveira de Azeméis, Aveiro 3720-210 Portugal Attn: Faculade de Farmácia da Universidade do Porto
Publisher Tax ID	GB 494 6272 12
Total	0.00 EUR
Terms and Conditions	

INTRODUCTION

1. The publisher for this copyrighted material is Elsevier. By clicking "accept" in connection with completing this licensing transaction, you agree that the following terms and conditions apply to this transaction (along with the Billing and Payment terms and conditions established by Copyright Clearance Center, Inc. ("CCC"), at the time that you opened your RightsLink account and that are available at any time at <https://myaccount.copyright.com>).

GENERAL TERMS

2. Elsevier hereby grants you permission to reproduce the aforementioned material subject to the terms and conditions indicated.

3. Acknowledgement: If any part of the material to be used (for example, figures) has appeared in our publication with credit or acknowledgement to another source, permission must also be sought from that source. If such permission is not obtained then that material may not be included in your publication/copies. Suitable acknowledgement to the source

27/06/23, 13:12

RightsLink Printable License

must be made, either as a footnote or in a reference list at the end of your publication, as follows:

"Reprinted from Publication title, Vol /edition number, Author(s), Title of article / title of chapter, Pages No., Copyright (Year), with permission from Elsevier [OR APPLICABLE SOCIETY COPYRIGHT OWNER]." Also Lancet special credit - "Reprinted from The Lancet, Vol. number, Author(s), Title of article, Pages No., Copyright (Year), with permission from Elsevier."

4. Reproduction of this material is confined to the purpose and/or media for which permission is hereby given. The material may not be reproduced or used in any other way, including use in combination with an artificial intelligence tool (including to train an algorithm, test, process, analyse, generate output and/or develop any form of artificial intelligence tool), or to create any derivative work and/or service (including resulting from the use of artificial intelligence tools).

5. Altering/Modifying Material: Not Permitted. However figures and illustrations may be altered/adapted minimally to serve your work. Any other abbreviations, additions, deletions and/or any other alterations shall be made only with prior written authorization of Elsevier Ltd. (Please contact Elsevier's permissions helpdesk [here](#)). No modifications can be made to any Lancet figures/tables and they must be reproduced in full.

6. If the permission fee for the requested use of our material is waived in this instance, please be advised that your future requests for Elsevier materials may attract a fee.

7. Reservation of Rights: Publisher reserves all rights not specifically granted in the combination of (i) the license details provided by you and accepted in the course of this licensing transaction, (ii) these terms and conditions and (iii) CCC's Billing and Payment terms and conditions.

8. License Contingent Upon Payment: While you may exercise the rights licensed immediately upon issuance of the license at the end of the licensing process for the transaction, provided that you have disclosed complete and accurate details of your proposed use, no license is finally effective unless and until full payment is received from you (either by publisher or by CCC) as provided in CCC's Billing and Payment terms and conditions. If full payment is not received on a timely basis, then any license preliminarily granted shall be deemed automatically revoked and shall be void as if never granted. Further, in the event that you breach any of these terms and conditions or any of CCC's Billing and Payment terms and conditions, the license is automatically revoked and shall be void as if never granted. Use of materials as described in a revoked license, as well as any use of the materials beyond the scope of an unrevoked license, may constitute copyright infringement and publisher reserves the right to take any and all action to protect its copyright in the materials.

9. Warranties: Publisher makes no representations or warranties with respect to the licensed material.

10. Indemnity: You hereby indemnify and agree to hold harmless publisher and CCC, and their respective officers, directors, employees and agents, from and against any and all claims arising out of your use of the licensed material other than as specifically authorized pursuant to this license.

11. No Transfer of License: This license is personal to you and may not be sublicensed, assigned, or transferred by you to any other person without publisher's written permission.

12. No Amendment Except in Writing: This license may not be amended except in a writing signed by both parties (or, in the case of publisher, by CCC on publisher's behalf).

27/06/23, 13:12

RightsLink Printable License

13. **Objection to Contrary Terms:** Publisher hereby objects to any terms contained in any purchase order, acknowledgment, check endorsement or other writing prepared by you, which terms are inconsistent with these terms and conditions or CCC's Billing and Payment terms and conditions. These terms and conditions, together with CCC's Billing and Payment terms and conditions (which are incorporated herein), comprise the entire agreement between you and publisher (and CCC) concerning this licensing transaction. In the event of any conflict between your obligations established by these terms and conditions and those established by CCC's Billing and Payment terms and conditions, these terms and conditions shall control.

14. **Revocation:** Elsevier or Copyright Clearance Center may deny the permissions described in this License at their sole discretion, for any reason or no reason, with a full refund payable to you. Notice of such denial will be made using the contact information provided by you. Failure to receive such notice will not alter or invalidate the denial. In no event will Elsevier or Copyright Clearance Center be responsible or liable for any costs, expenses or damage incurred by you as a result of a denial of your permission request, other than a refund of the amount(s) paid by you to Elsevier and/or Copyright Clearance Center for denied permissions.

LIMITED LICENSE

The following terms and conditions apply only to specific license types:

15. **Translation:** This permission is granted for non-exclusive world **English** rights only unless your license was granted for translation rights. If you licensed translation rights you may only translate this content into the languages you requested. A professional translator must perform all translations and reproduce the content word for word preserving the integrity of the article.

16. **Posting licensed content on any Website:** The following terms and conditions apply as follows: Licensing material from an Elsevier journal: All content posted to the web site must maintain the copyright information line on the bottom of each image; A hyper-text must be included to the Homepage of the journal from which you are licensing at <http://www.sciencedirect.com/science/journal/xxxx> or the Elsevier homepage for books at <http://www.elsevier.com>; Central Storage: This license does not include permission for a scanned version of the material to be stored in a central repository such as that provided by Heron/XanEdu.

Licensing material from an Elsevier book: A hyper-text link must be included to the Elsevier homepage at <http://www.elsevier.com>. All content posted to the web site must maintain the copyright information line on the bottom of each image.

Posting licensed content on Electronic reserve: In addition to the above the following clauses are applicable: The web site must be password-protected and made available only to bona fide students registered on a relevant course. This permission is granted for 1 year only. You may obtain a new license for future website posting.

17. **For journal authors:** the following clauses are applicable in addition to the above:

Preprints:

A preprint is an author's own write-up of research results and analysis, it has not been peer-reviewed, nor has it had any other value added to it by a publisher (such as formatting, copyright, technical enhancement etc.).

Authors can share their preprints anywhere at any time. Preprints should not be added to or enhanced in any way in order to appear more like, or to substitute for, the final versions of

27/06/23, 13:12

RightsLink Printable License

articles however authors can update their preprints on arXiv or RePEc with their Accepted Author Manuscript (see below).

If accepted for publication, we encourage authors to link from the preprint to their formal publication via its DOI. Millions of researchers have access to the formal publications on ScienceDirect, and so links will help users to find, access, cite and use the best available version. Please note that Cell Press, The Lancet and some society-owned have different preprint policies. Information on these policies is available on the journal homepage.

Accepted Author Manuscripts: An accepted author manuscript is the manuscript of an article that has been accepted for publication and which typically includes author-incorporated changes suggested during submission, peer review and editor-author communications.

Authors can share their accepted author manuscript:

- immediately
 - via their non-commercial person homepage or blog
 - by updating a preprint in arXiv or RePEc with the accepted manuscript
 - via their research institute or institutional repository for internal institutional uses or as part of an invitation-only research collaboration work-group
 - directly by providing copies to their students or to research collaborators for their personal use
 - for private scholarly sharing as part of an invitation-only work group on commercial sites with which Elsevier has an agreement
- After the embargo period
 - via non-commercial hosting platforms such as their institutional repository
 - via commercial sites with which Elsevier has an agreement

In all cases accepted manuscripts should:

- link to the formal publication via its DOI
- bear a CC-BY-NC-ND license - this is easy to do
- if aggregated with other manuscripts, for example in a repository or other site, be shared in alignment with our hosting policy not be added to or enhanced in any way to appear more like, or to substitute for, the published journal article.

Published journal article (JPA): A published journal article (PJA) is the definitive final record of published research that appears or will appear in the journal and embodies all value-adding publishing activities including peer review co-ordination, copy-editing, formatting, (if relevant) pagination and online enrichment.

Policies for sharing publishing journal articles differ for subscription and gold open access articles:

Subscription Articles: If you are an author, please share a link to your article rather than the full-text. Millions of researchers have access to the formal publications on ScienceDirect, and so links will help your users to find, access, cite, and use the best available version.

Theses and dissertations which contain embedded PJAs as part of the formal submission can be posted publicly by the awarding institution with DOI links back to the formal publications on ScienceDirect.

If you are affiliated with a library that subscribes to ScienceDirect you have additional private sharing rights for others' research accessed under that agreement. This includes use for classroom teaching and internal training at the institution (including use in course packs and courseware programs), and inclusion of the article for grant funding purposes.

27/06/23, 13:12

RightsLink Printable License

Gold Open Access Articles: May be shared according to the author-selected end-user license and should contain a [CrossMark logo](#), the end user license, and a DOI link to the formal publication on ScienceDirect.

Please refer to Elsevier's [posting policy](#) for further information.

18. **For book authors** the following clauses are applicable in addition to the above: Authors are permitted to place a brief summary of their work online only. You are not allowed to download and post the published electronic version of your chapter, nor may you scan the printed edition to create an electronic version. **Posting to a repository:** Authors are permitted to post a summary of their chapter only in their institution's repository.

19. **Thesis/Dissertation:** If your license is for use in a thesis/dissertation your thesis may be submitted to your institution in either print or electronic form. Should your thesis be published commercially, please reapply for permission. These requirements include permission for the Library and Archives of Canada to supply single copies, on demand, of the complete thesis and include permission for Proquest/UMI to supply single copies, on demand, of the complete thesis. Should your thesis be published commercially, please reapply for permission. Theses and dissertations which contain embedded PJAs as part of the formal submission can be posted publicly by the awarding institution with DOI links back to the formal publications on ScienceDirect.

Elsevier Open Access Terms and Conditions

You can publish open access with Elsevier in hundreds of open access journals or in nearly 2000 established subscription journals that support open access publishing. Permitted third party re-use of these open access articles is defined by the author's choice of Creative Commons user license. See our [open access license policy](#) for more information.

Terms & Conditions applicable to all Open Access articles published with Elsevier:

Any reuse of the article must not represent the author as endorsing the adaptation of the article nor should the article be modified in such a way as to damage the author's honour or reputation. If any changes have been made, such changes must be clearly indicated.

The author(s) must be appropriately credited and we ask that you include the end user license and a DOI link to the formal publication on ScienceDirect.

If any part of the material to be used (for example, figures) has appeared in our publication with credit or acknowledgement to another source it is the responsibility of the user to ensure their reuse complies with the terms and conditions determined by the rights holder.

Additional Terms & Conditions applicable to each Creative Commons user license:

CC BY: The CC-BY license allows users to copy, to create extracts, abstracts and new works from the Article, to alter and revise the Article and to make commercial use of the Article (including reuse and/or resale of the Article by commercial entities), provided the user gives appropriate credit (with a link to the formal publication through the relevant DOI), provides a link to the license, indicates if changes were made and the licensor is not represented as endorsing the use made of the work. The full details of the license are available at <http://creativecommons.org/licenses/by/4.0>.

CC BY NC SA: The CC BY-NC-SA license allows users to copy, to create extracts, abstracts and new works from the Article, to alter and revise the Article, provided this is not done for commercial purposes, and that the user gives appropriate credit (with a link to the formal publication through the relevant DOI), provides a link to the license, indicates if changes were made and the licensor is not represented as endorsing the use made of the

27/06/23, 13:12

RightsLink Printable License

work. Further, any new works must be made available on the same conditions. The full details of the license are available at <http://creativecommons.org/licenses/by-nc-sa/4.0>.

CC BY NC ND: The CC BY-NC-ND license allows users to copy and distribute the Article, provided this is not done for commercial purposes and further does not permit distribution of the Article if it is changed or edited in any way, and provided the user gives appropriate credit (with a link to the formal publication through the relevant DOI), provides a link to the license, and that the licensor is not represented as endorsing the use made of the work. The full details of the license are available at <http://creativecommons.org/licenses/by-nc-nd/4.0>. Any commercial reuse of Open Access articles published with a CC BY NC SA or CC BY NC ND license requires permission from Elsevier and will be subject to a fee.

Commercial reuse includes:

- Associating advertising with the full text of the Article
- Charging fees for document delivery or access
- Article aggregation
- Systematic distribution via e-mail lists or share buttons

Posting or linking by commercial companies for use by customers of those companies.

20. Other Conditions:

v1.10

Questions? customercare@copyright.com.

- Figure 3.9

27/06/23, 14:44

Creative Commons — Attribution-ShareAlike 4.0 International — CC BY-SA 4.0

This page is available in the following languages:



Creative Commons License Deed



Attribution-ShareAlike 4.0 International (CC BY-SA 4.0)

This is a human-readable summary of (and not a substitute for) the [license](#).

You are free to:

Share — copy and redistribute the material in any medium or format

Adapt — remix, transform, and build upon the material

for any purpose, even commercially.

The licensor cannot revoke these freedoms as long as you follow the license terms.

Under the following terms:

Attribution — You must give appropriate credit, provide a link to the license, and indicate if changes were made. You may do so in any reasonable manner, but not in any way that suggests the licensor endorses you or your use.

ShareAlike — If you remix, transform, or build upon the material, you must distribute your contributions under the same license as the original.

No additional restrictions — You may not apply legal terms or technological measures that legally restrict others from doing anything the license permits.

Notices:

You do not have to comply with the license for elements of the material in the public domain or where your use is permitted by an applicable exception or limitation.

No warranties are given. The license may not give you all of the permissions necessary for your intended use. For example, other rights such as publicity, privacy, or moral rights may limit how you use the material.

- Figure 3.10

27/06/23, 14:44

Creative Commons — Attribution 4.0 International — CC BY 4.0

This page is available in the following languages:



**Creative Commons License
Deed**

Attribution 4.0 International (CC BY 4.0)



This is a human-readable summary of (and not a substitute for) the [license](#).

You are free to:

Share — copy and redistribute the material in any medium or format

Adapt — remix, transform, and build upon the material

for any purpose, even commercially.

The licensor cannot revoke these freedoms as long as you follow the license terms.

Under the following terms:

Attribution — You must give appropriate credit, provide a link to the license, and indicate if changes were made. You may do so in any reasonable manner, but not in any way that suggests the licensor endorses you or your use.

No additional restrictions — You may not apply legal terms or technological measures that legally restrict others from doing anything the license permits.

Notices:

You do not have to comply with the license for elements of the material in the public domain or where your use is permitted by an applicable exception or limitation.

No warranties are given. The license may not give you all of the permissions necessary for your intended use. For example, other rights such as publicity, privacy, or moral rights may limit how you use the material.